Ex vivo gene therapy using human muscle stem cells and bacterial nanocellulose as a new culture strategy

Inaugural-Dissertation
to obtain the academic degree
Doctor rerum naturalium (Dr. rer. nat.)

submitted to the Department of Biology, Chemistry, Pharmacy
of Freie Universität Berlin

by

Silvia Di Francescantonio
from Teramo, Italy

2021

The work was conducted from January 2017 to January 2021 under the supervision of Professor Simone Spuler at the Experimental and Clinical Research Center (a joint cooperation of the Charité Medical Faculty and the Max Delbrück Center for Molecular Medicine, Berlin, Germany). The experiments were conducted in the laboratories of Professor Simone Spuler.

1st reviewer: **Prof. Dr. Simone Spuler**
Institute for Chemistry and Biochemistry
Department of Biology, Chemistry and Pharmacy
Freie Universität Berlin

and

Department of Muscle Sciences and
University Outpatient Clinic for Muscle Disorders
Experimental and Clinical Research Center, Berlin

2nd reviewer: **Prof. Dr. Michael Gotthardt**
Experimental and Translational Cardiology at the
Max Delbrück Center for Molecular Medicine, in
the Helmholtz Association, Berlin and Charité-
Universitätsmedizin, Berlin

Date of defense: 03.06.2021

SELBSTSTÄNDIGKEITSERKLÄRUNG

Ich erkläre gegenüber der Freien Universität Berlin, dass ich die vorliegende Dissertation selbständig und ohne Benutzung anderer als der angegebenen Quellen und Hilfsmittel angefertigt habe.

Die vorliegende Arbeit ist frei von Plagiaten. Alle Ausführungen, die wörtlich oder inhaltlich aus anderen Schriften entnommen sind, habe ich als solche kenntlich gemacht. Diese Arbeit wurde in gleicher oder ähnlicher Form noch bei keiner anderen Universität als Prüfungsleistung eingereicht.

_____ _____

Datum Unterschrift

ACKNOWLEDGEMENTS

First, I would like to express my gratitude to Professor Simone Spuler for supervising my work and giving me the opportunity to develop this PhD project in her laboratory. Her guidance and advice were essential to achieve my goals. I would also like to thank Professor Michael Gotthardt, for reviewing my Thesis and for the supervision as PhD committee member, together with Dr. Mina Gouti.

I want to thank MyoGrad and the MDC PhD program for financially supporting my doctoral studies as well as my participation in scientific events. I also want to thank Susanne Wissler for helping with all the organizational and administrative aspects of my PhD.

I thank Dr. MD Elisabetta Gazzerro for her support, persistent trust and for being such an inspiring woman of science. Her contribution was essential for my professional growth.

I would like to thank Dr. Helena F. Escobar for her mentoring in the field of gene editing, for the inspiring discussions and the constructive criticisms. I am also grateful for the encouragement and the emotional support throughout the last four years.

I thank Dr. Eric Metzler for being a great fellow PhD student as well as a very good friend since the very beginning. His continuous support, especially during the last months, was crucial for finalizing my doctoral Thesis.

I would like to thank Stephanie Meyer-Liesener and Stefanie Haafke for helping me with primary muscle cell culture and for their assistance throughout the PhD.

I thank Dr. Andreas Marg for sharing his expertise in performing the laser wounding assay.

I would like to thank Dr. Yumi Sunaga-Franze for her collaboration in the analysis of the RNA sequencing data and Kirsten Richter for the introduction to library preparation.

I thank Dr. Devakumar Sundaravinayagam from the laboratory of Dr. Michela Di Virgilio for sharing his knowledge in cell cycle analysis techniques.

I would like to thank current and past members of the AG Spuler, Dr. Helena Escobar, Dr. Henning Langer, Dr. Jakub Malcher, Dr. Stefanie Müthel, Dr. Eric Metzler and Anne Krause. We shared funny moments and fruitful conversations inside and outside the lab. A special mention to Dr. Stefanie Müthel for being the perfect office- and bench-mate, because “no question is a stupid one”. I also want to thank Dr.

Jakub Malcher for being a great desk-neighbor and for sharing his knowledge about virus production and usage.

I would like to thank my “Berlin family”, as no one can succeed in life without good friends. I have been very lucky as we shared fun, trips, dinners and difficult moments. A special mention goes to Vero, for supporting when most needed, and to Dimitra for being a great flatmate and friend during a tough time of our lives. I also thank Matte and Cris for making me feel always at home.

A special thank goes to Silvia who, since the very beginning, has been sharing joys and pains of our Berlin adventure. She is a colleague, a friend, a flatmate and her support has never failed. I own her a lot.

I need to thank all the friends that have been close despite the distance. Sara, “discovering” life together ever since we didn’t know much about it. Emanu, my “better half”, side by side through any hurdles and challenging steps of life. Ile and Lori, as we still have such a good friendship after so many years.

Last but not least, my family: my parents Pasquale and Grazia and my sisters Valeria and Paola. I own them everything I have achieved in my life. I want to thank them for the encouragement, the trust, the good food sent from Italy and for giving me the opportunity to always follow my path, even when it was leading so far away from home.

TABLE OF CONTENTS

SUMMARY

Muscular dystrophies (MDs) are a group of inherited degenerative disorders characterized by progressive muscle wasting and, in some cases, short life expectancy. More than 40 genes have been identified as causative for MDs and there is still no cure for these disorders. Cell replacement therapy holds the promise to regenerate and restore the dystrophic muscle after allogeneic or autologous transplantation. The ability of skeletal muscle to regenerate relies on a population of quiescent muscle stem cells called satellite cells (SCs). Upon injury, they proliferate and generate a committed progeny (a.k.a. myoblasts) that is responsible for muscle repair. SCs can be isolated from muscle biopsies and, when transplanted into regenerating muscles, show a robust engraftment potential. Therefore, SCs represent an optimal candidate for cell-therapies, although there are limitations as the loss of their stemness during in vitro amplification. Cell-based strategies can be combined with gene editing technologies for autologous transplantation of corrected cells. The CRISPR/Cas9 system relies on single guide RNAs (sgRNAs) and a Cas9 nuclease to induce site-specific double strand breaks (DSBs). The genome editing is then achieved via intrinsic repair mechanisms such as non-homologous end joining (NHEJ) or the homology-directed (HDR) DNA repair pathway. CRISPR/Cas9-based gene editing has been reported for correction of several MD-causing mutations in vivo and ex vivo systems. However, no results have been published yet for the correction of disease-causing mutations in human myoblasts. Therefore, the establishment of optimal gene correction strategies, as well as new culture conditions that preserve the regenerative potential of myoblasts have been extensively investigated to improving cell-based treatments.

In this study, I first developed a CRISPR/Cas9-based ex vivo gene editing method in human primary myoblasts (hPMs) to repair a mutation in the dysferlin gene (DYSF) that is known to cause limb girdle muscular dystrophy type 2B (LGMD2B) which is an autosomal recessive disease characterized by severe weakness and atrophy of the pelvic and girdle muscles. The mutation in the exon 44 of the DYSF gene (c.4872_4876delinsCCCC) causes a shift of the open-reading frame resulting in the absence of the encoded protein. Here, I showed that the DYSF coding sequence can be re-framed via a single nucleotide insertion combining the Cas9 nuclease with a mutation-specific sgRNA. As consequence, the missing protein was re-expressed in edited myoblasts and correctly localized at the membrane of terminally differentiated myotubes. These results proved the feasibility of CRISPR/Cas9-based editing to correct a specific mutation in LGMD2B patient-derived PMs.

As a second aim of this study, to preserve the regenerative potential of in vitro cultured myoblasts by avoiding extensive cell proliferation, I characterized bacterial nanocellulose (BNC) as an alternative substrate for hPMs. BNC is a water-insoluble polysaccharide consisting of cellulose nano-fibers produced by bacteria (e.g Gluconacetobacter xylinus). BNC is biocompatible, extensively used in regenerative medicine and tissue engineering and displays similarities with extracellular matrix (ECM) proteins like collagen. I showed that hPMs on the BNC substrate were able to be cultured for weeks without reaching confluence, suggesting a substantial reduction of

their proliferation rate compared to standard culture on plastic dishes (Standard). I investigated hPMs cellular morphology, proliferation capability and total gene expression profiles comparing BNC to Standard. The results confirmed that BNC substrate induces a slow-dividing state of hPMs, avoiding extensive propagation and preserving cells for weeks without undergoing terminal differentiation or senescence. Remarkably, hPMs were able to recover proliferation and myogenic potential (e.g. differentiation in multinucleated myotubes) when placed back in Standard after 2 weeks of BNC culture. Lastly, I proved that CRISPR/Cas9-based gene editing is also functional in hPMs on BNC using NCAM1 (neural cell adhesion molecule 1) knockout as readout strategy. Therefore, BNC is a suitable in vitro method for testing genetic manipulation in slowly-dividing primary cells.

ZUSAMMENFASSUNG

Muskeldystrophien (MD) sind eine heterogene Gruppe von vererbbaren, degenerativen Muskelerkrankungen, die durch einen progressiven Verlust der Muskulatur und, in einigen Fällen, einer verminderten Lebenserwartung charakterisiert sind. Es wurden bereits mehr als 40 Gene, die MDs auslösen, identifiziert, aber bis jetzt konnte keine Therapie gefunden werden. Die Zellersatztherapie ist eine vielversprechende Methode, um dystrophe Muskeln nach einer allogenen oder autologen Zelltransplantation zu regenerieren und wiederherzustellen. Die Fähigkeit des Skelettmuskels sich selbst zu regenerieren, beruht auf einer bestimmten Anzahl von quieszenten Muskelstammzellen, den sogenannten Satellitenzellen (SCs). Nach einer Verletzung, beginnen sie zu proliferieren und generieren die sogenannten Myoblasten, eine Zellpopulation, die verantwortlich für die Muskelreparatur ist. SCs können aus Muskelbiopsien isoliert werden und zeigen nach Transplantation in einen regenerierenden Muskel ein robustes Einwachsen in diesen. Daher sind SCs ein optimaler Kandidat für Zelltherapien, obwohl sie während der *in vitro* Vermehrung ihre Stammzelleigenschaften verlieren können.

Zell-basierte Therapien können zusammen mit Geneditierungstechnologien für eine autologe Transplantation von korrigierten Muskelzellen genutzt werden. Das CRISPR/Cas9 System benötigt hierbei eine single guide RNAs (sgRNAs) und die Nuklease Cas9, um an spezifischen Stellen im Genom Doppelstrangbrüche hervorzurufen. Die Editierung des Genoms erfolgt dann mittels intrinsischer Reparaturmechnismen zum einen über Non-homologous end-joining (NHEJ) oder zum anderen über Homology-directed repair (HDR). Die CRISPR/Cas9-basierte Geneditierung wurde bereits für die Korrektur verschiedener MD-auslösender Mutationen *in vivo* und *ex vivo* genutzt. Allerdings wurde bis jetzt noch keine Geneditierung von humanen Myoblasten publiziert. Daher wurden hier die Etablierung einer optimalen Strategie zur Genkorrektur sowie neue Zellkultur-Methoden, die das regenerative Potential von Myoblasten unterstützen, intensiv untersucht, um zell-basierte Therapien zu verbessern.

In dieser Studie, habe ich zuerst eine CRISPR/Cas9-basierte Geneditierungsmethodik entwickelt, um eine Mutation im Dysferlin (*DYSF*) Gen in primären humanen Myoblasten (hPM) zu reparieren. Diese Mutation führt zur Ausprägung der Gliedergürteldystrophie vom Typ 2B (LGMD2B), bei der es sich um eine autosomal rezessive Krankheit handelt, die durch eine starke Muskelschwäche und Atrophie der Becken- und Hüftmuskulatur charakterisiert ist. Die hier untersuchte Mutation liegt in Exon 44 des *DYSF* Gens (c.4872_4876delinsCCCC) und führt zu einer Verschiebung des offenen Leserahmens, was wiederum zu einem Verlust des kodierten Proteins führt. Ich zeige hier, dass der offene Leserahmen von *DYSF* durch die Insertion eines Nukleotids wiederhergestellt werden kann, wenn Cas9 mit einer mutations-spezifischen sgRNA genutzt wird. Daraus resultiert eine Re-Expression des DYSF Proteins in editierten Myoblasten sowie eine korrekte Lokalisierung des Proteins in der Membran von terminal differenzierten Myotuben. Diese Ergebnisse zeigen, dass die CRISPR/Cas9-basierte Geneditierung genutzt werden kann, um spezifische Mutationen in hPMs von LGMD2B Patienten zu korrigieren.

Das zweite Ziel dieser Studie war es, das regenerative Potential von *in vitro* kultivierten Myoblasten zu erhalten, ohne dass übermäßiges Zellwachstum stattfindet. Dafür habe ich bakterielle Nanocellulose (BNC) als ein alternatives Substrat für die Kultivierung von hPMs charakterisiert. BNC ist ein wasserunlösliches Polysaccharid, das Zellulose Nanofibrillen enthält, die von Bakterien (z.B. *Gluconacetobacter xylinus)* produziert werden. BNC ist biokompatibel, bereits intensiv genutzt in der regenerativen Medizin sowie dem Tissue Engineering und verhält sich ähnlich wie extrazelluläre Matrixproteine (ECM), z.B. Kollagene. Ich zeige hier, dass hPMs auf BNC als Substrat über Wochen kultiviert werden können, ohne dass sie volle Konfluenz erreichen. Das weist darauf hin, dass eine erhebliche Reduktion der Proliferationsrate verglichen mit Standard Zellkulturmethoden auftritt. Neben der zellulären Morphologie habe ich das Proliferationspotential und die Veränderung der Genexpression in hPMs auf BNC mit Standard Zellkulturmethoden verglichen. Die Ergebnisse bestätigen, dass das BNC Substrat bei hPMs einen langsam-teilenden Zustand hervorruft, wobei übermäßiges Wachstum über Wochen verhindert wird ohne dass die Zellen terminal differenzieren oder seneszent werden. Bemerkenswert ist, dass hPMs sowohl Proliferation als auch ihr myogenes Potential wieder aufnehmen, sobald sie in Standard Zellkultur überführt werden, nachdem sie 2 Wochen auf BNC kultiviert wurden. Zuletzt konnte ich zeigen, dass CRISPR/Ca9 basierte Geneditierung auch funktioniert, wenn hPMs auf BNC kultiviert werden. Dies konnte ich mittels Knock-out von *NCAM1* (neural cell adhesion molecule 1) als Readout zeigen. Daher eignet sich BNC als *in vitro* Methode zur Untersuchung genetischer Manipulationen in langsam teilenden Zellen.

LIST OF FIGURES

LIST OF TABLES

LIST OF ABBREVIATIONS

A	Adenine
a.k.a.	also known as
AAV	Adeno-associated virus
ASOs	Antisense oligonucleotides
BF	Bright field
BMD	Becker muscular dystrophy
BNC	Bacterial nanocellulose
BrdU	Bromodeoxyuridine
CALCR	Calcitonin receptor
CAPN3	Calpain 3
Cas	CRISPR-associated protein
CCNs	Cyclins
CDC42	RAC1 and the cell division cycle 42
CDKs	Cyclin-dependent protein kinases
CLEC14	C-type lectin domain containing 14A
COL28	Collagen type XXVIII
COL5	Collagen type V
COL6	Collagen type VI
COL7A1	Collagen type VII α1 chain
CRISPR	Clustered Regularly Interspersed Short Palindromic Repeats
crRNA	CRISPR RNA
Ct	Cycle threshold
CXCR4	C-X-C chemokine receptor type 4
DETs	Differentially expressed transcripts
DMD	Duchenne muscular dystrophy
DMD	Dystrophin gene
dsDNA	double strand DNA
DYSF	Dysferlin gene
e.g.	exempli gratia
E2F1	E2 promoter binding factor 1
ECM	Extracellular matrix
EHD2	EH-domain containing protein
etc.	et cetera
eSpCas9	Enhanced-specificity SpCas9
FACS	Fluorescence activated cell sorting

FAPs	Fibroadipogenic progenitors
FCS	Fetal calf serum
FGF	Fibroblast growth factor
FN1	Fibronectin 1
FSHD	Facioscapulohumeral muscular dystrophy
GAPDH	Glyceraldehyde 3-phosphate dehydrogenase, housekeeping gene
GFP	green fluorescent protein
HDR	Homology directed repair
hiPSCs	Human induced pluripotent stem cells
hPMs	Human primary myoblasts
HUVEC	Human umbilical vein endothelial cells
i.e.	id est (in other words)
i.m.	intramuscular
ICE	Inference of CRISPR Edits
IF	Immunofluorescence
iPSCs	Induced pluripotent stem cells
LGMD	Limb girdle muscular dystrophy
MABs	Mesoangioblasts
MDs	Muscular dystrophies
mESCs	Mouse embryonic stem cells
MG53	Protein mitsugumin 53
MMD1	Miyoshi myopathy with primarily distal weakness
MMP2	Matrix metalloproteinase-2
MOI	Multiplicity of infection
MRF4	Myogenic regulatory factor 4
MRFs	Myogenic regulatory factors
MSCs	Mesenchymal stem cells
Myf5	Myogenic factor 5
MYHC	Myosin heavy chain protein
MyoD1	Myogenic differentiation 1
MYOG	Myogenin
N	Nucleotide
n.s.	not significant
NCAM1	Neural cell adhesion molecule 1, also known as CD56
NHEJ	Non-homologous end joining
NOG	Immunodeficient mice
NSG	Immunodeficient NOD/SCID-gamma null mice

OPMD	Oculopharyngeal muscular dystrophy
padj	p value adjusted
PAM	Protospacer adjacent motif
Pax7	Paired-box protein 7
PCR	Polymerase chain reaction
PI	Propidium iodide
PMs	Primary myoblasts
Post-BNC	hPMs after detachment from BNC
RAC1	Rac family small GTPase 1
Rb	Retinoblastoma protein
RHO	Ras homolog family member
RIN	RNA integrity number
RMP	Recombinant protein
RT	Room temperature
RTq-PCR	Real-time quantitative polymerase chain reaction
SCs	Satellite cells
SEM	Scanning electron microscopy
sgRNA	Single guide RNA
SICD	Severe combined immunodeficiency
SMCs	Smooth muscle cells
SpCas9	*Streptococcus pyogenes* Cas9
Standard	Standard plastic dishes
T2A	*Thosea asigna* virus
T7E1	T7 Endonuclease I
TEBVs	Tissue-engineered blood vessels
TEM	Transmission electron microscopy
tracrRNA	trans-activating crRNA
T-tubule	Transverse tubule
VCAM-1	Vascular cell adhesion protein 1
vs.	versus
WB	Western blot
WGA	Wheat germ agglutinin
WT	Wild-type

1. INTRODUCTION

1.1. Skeletal muscle and adult muscle stem cells

Skeletal muscle is one of the most dynamic and plastic post-mitotic tissues in the human body. It covers more than 40% of the whole mass and contributes to multiple mechanical (e.g. locomotion, postural support, and breathing) and metabolic functions (Hoppeler and Fluck 2002; Frontera and Ochala 2015; Schnyder and Handschin 2015). The functional unit of the skeletal muscle is the muscle fiber or myofiber. Myofibers are grouped in longitudinal-organized fascicles and generate force by sarcomeres' contraction (Frontera and Ochala 2015). Each single myofiber is a giant multinucleated cell derived from the fusion of committed muscle progenitors or myoblasts during embryonic and fetal development (Mintz and Baker 1967; Relaix and Zammit 2012). Adult skeletal muscle tissue has a high regenerative potential. Since myonuclei are post-mitotic, muscle maintenance and regeneration potency rely on a population of adult stem cells, called satellite cells (SCs) (Almeida et al. 2016). SCs were first identified in 1961 by Alexander Mauro as rare mononucleated cells at the periphery of myofibers with a high nucleus to cytoplasm ratio. For many years, these cells were described only by their anatomical localization as "wedged" between the plasma membrane (also known as sarcolemma) and the basal lamina of each myofiber (Mauro 1961; Scharner and Zammit 2011; Yin, Price, and Rudnicki 2013) (Figure 1.1). Their involvement in muscle regeneration was just a hypothesis (Mauro 1961).

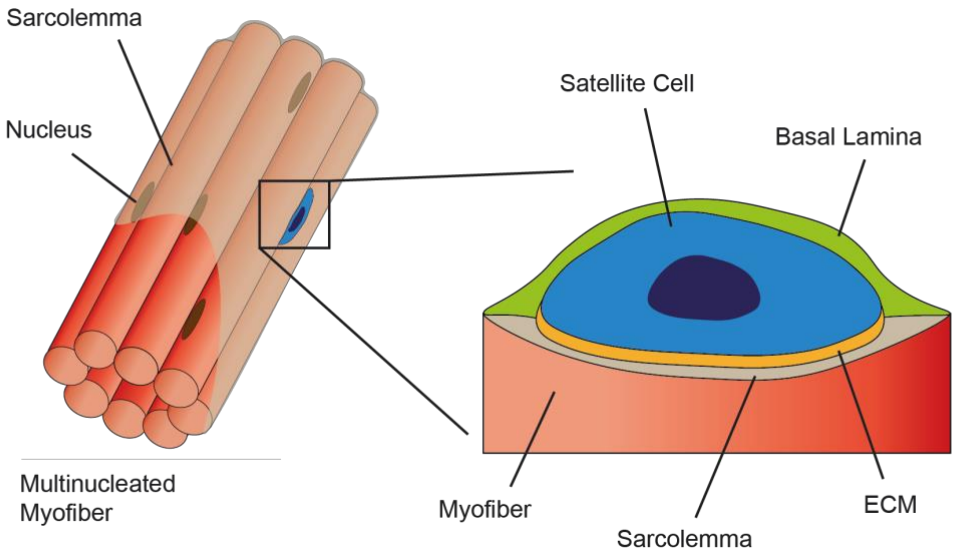

Figure 1.1: Localization of SCs in skeletal muscle.
SCs are quiescent muscle stem cells "wedged" between the basal lamina (green) and the sarcolemma (grey) of each myofiber surrounded by extracellular matrix or ECM (yellow).

Later on, [3H] thymidine tracing experiments demonstrated that SCs are mitotically quiescent cells resting in G0 cell cycle phase, but able to enter the cell cycle quickly after muscle injury, i.e. due to exercise or to disease (Reznik 1969; Moss and Leblond 1970). Moreover, SCs dissected from myofibers and cultured *in vitro*, undergo outgrowth, clonal expansion, and fusion to form functional myotubes (i.e. immature myofibers) (Bischoff 1975; Konigsberg, Lipton, and Konigsberg 1975).

Adult stem cells, by definition, should be able to both give rise to further committed progeny and to replicate themselves to maintain the tissue stem cells pool (a.k.a. self-renew). The ability of SCs to self-renew was proven by a myofiber transplantation assay. This experiment showed that, the engraftment of freshly isolated myofibers into irradiated muscles of dystrophic-nude mice gives rise to hundreds of SCs and a much higher number of myonuclei. Moreover, new generated SCs were able to support muscle regeneration despite subsequent rounds of experimental-induced injuries (Collins et al. 2005). It was then concluded that SCs are bona fide adult stem cells.

In 2000, Seale et al. demonstrated that mouse quiescent SCs and proliferating early myoblasts express the transcription factor paired box protein Pax7 (Seale et al. 2000). This was proven to be true across many other species, including humans (Morrison et al. 2006; Lindstrom and Thornell 2009; Lindstrom, Pedrosa-Domellof, and Thornell 2010; Yablonka-Reuveni 2011).

Pax7 is not only a canonical marker for SCs detection and various functions of this gene in SCs were proposed and controversially discussed. SCs become quiescent after birth from a pool of highly proliferative muscle progenitors (Relaix et al. 2005). It has been proven that Pax7 germline mutant mice, which survive after birth, show severe depletion of skeletal muscle stem cells and compromised post-natal muscle growth and regeneration after acute injury (Seale et al. 2000; Kuang et al. 2006; Relaix et al. 2006). As published in 2009, muscle regeneration fails after genetic ablation of Pax7 positive (Pax7+) cells in juvenile mice only. These results show that the transition from muscle progenitor cells to an adult stem cell state (a.k.a. SCs specification), is depended on Pax7 abundance. Other studies suggested that muscle regeneration and self-renewal after cardiotoxin injury is not impaired when Pax7 is ablated in mutant mice, showing that Pax7 is not required for injury-induced myogenesis in adulthood (Lepper, Conway, and Fan 2009; McCarthy et al. 2011). In contrast with these results, Pax7 has been described as a crucial gene for self-renewal and maintenance, as in its absence SCs are progressively lost postnatally because of apoptosis and cell cycle defects (Relaix et al. 2006) or precocious differentiation (von Maltzahn et al. 2013). The role of Pax7 was then considered important for SCs expansion and differentiation during both neonatal and adult myogenesis (Olguin and Olwin 2004; von Maltzahn et al. 2013; Lilja et al. 2017).

1.1.1. Myogenic regulatory factors in skeletal muscle regeneration

In the process of regeneration, SCs activate, re-enter cell cycle, expand in myoblasts and differentiate (Collins et al. 2005). This process is controlled by sub-sequential expression of transcription factors, partially resembling the differentiation program of embryonic myogenesis (von Maltzahn, Bentzinger, and Rudnicki 2014; Hernandez-Hernandez et al. 2017). Some of the

important “players” of myogenesis and regeneration are the myogenic regulatory factors (MRFs), basic helix-loop-helix transcription factors: myoblast determination protein 1 (MyoD1), myogenic factor 5 (Myf5), myogenin (MYOG), and MRF4 (Zanou and Gailly 2013; Hernandez-Hernandez et al. 2017) (Figure 1.2: Myogenic lineage progression and protein expression profile of the main MRFs.).

As previously discussed, Pax7 is expressed in SCs when localized in their anatomical niche between the basal lamina and the sarcolemma of skeletal muscle fibers (Cheung and Rando 2013). Upon activation (e.g. muscle injury), SCs express Myf5 and MyoD1 as early markers for myogenic commitment (Tajbakhsh et al. 1996). A subset of these dividing SCs commits to differentiation, through the expression of MYOG and downregulation of Pax7. After few rounds of proliferation, the majority of SCs-derived myoblasts ultimately exit the cell cycle, terminally differentiate and fuse to repair existing damaged muscle fibers or fuse among themselves to generate new myosin heavy chain (MYHC) positive muscle myofibers (Zammit et al. 2004) (Figure 1.2).

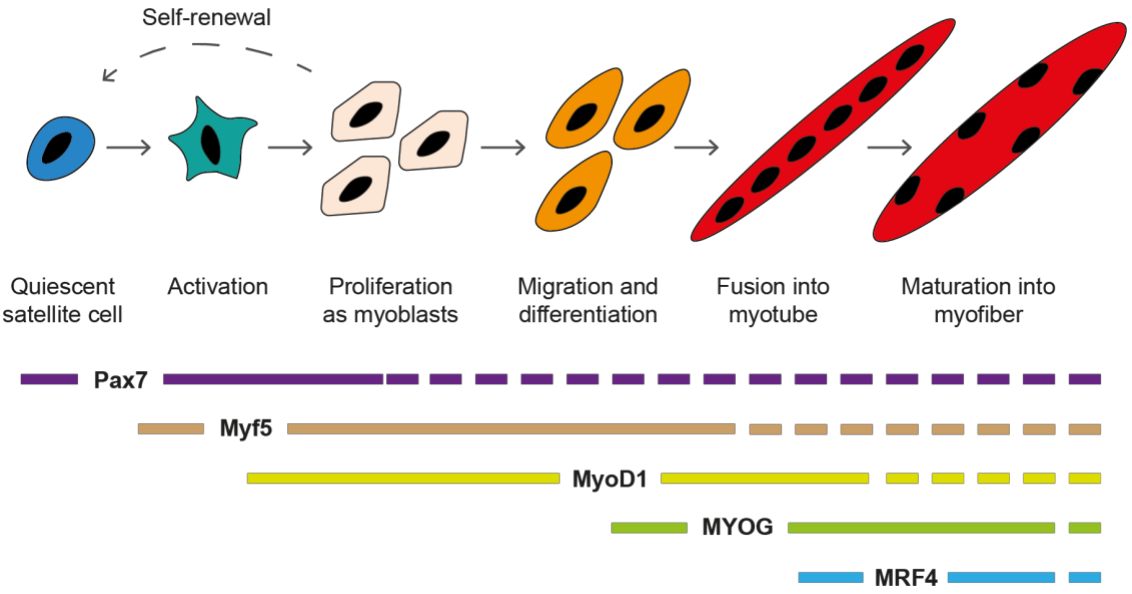

Figure 1.2: Myogenic lineage progression and protein expression profile of the main MRFs.
In the presence of tissue injury, SCs are able to activate (i.e., enter the cell cycle) and to generate a new tissue-specific committed progeny (a.k.a. myoblasts) that differentiate and fuse into myotubes and mature to become myofibers, the contractile unit of skeletal muscle. This process is characterized by sub-sequential expression of key modulators of myogenic lineage progression (modified from Schmidt et al. (2019)).

A subset of activated SCs downregulates Myf5 and MyoD1, resists the differentiation process and re-acquires a mitotically inactive quiescent state. These cells re-establish the pool of SCs in the niche and ensure that the response to future injuries is maintained (Kuang et al. 2007; Sacco et al. 2008; Olguin and Pisconti 2012; Almada and Wagers 2016)

Muscle regeneration could be partially reproduced *in vitro.* Mouse or human SCs can be isolated and placed in culture on plastic dishes (Montarras et al. 2005; Charville et al. 2015; Garcia

et al. 2018). After isolation, they are considered activated. In culture, they proliferate as myoblasts and can spontaneously fuse in functional myotubes when confluent or after differentiation induction (by starvation) (Bischoff 1975; Montarras et al. 2005; Kuang and Rudnicki 2008). If myoblasts are not differentiating, they undergo senescence after a certain number of divisions, depending on cell origin and donor age (Decary, Mouly, and Butler-Browne 1996; Montarras et al. 2005; Soriano-Arroquia et al. 2017). *In vitro* cultured myoblasts can be intramuscularly transplanted and are capable to engraft, regenerate muscle fibers and repopulate the pool of self-renewed muscle stem cells (Collins et al. 2005; Sacco et al. 2008).

1.1.2. Muscle stem cells heterogeneity and engraftment potency.

The identification of Pax7 and other canonical biomarkers for SCs (e.g. CD34, C-X-C chemokine receptor type 4 (CXCR4), syndecan-4, vascular cell adhesion protein 1 (VCAM-1) and β1-integrin etc., as well as the generation of transgenic reporter mouse lines, has been useful to investigate their phenotypic and functional heterogeneity (Kuang and Rudnicki 2008).

First studies suggested the coexistence of at least two distinct cell populations: on one hand, the committed muscle progenitors that are ready for myogenic differentiation, and on the other the self-renewing population that is capable of replenishing the SCs pool in the niche (Chakkalakal et al. 2012; Rocheteau et al. 2012; Chakkalakal et al. 2014). Lineage tracing experiments showed that about 10% of the total pool of muscle stem cells had never expressed Myf5 during development. This cell population was found to be more efficient in repopulating the SCs compartment (compared to Myf5-expressing SCs) when transplanted into Pax7-null mice (Kuang et al. 2007). Two populations of SCs have been identified according to the Pax7 RNA level: cell expressing high (Pax7hi) or low (Pax7low) level of Pax7. Pax7hi cells have a lower metabolic activity, are more dormant in their cell cycle activity and, in contrast to Pax7low cells, are able to replenish both Pax7hi and Pax7low SCs upon transplantation in cryodamaged muscles of immunocompromised mice (Rocheteau et al. 2012). Moreover, it has been discovered that low-cycling SCs have a higher engraftment potency than high-cycling cells after transplantation in injured mice (Ono et al. 2012; Chakkalakal et al. 2014).

Recently, single cell sequencing techniques allowed the identification of transcriptionally distinct populations of human SCs with a heterogeneous gene expression pattern (Charville et al. 2015; Cho and Doles 2017; Marg et al. 2019; Barruet et al. 2020). The engraftment potential of each different population is currently investigated. Interestingly, Marg A et al. identified a new Pax7-negative myogenic population which is positive for the marker CLEC14 (C-type lectin domain containing 14A). This population of cells is able to engraft and form new myofibers after transplantation into immunodeficient NOG mice (Marg et al. 2019), thus demonstrating that the regeneration potential of myogenic cells does not depend on Pax7 abundance. In a different study, a subpopulation of human SCs, Pax7+ cells marked by caveolin 1, showed to be more efficient in engraftment, differentiation and self-renewal after transplantation in immunodeficient NOD/SCID-

gamma null (NSG) mice, compared to caveolin 1 negative SCs (Barruet et al. 2020), suggesting again that not only Pax7 expression is a marker for defining SCs engraftment capacity.

1.1.3. Muscle stem cells and the niche

As general knowledge, a specialized microenvironment or niche is critical to sustain the SCs pool maintenance and to regulate stem cell-specific properties (e.g. self-renewal, multi-potentiality and quiescence) (Schofield 1978; Scadden 2006; Arai and Suda 2008).

SCs regulation and maintenance relies on intrinsic mechanisms as well as extrinsic factors that are strongly depending on their specific anatomic microenvironment (Mashinchian et al. 2018; Gonzalez et al. 2020).

The SCs niche (Figure 1.3) is composed of stromal cells (e.g. fibroadipogenic progenitors or FAPs, Pw1+ interstitial cells and resident macrophages), ECM structural elements (e.g. collagens VI and V, laminins, fibronectin, syndecan 3/4) and a complex set of signaling molecules (Evano and Tajbakhsh 2018). Specific receptors that are expressed on the SCs surface allow cell-cell interaction and the communication between the ECM of the basal lamina and the surrounding microenvironment. SCs-niche interplay is necessary in several muscle stem cells states: developmental, perinatal, quiescent and regenerative (Dumont, Wang, and Rudnicki 2015).

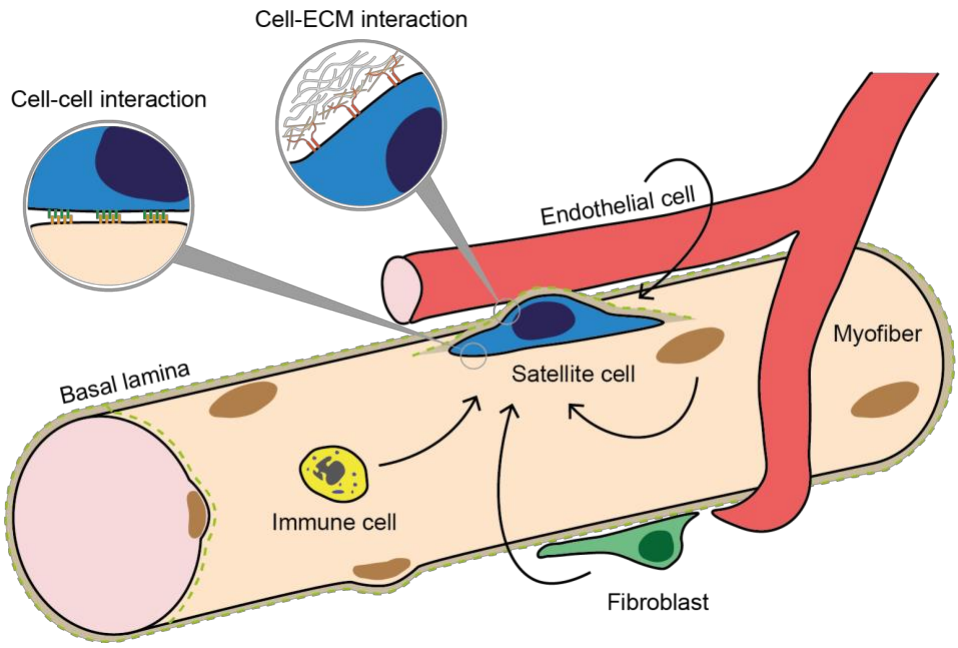

Figure 1.3: The SC in the niche.
SCs are localized in a specialized microenvironment or niche. Cell-matrix and cell-cell interaction are crucial for SCs polarization and asymmetric division. Communication with several other types of cells (e.g. immune cells, fibroblasts, vessel-associated cells) also influence SCs behavior during homeostasis and regeneration (modified from Bentzinger, Wang, von Maltzahn, and Rudnicki (2013)).

Many studies have focused on investigating the contribution of the SCs niche in supporting cell quiescence. Quiescent SCs are characterized by a low cytoplasmic/nuclear volume ratio, a low metabolic activity and mitotic inactivity (Cheung and Rando 2013). SCs in the niche show intimate interaction with basal lamina ECM, polymerized collagens and laminins. The importance of this interaction has been reported in several studies. For instance, Integrin β1 loss induces SCs to quit quiescence and to undergo cell cycle entry (Rozo, Li, and Fan 2016). Laminin α2 deficiency in mouse leads to a dramatic reduction of Pax7+ SCs, to a low number of differentiated myoblasts and therefore failure of fetal myofibers growth (Nunes et al. 2017).

In other studies, the p53 protein was found to regulate SCs balance between differentiation and self-renewal when they are in the niche. When SCs are associated to myofibers, sustained p53 expression during SCs activation inhibits differentiation while promoting quiescence (Flamini et al. 2018). It has also been reported that adult SCs release the ECM component collagen V (COLV) in the niche to maintain quiescence through the interaction with the calcitonin receptor (CALCR) (Baghdadi et al. 2018), demonstrating that SCs themselves have a crucial role in the regulation of the cell-niche interplay.

1.2. Inherited muscular dystrophies (MDs)

The terminology “muscular dystrophy” was introduced in the early 20th century and defined as an inherited “childhood progressive muscle disease” (Tyler and Stephens 1951). Afterward, muscular dystrophies (MDs) were recognized as a group of heterogeneous genetic disorders and distinguished in the following sub-categories: Duchenne muscular dystrophy (DMD) and Becker muscular dystrophy (BMD), limb-girdle muscular dystrophy (LGMD), distal myopathies, congenital muscular dystrophy, facioscapulohumeral muscular dystrophy (FSHD), myotonic dystrophy, Emery-Dreifuss and oculopharyngeal muscular dystrophy (OPMD) (Kang and Griggs 2015; Mercuri and Muntoni 2013). More precisely, MDs are inherited myogenic disorders characterized by progressive muscle wasting and weakness associated with muscle atrophy of variable distribution and severity. The affected muscles can be limb, axial, and facial muscles to a variable degree. The distribution of the skeletal muscle weaknesses helps to distinguish between the different forms of MDs (Figure 1.4) (Emery 2002).

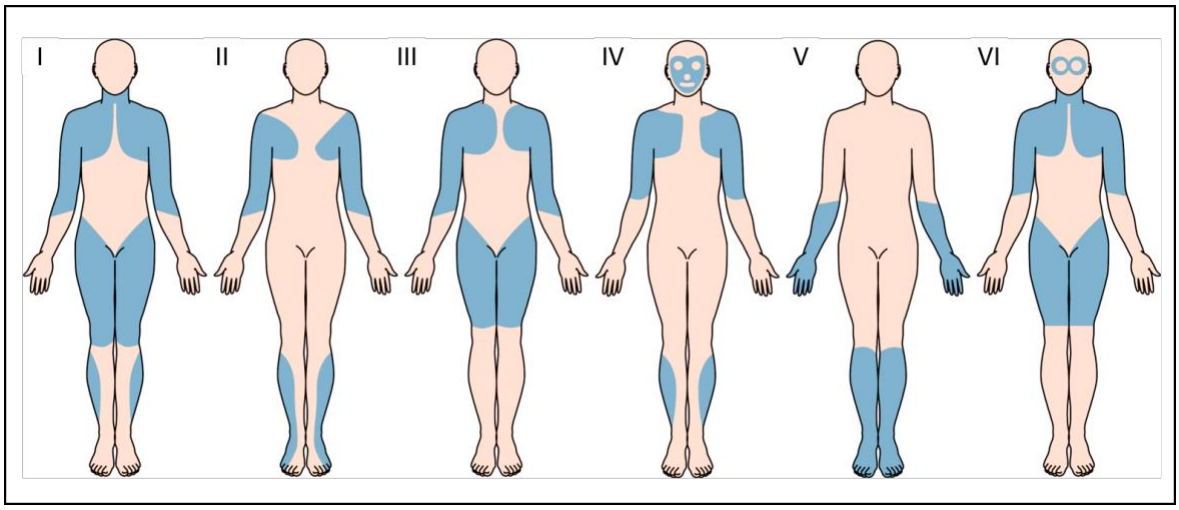

Figure 1.4: Patterns of muscle weakness distribution in different types of MDs.
I) DMD and BMD. **II)** Emery-Dreifuss muscular dystrophy. **III)** LGMD. **IV)** FSHD. **V)** Distal muscular dystrophy. **VI)** OPMD. Blue shading represents affected areas (modified from Mercuri and Muntoni (2013)).

Age of onset, severity and rate of progression, and consequent prognosis, are variable. Childhood-onset dystrophies are associated often to a reduced life-expectancy since the associated cardiac or respiratory muscle weakness (Mercuri and Muntoni 2013).

Whole-exome/genome sequencing and sophisticated bioinformatics strategies permitted to identify numerous genes whose gain-of-function or loss-of-function leads to a dystrophic phenotype, thus enhancing the heterogeneity of these disorders (Kang and Griggs 2015) .

DMD is the most common inherited muscle dystrophy of childhood with an incidence of 1:3500 live born male boys. With disease progression, the patients are forced to wheelchair dependency around 13 years of age and eventually die for respiratory failure in early adulthood. BMD is the milder allelic variant of DMD and has a slightly lower prevalence (Domingos et al. 2017). Both DMD and BMD are caused by mutations of the dystrophin gene (*DMD*) (Hoffman et al. 1987). The majority of mutations affect the reading frame of dystrophin gene leading to the DMD phenotype, while the in-frame mutations cause the milder BMD phenotype. As consequence, dystrophin protein is absent in DMD and partially functional in BMD patients (Monaco et al. 1988; Domingos et al. 2017). The high incidence and severity of DMD have stimulated in the last two decades an enormous research effort to identify new pharmacological and/or gene therapies that has paved the way of new approaches for other genetic muscle disorders.

LGMDs are rare and heterogeneous pathologies, characterized by severe muscle weakness and atrophy of the pelvic and girdle muscles, loss of ambulation and eventually premature death. Classified into dominant and recessive, more than 30 genetic forms are currently recognized. LGMDs are divided into autosomal dominant disorders (type 1) (e.g. LGMD1A, LGMD1B), which are rare and less severe, and autosomal recessive (type 2) disorders (e.g. LGMD2A, and LGMD2B) (Domingos et al. 2017; Emery 2002). Disease onset and progression appear to be variable within each group.

Advances in the definition of the pathophysiology mechanisms, together with the evolution of medical care and new treatment options, have improved the understanding of these disorders and

increased number of clinical trials (Kang and Griggs 2015; Shieh 2015). However, despite all efforts, a cure for muscular dystrophies is not available yet (Shieh 2015).

1.2.1. LGMD type 2B (LGMD2B)

LGMD-causing mutations can be found in a variety of genes encoding proteins associated to different cellular compartments (e.g. membrane-associated, cytosolic, sarcomeric or nuclear envelope) (Table 1.1) (Wicklund and Hilton-Jones 2003; Nigro and Savarese 2014; Domingos et al. 2017).

Name	***Gene***	***Locus***	***Protein***
LGMD 2A	CAPN3	15q15.1	Calpain-3
LGMD 2B	DYSF	2p13.2	Dysferlin
LGMD 2C	SGCG	13q12.12	γ-sarcoglycan
LGMD 2D	SGCA	17q21.33	α-sarcoglycan
LGMD 2E	SGCB	4q12	β-sarcoglycan
LGMD 2F	SGCD	5q33.3	δ-sarcoglycan
LGMD 2G	TCAP	17q12	Telethonin
LGMD 2H	TRIM32	9q33.1	Tripartite Motif containing protein-32
LGMD 2I	FKRP	19q13.32	Fukutin-Related-Protein
LGMD 2K	POMT1	9q34.13	Protein O-Mannosyl Transferase-1
LGMD 2L	ANO5	11p14.3	Anoctamin-5
LGMD 2M	FKTN	9q31.2	Fukutin
LGMD 2N	POMT2	14q24.3	Protein O-Mannosyl Transferase-2
LGMD 2O	POMGnT1	1p34.1	Protein O-Mannose N-acetyl-Glucosaminyl Transferase-1
LGMD 2P	DAG1	3p21	Dystroglycan
LGMD 2Q	PLEC1	8q24.3	Plectin-1
LGMD 2R	DES	2q35	Desmin
LGMD 2S	TRAPPC11	4q35.1	Trafficking-protein-particle-complex-11
LGMD 2T	GMPPB	3p21.31	GDP-mannose-pyrophosphorylase B
LGMD 2U	ISPD	7p21	Isoprenoid synthase
LGMD 2V	GAA	17q25.3	Acid alpha-glucosidase
LGMD 2W	LIMS2	2q14.3	LIM Zinc Finger Domain Containing 2
LGMD 2X	BVES	6q21	Blood vessel epicardial substance
LGMD 2Y	TOR1AIP1	1q25.2	Torsin a-interacting protein 1
LGMD 2Z	POGLUT1	3q13.33	Protein O-glucosyltransferase 1

Table 1.1: Autosomal recessive LGMD type 2 classification.
Modified from Angelini, Giaretta, and Marozzo (2018).

Mutations in the dysferlin (*DYSF*) gene cause a family of LGMD disorders also defined as dysferlinopathies: Miyoshi myopathy with primarily distal weakness (MMD1) (Miyoshi et al. 1986) and LGMD2B with primarily proximal weakness (Liu et al. 1998; Bashir et al. 1998). LGMD2B is an autosomal recessive myopathy reported to be more prevalent in southern than in northern Europe, with a frequency of 15–25% circa within the group of the LGMDs (Argov et al. 2000; Cagliani et al. 2003; Vilchez et al. 2005). Symptoms generally appear in early adulthood and the progression is typically slow but by late stages all limb girdle muscles are affected. In later stages patients are wheelchair bound and need often respiratory assisted ventilation because of diaphragm and thoracic muscle weakness (Nigro and Savarese 2014; Domingos et al. 2017).

In both LGMD2B and MMD1, loss of dysferlin functionality results in impaired myofiber plasma membrane integrity, due to a defective resealing mechanism, and progressive myonecrosis (Han and Campbell 2007). Indeed, defects in membrane repair have been observed in the sarcolemma of dysferlin-deficient muscle fibers (Bansal et al. 2003) and in myotubes of patients affected by dysferlinopathy (Philippi et al. 2015). Myofiber necrosis is the primary cause of inflammatory response in dystrophic muscles. Once triggered, chronic inflammation maintains itself by autocrine/paracrine mechanisms and it is involved in the progressive muscle degeneration and atrophy (Han 2011; Wenzel et al. 2005).

Histologically affected skeletal muscle is characterized by myofiber necrosis, central nucleation, reactive inflammatory infiltrates and progressive connective and adipose tissue replacement (Rosales et al. 2010; Gayathri et al. 2011; Patel, Van Dyke, and Espinoza 2017).

1.2.1.1. The dysferlin gene and protein function in LGMD2B

The *DYSF* gene is localized in chromosome 2p13 and encodes for different transcripts and several splice isoforms (Salani et al. 2004; Pramono et al. 2009). The major transcript found in skeletal muscle (Pramono et al. 2009) corresponds to isoform 8 (RefSeq accession: NM_003494.2). *DYSF* isoform 8 is a 6.3 kb transcript divided into 55 exons, spans 150 kb of genomic DNA and encodes a 2080 amino acid protein (Anderson et al. 1999; Barthelemy et al. 2011; Mercuri and Muntoni 2013). The 230-kDa dysferlin protein, is a large type II transmembrane polypeptide belonging to the ferlin family. In skeletal muscle, dysferlin is localized predominantly at the myofiber plasma membrane, also called sarcolemma (Anderson et al. 1999; Bansal et al. 2003), or in the T-tubules (Ampong et al. 2005; Klinge et al. 2010), which are deep membrane invaginations into the muscle cell. Dysferlin is also expressed in cultured human myoblasts and SCs (De Luna, Gallardo, and Illa 2004; Salani et al. 2004), even if more robustly expressed in *in vitro* differentiated myotubes where it is localized at the sarcolemma and to intracellular membrane compartments (Doherty et al. 2005; Klinge et al. 2010).

Dysferlin contains up to seven C2 domains (C2A to C2G) (Therrien et al. 2006) and it anchors to the membrane by its C-terminal transmembrane domain while the N-terminus of the

protein resides in the cytoplasm (Figure 1.5). The C2 domains are reported to be necessary for Ca^{2+} and/or phospholipids binding (Bansal and Campbell 2004; Klinge et al. 2007).

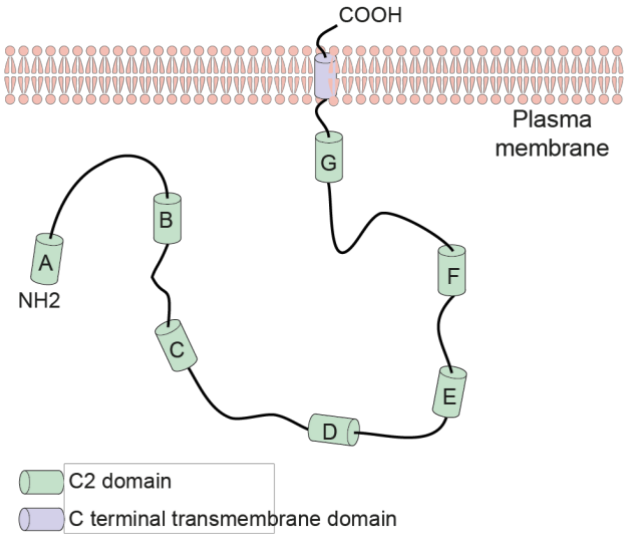

Figure 1.5: Protein structure and topology of dysferlin.
Dysferlin protein includes seven tandem C2 domain (C2A to C2G), anchors to the plasma membrane by its C-terminal transmembrane domain and the N-terminus of the protein is localized in the cytoplasm (modified from Bansal and Campbell (2004)).

Among all C2 domains, only the C2A shows high Ca^{2+} affinity and strongly binds lipids. The rest of the C2 domains shows weaker or rather Ca^{2+}-independent phospholipids binding (Therrien et al. 2009; Abdullah et al. 2014) and not all of them are necessary for the membrane repair process (Therrien et al. 2009; Krahn et al. 2010; Cárdenas et al. 2016).

Dysferlin is responsible for muscle fiber Ca^{2+}-depended plasma membrane repair after micro-injuries (Bansal et al. 2003; Han and Campbell 2007; Han 2011). Such membrane repair process requires fusion of intracellular vesicles at the damage site to form a “membrane patch” through a Ca^{2+}-triggered endocytosis mechanism (McNeil 2002) (Figure 1.6). In infrared laser wounding assays, skeletal muscle plasma membrane failed to be repaired in absence of Ca^{2+} and in dysferlin-null muscle fibers (Bansal et al. 2003; Marg et al. 2012), showing that the Ca^{2+}-dependent membrane repair requires dysferlin. It was then discovered that dysferlin, as Ca^{2+} sensor, regulates vesicle-membrane fusion during this repair process (Han 2011). Indeed, loss of plasma membrane integrity and subsarcolemmal vesicles accumulation have been observed in muscle fibers from dysferlin-deficient mice (Bansal et al. 2003; Hornsey et al. 2013).

Several proteins have been identified as dysferlin partners in sarcolemma repair. For instance, caveolin-3 (Matsuda et al. 2001) and tri-partite motif (TRIM) family protein mitsugumin 53 (MG53) (Matsuda et al. 2001; Cai, Weisleder, et al. 2009) interact with dysferlin and are necessary for sarcolemma healing (Cai, Masumiya, et al. 2009). MG53 facilitates the recruitment of vesicles containing dysferlin to the site of injury in a Ca^{2+} depended manner (Cai, Weisleder, et al. 2009; Matsuda et al. 2001). Dysferlin subsequently promotes vesicles aggregation and fusion, in association with annexins, for the resealing of the membrane (Han 2011) (Figure 1.6). The complete repair of the wound in normal myotubes gives rise to a rigid endo-membrane structure at the injury site, so-called “repair dome”. F-actin, annexin 1, EH-domain containing protein (EHD2) and dysferlin are strongly expressed at the “repair dome” before it is physiologically removed (Marg et al. 2012).

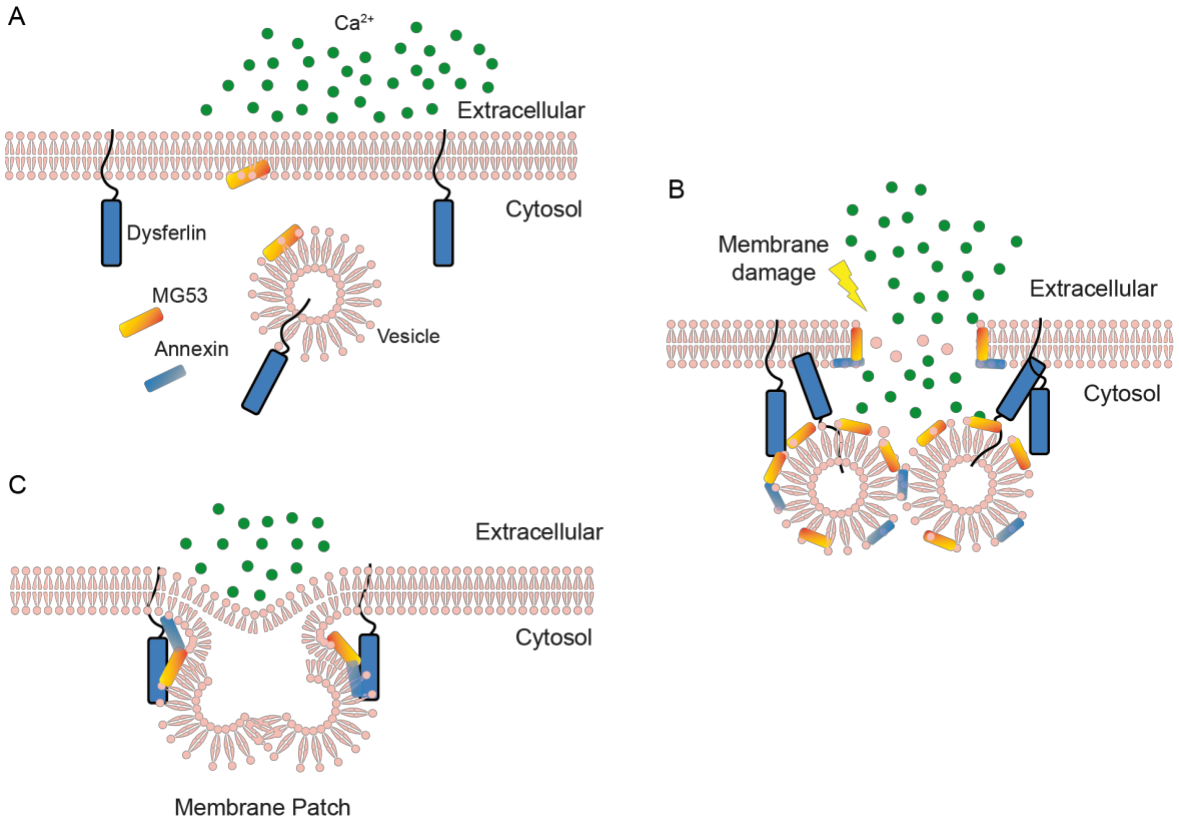

Figure 1.6: Dysferlin participate to the Ca^{2+}-depended plasma membrane repair mechanism.
A) In absence of injury, the protein is localized at the sarcolemma and cytoplasmic vesicles. **B)** Membrane disruption leads to Ca^{2+} influx. In response to high Ca^{2+} level, dysferlin and MG53, supported by annexins, mediate the transportation of membrane repair vesicles towards the damage site. Intracellular vesicles fuse with each other and to the original plasma membrane. **C)** A membrane "patch" is consequently formed and the membrane injury is resealed (modified from Han (2011)).

Besides its role in sarcolemma repair, dysferlin has also been associated with other functions: vesicles trafficking (Azakir et al. 2010), endocytosis, membrane receptor recycling (Demonbreun et al. 2011; Cooper and McNeil 2015) and T-tubules biogenesis (Klinge et al. 2010; Demonbreun et al. 2011; Kerr et al. 2013). Moreover, the roles of dysferlin in adipogenesis and metabolic regulation have been recently considered (Agarwal et al. 2019; Haynes et al. 2019). Indeed, lipid droplets accumulation has been observed in dysferlin-deficient aged mice and within human myofibers from patients affected by dysferlinopathy (Grounds et al. 2014). Progressive replacement of myofibers with adipocytes in dysferlin-deficient tissue was considered as a possible reason (Haynes et al. 2019). However, the implication of dysferlin deficiency in lipid metabolism needs to be better investigated.

1.2.1.2. *DYSF* mutations in LGMD2B

In LGMD2B patients, several *DYSF* disease-causing mutations have been described (Table): missense, nonsense, frameshift deletions/insertions, splicing mutations and large deletions (Table 1.2) (Krahn et al. (2009); Leiden Open Variation Database, last update March 31, 2017).

Since the broad range of genetic defects associated to the *DYSF* gene, no mutations hotspots were found in the context of LGMD2B. However, some founder mutations have been identified as more frequent in specific populations (Weiler et al. 1999; Argov et al. 2000; Cagliani et al. 2003; Leshinsky-Silver et al. 2007).

Natural variant ID	***AA Position(s)***	***Description***
[i]*VAR_057834*	52	W → R in LGMD2B.
[i]*VAR_057835*	67	V → D in MMD1 and LGMD2B; Reduces calcium-sensitive phospholipid binding and interaction with AHNAK and AHNAK2
[i]*VAR_057837*	155	G → R in LGMD2B.
[i]*VAR_024853*	170	A → E in MMD1 and LGMD2B
[i]*VAR_057838*	234	G → E in LGMD2B.
[i]*VAR_057839*	284	I → T in LGMD2B.
[i]*VAR_057840*	299	G → R in LGMD2B and proximodistal myopathy.
[i]*VAR_024859*	555	R → W in LGMD2B and MMD1
[i]*VAR_057851*	618	G → R in MMD1 and LGMD2B.
[i]*VAR_057852*	621	G → R in LGMD2B.
[i]*VAR_057853*	625	D → Y in LGMD2B.
[i]*VAR_057854*	731	P → R in LGMD2B.
[i]*VAR_012308*	791	P → R in MMD1 and LGMD2
[i]*VAR_057856*	930	W → C in LGMD2B; unknown pathological significance.
[i]*VAR_024860*	959	R → W in MMD1 and LGMD2B.
[i]*VAR_024861*	1022	R → Q in LGMD2B; unknown pathological significance.
[i]*VAR_024862*	1038	R → Q in LGMD2B.
[i]*VAR_024865*	1208	I → M in LGMD2B.
[i]*VAR_057860*	1228	L → P in LGMD2B.
[i]*VAR_012309*	1298	I → V in MMD1 and LGMD2B.
[i]*VAR_024868*	1335	E → K in MMD1 and LGMD2B.
[i]*VAR_057862*	1341	L → P in LGMD2B.
[i]*VAR_057864*	1505	Y → C in LGMD2B.
[i]*VAR_057865*	1526	K → T in LGMD2B.
[i]*VAR_057866*	1543	G → D in LGMD2B.
[i]*VAR_057872*	1734	E → G in LGMD2B.
[i]*VAR_057873*	1768	R → W in LGMD2B and proximodistal myopathy; unknown pathological significance.
[i]*VAR_057880*	1970	P → S in LGMD2B.

Table 1.2: Different types of LGMD2B-causing mutations identified.
Modified from https://www.uniprot.org/uniprot/O75923.

As a consequence of nonsense or frameshift *DYSF* mutations, mRNA instability/degradation (Wenzel et al. 2006) and loss of protein expression have been observed. Dysferlin dysfunction has also been related to protein misfolding, aggregation, amyloid formation and premature degradation (Wenzel et al. 2006; Spuler et al. 2008).

1.3. Therapeutic strategy developed for the treatment of MDs

In the last decade, treatment and management of MDs have been drastically improved but no definitive cure is available. The current approaches are indeed limited to the handling of symptoms, to slow-down disease progression and to prevent severe complications (e.g. respiratory failure or cardiomyopathy) (Mercuri and Muntoni 2013) .

Corticosteroid therapies represents the pharmacological standard of care for DMD patients (Griggs et al. 2013), however it is not commonly applied to treat other MDs. Indeed, the efficacy of anti-inflammatory corticosteroids in patients affected by LGMDs is still controversial (Hoffman, Rao, and Pachman 2002; Walter et al. 2013; Domingos et al. 2017). Different approaches to counteract the initiation of inflammation are considered but they are still far from the clinical application (Han 2011). Current efforts are going towards the development of alternative therapies aiming to directly correct the pathology of the disease (Barthelemy et al. 2011).

1.3.1. Gene therapy approaches

Gene replacement is probably the most direct way to treat monogenetic, recessive diseases with a known genetic cause. Adeno-associated virus (AAV)-based muscle specific delivery of truncated forms of the dystrophin gene, like mini-dystrophin (Wang, Li, and Xiao 2000) or micro-dystrophin (Harper et al. 2002; Gregorevic et al. 2008) has been successful in ameliorating the disease phenotype in both mouse and canine models of DMD (Watchko et al. 2002; Le Guiner et al. 2017; Shin et al. 2013; Duan 2018; Ramos et al. 2019). Currently, there are several on-going clinical trials using different variants of micro-dystrophin and showing encouraging results (Pfizer, NCT03362502; Sarepta Therapeutics, NTC03375164; Solid Biosiences IGNITE DMD, NTC03368742) (Crudele and Chamberlain 2019; Mendell et al. 2019). Approaches based on gene replacement through AAV delivery have been explored for dysferlinopathy (Grose et al. 2012; Lostal et al. 2012; Sondergaard et al. 2015) α/ß-sarcoglycanopaty (Mendell et al. 2019) and other types of LGMDs (Crudele and Chamberlain 2019). However, limitations of AAV packaging size (Dong, Fan, and Frizzell 1996), unwanted immune responses (against AAV vector or the newly expressed transgene) (Shayakhmetov, Di Paolo, and Mossman 2010; Mendell et al. 2010; Martino et al. 2011; Mingozzi and High 2013) and questionable improvement of the muscle function are still unsolved challenges.

Exon skipping-based therapy has been applied for the treatment of several MDs forms, including DMD, BMD and LGMDs (Aartsma-Rus et al. 2003; Aartsma-Rus et al. 2010; Aoki et al. 2013; Wyatt et al. 2018). This approach is based on short antisense oligonucleotides

(ASOs) which hybridize to pre-mRNA target sequences altering exons splicing. The skipping of one or more exons in a mutated gene can induce re-framing of the coding sequence and the synthesis of a truncated but still functional protein (Matsuo et al. 1991; Dunckley et al. 1998; Aartsma-Rus et al. 2002). A morpholino ASO (a.k.a. eteplirsen), developed by Sarepta Therapeutics, is currently used to skip out exon 51 and restore ~13% of the functional protein when intravenously infused in DMD patients (Stein 2016; Lim, Maruyama, and Yokota 2017). Exon 32 skipping efficiency was also tested to correct *DYSF* mutations. Dysferlin function was partially rescued in treated LGMD2B patient-derived myoblasts (Barthelemy et al. 2015). Also, U7 small nuclear RNA-encoded antisense RNAs have been tested as alternative to the DNA-analogue based ASOs and proved successfully in skipping exons 37 and 38 when delivered in a mouse model for dysferlinopathy (Malcher et al. 2018).

Exon-skipping, as well as other currently developing gene editing approaches, can be also achieved using the Clustered Regularly Interspersed Short Palindromic Repeats (CRISPR)/CRISPR-associated (Cas) systems (Crudele and Chamberlain 2019). The CRISPR/Cas systems, first identified as defensive immune response in prokaryotic organisms (Ishino et al. 1987; Makarova et al. 2015), induce DNA cleavages at specific target sites defined by guide RNAs and have been applied for genome engineering in the context of different monogenic diseases (Jinek et al. 2012; Cong et al. 2013; Mali et al. 2013; Pickar-Oliver and Gersbach 2019). For instance, CRISPR/Cas9-based editing has been tested *in vivo* in a canine model bringing an exon 50 deletion in the *DMD* gene. A single cut at the exon 51 splice acceptor site of the *DMD* gene induced skipping and splicing from exon 49 to 52 which restored the open reading frame of the gene (Amoasii et al. 2018). Other CRISPR/Cas9 approaches for gene correction are currently explored and they will be discussed further ahead (see section 1.4.1.).

1.3.2. Cell replacement therapy approaches

Damage and degeneration of muscle fibers are physiologically followed by SCs-mediated regeneration process (Collins et al. 2005; Tedesco et al. 2010; Wang and Rudnicki 2011). In pathological conditions (e.g. MDs), mutated SCs regenerate muscle fibers that will carry the genetic defect. Moreover, repeated cycles of muscle degeneration/regeneration lead to stem cells pool exhaustion and loss of regenerative capability, exacerbating the disease pathology (Wallace and McNally 2009; Goldstein and McNally 2010; Negroni et al. 2015).

With the aim of restoring the structural integrity of the muscle tissue, correcting and replenishing the SCs pool, different cell-based approaches have been investigated as long-term treatments for MDs. The general strategy is based on transplantation of healthy or genetically corrected myogenic cells that have been isolated from donor or patients. Once engrafted, cells can contribute to muscle regeneration and tissue repair (Skuk et al. 2006; Skuk, Goulet, Roy, Piette, Cote, et al. 2007; Negroni et al. 2015). For this purpose, different sources of both muscle and non-muscle-derived myogenic cells have been considered.

1.3.2.1. SCs-derived muscle progenitors

Since SCs have a fundamental role in muscle repair, regeneration and commitment to the myogenic lineage (Collins et al. 2005; Tedesco et al. 2010; Wang and Rudnicki 2011), they have been explored first as promising candidates in heterologous cell transplantation.

Pioneer experiments demonstrated that intramuscular (i.m.) injection of healthy murine SCs-derived myoblasts into DMD animal models (i.e. *mdx* mice that have a spontaneous nonsense mutation in *DMD* exon 23 and a complete absence of the protein) can contribute to muscle repair, repopulate the SCs compartment and restore the expression of the dystrophin in newly generated fibers (Partridge et al. 1989; Kinoshita et al. 1994; Montarras et al. 2005). The first clinical trials using donor-derived healthy myoblasts in DMD patients produced poor results showing only 10% of newly generated donor-derived dystrophin fibers and no improvement in muscle functionality (Mendell et al. 1995). Despite that, those first studies demonstrated the overall safety of the transplantation procedure if an immunosuppression protocol was applied (Tremblay et al. 1993). Few years later, a phase IA clinical trial using different cell delivery conditions (e.g. high density injections), which were previously tested on non-human primate models (Skuk et al. 2002), started. The aim was to overcome challenges like poor cell survival, low migration from the injection site and unexpected immune responses (Guérette et al. 1994; Fan et al. 1996; Guérette et al. 1997). The new protocol led to a significant increase in the engraftment efficiency with a 34.5% of myofibers expressing donor-derived dystrophin at the injection sites (Skuk, Goulet, Roy, Piette, Cote, et al. 2007), but it failed to provide clinical improvement. Additional studies in non-human primates have been used to further evaluate the effect of needle size, cell number and injection volume in transplantation efficiency (Skuk, Goulet, and Tremblay 2014). To date, an on-going clinical trial is evaluating safety and efficiency of high-density myoblasts injection in the muscle of DMD patients (ClinicalTrials.gov: NCT02196467).

Since SCs are not able to transverse the blood vessels, they cannot be delivery in other ways than i.m. injection (Briggs and Morgan 2013). Indeed, local delivery in accessible muscles is the only current application of myoblasts. A recent clinical trial has reported encouraging results when autologous healthy myoblasts were locally administrated in patients affected by OPMD (OMIM 164300; Périé et al. (2014)). Autologous setting, local cell delivery and limited size of the affected muscle were most likely related to the positive clinical outcome of this study.

Other experimental strategies involve the *ex vivo* genetic manipulation of autologous donor myoblast prior to transplantation. First attempts to genetically correct SCs-derived myoblasts have been made for the treatment of DMD using viral-based methods. Moisset et al. showed that expression of a *DMD* minigene construct by adenovirus infection of myoblasts restored functional dystrophin expression after xenograft (Moisset et al. 1998). In other studies, introduction of full length-*DMD* was achieved via adeno/AAVs vectors (Floyd et al. 1998; Gonçalves et al. 2006). To avoid the limitation of AAV packaging size, Tedesco et al. proved that SCs transduced with a human artificial chromosome (HAC) containing the *DMD* locus ameliorate the disease phenotype when transplanted in a DMD mouse model (Tedesco et al. 2011). In addition, lentiviral-based exon

skipping has been tested to rescue the expression of a so-called “quasi-dystrophin” in patient-derived myoblasts (Quenneville et al. 2007).

Autologous transplantation can overcome the limitation of immune reactions against the donor cells that are used for heterologous transplantation (Guérette et al. 1994). However, the impact of unwanted immune responses towards the vectors (e.g. AAVs) and the therapeutic gene is still discussed (Shayakhmetov, Di Paolo, and Mossman 2010; Mendell et al. 2010; Martino et al. 2011; Mingozzi and High 2013).

In heterologous or autologous transplantation approaches one of the main challenges is to obtain a large number of SCs-derived myoblasts that have the potential to both self-renew and differentiate after engraftment (Charville et al. 2015). In human muscle SCs are 2-5% of the total nuclei (Allbrook, Han, and Hellmuth 1971); Bischoff, et al. 1994). Since the contribution of SCs to muscle regeneration correlates also with the number of transplanted cells (Sacco et al. 2008), *ex vivo* expansion of human SCs is necessary for clinical application (Negroni et al. 2015; Xu et al. 2015). When isolated, SCs are cultured out of their niche in a non-physiological condition and they spontaneously activate and proliferate as committed myoblasts, which show a lower regenerative potential upon extensive proliferation. Indeed, *in vitro* expansion of freshly isolated mouse (Montarras et al. 2005), canine (Parker et al. 2012) and human SCs (Cooper et al. 2003; Brimah et al. 2004) reduces their stemness and contribution to muscle regeneration *in vivo.* Moreover, myoblasts derived from dystrophic patients in most of the case exhibit lower proliferation and regenerating capability, making difficult to apply genetic manipulation *ex vivo* without losing their engraftment efficiency (Wallace and McNally 2009; Goldstein and McNally 2010; Negroni et al. 2015). For this reason, several studies have focused on improving culture condition to preserve myoblasts regenerative potential for cell-therapy (Briggs and Morgan 2013).

SCs isolation procedures significantly influence their biology and have an impact on their efficiency in regeneration. Indeed, during the initial step of cell isolation via enzymatic digestion, SCs undergo many biochemical changes and their molecular profile quickly changes in comparison with the one of quiescent cells in the *in vivo* niche (Machado et al. 2017). In a different isolation method, myogenic cells are overgrown from single human muscle fibers and unwanted non-myogenic cells (e.g. fibroblasts) are negatively selected using hypodermic treatment). In these conditions, the basal lamina of SCs niche is preserved and they are expanded in a more physiological condition. Direct transplantation of human muscle fibers into irradiated muscle of NOG mice showed robust engraftment and contribution to muscle fibers formation (Marg et al. 2014).

Cell replacement efficacy can be also influenced by SCs and myoblasts heterogeneity (Kuang and Rudnicki 2008). As already mentioned, single cell sequencing experiments showed that the pool of isolated SCs includes genetically and functionally different sub-population of cells (Barruet et al. 2020; Charville et al. 2015; Cho and Doles 2017; Marg et al. 2019). Currently, the efficiency of SCs distinct populations in regeneration after engraftment is investigated (see section 1.1.4.). Elucidating which sub-populations exhibit the best regenerative potential and how to isolate them is crucial for improving cell-therapy approaches in MDs.

1.3.2.2. Non-muscle-derived cells

Multipotent precursor cells like CD133 positive (CD133+) hematopoietic cells (Torrente et al. 2004) and mesoangioblasts (MABs) or pericytes (Dellavalle et al. 2007) have shown to be myogenic when intramuscularly or systematically injected in dystrophic hosts (Tedesco et al. 2010). Human CD133+ (hCD133+) cells can be obtained from both peripheral blood and skeletal muscle, proliferate and differentiate *in vitro*. As reported, hCD133+ that are intramuscularly injected in immunodeficient *mdx* mice can efficiently participate in muscle regeneration and generate fibers that are positive for human markers (lamin A/C and spectrin). Moreover, they colonize the SCs niche and express Pax7 (Meng et al. 2014). The safety of CD133+ cells when autonomously transplanted in DMD patients' muscle has been evaluated and confirmed in a phase I clinical trial (Torrente et al. 2007). However, as recently observed, the contribution to muscle regeneration of CD133+ derived from DMD patients is inferior compared to the healthy counterpart (Meng, Muntoni, and Morgan 2018), thus discouraging their use in autologous treatments. Moreover, their myogenic potential is drastically reduced after amplification in culture, as also observed in myoblasts, and the *in vitro* conditions needs to be further defined (Meng et al. 2014).

MABs are mesodermal progenitors isolated for the first time in 1999 (De Angelis et al. 1999) and well characterized in animal models (Sampaolesi et al. 2003; Sampaolesi, Blot, and D'Antona 2006) and humans (Dellavalle et al. 2007; Minasi et al. 2002). *In vitro,* human MABs efficiently proliferate and can spontaneously differentiate into MYHC positive myotubes. MABs ability to cross the vessel wall and to reach muscle tissue via systemic delivery, is an advantage in cell-therapy for MDs. Indeed, when systematically injected in immunodepressed *mdx* mice, they migrate into the muscle, regenerate dystrophin expressing fibers and re-colonized the SCs niche (Dellavalle et al. 2007). In addition, gene corrected patient-derived MABs have been proved to improve muscle function of DMD animal models (e.g. mice and dogs) (Sampaolesi, Blot, and D'Antona 2006; Dellavalle et al. 2007). Based on these results, a first clinical trial for the treatment of DMD patients started in 2015 (https://www.clinicaltrialsregister.eu; EudraCT, 2011-000176-33). This study demonstrated the safety of MABs when transplanted in patients, but the clinical outcome was not successful as the one obtained in animal models (Cossu et al. 2015).

1.3.2.3. Induced pluripotent stem cells

Human induced pluripotent stem cells (hiPSCs) have a limitless self-renewal capacity and can in theory differentiate into all types of cells in the human body (Thomson et al. 1998). hiPSCs can be obtained from different somatic cell types (e.g. fibroblasts of the skin or muscle), genetically manipulated, differentiated *in vitro* into muscle progenitor cells and used for autologous transplantation (Kazuki et al. 2010; Goudenege et al. 2012). Currently, several differentiation protocols have been applied aiming to obtain the best efficiency in muscle engraftment and regeneration (Tedesco et al. 2012; Darabi et al. 2012; Shelton et al. 2014; Chal et al. 2015; Ortiz-Vitali and Darabi 2019). CRISPR/Cas9-based methods have been successfully used in patient-

derived hiPSCs to correct several MD-causing mutations, including dysferlinopathies (Turan et al. 2016). In addition, several studies proved that i.m. transplantation of corrected hiPSCs-derived muscle progenitors can generate fibers expressing dystrophin and α-sarcoglycan in immunosuppressed mouse models of DMD and LGMD2D respectively (Tedesco et al. 2012; Young et al. 2016; Hicks et al. 2018). The improvements in using hiPSCs for cell-therapy are encouraging, however their karyotype instability and their teratogenic potential after differentiation are still unsolved safety issues (Hicks et al. 2018).

1.3.3. Therapeutic strategies and current clinical trials for LGMD2B

Up to date, no cure for LGMD2B exists (Barthelemy et al. 2011). As previously mentioned, strong inflammatory responses play a significant role in the pathology of the disease (Han 2011). In a clinical trial from 2003 (Table 1.3; ClinicalTrials.gov: NCT00527228), deflazacort, a glucocorticoid used as an anti-inflammatory and immunosuppressant, was tested in patients affected by dysferlinopathies. The treatment was unfortunately not effective and the authors concluded that steroids should be avoided in these pathologies (Walter et al. 2013). An increase of muscle strength was observed in dysferlinopathy patients treated with Rituximab™, a monoclonal antibody directed against CD20 positive B cells, suggesting that B cells have a role in the pathophysiology of the disease (Lerario et al. 2010). Resolaris (or ATYR1940) is an intravenous protein therapy being developed by aTyr Pharma Inc. to treat FSHD and LGMD2B (Table 1.3; ClinicalTrials.gov: NCT02579239). Resolaris acts to reduce the excessive innate and adaptive immune response involved in the disease pathology and first outcomes showed that it is safe and well-tolerated (Lo et al. 2014; Zhou et al. 2014). Further results of the clinical trial are not available yet.

Cell transplantation approaches have been investigated using both myoblasts and MABs. Leriche-Guerin et al. showed first that human healthy myoblasts transplanted into SCID mice induce formation of dysferlin positive fibers in ~40% of the analyzed muscles. Protein expression was rescued by transplantation of healthy mouse myoblasts in a mouse model for both LGMD2B and MMD1 (Leriche-Guérin et al. 2002). Few years later, Manera JD at al. demonstrated that, wild-type (WT) mouse MABs intramuscularly or systemically delivered to dysferlin-deficient mice, fuse with the host muscle fibers and restore dysferlin protein level to ~20% of WT. Dysferlin positive fibers also rescued their function in membrane resealing. However, no significant improvement in muscle function was observed in the treated mice (Díaz-Manera et al. 2010).

Gene therapy treatments aim to restore dysferlin expression in dystrophic muscles. Full length *DYSF* DNA was successfully delivered into dysferlin-deficient immortalized myoblasts using *Sleeping Beauty* Transposase. The engineered cells were transplanted in immunocompromised dysferlin-deficient mice and gave rise to dysferlin expressing myofibers (Escobar et al. 2016). Antisense-mediated exon skipping has also been proposed. A modest reconstitution of dysferlin expression was reported in a dysferlin-deficient mouse model (Malcher et al. 2018) or patient myoblasts (Dominov et al. 2014; Barthelemy et al. 2015; Lee et al. 2018). Some of these studies

also demonstrated the rescue of the plasma membrane resealing function in corrected myotubes via membrane-wounding assay (Barthelemy et al. 2015; Malcher et al. 2018; Lee et al. 2018).

In the last years, it has been proved that a dual AAV system can be used to express a full length *DYSF* and restore the protein expression and the muscle function in mouse and primates models of dysferlinopathy (Grose et al. 2012; Sondergaard et al. 2015). Based on these findings, in 2016 a phase I clinical trial started with the aim to test recombinant AAVs (arAAVrh74.MHCK7.DYSF.DV) carrying dysferlin transgene under the control of a skeletal and cardiac muscle-specific promoter (MHCK7) to treat dysferlinopathies (Table 1.3; ClinicalTrials.gov: NCT02710500). The study was completed in July 2019 but the outcome details are still not publicly available.

Clinical Trial name	***Date***	***Status***	***References***
Deflazacort in Dysferlinopathies (NCT00527228)	2003/2008	Completed	(Walter et al. 2013)
The Safety and Biological Activity of ATYR1940 in Patients With Limb Girdle or Facioscapulohumeral Muscular Dystrophies (NCT02579239)	2015/2017	Completed	https://clinicaltrials.gov/ct2/show/NCT02579239?recrs=abdefghim&cond=LGMD2B&draw=2&rank=3
Clinical Outcome Study for Dysferlinopathy (NCT01676077)	2012/2018	Unknown	(Moore et al. 2018) (Diaz-Manera et al. 2018) (Moore et al. 2019)
rAAVrh74.MHCK7.DYSF.DV for Treatment of Dysferlinopathies (NCT02710500)	2016/2020	Completed	(Grose et al. 2012) (Sondergaard et al. 2015)

Table 1.3: Current clinical trials in Dysferlinopathies.
Each study is specified by its ClinicalTrials.gov identifier NCT number that is indicated in the table. Modified from: www.clinicaltrials.gov.

Together with the development of clinical strategies, a better understanding of the pathogenic mechanisms and disease progression of LGMD2B is required to identify novel therapeutic approaches and clinical trial possibilities. A natural history study (Clinical Outcome Study for Dysferlinopathy) started in 2012 from the collaboration of different institutes in Europe, USA, Japan and Australia (Table 1.3; ClinicalTrials.gov: NCT01676077). The aim is to collect biological samples for the identification of new disease markers, to study the disease progression and determine clinical outcome measures required for future trials.

1.4. CRISPR/Cas systems: from bacterial adaptive immunity to molecular tools for genome editing

CRISPR/Cas systems were initially discovered as an RNA-mediated adaptive immune response of bacteria and archaea against phage infections (Mojica et al. 2005; Labrie, Samson, and Moineau 2010; Makarova et al. 2015) enabling the host to respond to and eliminate foreign genetic material. Cas proteins are the main players of the CRISPR-Cas response (Makarova et al. 2006) and they are encoded by genes flanking the CRISPR array (Jansen et al. 2002). CRISPR/Cas-mediated immunity follows three steps. Upon first viral infection, short fragments of invasive DNA (a.k.a. protospacer) are integrated in the CRISPR array locus of the host genome as complementary sequences (a.k.a spacer). This step is also known as spacer acquisition phase (Ishino et al. 1987; Jansen et al. 2002; Kunin, Sorek, and Hugenholtz 2007). The selection of new protospacer sequences depends on the presence of a 2-5 nucleotide sequence, so-called protospacer adjacent motif (PAM), located next to the protospacer sequence. CRISPR repeat-spacer elements are then transcribed into a CRISPR RNAs (crRNAs) sequence (a.k.a. biogenesis phase), containing a conserved fragment and a variable spacer sequence (guide) complementary to the viral nucleic acid. crRNAs combine with Cas effector proteins to form a complex that recognizes the phage genome (or plasmid) harboring a target sequence complementarity to the crRNA guide and induces sequence-specific cleavage via nuclease activity. This last step prevents the propagation of viral genome and it is known as interference phase (van der Oost et al. 2009; Makarova et al. 2011). crRNA-dependent detection and destruction of foreign DNA rely on the PAM sequence to avoid self-targeting at the complementary endogenous spacer in the CRISPR array (Figure 1.7) (Sternberg et al. 2014).

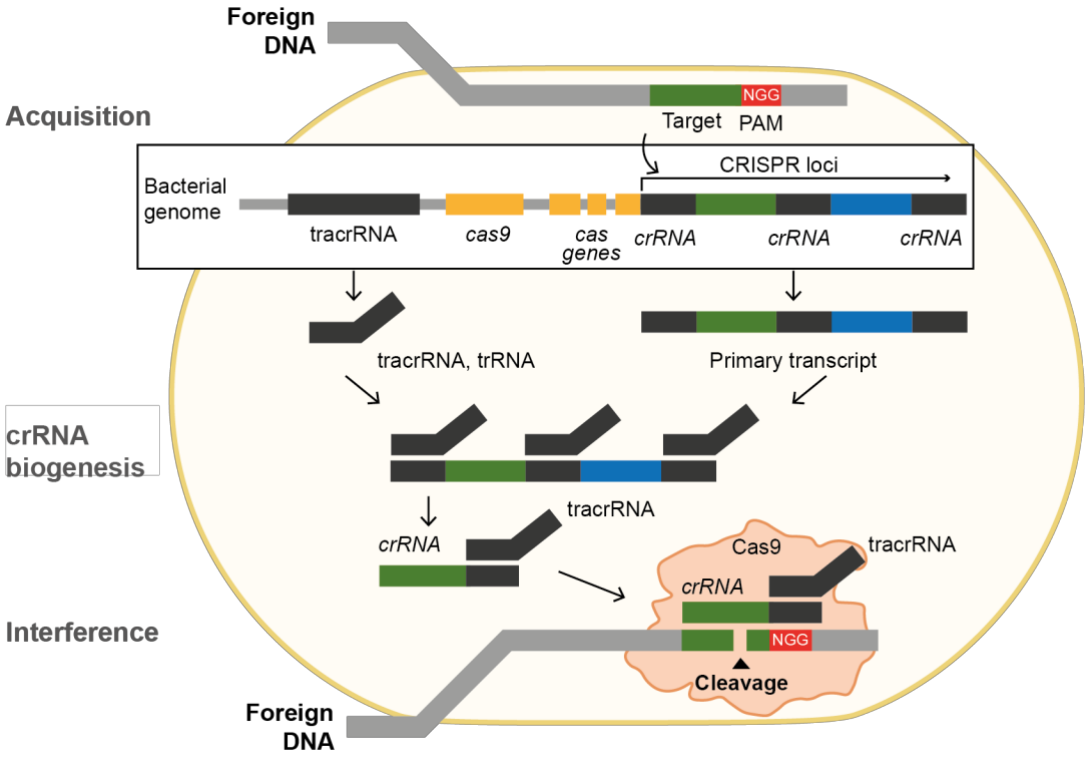

Figure 1.7: CRISPR/Cas adaptive immune response.
CRISPR/Cas9-mediated immune response comprises 3 consecutive phases. Acquisition phase: foreign DNA (protospacer) is integrated into the bacterial CRISPR locus as a new spacer. Biogenesis phase: the repeat spacer element in the CRISPR locus is transcribed and processed into crRNA. Interference phase: Cas9 endonuclease, complexed with a crRNA and tracrRNA, cleaves foreign DNA containing a 20-nucleotide sequence complementary to the crRNA and adjacent to a PAM sequence (modified from https://international.neb.com).

According to the *Cas* genes involved in the process, CRISPR/Cas systems can be classified in six types (I, II, III, IV, V, VI) (Makarova et al. 2011; Makarova et al. 2015). The most extensively studied is type II, in which *Cas1* and *Cas2* genes are the minimum requirements for the viral DNA integration into the CRISPR array, while *Cas9* is necessary for the interference phase. Cas9 is an endonuclease effector protein that, in order to mediate foreign DNA cleavage, must be complexed with both a crRNA and a so-called trans-activating crRNA (tracrRNA or trRNA), that is partially complementary to the crRNA and acts as a scaffold to promote the formation of the Cas9/crRNA complex (Sternberg et al. 2014; Shmakov et al. 2015).

Streptococcus pyogenes Cas9 (SpCas9) belongs to the type II CRISPR-Cas systems and was the first Cas protein to be engineered to specifically target DNA sites in mammalian cells (Figure 1.8) (Cong et al. 2013; Mali et al. 2013). PAM recognized by SpCas9 consists of the 5′-NGG (N represents any nucleotide) consensus sequence located downstream the protospacer (Deltcheva et al. 2011). The tracrRNA::crRNA required for Cas9 site-specific cleavage of the viral genome has been engineered as a single guide RNA (sgRNA). The sgRNA displays two critical features: a specific sequence that defines the DNA target of interest by complementarity and a duplex RNA structure that binds to Cas9 (Jinek et al. 2012). PAM recognition of the Cas9/sgRNA complex (at the 3‘of the target sequence) allows Cas9 conformational changes and target binding

(Figure 1.8) (Jinek et al. 2012; Jinek et al. 2014; Nishimasu et al. 2014). Afterward, the Cas9 HNH and RuvC/RNaseH-like endonuclease domains induce the cleavage of both DNA strands three nucleotides upstream of the PAM sequence (Jinek et al. 2014; Nishimasu et al. 2014; Anders et al. 2014).

The HNH domain cleaves the complementary strand, while the RuvC domain cleaves the non-complementary PAM-containing strand (Gasiunas et al. 2012; Jinek et al. 2012). Thus, sgRNA-mediated Cas9 binding to its DNA target results in the generation of a blunt DNA double-strand break (DSB) (Gasiunas et al. 2012; Jinek et al. 2012) or occasionally a staggered-end DBS resulting in 5´ one N overhangs (Zuo and Liu 2016; Gisler et al. 2019).

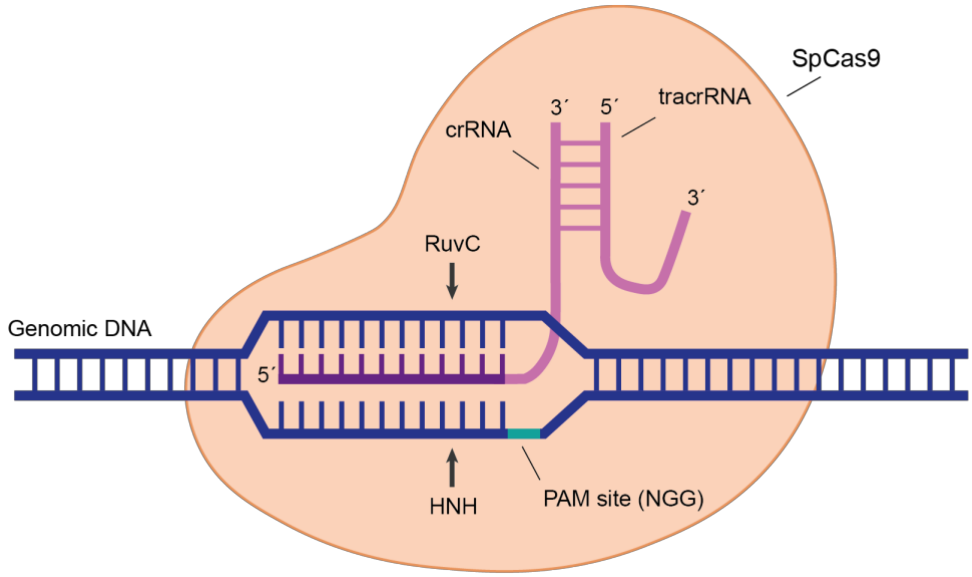

Figure 1.8: CRISPR/Cas9 complex cutting a double strand DNA (dsDNA).
SpCas9 proteins use an RNA guide to specifically target genomic DNA. In engineered CRISPR/Cas9 systems, SpCas9 forms a ribonucleotide complex with the backbone of the sgRNA. A portion of the sgRNA is complementary to a DNA target sequence positioned next to a 5´ PAM. RuvC/RNaseH-like and HNH endonuclease domains induce DSBs of DNA upstream of the PAM.

In 2012, Emmanuelle Charpentier and Jennifer Doudna first realized the potential of type II CRISPR nuclease and harnessed it for developing precise genome-targeting/editing technologies (Jinek et al. 2012). For the invention of this extremely powerful tool, they have been awarded the Nobel Prize in Chemistry in October 2020. In the last years, CRISPR/Cas systems have been intensively applied in both research and therapeutics (Pickar-Oliver and Gersbach 2019).

1.4.1. CRISPR/Cas9-based genome editing

Only few months after the functional characterization of Cas9 (Jinek et al. 2012), more than one study proved that Cas9/sgRNA complex can be used to specifically edit the genomes of human cells (Cong et al. 2013; Mali et al. 2013; Cho et al. 2013; Jinek et al. 2013). The application of CRISPR/Cas9 systems in gene editing is superior in convenience and versatility compared to

previous technologies (e.g. ZFN, Zinc Finger Nuclease and TALEN, Transcription Activator-Like Effector Nucleases). CRISPR/Cas9 is easy to design and more affordable. Its specificity can be programmed by changing the sequence of the sgRNA for any target DNA sequence of interest.

CRISPR/Cas9 has been used in genetic studies (e.g. high-throughput loss-of-function screenings) (Shalem et al. 2014; Koike-Yusa et al. 2014; Hart et al. 2015), for disease modelling (Wang et al. 2013; Platt et al. 2014; Paquet et al. 2016) and as new therapeutic approach for a large number of diseases (Jacinto, Link, and Ferreira 2020). Great achievements have been made in the treatment of diseases like cystic fibrosis (Schwank et al. 2013; Bellec et al. 2015; Maule et al. 2019), DMD (Long et al. 2014; Li et al. 2015; Moretti et al. 2020; Zhang, Li, et al. 2020), β-thalassemia (Xie et al. 2014; Song et al. 2015; Gabr et al. 2020) and Sickle cell disease (Frangoul et al. 2020).

Classical CRISPR/Cas9-based genome editing involves first the DNA cleavage and then a second step of DNA repair. In eukaryotes, the induced DSB triggers DNA repair through intrinsic cellular pathways, such as homology-directed repair (HDR) or non-homologous end joining (NHEJ) (Figure 1.9) (Doudna and Charpentier 2014). HDR is considered an error-free pathway and can be used to generate a precise replacement of the sequence at the DSB site through homologous recombination (Rong and Golic 2000). This process relies on DNA templates like sister chromatids or exogenously provided templates. HDR is restricted in S and G2 phases of the cell cycle since a sister chromatid is available only after DNA replication (Rudin, Sugarman, and Haber 1989; Zhao et al. 2017). When Cas9 delivery is combined with a donor DNA, HDR induces sequence substitutions or insertion of the designed nucleotide sequence into a targeted site. HDR is the pathway of choice for installing precise edits for gene correction (Paquet et al. 2016), however, since it is limited in dividing cells, it is not always possible to rely on it. Therefore, HDR-independent strategies need to be developed (Chu et al. 2015; Maruyama et al. 2015; Nami et al. 2018).

The NHEJ pathway is a template-independent and error-prone mechanism. It is a fast and flexible mechanism, which is more predominant compared to HDR since it is not restricted to cycling cells. In most cases, its efficiency can be nearly 90% (Mao et al. 2008; Lieber 2010). After Cas9-induced DSBs, NHEJ repair results in random N insertion or deletion (a.k.a. indels) at the cleavage site (Hilton and Gersbach 2015). Indel formation can lead to gene knockout if it disrupts the reading frame, usually by introducing a premature stop codon (Figure 1.9) (Hsu, Lander, and Zhang 2014).

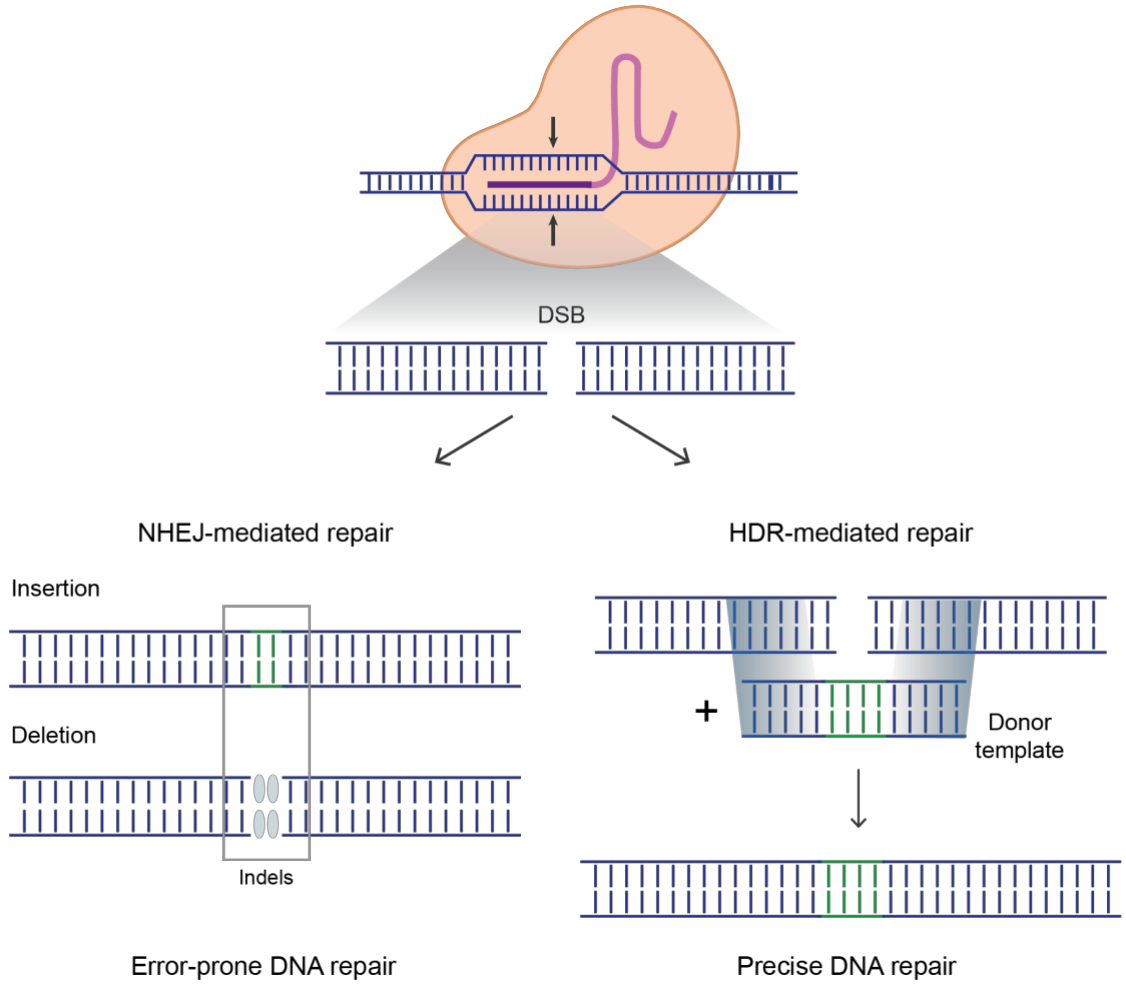

Figure 1.9: DNA repair mechanisms following Cas9-induced DSBs.
CRISPR/Cas9-induced DSBs result in DNA repair by NHEJ or HDR. The error-prone NHEJ leads to indels, enabling gene knockout. On the contrary, HDR can be used to install precise edits by providing either a double-stranded or a single-stranded oligodeoxynucleotide donor template that contains homology arms (light blue rectangles) to the cleaved target site (modified from Yang and Huang (2019)).

Cas9-induced NHEJ has also been proposed as therapeutic strategy for diseases caused by frameshift mutations, where the reading frame of the gene is disrupted (Amoasii et al. 2017; Takashima et al. 2019). For example, Kocher et al. showed that a frameshift mutation in the collagen type VII α1 chain gene (*COL7A1*), that causes Dystrophic Epidermolysis Bullosa, can be corrected with a precise single adenine insertion induced by CRISPR/Cas9-induced NHEJ. After editing, affected keratinocytes show a reframing efficiency of ~75% (Kocher et al. 2020).

A drawback of CRISPR/Cas9 systems is that Cas9 can cleave off-target sites as a result of an incorrect complementarity between the DNA sequence and the sgRNA (Fu et al. 2013; Kuscu et al. 2014). Off-target events may cause pathogenic mutations and make CRISPR/Cas9 unsafe for clinical applications. For this reason, great efforts have been made to develop more precise methods to detect on- and off-target mutations (Kuscu et al. 2014; Kim et al. 2015; Tsai et al. 2015; Akcakaya et al. 2018), as well as to enhance Cas9 protein specificity. SpCas9 nucleases have been engineered to obtain variants with an increased target specificity, so to reduce off-target cleavage (Ishida, Gee, and Hotta 2015; Slaymaker et al. 2016). The enhanced-specificity SpCas9

(eSpCas9) proteins (Slaymaker et al. 2016) have been generated by mutating positively-charged residues responsible for the high Cas9 binding affinity to the DNA backbone, thus reducing cleavage activity at off-target sites. The same principle was applied for the generation of SpCas9-HF1 (for high-fidelity variant number 1) (Kleinstiver et al. 2016).

1.4.1.1. *In vivo* and *ex vivo* CRISPR/Cas9-based genome editing for correction of MD-causing mutations

Since MDs can be correlated with a specific mutation, CRISPR/Cas9-mediated gene therapy was explored as possible treatment. Recently, several studies have also combined CRISPR/Cas9-based genome editing with cell-therapy for allogeneic transplantation. *Ex vivo* corrected myogenic cells could ideally replace dystrophic muscle for a long-term therapeutic effect (Sun et al. 2020).

In the context of MDs, *in vivo* gene editing was first reported in the *mdx* mouse model by Taberdbar et al. in 2016. The authors demonstrated that the AAV-mediated delivery of Cas9 with two sgRNAs flanking the mutated exon 23 resulted in its excision and consequent rescue of dystrophin expression in dystrophic muscles (Tabebordbar et al. 2016). In other studies, humanized mouse models have been used to test the restoration of the shifted reading frame in the mutated *DMD* sequence (Sun et al. 2020). In 2017, an humanized mouse model carrying the exon 45 deletion in the human *DMD* gene (out of frame mutation) was used to demonstrate that muscle electroporation of specific gRNAs and a Cas9 plasmids can induce exon 45-55 deletion and restore dystrophin expression (Young et al. 2017).

AAV vectors have been used to systemically or intramuscularly deliver the CRISPR/Cas9 components *in vivo*. An *mdx* mouse model harboring a nonsense mutation within exon 53 (Im et al. 1996) was used to test either excision of exons 52-53 via NHEJ-repair, re-establishing the correct reading frame, or to precisely resolve the mutation in exon 53 inducing HDR-mediated repair. All treated mice showed a recovery of the dystrophin expression following local or systemic AAV serotype 6-mediated delivery of the CRISPR/Cas9 components with consequent amelioration of the dystrophic phenotype (Bengtsson et al. 2017). More recently, *DMD* correction was achieved also in mice and dogs harboring an exon 50 dystrophin mutation. Injection of two AAV serotype 9 (AAV9) (showing tropism to both skeletal muscle and heart) (Zincarelli et al. 2008) encoding Cas9 gene and specific sgRNAs allowed reframing of the mutation and skipping of exon 51, thus restoring gene expression (Amoasii et al. 2017; Amoasii et al. 2018). Lastly, another mouse model of DMD carrying an exon 44 deletion (Ex44 DMD) was generated by Yi-Li Min et al. and used to test correction strategies using CRISPR/Cas9–mediated skipping of surrounding exons. The authors demonstrated that systemic injection of AAV9 carrying the Cas9/sgRNAs complex induced *DMD* reframing of the exon 45, either via splicing between exons 41 and 45 or between exons 43 and 46. In addition, gene reframing can be achieved via one N insertion or two nucleotides deletion induced by a single sgRNA and NHEJ repair. *DMD* reframing resulted in restoration of dystrophin protein expression and recovered muscle function in Ex44 DMD mice (Min et al. 2019).

Gene correction has been applied also *ex vivo* in muscle progenitor cells or iPSCs for testing cell replacement therapies. CRISPR/Cas9-induced NHEJ was used in DMD patient-derived iPSCs to reframe the mutated *DMD* gene. The authors showed restoration of protein function both *in vitro* (e.g. iPSC-derived cardiomyocytes and skeletal muscle cells) and *in vivo* (Young et al. 2016). In another study, CRISPR/Cas9-based editing was applied to correct patient-derived iPSCs carrying *DMD* exon 44 deletion either by skipping exon 43/45 or, by inducing the NHEJ-depended reframing of exon 43/44. The edited iPSCs-derived cardiomyocytes showed restored dystrophin expression (Min et al. 2019).

Recent studies have reported correction of specific mutations in LGM2B and LGM2D patients-derived iPSCs as well. Turan and colleagues developed for the first time a strategy to reverse a missense and stop codon mutation respectively in α-sarcoglycan and *DYSF* gene using the SpCas9/sgRNAs complex and a template for HDR repair. Muscle progenitor cells derived from corrected human iPSCs showed rescued expression and correct localization for both proteins (Turan et al. 2016). More recently, Selvaraj et al. reported successful gene correction in LGMD2A patient-derived iPSCs. iPSCs carrying three different Calpain 3 (CAPN3) mutations were edited using CRISPR/Cas9 followed by HDR repair to enable gene knockin and to bypass the mutations localized between exon 15-24. As a consequence, they showed CAPN3 protein rescue *in vitro* and mRNA detection *in vivo* after cell engraftment in a CAPN3-deficient immunocompromised mouse model (Selvaraj et al. 2019).

To conclude, CRISPR/Cas9-based editing in combination with cell-therapy is promising in translational medicine (Jacinto, Link, and Ferreira 2020). First clinical trials have already reported encouraging results in non-MDs (e.g. β-thalassemia, ClinicalTrials.gov: NCT03655678 and Sickle cell anemia, ClinicalTrials.gov: NCT03745287) (Hirakawa et al. 2020). However, safety and ethical concerns as well as methodological issues must be considered and solved for translation of CRISPR/Cas9 approaches into the clinic.

1.5. Bacterial nanocellulose

Bacterial nanocellulose or BNC is a water-insoluble polysaccharide consisting of linear D-glucose molecules linked by β-1,4 glyosidic bonds and produced by a variety of bacteria species (Jahn et al. 2011). Among all microorganisms reported for cellulose biosynthesis, Gluconacetobacter xylinum (G. xylinus), is the most efficient species (Shoda and Sugano 2005; Valera et al. 2015; Gullo et al. 2018). G. xylinus is an aerobic, Gram-negative, rod-like bacterium that metabolizes glucose via glucose-6-phosphate, glucose-1-phosphate, and uracil-diphosphate (UDP)-glucose to cellulose. The BNC is most commonly synthetized under static or shaking culture conditions, where bacteria generate a cellulose membrane at the medium-air interface (Rajwade, Paknikar, and Kumbhar 2015). Crystallized cellulose nanofibers are a highly porous material that is deposited extracellularly by the producing bacterium. BNC appears to be necessary to maintain the organisms in an aerobic environment (Hestrin and Schramm 1954), transport nutrients by diffusion

(Iguchi, Yamanaka, and Budhiono 2000) and mechanically support the bacteria, giving a survival advantage under natural conditions (Römling 2002).

BNC exhibits high mechanical strength (Hutchens et al. 2006), high water retention (Gelin et al. 2007), purity, biocompatibility (Klemm et al. 2005; Helenius et al. 2006) and non-biodegradability *in vivo* (Andersson et al. 2010; Petersen and Gatenholm 2011; Feldmann et al. 2013; Rajwade, Paknikar, and Kumbhar 2015; Ullah et al. 2016). It possesses a fine nanofibril network (Yamanaka et al. 1989; Retegi et al. 2010), which mimics, to some extent, properties of ECM (Bäckdahl et al. 2006; Petersen and Gatenholm 2011; Geisel et al. 2016) (Figure 1.10).

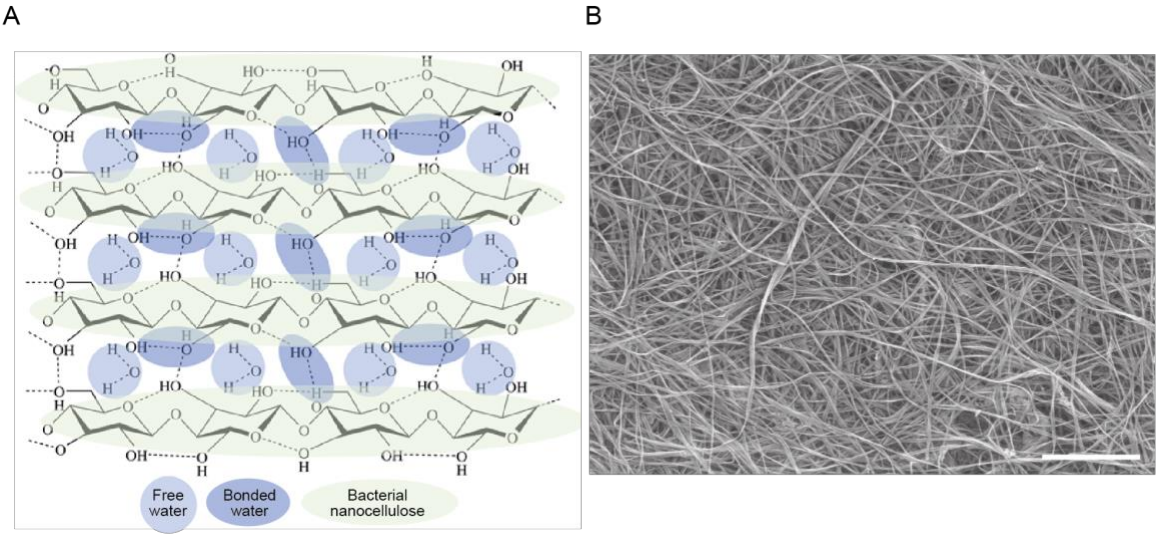

Figure 1.10: Molecular structure and ultrastructure of BNC
A) Typical molecular structure of hydrated BNC (modified from Portela et al. (2019)). **B)** Representative SEM picture of BNC nanofibril morphology. Scale bar = 2 µm

Its mechanical properties are similar to those ones of soft tissues with a Young´s modulus not greater than 30 GPa (Nishi et al. 1990). Of note, chemical/physical properties, porosity and shape of BNC strongly depend on the manufacturing conditions and can be adjusted according to necessity (Shah et al. 2013). All those features have contributed to a growing interest to this natural polymer as ideal biomaterial and cells substrate.

1.5.1. Applications of BNC as biomaterial

BNC is a biodegradable, non-toxic, biocompatible and pure substrate. It shows a unique reticulate 3D structure formed by a network of cellulose fibrils of 1.5 nm width, providing elasticity, flexibility and resistance. Many are the applications in regenerative medicine where BNC has been used as biomaterial (Svensson et al. 2005; Dutta, Patel, and Lim 2019). As first, the *in vivo* biocompatibility of the substrate was investigated (Helenius et al. 2006). In 1997 BNC was used to replace dura mater in dogs, showing great biocompatibility and adherence to the bone (Mello et al. 1997). Inflammation was assessed after subcutaneous implantation in rats and no immune response or fibrosis was observed at the engraftment area (Helenius et al. 2006).

The best-established application of native BNC is in wound dressing to treat burn or chronic lesions (Figure 1.11A) (Portela et al. 2019). Due to its capacity to retain moisture, absorbance and accelerate re-epithelization, BNC was used as an ideal scaffold for wound healing, tissue regeneration or as skin substitute (Czaja et al. 2006; Khalid et al. 2017). Biofill® (Fontana et al. 1990) was the first BNC product to be commercialized as skin substitute in 1990 and many others are currently in use (Picheth et al. 2017).

Native or chemically modified BNC has been also explored as scaffold for vascular/cardiovascular (Figure 1.11B,C) (Schumann et al. 2009), cartilage-meniscus (Andersson et al. 2010), bone (Zhang, Wang, et al. 2020) and neural (Kowalska-Ludwicka et al. 2013) tissue.

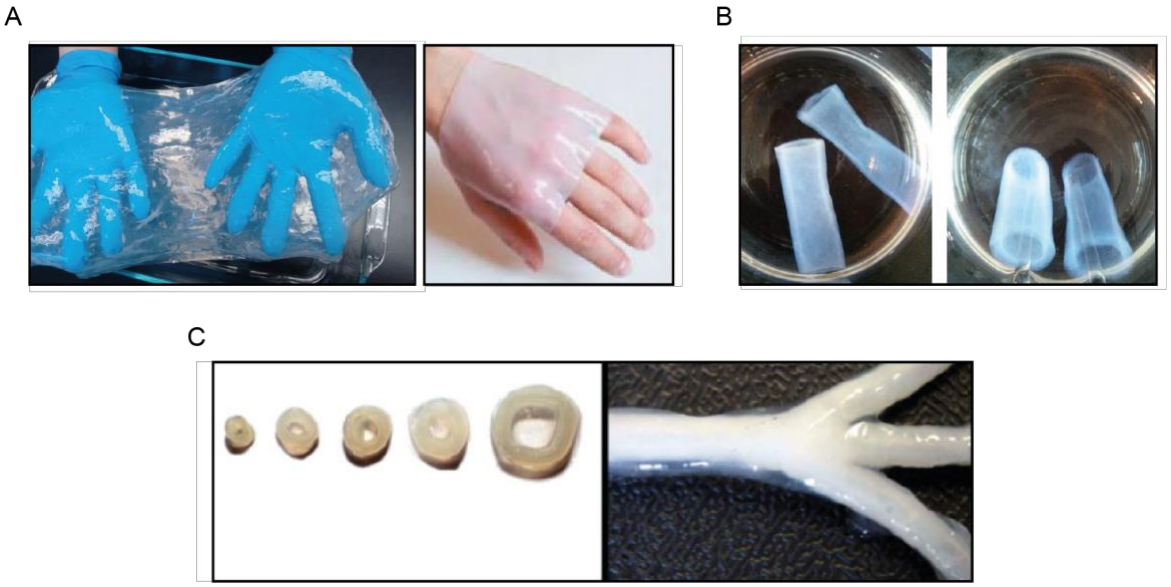

Figure 1.11: Examples of BNC biomaterials and scaffolds.
A) BNC bandage after production and when it is applied on wounded hand. **B)** Different sizes of BNC vascular graft and blood vessel tubes. **C)** On the left, BNC tubes with different diameters; on the right, branched BNC tube fermented on silicone tubes used as vascular scaffold (modified from Gorgieva and Trček (2019)).

1.5.2. BNC as *in vitro* cells scaffold for regenerative medicine applications

Given the potential of BNC as biomaterial (Svensson et al. 2005; Helenius et al. 2006; Bodin et al. 2007; Bäckdahl et al. 2008), several studies focused on the use of cellulose as scaffold for different type of cells to be applied for *in vivo* implantation and tissue regeneration.

The first studies have been made to assess biocompatibility for cell culture and to describe cell behavior on BNC-based substrates. In 1993 it has been reported that a L929 cells (a murine fibrosarcoma cell line) displayed reduced growth and adhesion when cultured on native BNC compared to cells in plastic dishes (Watanabe et al. 1993). Human umbilical vein endothelial cells (HUVEC) do not show significant differences in culture on a BNC substrate, as tested by Jeong et al. (Jeong et al. 2010). In another study, HUVEC showed horizontal growth, good adhesion and vertical migration when they are cultured on a three-dimensional BNC substrate (Recouvreux et al.

2011). In both cases, absence of cell toxicity and BNC biocompatibility, either *in vitro* or *in vivo,* was proved.

BNC modifications in mechanical and chemical features (e.g. BNC/poly-ethylene glycol, BNC/chitosan, BNC/gelatine and BNC/collagen etc.) have different effects on cell spreading, proliferation and adhesion capabilities (Andrade et al. 2010; Figueiredo et al. 2013; Shah et al. 2013; Huang et al. 2014) which could also vary with the cell types. Interestingly, high porosity BNC was evaluated as scaffold for cartilage tissue engineering. In this study it was observed that human chondrocytes are able to enter the cellulose pores of the scaffold, proliferate over time and produce ECM components within it. The authors concluded that porous BNC scaffold can be suitable to "host" chondrocytes for *in vivo* transplantation and cartilage regeneration (Andersson et al. 2010).

Culture of smooth muscle cells (SMCs) on BNC-based substrate has been investigated for tissue-engineered blood vessels (TEBVs). Human SMCs showed a lower proliferation rate on BNC substrate in comparison with polystyrene (Bäckdahl et al. 2006). In the same study, the authors observed that SMCs morphology and migration were influenced by BNC porosity and density. On the compact side of the BNC the cells were thin, elongated and distributed on one layer. On the porous side, SMCs were more rounded and migrate into the cellulose nanofibers (Bäckdahl et al. 2006). These findings have been important for designing tubular BNC as TEBVs.

BNC is extensively used for wound dressing as it was proved to avoid infection, accelerate granulation and re-epithelization of skin injuries (Portela et al. 2019). To improve the efficiency of BNC in wound healing, mesenchymal stem cells (MSCs) or keratinocytes can be incorporated in the scaffolds. These cells were expected to integrate into the host tissue after engraftment and to promote tissue regeneration. Indeed, it was reported that human MSCs can be cultured on native BNC and support wound healing when transplanted on burned skin of mice (Souza et al. 2014). Also, human keratinocytes and dermal fibroblasts that were included into a 3D BNC/acrylic acid hydrogel seemed to accelerate the wound healing process *in vivo* when placed on injured skin of mice. Both cell types attached well to the substrate, maintained viability with a limited proliferation and migration rate and could be transferred at the wounding site (Loh et al. 2018).

BNC properties and similarities with ECMs components like collagen (Bäckdahl et al. 2006; Petersen and Gatenholm 2011; Geisel et al. 2016) stimulated *in vitro* studies to optimize cell culture strategies. As reported by Feil et al., collagen-coated BNC preserved HUVEC native transcriptomic and proteomic phenotype mimicking cellular microenvironment. Specifically, they observed a reduction in proliferation-associated proteins and maintenance of receptor tyrosine kinase MAP/ERK and PI3K signaling pathways which are typical of their native biological functions (Feil et al. 2017). In another study, Tronsen and colleagues proved long-term maintenance of mouse embryonic stem cells (mESC) pluripotency when culture on BNC. Indeed, bio-mechanical features of cellulose nano-fibers appeared to inhibit mESC differentiation (Tronser et al. 2018).

Despite these first findings, BNC potentiality as substrate for stem cells culture is still unclear and further investigations are needed to evaluate its advantages in comparison to standard methods.

2. AIM OF THE STUDY

MDs are a heterogeneous group of inherited muscular disorders characterized by progressive degeneration and weakness of skeletal muscle and for which no definitive cure is currently available. MDs are caused by mutations of genes encoding for protein associated to a variety of cellular compartments (e.g. sarcolemma, extracellular matrix, nuclear membrane, and sarcomeric apparatus) and often essential for the maintenance of muscle integrity. *Ex vivo* cell-based gene therapy is being investigated as a promising approach for the treatment of monogenic muscular disorders. Importantly, cell-based strategies have been combined with the gene editing technology based on CRISPR/Cas9, which is currently explored as method for the correction of dystrophy-causing mutations. Ideally, patient-derived muscle precursor cells or myoblasts are genetically corrected *ex vivo*, subsequently expanded in culture and eventually used for autologous transplantation. For that reason, the development of an optimal gene correction strategy is crucial for the application of cell-therapy in the autologous context. A major obstacle to limit the clinical use of muscle stem-derived cells in cell-based therapy is the loss of their regenerative capabilities and stemness when expanded *ex vivo*. Culture conditions able to preserve the regenerative potential of myogenic cells by avoiding extensive proliferation are therefore of extreme interest.

The purpose of my work was to develop an *ex vivo* gene editing strategy able to efficiently correct dystrophy-causing mutations, while avoiding loss of human primary myoblasts (hPMs) stemness in culture.

To achieve this goal I aimed to:

1. Test a CRISPR/Cas9-based method for the correction of a founder mutation of the *DYSF* gene that is known to cause LGMD2B, in patient-derived PMs.
2. Explore a BNC substrate as an alternative culture method for hPMs and characterize their cellular behavior in comparison with the standard culture technique.
3. Verify that CRISPR/Cas9-based gene editing strategy is functional in donor-derived PMs when cultured on BNC.

3. MATERIALS AND METHODS

3.1. Cell culture

3.1.1. Primary human cell sources

Human muscle fiber fragments were prepared from muscle biopsy specimens obtained for diagnostic purposes. All human samples were collected after patients had signed informed consent forms in accordance with the requirements of the Charité Ethics Committee. Before human primary myoblasts (hPMs) isolation, muscle biopsy specimens underwent hypothermic treatment at 4°C as described in Marg et al. (Marg et al. 2014). Subsequently, isolation and culture of hPMs was performed as previously described (Marg et al. 2014; Schoewel et al. 2012). Research use of the material was approved by the regulatory agencies (EA1/203/08, EA2/051/10, EA2/175/17, Charité Universitätsmedizin Berlin). The hPMs used in this study are listed in table 3.1.

hPMs	Gender	Age	Cell Passage #*	Desmin %**	Pax7 %**	Ki-67 %**
hPM-1	male	67	P7	99	13	67
hPM-2	male	21	P6/P7	99	57	65
hPM-3	female	49	P8	99	22	51
hPM-4	female	25	P8	99	1	53
hPM-5	male	25	P7	99	25	64
hPM-6	female	56	P7	99	12	50
hPM-7	female	23	P7	99	17	60
hPM-8	female	58	P6	99	12	50
hPM-9	female	43	P7	99	55	84
hPM-10	female	27	P7	99	39	71
hPM-11	female	29	P7	99	5	73

* The column indicates the cell passage number (#) at which hPMs were used for performing experiments
** The markers were characterized in freshly isolated primary myoblasts before thawing

Table 3.1: Donor-derived PMs details.
The table shows the hPMs used for the all the experiments performed in the present study. The listed hPMs are from patients with different gender and ages. hPMs were all used between passage 6 and 8 and considered pure myogenic since at least 99% of cells were counted positive for desmin (myogenic marker). Ki-67 (proliferation marker) indicate the proliferation rate of cells after isolation. Myoblasts possessed a different percentage of Pax7 (SCs marker) positive cells. Differences are due to the donor-derived variability.

3.1.2. hPMs culture

3.1.2.1. hPMs culture on standard plastic dishes (Standard)

hPMs were grown in humidified atmosphere containing 5% CO_2 at 37°C on 10 cm plastic dishes (Corning) in skeletal muscle cell growth medium (SMCGM) (Provitro) enriched with fetal calf serum (FCS) supplement mix (Provitro), 10% fetal bovine serum (Biochrom) and 2.72 mM glutamine (GlutaMAX™, Thermo Fisher Scientific), Antibiotics (Provitro).

For cell passaging, hPMs were washed with Dulbecco's phosphate-buffered saline (DPBS) (Thermo Fisher Scientific) and treated with 0,25 % Trypsin/EDTA (Thermo Fisher Scientific) at 37°C for 5 min. Detached cells were collected in SMCGM + supplements to a dilution of 1:10 and centrifuged at 200 g for 5 min at room temperature (RT). Pellet was resuspended in an appropriate volume of SMCGM + supplements and seeded at a density of 1-2*10^4 cells/cm^2 on 10 cm plates. Cells were split every 2-3 days according to growth rate/confluence.

3.1.2.2. hPMs differentiation assay Standard

hPMs were seeded in 8-well ibidi µ-Slides (IBIDI GmbH Martinsried, Cat. # 80826, Germany) (10,000-15,000 cells per well) in SMCGM + supplements and incubated in humidified atmosphere containing 5% CO_2 at 37°C. At 70-80% of confluence, the medium was switched to OptiMEM (Thermo Fisher Scientific). After four days, cells were fixed for 10 min in 3.7% Formaldehyde (FA) (Sigma-Aldrich) and analyzed by immunofluorescence assay with antibodies against desmin, MYHC and MYOG (see Table 3.2 of section 3.2. for antibody list). Nuclei were stained with Hoechst 33258 (0.5 µg/ml, Sigma-Aldrich).

3.1.2.3. Production of BNC framed discs for cell culture

The BNC framed discs used in this study were produced by Xellulin® (Xellutec GmbH, Germany) as previously described (Hofinger, Bertholdt, and Weuster-Botz 2011; Feil et al. 2017). Currently, BNC manufacture is performed in our laboratory by Dr. Hans-Jürgen Peter, according to a modified protocol from Hofinger et al. and using Gluconacetobacter xylinus (Leibniz-Institut DSMZ - Deutsche Sammlung Mikroorganismen und Zellkulturen GmbH, Braunschweig, Germany, DSM 2325).

3.1.2.4. BNC framed discs and hPMs culture on BNC

hPMs on BNC were grown in humidified atmosphere containing 5% CO_2 at 37°C on BNC framed discs included in 6-well plates (Corning). Each well contained a total volume of 2.5 ml (1.5 ml inside and 1ml outside the frame) of SMCGM + supplements (see section 4.1.2.1.). Cell culture

medium was replaced twice a week. No cell passaging was needed during the culture period. hPMs grown on BNC were detached after washing with DPBS by an enzymatic treatment with 254 U/ml collagenase CLS II (Biochrom AG, Berlin, Germany), 100 U/ml Dispase II (Roche, Basel, Switzerland) and 0.25% trypsin/EDTA at 37°C for 45 min in 5% CO_2 at 37°C. Hence, hPMs were gently scraped (SPL Life Sciences Cat. # 90021, Korea), collected, counted, resuspended in an appropriate volume of SMCGM medium + supplements and seeded in standard 10 cm plastic dishes, 6-well plates as needed or 8-well ibidi µ-Slides (10,000-15,000 cells per well) (IBIDI GmbH Martinsried, Cat. # 80826, Germany) as needed. Bright field (BF) pictures of BNC substrate were taken before and after detachment using an EVOS FL Cell Imaging System.

3.1.2.5. hPMs proliferation from low number of cells on Standard and BNC

A low number of hPMs was seeded on 6-well plastic plates (Corning) and BNC discs ($1*10^3$ cells per well) and kept for 21 days in humidified atmosphere containing 5% CO_2 at 37°C. Cell culture medium (SMCGM + supplements) was replaced twice a week. No cell passaging was needed during the culture period. BF pictures were taken using an EVOS FL Cell Imaging System.

3.1.2.6. hPMs differentiation assay on BNC

hPMs were seeded on BNC discs ($2*10^5$ cells per well) in SMCGM + supplements and maintained in humidified atmosphere containing 5% CO2 at 37°C. After 30 days, the medium was switched to OptiMEM. After 4 days, cells were fixed for 10 min in 3.7% FA and analyzed by IF assay with antibodies against desmin, MYHC and MYOG (see Table 3.2 of section 3.2. for antibody list). Nuclei were stained with Hoechst 33258.

3.1.2.7. Fusion index calculation

After differentiation of hPMs on Standard and on BNC, the fusion index was calculated as the percentage of total nuclei incorporated into myotubes versus (vs.) the total number of nuclei. A myotube was defined as a muscle cell containing ≥3 nuclei.

3.2. Antibody list

Antibody	Catalog number and company	Working concentration
Desmin	ab15200, Abcam	1: 2.000 IF
MYF-5 (C-20)	sc-302, Santa Cruz Biotechnology	1: 2.000 IF
PAX7	sc-81648, Santa Cruz Biotechnology	1: 100 IF

Skeletal Myosin (fast)	M4276, Sigma-Aldrich	1: 200 IF
Myogenin (F5D)	ab1835, Abcam	1:500 IF
Ki-67 (SP6)	MA514520, Thermo Fisher	1:300 IF
MyoD1 (C-20)	sc-304, Santa Cruz Biotechnology	1:50 IF
BrdU	Ab6326, Abcam	1:50 FCS
CD56(NCAM1)	130090955, Milteny	1:200 FCS
Dysferlin (NCL-Hamlet)	Novocastra	1:500 WB
Dysferlin (Romeo)	ab124684, Abcam	1:200 IF
α-tubulin	T5168, Sigma-Aldrich	1:2000 WB
GAPDH	ab9485, Abcam	1:2000 WB
FITC	112-096-072, Jackson Immuno Research (Dianova)	1:1000 FCS
Alexa Fluor 488	A11001/ A11001, Invitrogen	1:1000 IF
Alexa Fluor 568	A11031/A11036, Invitrogen	1:1000 IF
Alexa Fluor 647	A21236, Invitrogen	1:500 IF
Alexa 488 conjugated WGA	W11261, Invitrogen	1:200 IF
Alexa Fluor™ 568 Phalloidin	94072, Sigma-Aldrich	1:250 IF

Table 3.2: List of primary and secondary antibodies.
Western blot (WB); Immunofluorescence (IF); Flow cytometry staining (FCS)

3.3. Immunofluorescence

3.3.1. Analysis of proliferation and myogenic markers expression in hPMs in Standard condition

hPMs were grown in 8-well ibidi µ-Slides (IBIDI GmbH Martinsried, Cat. # 80826, Germany) (10,000 cells per well), washed with DPBS and fixed with 3.7% FA at RT. After 10 min permeabilization with 0.2% Triton X-100 (Sigma Aldrich), cells were incubated in 1% bovine serum albumin (BSA) (Sigma Aldrich) in DPBS for 1h. Primary antibodies were used as described in Table 3.2of section 3.2., and incubated in 1% BSA/DPBS overnight at 4°C. After washing, samples were incubated with Alexa 488 or Alexa 568-conjugated secondary antibodies (see Table 3.2 of section 3.2. for antibody list) for 1h in DPBS at RT followed by Hoechst 33258 for 5 min.

3.3.2. Analysis of proliferation and myogenic markers expression in hPMs on BNC

hPMs were grown on 6-well plate BNC discs for various time points followed by fixation in 3.7% FA for 10 min at RT. BNC discs were then manually cut and divided into six to eight equal parts. BNC slices were transferred into 8-well ibidi µ-Slides (IBIDI GmbH Martinsried, Cat. # 80826, Germany) for further analysis. Cells were permeabilized for 20 min with 0.2% Triton X-100 and blocked in 1% BSA in DPBS for 1h. Primary antibodies (see Table 3.2 of section 3.2. for antibody list) were added overnight at 4°C. After washing, samples were incubated with Alexa 488 or Alexa 568-conjugated secondary antibodies (see Table 3.2 of section 3.2. for antibody list) and Hoechst 33258 for 1h in DPBS at RT. For imaging, BNC slices were mounted on slides using Aqua-Poly Mount (Polyscience, Cat. # 18606-5) solution.

3.3.3. Wheat germ agglutinin (WGA) conjugate membrane staining of hPMs on BNC

hPMs were grown on 6-well plate BNC discs for 48h followed by fixation in 3.7% FA for 10 min at RT. Cells were washed three times in HBSS (Life Technologies) and incubated with 1.0 mg/mL WGA conjugate stock solution (see Table 3.2 of section 3.2. for antibody list) diluted in HBSS for 10 min at RT. After the labelling solution was removed, cells were washed twice in HBSS. For imaging, BNC slices were mounted on slides using Aqua-Poly Mount solution.

3.3.4. Alexa Fluor 488/568 Phalloidin staining of hPMs on Standard or BNC

hPMs were grown on 6-well plate BNC discs or in 8-well ibidi µ-Slides (IBIDI GmbH Martinsried, Cat. # 80826, Germany) (10,000 cells per well) for 48h followed by fixation in 3.7% FA for 10 min at RT. Cells were permeabilized for 10 min with 0.2% Triton X-100, washed in DPBS two times and incubated with Alexa Fluor 488 Phalloidin (see Table 3.2 of section 3.2. for antibody list) in DPBS for 45 min at RT. After the labelling solution is removed, the cells are washed twice in DPBS and incubated with Hoechst 33258 for 5 min. For imaging, BNC slices were mounted on slides using Aqua-Poly Mount solution.

3.4. SDS page and immunoblot

Protein lysate of hPMs was obtained using protein extraction RIPA buffer consisting of 50mM Tris-HCl, 150mM NaCl, 0.1% NP-40, 0.1% SDS, 0.1% sodium deoxycholate and protease inhibitors. The protein lysate was kept on ice for 30 minutes, centrifuged at 1500 rpm for 10 min at 4°C and supernatant were transferred into fresh 1.5ml tubes. Protein quantification was performed

using BCA Protein Assay Kit™ (Pierce) following manufacturer's protocol. Required amount of protein (15 to 20 µg) was mixed with appropriate amount of SDS sample running buffer (0.25M Tris-HCl, 50% Glycerol, 5% SDS, 0.05% bromophenol blue and 10% β-mercaptoethanol) and heated at 94°C for 10 min Samples were loaded onto Invitrogen Novex™ WedgeWell™ 8 to 16% gradient gel (Thermo Scientific, XP08165BOX). Proteins were separated in denaturing conditions and transferred to a PVDF membrane using a wet electroblotting system (Bio-Rad) in Tris-glycine buffer containing 10% methanol and 0.1% SDS. Following transfer, the membrane was incubated for 1h at RT in TBST solution containing 4% dry milk powder (blocking buffer). After blocking, the membrane was incubated with the corresponding primary antibody diluted in blocking buffer (anti-dysferlin NCL-Hamlet, overnight at 4°C / anti- α-tubulin, 2h at RT / anti-GAPDH 2h at RT) (see Table 3.2 of section 3.2. for antibody list) and washed 10 min with TBST. Incubation with horse radish peroxidase (HRP)-conjugated secondary antibodies against mouse IgG (Thermo Scientific, 31432) and rabbit IgG (Thermo Scientific, 31462), both diluted 1:5000 in blocking buffer, was performed at RT for 1h. Afterwards the membrane was washed three times and incubated with AmershamTM ECLTM Prime Western Blotting Detection Reagent (GE Healthcare, RPN2232) and developed with VWR® CHEMI only system (VWR International GmbH). Images were processed using Adobe Photoshop CC 17. Modifications were applied to the full image (all the lanes).

3.5. Laser-mediated membrane wounding

For laser wounding experiment primary human myoblasts were plated on 8-well ibidi µ-Slides well (IBIDI GmbH Martinsried, Cat. # 80826, Germany) and fused as described in section 3.1.2.2.. Before performing the membrane wounding, the medium was replaced with Tyrode solution (140 mM NaCl, 5mM KCl, 2mM $MgCl_2$ and 10 mM HEPES, pH 7.2). Myotubes were wounded by irradiation of a 2.5 x 2.5 µm boundary area of the plasma membrane at 100% maximum power (10 mWdiode laser, 488 nm laser line) for 76 seconds using Zeiss LSM 700 confocal microscope with 63x (oil) magnification objective (LCI Plan-Neofluar 63x/1.3 Imm Korr DIC M27; Zeiss). Digital images were acquired using the Zeiss LSM ZEN 2.3 software (Carl Zeiss Microscopy GmbH).

3.5.1. IF after laser-mediated membrane wounding

After performing laser wounding experiment, myotubes were washed with DPBS and fixed with 3.7% FA in DPBS for 10 min. After washing with DPBS, blocking was performed with 1% BSA in DPBS for 1h at RT. Then, the myotubes were incubated with primary antibodies (anti-annexin A1 and anti-dysferlin (Romeo), see Table 3.2 of section 3.2. for antibody list) with 1% BSA in DPBS o/n at 4°C. Alexa 488 or Alexa 568-conjugated secondary antibodies (see Table 2 of section 3.2. for antibody list) were applied for 1h in DPBS at RT followed by Hoechst 33258 for 5 min.

3.6. Image acquisition

3.6.1. Standard cell culture imaging

Cells were routinely monitored via BF microscopy using a Leica DM IL Fluo Invers microscope (Leica Microsystems) equipped with 4x, 10x, 20x and 40x magnification objectives (HI PLAN 4x/0.10, HI PLAN I 10x/0.22 Ph1, HI PLAN I 20x/0.30Ph1, HI PLAN I 40x/0.50 Ph2). hPMs were checked daily for density and cell quality, depending mainly on passage number and donor, to assess usability for experiments and to prevent spontaneous fusion for standard maintenance cell culture. BF pictures were taken with an inverted light microscope EVOS® FL Cell Imaging System (Thermo Fisher Scientific) with 4x or 10x magnification objectives (PL FL 4X LWD PH, 0.13NA/16.9WD, PL FL 10X LWD PH, 0.25NA/9.2WD).

3.6.2. Laser Scan Microscopy

Multi-color, confocal IF imaging was performed using the Laser Scan Microscope LSM 700 (Carl Zeiss) equipped with a 1-2-channel scanning module corresponding to laser class 3B (DIN EN 60825-1) (405 nm (5 mW), 488 nm (10 mW), 555 nm (10 mW), 639 nm (5 mW)). The LSM is attached to an Axio Observer Z1 inverted microscope (Carl Zeiss) equipped with 40x or 63x (oil) magnification objectives (N-Achroplan 10x/0.25 M27, Plan-Apochromat 40x/0.95 Korr M27, LCI Plan-Neofluar 63x/1.3 Imm Korr DIC M27). Images were acquired with the ZEN 2010 SP1 software (Carl Zeiss). Control samples were used to adjust laser parameters to sample auto-fluorescence and secondary antibody fluorescence.

Same scan-settings were used for different samples that shared the same staining conditions. Image analysis and composition was done using the ZEN 2.3 software (Carl Zeiss Microscopy GmbH), ImageJ and Adobe Illustrator CC 2017.

3.6.3. Scanning electron microscopy (SEM) of BNC

BNC was fixed with 1 % (v/v) osmium tetroxide and, after washing with cacodylate buffer, dehydrated with Hexamethyldisiazane solution and placed on aluminum holders. For imaging, the samples were coated with gold/palladium and examined at Zeiss DSM 982 Gemini electron microscope (Carl Zeiss Microscopy GmbH Oberkochen, Germany).

3.6.4. Transmission electron microscopy (TEM) of hPMs on BNC

hPMs on BNC were fixed with 2.5% (v/v) glutaraldehyde in 0.1 M cacodylate buffer for 2h at RT. Blocs of 1-2 mm^3 were post-fixed with 1 % (v/v) osmium tetroxide, dehydrated in a graded series of ethanol and embedded in PolyBed® 812 resin (Polysciences, Inc., Warrington, USA).

Ultrathin sections (80 nm) were stained with uranyl acetate and lead citrate and examined at 80 kV with a Zeiss EM 910 electron microscope (Carl Zeiss Microscopy GmbH). Acquisition was done with a Quemesa CDD camera and the iTEM software (Emsis).

3.7. Flow cytometric assays

3.7.1. Flow cytometric assessment of cell viability

Propidium iodide (PI) staining was utilized for the determination of cell viability of hPMs cultured on BNC. After detachment, hPMs were washed with DPBS and labelled with PI - 1.0 mg/mL (Life technologies, P3566) (1:600). The signal was detected using BD FACS Canto II and normalized to unstained cells. PI as membrane impermeant dye is excluded from viable cells.

3.7.2. Flow cytometric cell cycle analysis using the Bromodeoxyuridine (BrdU) assay

On day after seeding (on Standard or on BNC), hPMs were incubated with 10nM BrdU (Roche, Germany) for 60 min. BrdU incorporated in newly synthesized DNA reflects the cell cycle progression status. The cells were collected as described in section 3.1.2.2. and 3.1.2.4., fixed with ice-cold ethanol (99%) (Sigma Aldrich) and denatured by treatment with 2 M HCl (Roth, Germany) / 0.5% Triton X-100 in DPBS for 30 min at RT. After neutralization with 0.1 M $Na_2B_4O_7$ (disodium tetraborate) (Roth, Germany) buffer at pH 8.5 for 2 min at RT, cells were washed and incubated with an anti-BrdU antibody (see Table 3.2 of section 3.2. for antibody list) for 30 min at RT. After washing, hPMs were incubated with a FITC secondary antibody (see Table 3.2 of section 3.2. for antibody list) for 30 min at RT. After washing, cells were resuspended in 3% FBS/DPBS containing 10mg/ml RNaseA (Qiagen) for 30 min at 37°C in the dark. Finally, 1mg/ml PI was added and the measurement was carried out with Flow Cytometry (Cell Analyser BD LSRFortessa). The percentages of cells distribution in G0/G1, S, and G2/M phases of the cell cycle were quantified using Flow Jo software version 10.6.0.

3.7.3. Flow cytometry protocol for neural cell adhesion molecule 1 (CD56 or NCAM1) staining

hPMs cultured on Standard or BNC were collected (see section 3.1.2.2. and section 3.1.2.4.) for CD56/NCAM1 FACS staining and washed in 2 ml of ice-cold staining buffer (1% BSA in DPBS). After washing, hPMs were incubated with the anti-CD56 primary antibody (see Table 3.2 of section 3.2. for antibody list), 15 min at 4°C (mix gently every 5 min) and washed two times with 500 µl staining buffer before the incubation with the secondary antibody Alexa Fluor 647 (see Table 3.2 of

section 3.2. for antibody list), 15 min at 4°C. Cells were washed two times, resuspended in 500µl staining buffer and transferred to FACS tubes with 40µm cell strainer caps (Corning) to remove cell clumps. NCAM1 signal was detected using flow cytometry (Cell Analyser BD LSRFortessa).

3.8. Lentivirus-GFP infection

3.8.1. Lentivirus production

Third generation (Dull et al. 1998), self-inactivating lentiviral vectors (Zufferey et al. 1998) were produced using quadri-transfection of 293TN human kidney producer cells (System Biosciences) on 0.01% Poly-L-Lysin (Sigma-Aldrich, Munich, Germany)-coated plates in OptiMEM Medium using Lipofectamin® 3000 Reagent (Thermo Fisher Scientific, Germany) (Diecke et al. 2013). Sequences encoding Gag, Pol and Rev proteins were delivered on pMD2L_PRE and pRSV-Rev packaging plasmids, whereas the vesicular stomatitis virus envelope glycoprotein (VSV-G) on pMD2.G plasmid. The viral LTRs and the enhanced GFP, under the control of human phosphoglycerate kinase-1 (PGK-1) promoter, were delivered on the pRRLSINcPPT_PGKGFP_WEPRE plasmid. Supernatant was collected for three days after transfection and centrifuged at 500 g for 15 min. 1 volume of cold Lenti-X-Concentrator was mixed with 3 vol of supernatant, incubated overnight and centrifuged at 1500 g for 45 min at 4°C. Pelleted Lentivirus was resuspended in ice-cold DPBS, aliquoted and stored at -80°C. Viral titer was estimated by means of Lenti-X qRT-PCR Titration Kit (Clontech, Saint-Germain-en-Laye, France) and titration by infection using flow cytometry.

3.8.2. hPMs infection with Lentivirus-GFP

Under culture conditions in plastic dishes, $5*10^4$ hPMs were seeded in 12-well plates and infected with Lentivirus-GFP in 0.5 ml SMCGM + supplements, without (w/o) antibiotics (MOI: 1). One day later, a supplement of 0.5 ml of SMCGM + supplements (w/o antibiotics) was added. After 48 h, cells were pelleted, washed and fixed.

On BNC, $1*10^5$ hPMs were seeded on 6-well plates and infected in 0.75 ml SMCGM + supplements (w/o antibiotics) (MOI: 1). The day after the infection, a supplement of 0.75 ml of SMCGM + supplements (w/o antibiotics) was added to the cells. After 72h cells were pelleted, washed and fixed with 3.7 % FA and the GFP signal was detected using BD FACS Canto II and compared to uninfected cells.

3.9. CRISPR/Cas9-based gene editing

3.9.1. Cloning of sgRNAs

For targeting experiments a one vector system was used, where sgRNA and Cas9 are expressed by the same plasmid. Apart from the sgRNA cassette that is regulated by the U6 promoter, the plasmid contains either SpCas9 (Jinek et al. 2012) (HE_p4.1) or eSpCas(1.1) (Slaymaker et al. 2016) (HE_p3.1) under the control of a mammalian codon-optimized CAG-promoter. Additionally, Cas9 is followed by a T2A-Venus cassette for monitoring gene expression. HE_p3.1 and HE_p4.1 were previously cloned by Dr. Helena E. Fernandez and here named as eSpCas9(1.1)::Venus and SpCas9::Venus respectively (see Appendix section 7.1.).

For this study, the sgRNA sequences against human *NCAM1* exon 3 and DYSF exon 44 were cloned into HE_p3.1 or HE_p4.1 plasmids and then tested in hPMs. sgRNAs were designed with CRISPOR online tool (Concordet and Haeussler 2018) and assembled with oligo annealing with 37 °C for 30 min and 95°C for 5 min. Annealed oligoes were cloned into HE_p3.1 and HE_p4.1 using BpII restriction sites and ligation was performed using T4 DNA ligase (NEB), overnight at 16°C. After transformation in electrocompetent *E. coli* bacteria, positive clones were verified by Sanger sequencing. sgRNAs targeting human DYSF exon 44 (Table 3.3) were designed by Dr. Helena E. Fernandez.

Locus	Target allele	Guide ID	Guide sequence	PAM	Orientation
hNCAM1	WT	*NCAM1*ex3wt#1	AACGCCAACATCGACGACGC	CGG	sense
hDYSF	mutated	*DYSF*ex44mut#3	AAATAGGGGTCCAGCGTGCA	GGG	sense
	mutated	*DYSF*ex44mut#3 + [G]	gAAATAGGGGTCCAGCGTGCA	GGG	sense

Table 3.3: sgRNA sequences used for the CRISPR/Cas9 experiments.

3.9.2. Lipo-transfection of the Cas9/sgRNA complex

For the CRISPR/Cas9 experiments on Standard, hPMs were seeded at a density of 75.000 cells/well of a 6-well plates a day before transfection. 1µg eSpCas9(1.1)::Venus or SpCas9(1.1)::Venus DNA (with and without sgRNAs; see Table 3.3 of section 3.9.1.) was transfected using Lipofectamine® 3000 transfection reagent (Invitrogen, Germany), according to the manufacturer's instructions.

For the CRISPR/Cas9 experiments on BNC discs, hPMs were seeded at a density of ~$2*10^5$ cells/well a day before transfection. 2µg eSpCas9(1.1)::Venus DNA (with and without sgRNAs; see Table 3.3 of section 3.9.1.) were transfected using Lipofectamine® 3000 transfection reagent (Invitrogen, Germany), according to the manufacturer's instructions.

In all experiments, 48h after transfection the Venus signal was detected using an EVOS FL Cell Imaging System and BD FACS Canto II and Venus positive (+) cells were sorted using Cell Analyser BD LSRFortessa. Sorted cells were in part used for genomic DNA isolation and in part plated again on Standard condition for further analyses.

3.10. DNA assays

3.10.1. Genomic DNA (gDNA) isolation

gDNA of hPMs was isolated using an AMPure XP Beads (Beckman Coulter) based purification protocol. Pelleted cells were lysed with 50µl Lysis Buffer AL (Qiagen) (for less than $1*10^6$ cells) and Proteinase K (Qiagen) (50-100µg/ml). After incubation at 56˚C for 10 min while shaking at low speed (300 rpm), 1.8 volumes of AMPure XP Beads were added to the mixture. The rest of the protocol was performed following the manufacturer's procedure.

3.10.2. Polymerase chain reaction (PCR) amplification of gDNA and Sanger sequencing of PCR products

gDNA was PCR amplified using Q5 High-Fidelity DNA Polymerase (NEB) and *NCAM1* or *DYSF* primers (Table 3.4). PCR products were gel purified (Nucleospin Gel and PCR Clean-up kit, Macherey-Nagel) and analyzed by bulk Sanger sequencing (LGC Genomics). The Sanger data analysis was performed using Inference of CRISPR Edits (ICE) from Synthego (ice.synthego.com) free bioinformatics tool.

3.10.3. T7 Endonuclease I (T7E1) assay

0.5 µg of purified PCR product was used to perform a T7E1 assay according to the manufacturer's instructions. First, the PCR products were incubated with NEBbuffer 2 (NEB, B7002S) and T7E1 (NEB, M0302S) at 37°C for 20 min. Then, the DNA was denatured at 95°C and the re-annealing was performed by decreasing temperature from 95°C to 85°C at -2°C/s and from 85°C to 5°C at -0.1°C/s. The annealed PCR products were analyzed via 2% agarose gel electrophoresis.

3.10.4. Sub-cloning

Sub-cloning experiments were performed using CloneJET PCR Cloning Kit (Thermo Fisher) according to the manufacturer's instructions. The CloneJET PCR Cloning Kit is a positive selection

system for cloning PCR products. The vector pJET1.2/blunt, T4 DNA ligase and primers for cloning PCR and sequencing are included in the kit (Table 3.4).

Gene	Primers		Annealing temperature (°C)
hNCAM1	Forward	CATTCCAGCAGCCATACTCAC	60
	Reverse	CGTAATAGCCCTCTGGGAAC	
hDYSF	Forward	CAGGACACAGCCCACATCT	60
	Reverse	CTATGCCCCCATAGACATGC	
pJET1.2	Forward	CGACTCACTATAGGGAGAGCGGC	60
	Reverse	AAGAACATCGATTTTCCATGGCAG	

Table 3.4: Primer list for PCR and sub-cloning.

3.11. RNA assays

3.11.1. RNA isolation

hPMs cultured on Standard or BNC were washed once and 175 µl of RP1 buffer (NucleoSpin® RNA/Protein isolation kit (Macherey-Nagel) were added to each well. The cell-lysate was collected using a scraper, frozen immediately on dry ice and stored at – 80 °C until RNA isolation. For RNA isolation, the NucleoSpin® RNA/Protein isolation kit (Macherey-Nagel) was used according to the manufacturer´s instructions. Elution volumes of 20-40 µl were used, depending on the size of the cell pellet. RNA concentration was determined using the NanoDrop™ One Microvolume UV-Vis Spectrophotometer (Thermo Fisher Scientific)

3.11.2. Reverse Transcription and quantitative real-time PCR (RTq-PCR)

500 or 1000 ng of isolated RNA were reverse transcribed using the QuantiTect Reverse Transcription Kit (Qiagen) according to the manufacturer´s instructions and the complementary DNA (cDNA). The resulting cDNA was diluted to 20 ng/1 µl and stored at -20°C. For testing the used primers, different annealing temperatures were tested with standard curve assays using 32 ng, 8 ng, 2 ng and 0.5 ng cDNA input in order to define the amount of cDNA and annealing temperature needed for optimal primer efficiencies (Primer sequences and corresponding used annealing temperatures are listed in Table 3.5).

For real time PCR reactions, KAPA SYBR® FAST qPCR Master Mix (2X) Universal (Sigma-Aldrich) was used following the manufacturer´s instructions.

For analysis, the QuantStudio™ 6 Flex Real-Time PCR System (Thermo Fisher Scientific) together with MicroAmp® Optical 96-Well Reaction plates (Thermo Fisher Scientific) were used with three technical replicates per sample and per primer pair.

For primer pairs with optimal annealing temperature at 60 °C, a two-step protocol with 40 cycles with denaturation at 95 °C and annealing at 60 °C was used. For primer pairs with optimal annealing temperatures different from 60 °C, a three-step protocol was used with 40 cycles with denaturation at 95 °C, annealing see Table 3.5, and elongation and acquisition at 72 °C. For all primers, two control samples were used, a water control and a RTq-PCR reaction mix using a reverse transcription product without reverse transcriptase enzyme.

Ct values were normalized to the housekeeping gene GAPDH (DCt values) for each sample, primer pairs and each PCR plate. Relative gene expression levels were calculated using the formula $2^{-\Delta\Delta Ct}$ according to the MIQE guidelines (Bustin et al. 2009).

Gene	**Primers**		**Annealing temperature (°C)**
hGAPDH	Forward	GAAGGTGAAGGTCGGAGTC	60
	Reverse	GAAGATGGTGATGGGATTTC	
hKI67	Forward	TTGGAAGGGGTATTGAATGT	60
	Reverse	TCCATGTTTTAGCCGTACA	
hPAX7	Forward	TGGGCGACAAAGGGAA	60
	Reverse	GGTAGTGGGTCCTCTCAAA	
hMYOD1	Forward	GCGGAACTGCTACGAA	57
	Reverse	AGATGCGCTCCACGAT	
hMYF5	Forward	CCACCTCCAACTGCTC	57
	Reverse	CCAAGCTGGATAAGGAGT	
hDYSF exon52-53	Forward	TCCACCCAGAATGGTTTGTGT	60
	Reverse	CGCTCCTCATGCTCACTCTC	

Table 3.5: Primer list for RTq-PCR.

3.11.3. RNA library preparation

Total RNA was isolated and stored at – 80 °C as described in section 3.9.1. RNA quantity was assessed using the Qubit® 2.0 Fluorometer with the Qubit™ RNA HS Assay Kit (Thermo Fisher Scientific). The quality was evaluated by the 4200 TapeStation System together with the high sensitivity RNA ScreenTape (Agilent). RIN values were above 7 for all samples. Library preparation for total RNA sequencing was performed using the NEBNext Ultra II Directional RNA Library Prep Kit for Illumina® (New England Biolabs) together with the NEBNext rRNA

Depletion Kit (Human/Mouse/Rat) (New England Biolabs). 500 ng total RNA were used per sample following the manufacturer´s instructions. NEBNext® Multiplex Oligos for Illumina® (New England Biolabs) were used for indexing with a final PCR enrichment of adapter ligated DNA of 10 cycles due to the 500 ng initial RNA. Purification of the final PCR reaction using Agencourt®

AMPure XP PCR cleanup beads (Beckman Coulter Life Sciences) was performed twice to assure a clean end product without contaminating small fragments or adapters.

Library quality was checked with the 2100 Bioanalyser together with the Bioanalyser High Sensitivity DNA Analysis chips and reagents (Agilent). Library quantity was determined using the Qubit™ dsDNA HS assay kit (Agilent). Finally, samples were appropriately pooled with a final concentration of 10 mM per sample and delivered to the Genomics Platform (Dr. Sascha Sauer, Max Delbrück Center for Molecular Medicine, Berlin, Germany) to be sequenced with 2*76+16In (paired end, 76 cycles, 16 indices) using the HiSeq 4000 System (Illumina).

3.11.4. Total RNA sequencing and analysis

RNA sequencing data processing was done by the Genomics Platform (Dr. Sascha Sauer, Max Delbrück Center for Molecular Medicine, Berlin, Germany) by Dr. Daniele Yumi Sunaga-Franze. For each sample, the transcript quantification at isoform level was estimated by RSEM (bowtie2 default parameters, GRCh38) (Li & Dewey, 2011). DEseq2 paired designed and adjusted p value (padj) < 0.05 was used for the differential expression analysis (Anders & Huber, 2010) between hPMs cultured on Standard and BNC at different points of time. The differentially expressed isoforms were further annotated via Biomart R package (hsapiens_gene_ensembl). Pathway analysis was performed using ConsensusPathDB (http://cpdb.molgen.mpg.de/). GraphPad Prism 8 software and ClastVis online tool were used for volcano plots and visualizing clustering of multivariate data respectively (https://biit.cs.ut.ee/clustvis/).

3.12. Statistics

Data are presented as mean ± standard deviation (SD) or as the mean ± standard error of the mean (SEM). Statistical analyses were performed using the GraphPad Prism 8 software (GraphPad) or Excel 2016. Differences were considered statistically significant for $p<0.05$. Statistical tests performed for each specific experiment are indicated in the legends of the Figures.

4. RESULTS

4.1. *Ex vivo* CRISPR/Cas9-based gene editing in hPMs

Gene editing is a powerful tool to repair disease-causing mutations. CRISPR/Cas9 methods have already been tested *in vitro* or *in vivo* systems in the context of MDs, (Long et al. 2014; Nelson et al. 2016; Zhang et al. 2017; Zhu et al. 2017; Bengtsson et al. 2017)). Moreover, CRISPR/Cas9-based editing can be combined with cell-therapy for autologous transplantation as a clinical approach (Biressi, Filareto, and Rando 2020). To date, muscle disease-causing mutations have been corrected in patient-derived iPSCs (Turan et al. 2016; Young et al. 2016; Selvaraj et al. 2019; Min et al. 2019). However, no data were published yet on CRISPR/Cas9-based gene editing in hPMs, although this cell population is considered a valuable source for cell-therapy (Marg et al. 2014). Here, I tested the ability of the Cas9 nuclease and specific sgRNAs for *in vitro* editing of donor-derived PMs.

4.1.1. CRISPR/Cas9-based gene editing induces *NCAM1* knockout in donor-derived PMs

In order to target hPMs *in vitro*, I used a plasmid carrying an eSpCas9(1.1) nuclease and a sgRNA expression cassette driven by the human U6 promoter. This vector (named as eSpCas9(1.1)::Venus) also contains the fluorescent Venus reporter, which is expressed together with eSpCas9(1.1) from the CAG-promoter. Both proteins are separated by a T2A self-cleaving peptide which allows the independent expression of eSpCas9(1.1) and Venus from the same promoter. By this, eSpCas9(1.1) positive cells can be selected according to the fluorescent Venus protein. Once the eSpCas9(1.1)/sgRNA complex is formed in the cells, a DSB at the expected cleavage site is induced.

I chose *NCAM1* (also named *CD56* or Antigen Leu-19) as a candidate gene to test cleavage and editing efficiency in hPMs. NCAM1 is a membrane protein expressed constitutively in myoblasts (Figure 4.1A) (Illa, Leon-Monzon, and Dalakas 1992; Belles-Isles et al. 1993). This protein is localized at the membrane and can easily be detected by immunolabeling or flow cytometry (Capkovic et al. 2008). Therefore, loss of NCAM1 after Cas9-induced DSBs, was used as the experimental read-out.

To perform this experiment, I used donor-derived PMs that were isolated according to a protocol established in our laboratory (see Methods section 3.1.). After isolation, cells were characterized for purity (desmin), proliferation capability (Ki-67) and Pax7 (SCs marker) expression (see Methods section 3.1., Table 3.1). I transfected donor-derived PMs with the eSpCas9(1.1)::Venus plasmid containing a sgRNA targeting *NCAM1* exon 3 (sgRNA name: *NCAM1*ex3wt#1) (Figure 4.1B, C and see Methods section 3.9.1., Table 3.3). The eSpCas9::Venus vector w/o sgRNA was used as control. After enrichment for eSpCas9(1.1)::Venus+ cells through

FACS (Figure 4.1C), I extracted gDNA from each condition and I PCR amplified the region around *NCAM1* exon 3 for Sanger sequencing.

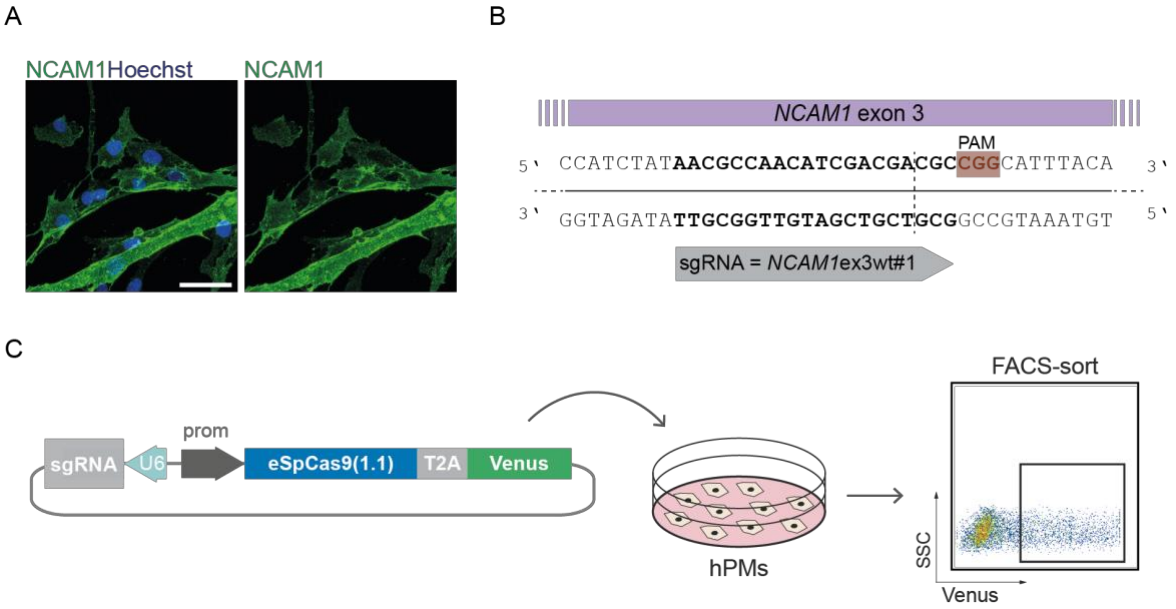

Figure 4.1: CRISPR/Cas9 strategy for *NCAM1* gene editing.
A) IF membrane staining for NCAM1 of hPMs. Scale bar = 50 µm. **B)** Illustration of the sgRNA binding site (arrow) and sequence targeting *NCAM1* exon 3. The PAM sequence for the sgRNA is indicated in red. The black dotted line indicates the expected cleavage site. **C)** Illustration of the plasmid encoding eSpCas9(1.1)::Venus used for hPMs transfection. Transfected cells express Venus and were selected according to their green fluorescence by FACS.

To analyze the editing efficiency of hPMs, I used a bioinformatics tool called inference of CRISPR Edits (ICE) from Synthego (ice.synthego.com). The ICE tool requires the chromatograms derived from Sanger sequencing of unedited (w/o sgRNA) and edited (sgRNA) samples. The de-convolution of Sanger-derived chromatograms allows to predict the percentage of sequence types in the bulk population of the edited cells.

Unedited cells displayed a clean chromatogram compared to the test sample (Figure 4.2A). The chromatogram of edited cells on the contrary showed aberrant peaks after the expected cut site which is 3 nucleotides 5' of the PAM sequence (Figure 4.2A). This can be explained by the formation of indels due to NHEJ, which randomly inserts or deletes nucleotides to repair DSBs (Hilton and Gersbach 2015). This suggested successful gene editing in the sgRNA sample only.

Quantification of the editing efficiency is displayed using indel plots, where the predicted distribution of indels in the test sample is shown. The prediction is calculated according to the chromatogram peak area of individual indels. Each bar of the plot shows the size of the insertion or deletion (+ or - 1 or more nucleotides), along with the percentage of sequences that contain that type of indel (Figure 4.2B, left). The indel plots revealed a predicted editing efficiency of 44.7%, average of 7 independent experiments (Figure 4.2B, right).

To further confirm CRISPR/Cas9-induced indel formation at gDNA-level, I performed a mismatch-specific T7E1 assay. This assay is based on the detection and cleavage by T7E1 of heteroduplex dsDNA that derive from the annealing of a DNA strand containing mutations with the

WT DNA strand (Mashal, Koontz, and Sklar 1995). Only gDNA derived from sgRNA-transfected samples when digested with T7E1 is cleaved at the predicted site of *NCAM1* exon 3 (Figure 4.2C). This further confirms the successful targeting of *NCAM1* on gDNA level.

Lastly, I evaluated NCAM1 protein expression via immunostaining and flow cytometry analysis. Due to the previously described indel formation by NHEJ, the open-reading frame of *NCAM1* was expected to be disrupted which leads to a loss of protein expression. Indeed, FACS analysis revealed a mean of 46.7% loss of NCAM1 in the edited cells after ~10 days of culture expansion (Figure 4.2D).

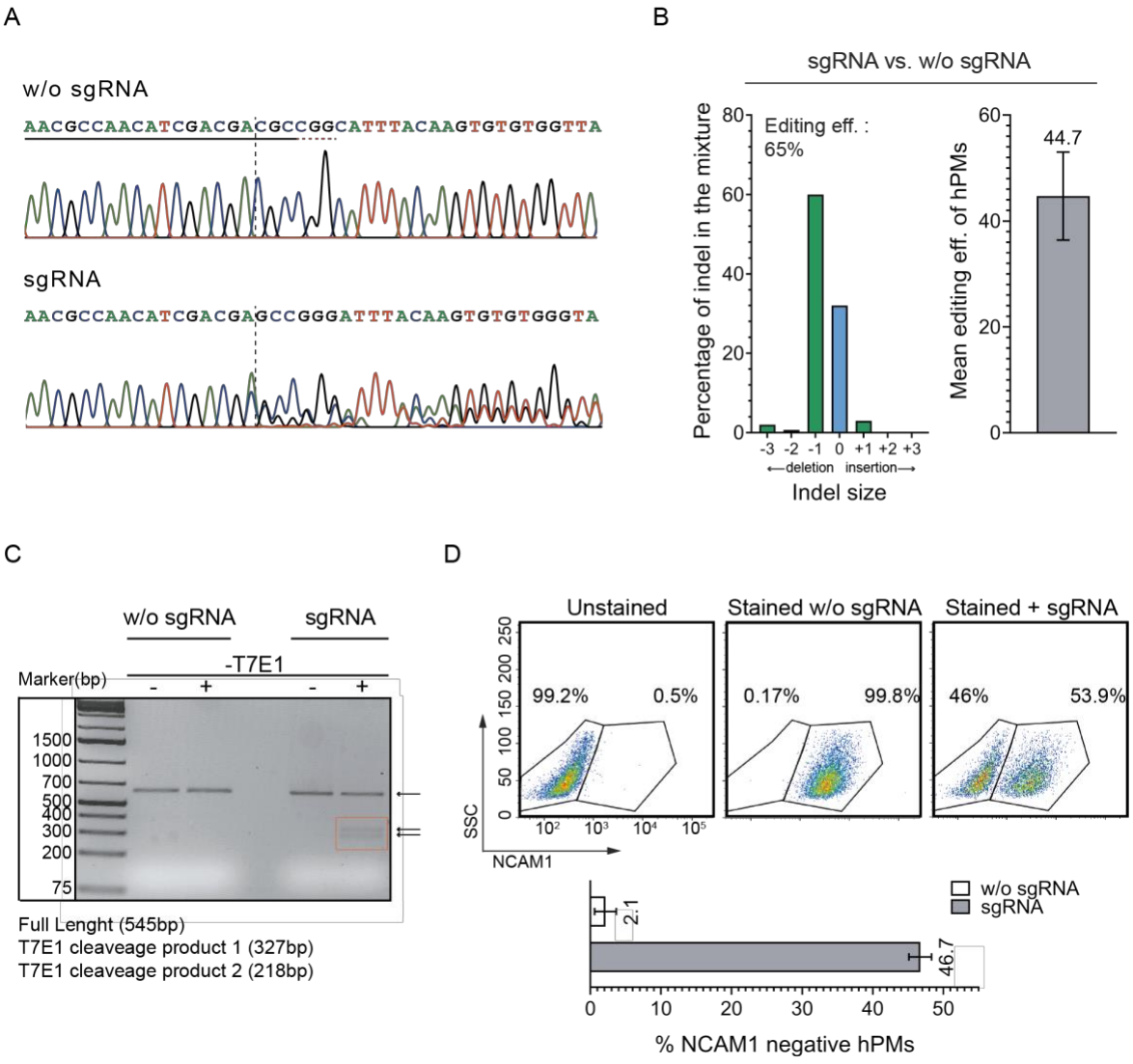

Figure 4.2: Depletion of NCAM1 protein in hPMs using a CRISPR/Cas9-mediated genome editing approach.

A) Sanger sequences of the region surrounding the sgRNA sequence obtained from a single sample of donor-derived PMs (hPM-2) transfected with sgRNA (sgRNA) compared to a control sequence (w/o sgRNA). Chromatogram variability is observed after the cleavage site (black dotted line). Horizontal black underline: sgRNA. Red dotted line: PAM site. **B)** Left, representative example of indel plot from ICE analysis showing the predicted editing efficiency relative to hPM-2. Right, editing efficiency (ICE) mean of different hPMs donors (n=7 donors; mean±SEM. **C)** T7E1 assay for detecting CRISPR/Cas9-induced indel formation in *NCAM1* exon 3 targeted locus of the hPM-2. **D)** Upper, example of FACS dot plots from NCAM1 staining of w/o sgRNA and

sgRNA relative to the hPM-2. Lower, percentage mean value of NCAM1 negative cells of different hPMs donors after editing (n=4 donors; mean±SD).

Here, I proved a successful gene knockout in hPMs based on CRISPR/Cas9. In addition, using *NCAM1* as model gene, I provided a reliable experimental read-out for testing gene editing efficiency in hPMs.

In this experiment, the eSpCas9/sgRNA complex was delivered without a donor template that is generally required for HDR-based repair. This is indicating that the NHEJ mechanism was the one responsible of the editing outcome. I also observed that using *NCAM1*ex3wt#1 to target *NCAM1* locus, NHEJ-induced deletion of a single nucleotide (N) is the preferential indel in the population of edited hPMs as shown by ICE analysis (Figure 4.2B, left). This suggested that the *NCAM1* knockout was caused by a NHEJ-induced frameshift mutation mainly via single N deletion.

4.1.2. CRISPR/Cas9 induces re-framing of *DYSF* exon 44 in patient-derived PMs

In order to proof the feasibility of the CRISPR/Cas9 method to repair MD-causing mutations in hPMs we chose LGMD2B as a model disease. LGMD2B is an autosomal recessive type of muscular dystrophy caused by mutations in the *DYSF* gene (Liu et al. 1998; Illa et al. 2001; Aoki et al. 2001; Bansal et al. 2003). *DYSF* c.4872_4876delinsCCCC is a founder mutation in *DYSF* exon 44 with a 10% carrier frequency in the Libyan Jew population (Argov et al. 2000). This mutation is characterized by single base (G) deletion in position 4872 (4872delG) of the *DYSF* coding sequence and a single N exchange (c.4876G>C). 4872delG causes a frameshift of the *DYSF* reading frame and the generation of a premature stop codon downstream in exon 45. Patients carrying this mutation in the homozygous state show a complete absence of dysferlin protein (Figure 4.3) (Argov et al. 2000).

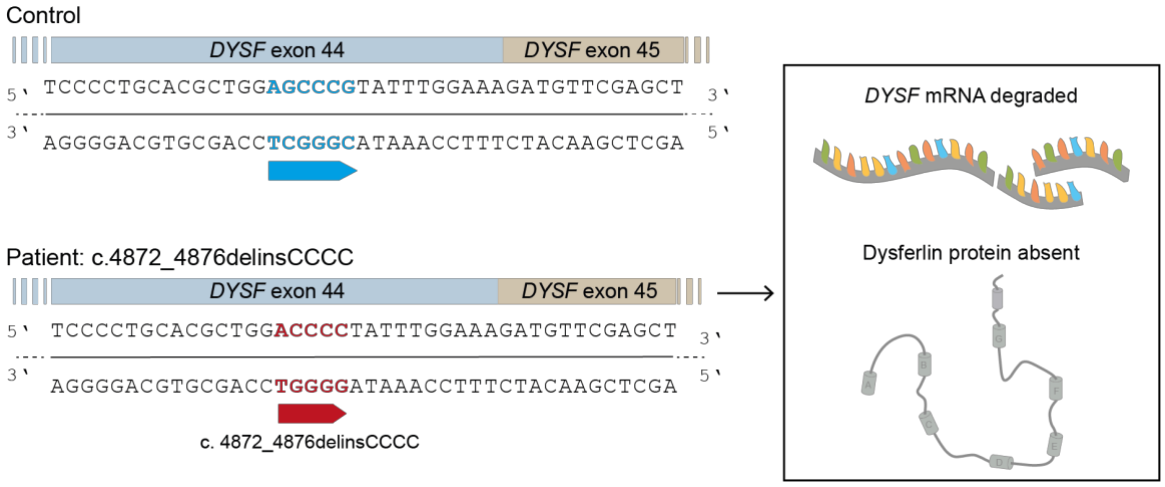

Figure 4.3: *DYSF* exon 44 homozygous c.4872_4876delinsCCCC.
A) Illustration showing the *DYSF* exon 44 c.4872_4876delinsCCCC founder mutation compared to a WT DNA sequence and the consequences at mRNA and protein level.

We developed a classic CRISPR/Cas9-based approach, to correct the c.4872_4876delinsCCCC mutation *ex* vivo in hPMs derived from a homozygous patient (hPM-11; see Methods section 3.1., Table 3.1). NHEJ repair is the main pathway involved in Cas9-induced indel formation, when an exogenous repair template is not provided (Hsu, Lander, and Zhang 2014). Recent studies proved that the repair outcomes significantly vary amongst target sites and some genomic locations show highly preferred sequence alterations or indels (van Overbeek et al. 2016; Chakrabarti et al. 2019). Practically, CRISPR-mediated NHEJ repair could be exploited to obtain a specific editing outcome in a genomic site of interest. Indeed, previous experiments performed in our laboratory on patient-derived iPSCs (Dr. Helena F. Escobar, unpublished work), showed that targeting *DYSF* exon 44 with a mutation-specific sgRNA (*DYSF*ex44mut#3; see Methods section 3.9.1., Table 3.3) restores the *DYSF* open-reading frame by a single N insertion as preferential editing outcome. However, it was not clear whether this editing strategy is only possible in hiPSCs or also in hPMs.

To verify the efficiency of sgRNA *DYSF*ex44mut#3 in editing hPM-11, I tested several strategies. First, the sgRNA was combined with the eSpCas9(1.1), that was shown to cut DNA efficiently in hPMs at the *NCAM1* locus. Second, the sgRNA was cloned into a vector containing the WT SpCas9 (named as SpCas9::Venus). Third, I tested the same sgRNA that included an extra G before the start of the protospacer sequence, as "preferred" transcription start for the U6 promoter (sgRNA+G). This is reported to induce a more efficient expression of the sgRNA sequence (Gao et al. 2017). The sgRNA+G was combined with the WT SpCas9 (Figure 4.4). The SpCas9::Venus vector w/o sgRNA was used as control.

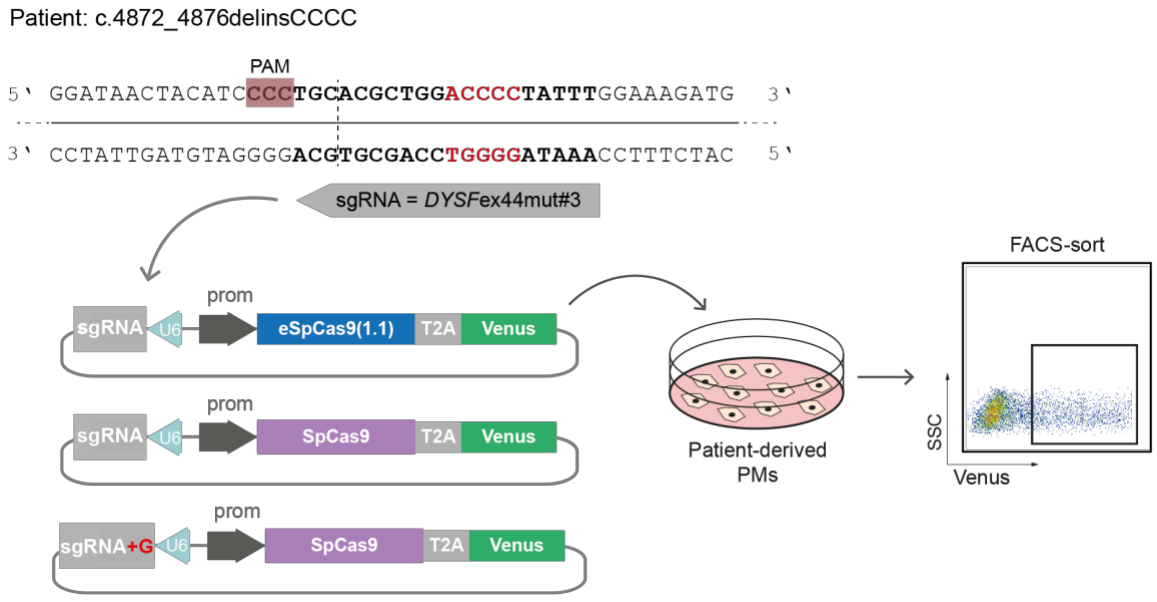

Figure 4.4: CRISPR/Cas9-based strategy for gene editing of *DYSF* exon 44 mutation.
Illustration of the sgRNA binding site (arrow) and sequence targeting *DYSF* exon 44. The PAM sequence is highlighted in red. The black dotted line indicates the expected cleavage site. Below, illustration of the used plasmids encoding eSpCas9(1.1)::Venus and SpCas9::Venus. Transfected cells expressed the fluorescent protein Venus (green) and were selected by FACS.

I transfected hPM-11 as previously described. After enrichment for Venus positive (+) cells via FACS, I extracted gDNA and I PCR-amplified the region around *DYSF* exon 44 for Sanger sequencing. ICE analysis revealed indel formation using both vectors and sgRNAs (with and w/o the extra G) (Figure 4.5A). The predicted editing efficiency was low (7%) with the eSpCas9(1.1)::Venus vector. However, it reached 49% and 50% for sgRNA and sgRNA+G, respectively, when the WT SpCas9 was used (Figure 4.5B). For this reason, I focused the following analysis on hPM-11 transfected with the SpCas9::Venus including sgRNA or sgRNA+G. In both conditions, I observed a single N insertion at the cleavage site as the preferred indel (Figure 4.5B). A single N insertion could restore the open-reading frame of the mutant *DYSF* exon 44.

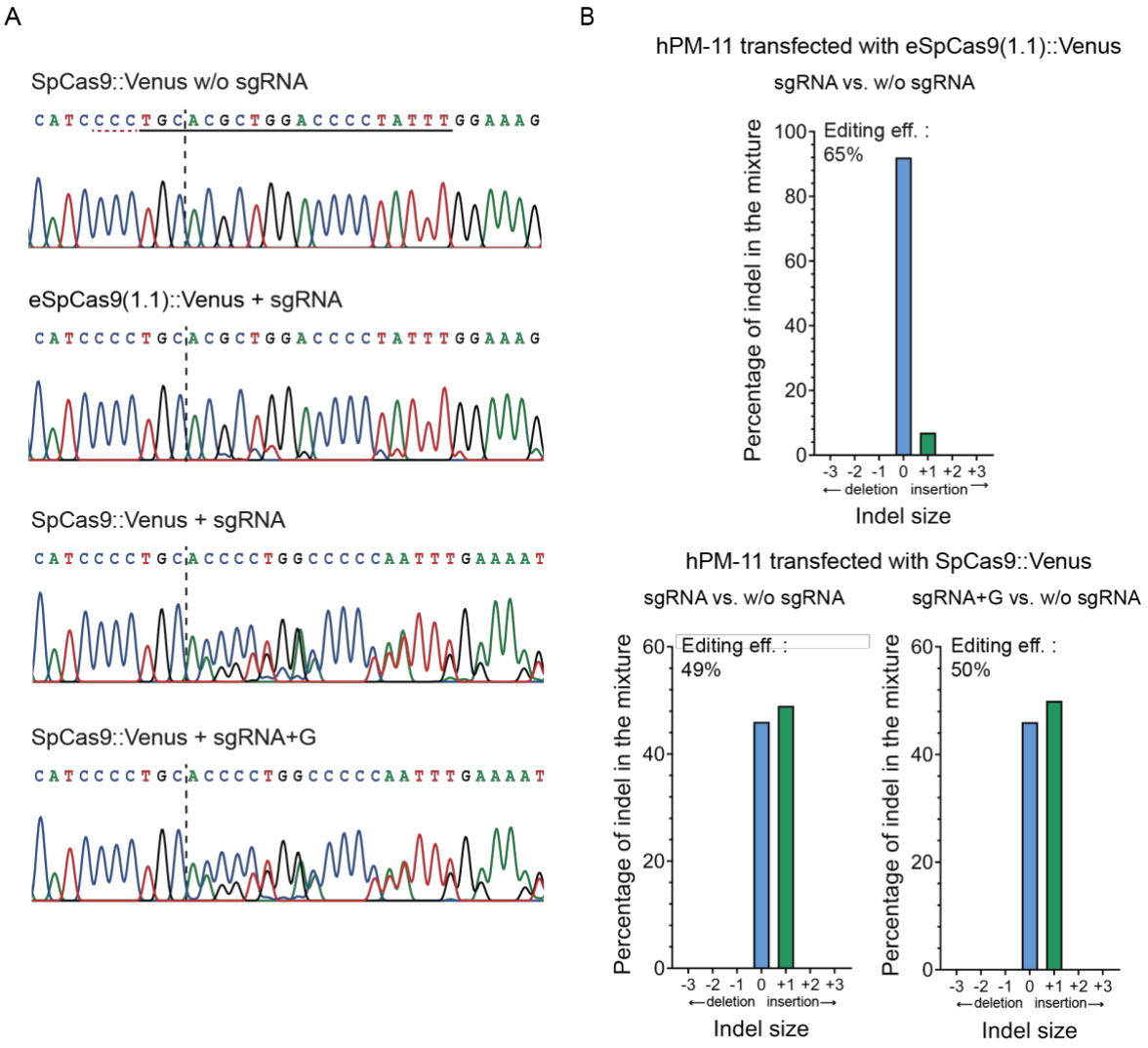

Figure 4.5: CRISPR/Cas9 induced re-framing of *DYSF* exon 44 in hPM-11.
A) Sanger sequences in the region surrounding the sgRNA from hPM-11 transfected with eSpCas9(1:1)::Venus + sgRNA and SpCas9::Venus + sgRNA or sgRNA+G compared to a control-non-edited sequence (w/o sgRNA) show chromatogram disturbance after the cleavage site (black dotted line). Horizontal black underline: sgRNA. Red dotted line: PAM. **B)** Indel plots from ICE analysis showing the predicted editing

efficiency of hPM-11, using both vectors (eSpCas9(1.1)::Venus and SpCas9::Venus) and sgRNAs (sgRNA and sgRNA+G).

To gain a better understanding of the Cas9 induced indel pattern and the mutation frequencies in the edited samples, I performed sub-cloning of the *DYSF* exon 44 PCR product from the edited samples. Single bacterial clones were picked, the *DYSF* exon 44 locus was amplified and the PCR product was send for Sanger sequencing analysis. Then, I analyzed indels found in each amplicon and plotted them in pie charts. The results showed that in both cases, the most frequent indel was a +1 Adenine (A) insertion at the DBS site (Figure 4.6). Similar results were previously observed in patient-derived iPSCs.

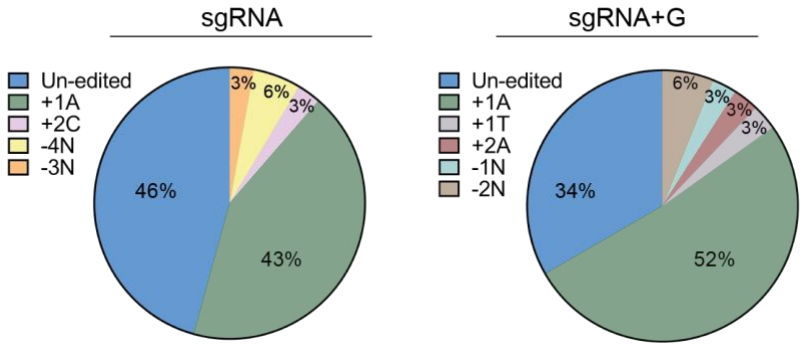

Figure 4.6: CRISPR/Cas9 induced re-framing of *DYSF* exon 44 in hPM-11 via +1A insertion.
Sub-cloning pie charts showing indel pattern distribution in sgRNA (total colonies analyzed: 35) and sgRNA+G (total colonies analyzed: 33) edited samples.

I showed that hPMs carrying a founder frameshift mutation in exon 44 of the *DYSF* gene were edited via SpCas9-induced single cut and NHEJ repair. Specifically, when a SpCas9 was driven by the mutation-specific *DYSF*ex44mut#3 sgRNA, the *DYSF* reading frame was restored by a preferred indel: a +1A insertion at the DSB site. In this manner we minimized the unwanted heterogeneity of repair outcomes that characterizes an error prone mechanism such us NHEJ repair, thus achieving a highly efficient and precise genome editing.

4.1.3. Re-framing of *DYSF* exon 44 restores protein expression and membrane localization in patient-derived PMs and myotubes

As described above, 4872delG mutation causes a frameshift of the *DYSF* coding sequence and generates a premature stop codon in exon 45. Restoring the reading frame of the mutant *DYSF* exon 44 via the +1A insertion is predicted to abolish the formation of a premature stop codon in exon 45 (Figure 4.7). As a consequence, *DYSF* mRNA should be transcribed as in control conditions.

To confirm this, I isolated mRNA from unedited and edited hPM-11 following ~10 days of culture expansion and evaluated the expression level of *DYSF* by RT-qPCR with primer pairs downstream (exon 52-53) of the mutation.

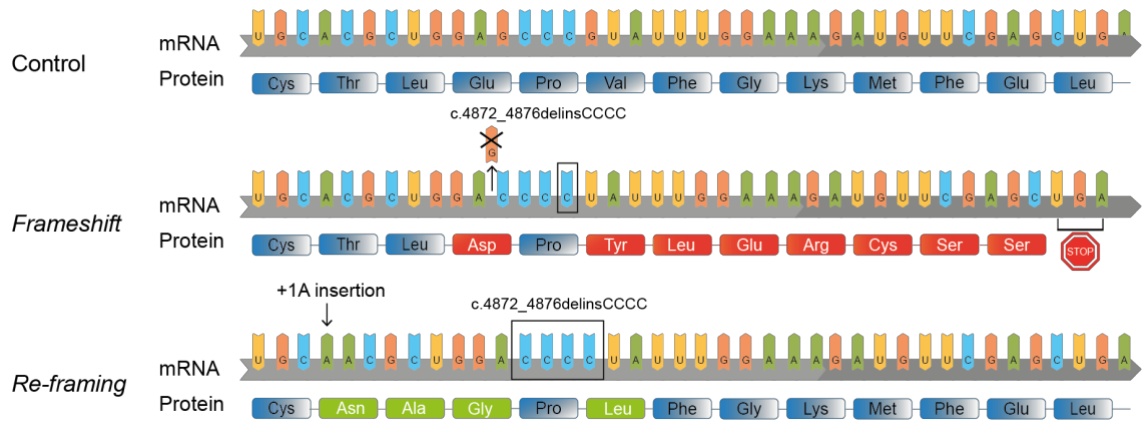

Figure 4.7: CRISPR/Cas9 induced re-framing of DYSF: prediction at mRNA and protein level.
Illustration showing the correction of the *DYSF* exon 44 mutated reading frame at mRNA and protein level. Due to a +1A insertion, the stop codon (UGA) in exon 45 is absent and the re-framed mRNA translation gives rise to a protein sequence where only 4 amino acids (aa) are exchanged.

Unedited patient cells showed a strong downregulation of *DYSF* mRNA when normalized to healthy control hPMs (Figure 4.8A). Degradation via nonsense-mediated decay (NDM) (Morse and Yanofsky 1969; Peltz, Brown, and Jacobson 1993) might explain a lower level of mRNA detected in unedited hPM-11. On the other hand, DYSF mRNA levels in sgRNA and sgRNA+G edited samples was significantly higher than unedited hPMs (Figure 4.8A), thus confirming a rescue of *DYSF* mRNA expression after gene editing.

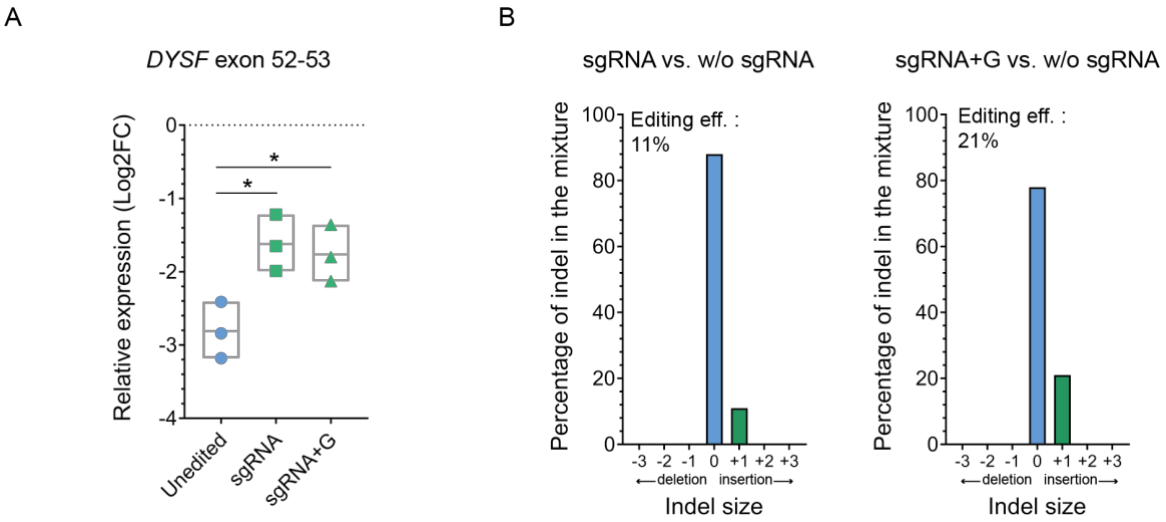

Figure 4.8: CRISPR/Cas9 induced re-framing of *DYSF* exon 44 rescued mRNA expression in hPM-11.
A) *DYSF* relative mRNA expression (amplified in exon 52-53) in sgRNA and sgRNA+G (~10 days of culture expansion) hPM-11 compared to the unedited sample (n=3 replicates). Data normalized to n=3 healthy control myoblasts. Two-sided unpaired t-test log2 fold change (Log2FC) values. *=p<0.05 **B)** Indel plots from ICE analysis showing the predicted editing efficiency of hPM-11 sgRNA and sgRNA+G samples, after ~10 of culture expansion.

However, I did not observe a total rescue of *DYSF* mRNA levels. This might depend on the "dilution" of edited cells within the unedited population occurring during *in vitro* expansion. Indeed, after ~10 days of culture the percentage of sequences carrying the re-framed *DYSF* exon 44 in edited hPM-11 dropped to 11% and 21% in sgRNA and sgRNA+G respectively (Figure 4.8B).

At the protein level, 4 aa would be exchanged compared to the WT sequence (Figure 4.7). Considering that *DYSF* loss of function is often caused by single point mutations with differences only in one or few aa (Leiden Open Variation Database, last update March 31, 2017), we asked whether those modifications are compatible with protein expression and membrane localization. To answer this, I first checked the expression of dysferlin in myoblasts via Western Blot (WB) using an antibody recognizing the C-terminal transmembrane domain of the protein. As shown in the WB, a band corresponding to the full-length dysferlin protein size was detected in both the sgRNA and sgRNA+G edited samples (Figure 4.9A, left plot). Dysferlin protein was undetectable in unedited patient cells. I confirmed this result in an independent experiment performed using sgRNA+G only (Figure 4.9A, right plot).

Additionally, I evaluated protein expression and localization via IF staining in edited (re-framed) patient myoblasts after differentiation into myotubes. As shown in Figure 4.9B, dysferlin was restored in single and multinucleated edited myotubes (Re-framed MT), and localized at the membrane as in healthy control myotubes (CTRL MT). As expected, no protein was detected in unedited patient myotubes (Unedited MT) (Figure 4.9B).

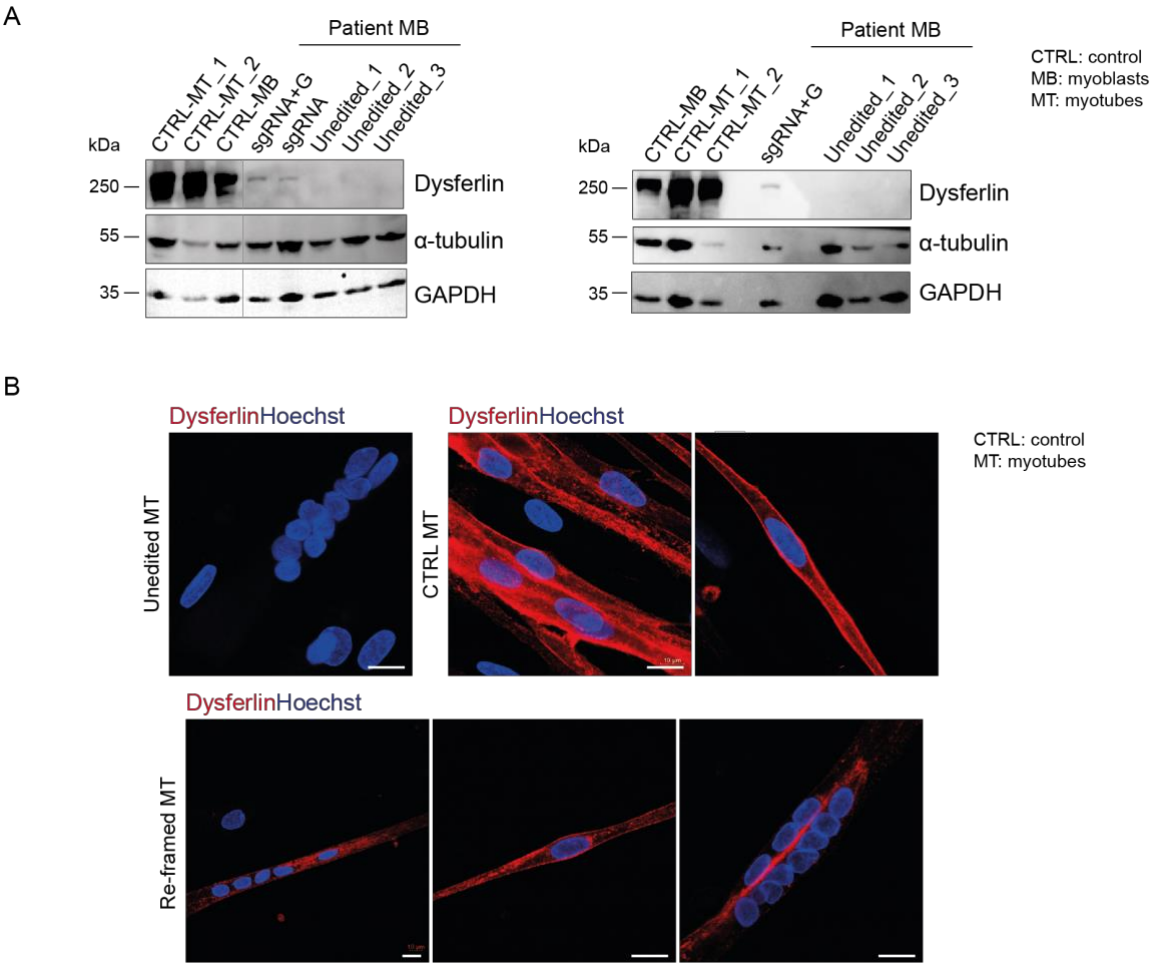

Figure 4.9: Re-framed dysferlin protein was re-expressed in patient-derived myoblasts and showed correct localization in differentiated myotubes.
A) Left plot, WB analysis of dysferlin of sgRNA and sgRNA+G samples compared to healthy CTRL myoblasts/myotubes and three unedited patient samples. Right plot, WB analysis of dysferlin from an independent experiment of sgRNA+G hPM-11. **B)** Representative pictures of dysferlin IF staining of unedited, CTRL and re-framed myotubes. (n=2 independent experiments). Scale bars = 20 µm.

Last, to investigate the capability of the re-framed dysferlin to participate in sarcolemmal repair after injury, I performed a laser-mediated wounding assay in patient-derived myotubes. Dysferlin and annexin A1 are known to localize at the wounding area or the “repair dome” (Marg et al. 2012). Here, I assessed their presence by IF 20 minutes after wounding in re-framed MT derived from edited patient PMs. Unedited MT and healthy CTRL MT were used as negative and positive controls, respectively. Re-framed MT showed both annexin A1 and dysferlin at the “repair dome” comparable to CTRL MT. In unedited MT, only annexin A1 was detected (Figure 4.10).

In conclusion, re-framing of the mutant *DYSF* exon 44 led to mRNA and protein rescue in patient myoblasts and to a correct localization of dysferlin at the membrane of myotubes as in healthy controls. After sarcolemmal injury, re-framed dysferlin participated in the membrane repair process together with annexin A1, indicating a functional rescue of the protein in mediating the resealing process.

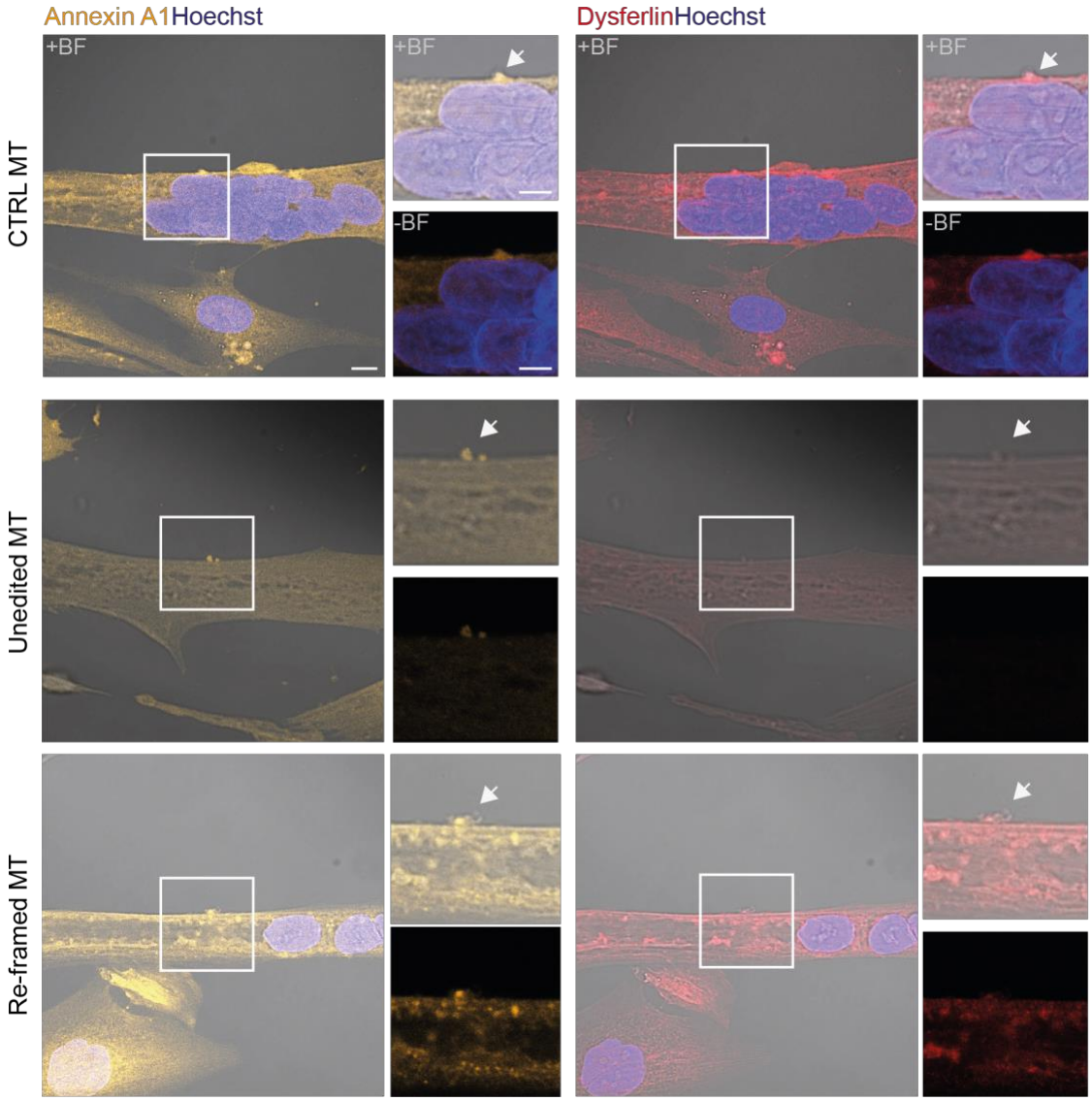

Figure 4.10: Annexin A1 and dysferlin were found enriched at the wounding area of re-framed myotubes after laser wounding.
Annexin A1 and dysferlin immunostaining and BF images of CTRL, unedited and re-framed MT performed up to 20 minutes after laser irradiation. Arrows indicate the wounding area (a.k.a. repair dome). Nuclei are counterstained with Hoechst. Scale bars = 5 µm, lower magnification and 10 µm, higher magnification.

4.2. Bacterial nanocellulose substrate maintains hPMs in a slowly-dividing and undifferentiated state

hPMs cultured in standard cell culture condition (named “Standard”) proliferate and progressively undergo differentiation or senescence thus resulting in a major decline of their regeneration potential and stemness properties for cell transplantation (Montarras et al. 2005; Gilbert et al. 2010). Preliminary data collected in our laboratory showed that hPMs cultured on a bacterial nanocellulose (BNC) substrate were able to be cultured longer than on Standard without the need to be passaged, suggesting a substantial reduction of hPMs proliferation rate.

BNC is a water-insoluble polysaccharide consisting of glucose molecules linked through β-1,4 linkages and can be produced by bacteria like *Gluconacetobacter xylinus* (Deinema and Zevenhuizen, 1971; Gullo et al., 2018; Kubiak et al., 2016). BNC has a good biocompatibility (Helenius et al. 2006), high water content (Gelin et al. 2007), and is chemically modifiable (Figueiredo et al. 2013; Huang et al. 2014). In our laboratory, BNC stiffness was evaluated to be ~15 KPa, much lower than the one of plastic dishes (~3GPa) and similar to the rigidity of skeletal muscle (~12 KPa) (Gilbert et al. 2010). Reproducing physiological tissue rigidity, organization and extracellular stimuli *in vitro* influence muscle stem cells behavior and could support self-renewal and regenerative potency when transplanted *in vivo* (Gilbert et al. 2010; Gillies and Lieber 2011; Quarta et al. 2016; Monge et al. 2017). Thus, we explored the BNC substrate as an alternative culture method able to avoid extensive hPMs propagation and differentiation.

Donor-derived PMs, isolated according to our established protocol (see Methods section 3.1.1.) were placed either on Standard or BNC and characterized as shown in Figure 4.11 for:

1. Morphology
2. Proliferation and differentiation properties
3. Molecular profiling, through a high-throughput RNA sequencing experiment

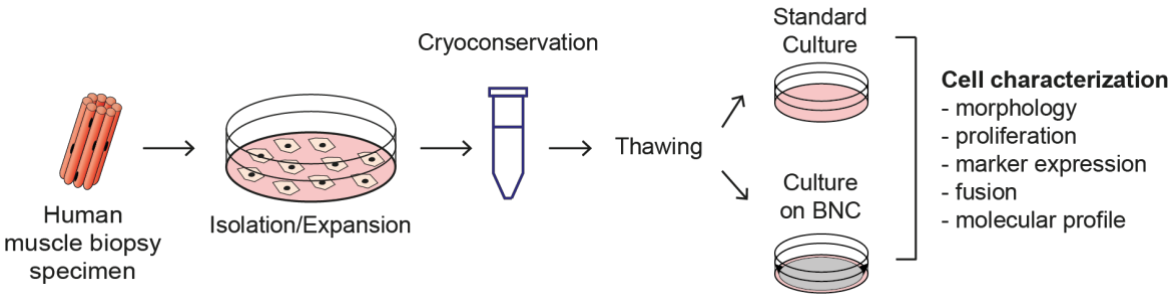

Figure 4.11: BNC characterization, experimental set-up.
Schematic illustration of isolation, expansion and conservation of hPMs. For each experiment, hPMs were seeded and compared on Standard or BNC.

4.2.1. hPMs morphology is altered on the BNC´s fibrils network

BNC thin fibrils are organized in a fine network (Yamanaka et al. 1989; Retegi et al. 2010) which mimics properties of the natural ECM (Petersen and Gatenholm 2011; Bäckdahl et al. 2006; Geisel et al. 2016). The same ultrastructure was observed in the BNC substrate used in this study via SEM (Figure 4.12A). I also investigated hPMs morphology using EM techniques. Representative SEM pictures showed how the fine network of the thin and long cellulose fibrils closely connect with the myoblasts after 2 days of culture (Figure 4.12B). In addition, the cells appeared round with thin elongations reaching into the BNC (Figure 4.12B). SEM higher magnification revealed vesicle-like structures on the myoblast´s membrane. Transmission EM pictures showed very close contact between adjacent hPMs on BNC, but no signs of fusion was detected (Figure 4.12C).

To better visualize hPMs membrane when cultured on BNC, I performed a WGA staining. IF analysis of the WGA staining showed round cell morphology and the presence of membrane vesicles, as observed in the SEM pictures (Figure 4.12D). The filamentous actin (F-Actin), detected with Phalloidin staining, appeared to be differently organized in comparison with cells on Standard. On BNC the Actin-protein was mainly localized at the sub-sarcolemmal space (Figure 4.12E, upper panel) instead of being structured as thin filaments along the cell cytoplasm, as observed in Standard (Figure 4.12E, lower panel).

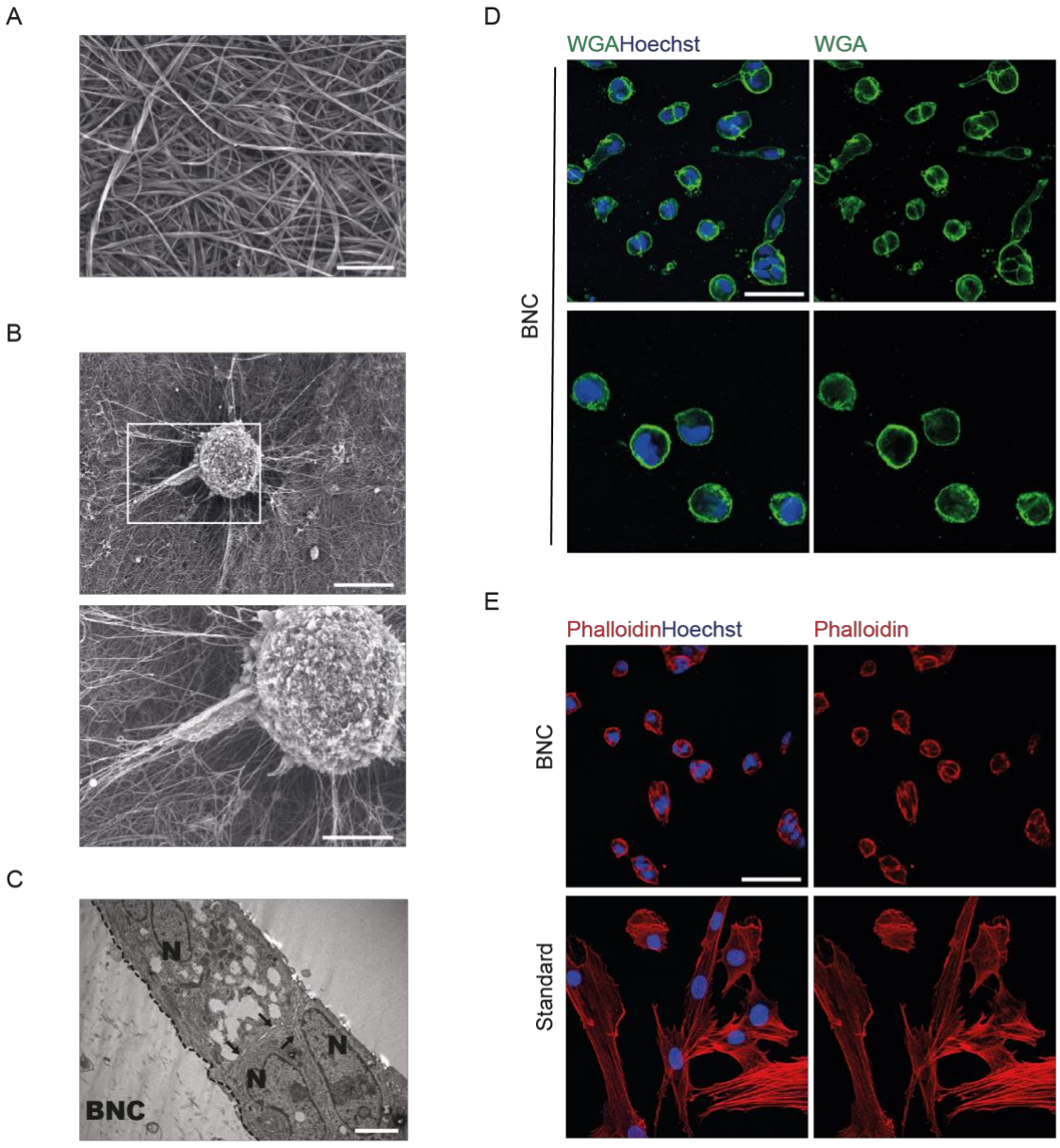

Figure 4.12: BNC substrate for hPMs culture: ultrastructure and morphology of hPMs on BNC.
EM pictures of pure BNC (scale bar = 1 µm) **(A)** and hPM-7 cultured on BNC **(B)** after 72 hours in culture (left, scale bar = 10 µm; right, scale bar = 5 µm). **C)** TEM pictures of hPMs on BNC. N: nucleus. Arrows: adherent junctions. Dotted line: hPMs/BNC interface. Scale bar = 100 µm. **E)** IF membrane stain for wheat germ agglutinin (WGA) of hPM-2 after 48h in culture on BNC. Scale bar = 50 µm. **E)** IF stain for Phalloidin detecting F-Actin of hPM-2 after 48h in culture on Standard (lower panel) or BNC (upper panel). Scale bar = 50 µm.

4.2.2. hPMs cultured on BNC show a slow proliferation rate

First data showed that donor-derived PMs cultured on BNC substrate were able to survive longer than the same number of cells seeded on Standard and did not require to be passaged (Figure 4.13A). In addiction we observed that, when hPMs were detached and counted after having been kept for 14 days in both culture conditions, cells on Standard had aged from P7 to P12 and had gone through 4 additional rounds of splitting with an at least 100 fold increase in cell number. Conversely, on BNC, hPMs had not been split for 14 days and had shown only ~2 fold increase in cell number (Figure 4.13B). Complementary experiments showed that hPMs reached confluence on BNC only after ~30 days of culture (Figure 4.13C).

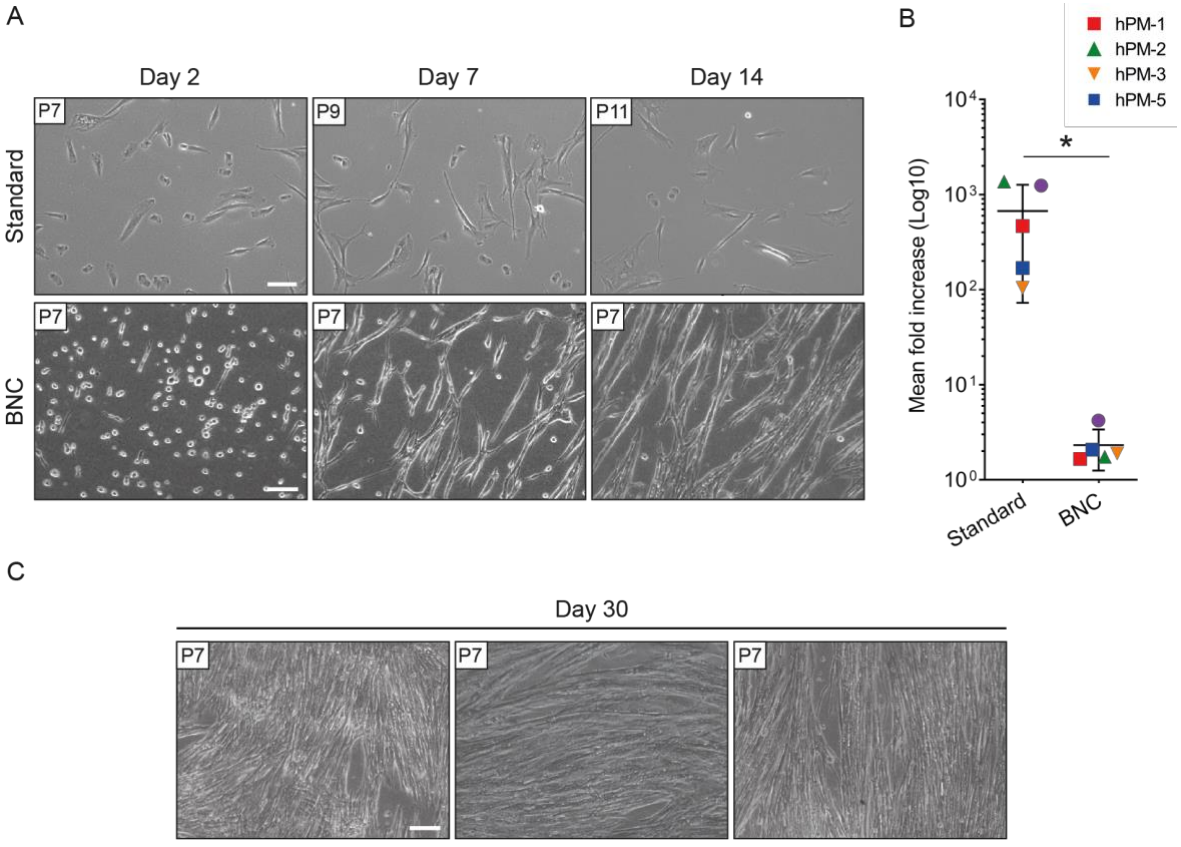

Figure 4.13: Long-term culture and proliferation evaluation of hPMs on BNC.
A) BF representative pictures of hPMs in Standard (upper panel) and on BNC (lower panel) on various time points. Scale bar = 25 µm. P, passage. **B)** Quantification of proliferation of hPMs cells under Standard and BNC (n=5 donors, hPM-1,2,3,4,5; mean±SD). Two-sided unpaired t-test. *=p<0.05. **C)** BF representative pictures of hPMs cultured on BNC until day 30. (n=3 donors, hPM-1,2,5). Scale bar = 25 µm. P, passage.

To further investigate this aspect, we seeded hPMs at low density (1000 cells) on Standard or BNC, monitoring the cell growth for 21 days (Figure 4.14). Interestingly, the cells on Standard reached confluence already after 14 days and at 21 days started to detach and die (Figure 4.14, upper panel). On the other hand, hPMs cultured on BNC never reached confluence and proliferated via a very slow clonal division pattern (Figure 4.14, lower panel).

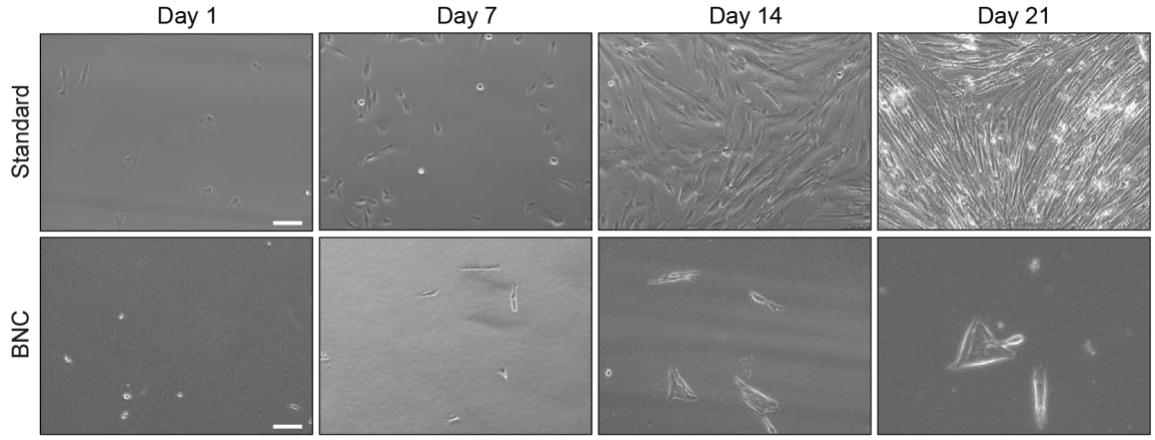

Figure 4.14: Low-density hPMs culture on BNC.
Representative BF pictures of hPMs seeded, on Standard (upper panel) and on BNC (lower panel), at low density (1000 cells) and cultured for 21 days (n=2 donors). Scale bar = 100 µm.

4.2.3. hPMs cultured on BNC are retained in G0/G1 cell cycle phase and maintain a myogenic phenotype

As a further analysis of cell division rate on BNC compared to Standard, I stained hPMs for Ki-67, widely used as a proliferation marker. Ki-67 protein has a variable expression pattern throughout the cell cycle. Its levels are low during the G1 and early S-phase and increases progressively reaching a maximum level during mitosis. A rapid reduction occurs during anaphase and telophase (Gerdes et al. 1983; Sun and Kaufman 2018; Booth and Earnshaw 2017; Cuylen et al. 2016). Ki-67 is thus expressed during all active phases of the cell cycle, and is absent from terminally differentiated, resting or quiescent cells. When hPMs were placed on BNC, Ki-67 protein expression was significantly downregulated after 7 ($p=0.001$) and 14 days of culture ($p=0.009$) compared to Standard (Figure 4.15A). On the mRNA level Ki-67 (*MKI67*) relative expression (RTq-PCR) was significantly reduced at 2 days and 7 days after seeding on the BNC in comparison to Standard (Figure 4.16).

Ki-67 expression analysis already showed that a high percentage of cells were in a resting cell cycle phase (G0 or G1-phase). However, to define the cells cycle status of hPMs on BNC, I performed a BrdU incorporation assay. BrdU as an analogue of thymidine, is efficiently incorporated into the DNA of replicating cells (the S-phase of mitosis). BrdU containing DNA was subsequently detected with a BrdU-specific antibody and cell's DNA content marked with PI.

The number of cells in each phase of the cell cycle was quantified via flow cytometry analysis. The percentage of hPMs in G0/G1-phase changes from a mean of 61.7% in Standard to 94.3% on BNC. Conversely the percentage of hPMs in S-phase goes form 25.8% in Standard to 1.1% on BNC. (Figure 4.15B). Notably, the S/G2-phases ratio resulted to be different between the two conditions. In Standard the number of cells in S-phase are ~2 fold higher compared to the one in G2 (25.8% vs. 11.5%) while on BNC the S/G2-phases ratio is equal to 0.5 (1.1% vs. 2.5%). This might indicate a higher velocity of DNA duplication in the Standard group compared to BNC.

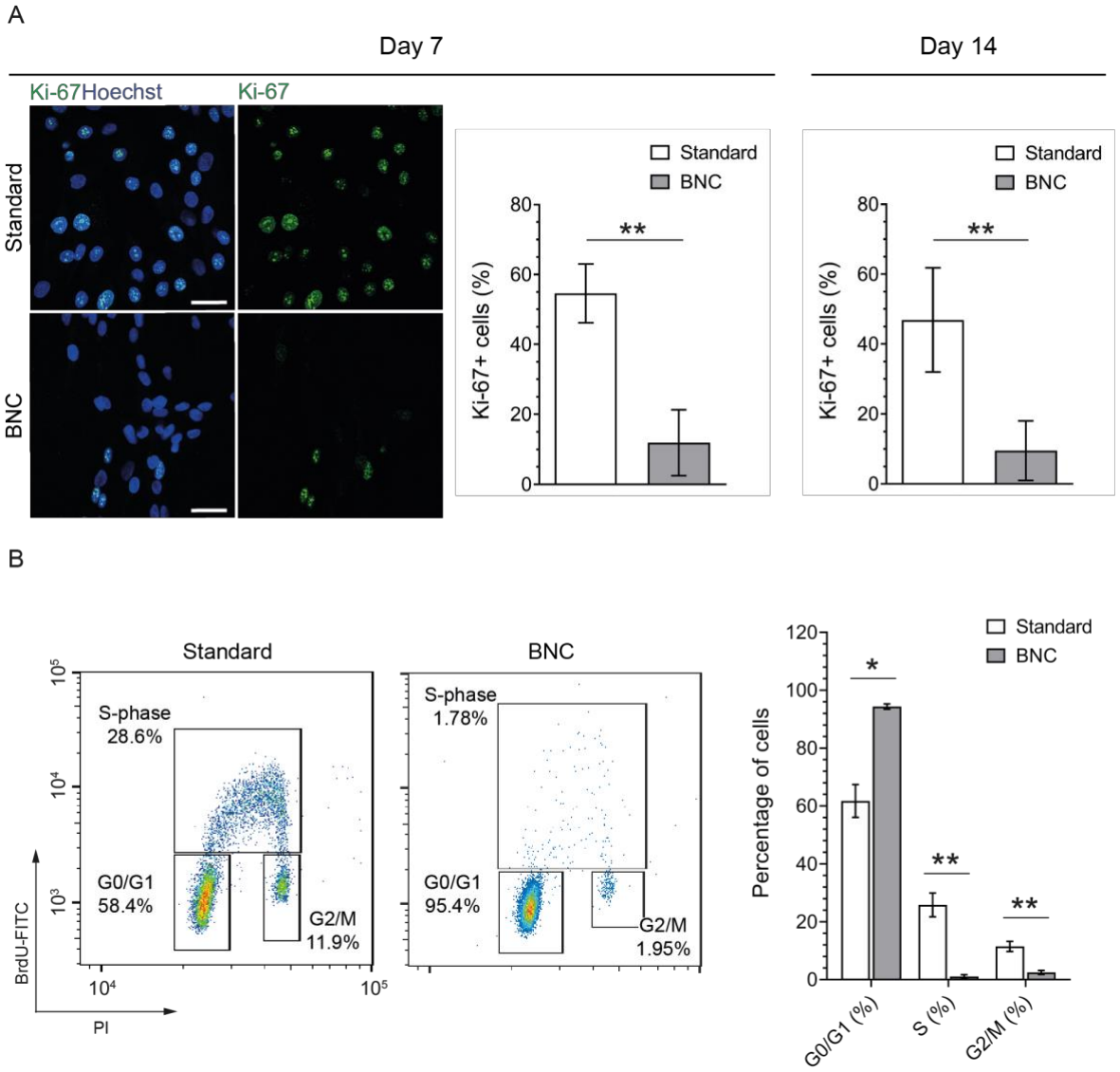

Figure 4.15: Slow-dividing state and cell cycle "arrest" in hPMs on BNC.
A) IF stain for Ki-67 (green) and Hoechst after 7 days in culture on BNC compared to Standard. Scale bar = 25 µm. Quantification of Ki-67 expression after 7 and 14 days (n=4 donors, hPM-1,2,3,5; mean±SD). **B)** Right, cell cycle analysis by FACS using combined PI and BrdU staining (PI-BrdU) (hPM-1). The gates are set according to PI-BrdU negative controls. Left, quantification of the percentage of hPMs in each phase of the cell cycle (n=3 donors, hPM-1,2,3; mean±SD). Two-sided unpaired t-test. *=p<0.05 **=p<0.01.

To ensure that the cells were maintained as myogenic, I quantified *PAX7*, *MYOD1* and *MYF5* mRNA levels by RTq-PCR, 2 days and 7 days after seeding on BNC or on Standard. The myogenic markers were equally expressed in hPMs cultured in either condition (Figure 4.16).

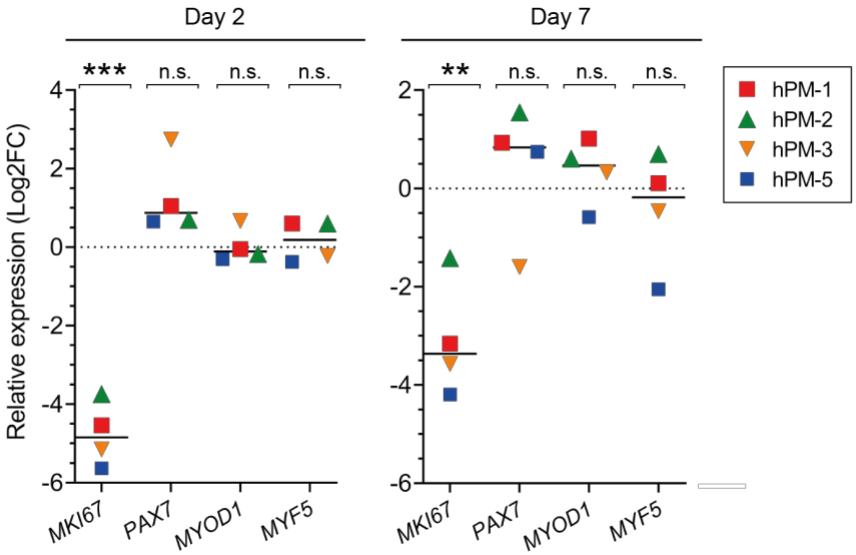

Figure 4.16: Myogenic characterization of hPMs on BNC.
MKI67 and myogenic markers relative mRNA expression in hPMs (day 2 and day 7 of culture) on BNC compared to Standard. Standard hPMs: Day 2 at P8; Day 7 at P10. BNC hPMs: P8 (n=4 donors; hPM-1,2,3,5; black bars show the median). Two-sided unpaired t-test calculated on Log2FC values. **=p<0.01; ***=p<0.001; n.s.= not significant.

To investigate the terminal differentiation efficiency, I induced differentiation of confluent hPMs in either culture condition through four days of starvation. Then, I detected the differentiation marker MYHC via immunostaining. Fusion of hPMs into myotubes was highly inhibited on BNC, as a drastic reduction of the number of multinucleated MYHC positive myotubes in BNC culture was observed compared to Standard. Reduction of the fusion efficiency was quantified by the analysis of the fusion index (Figure 4.17).

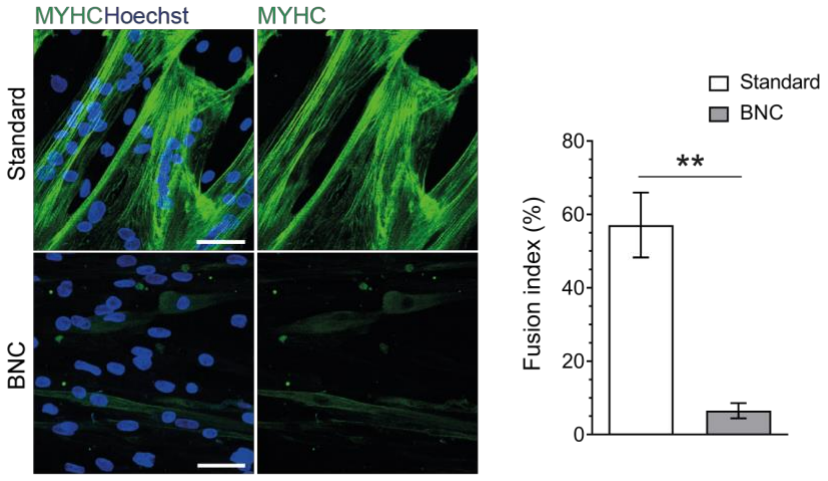

Figure 4.17: Evaluation of hPMs fusion property on BNC.
IF stain for MYHC (green) and Hoechst in hPMs 30 days in culture after fusion induction. Scale bar = 100µm. Fusion index calculated from hPMs in Standard (n=2 wells for each donors; n=4 donors; hPM-1,2,3,5) or on BNC (n=2 wells for each cell line; n=3 donors; hPM-1,3,5; mean±SD). Two-sided unpaired t-test. **=p<0.01.

From this first analysis, we concluded that BNC caused a cell cycle “arrest” in hPMs while preserving the expression of early myogenic markers for at least 7 days of culture. Even when confluent and in differentiating conditions, the hPMs on BNC did not fuse into myotubes maintaining an undifferentiated state.

4.2.4. hPMs recover proliferation and differentiation capability after detachment

With the intent to apply the BNC as a hPMs culture strategy for therapeutic approaches (e.g. autologous cell transplantation), we asked whether hPMs would recover proliferation, viability and differentiation properties once removed from the BNC substrate and re-plated in Standard.

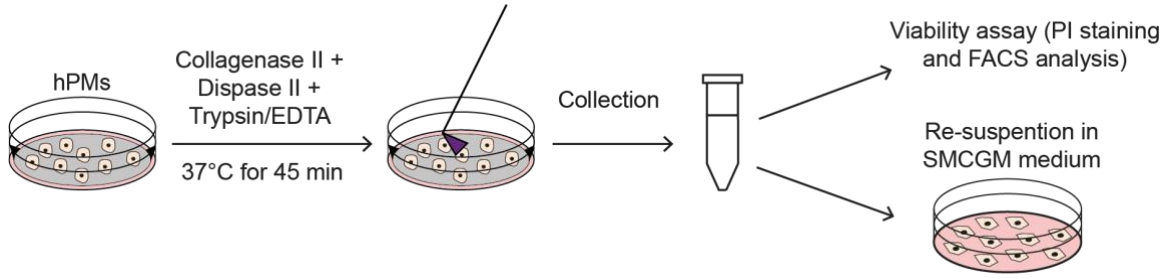

Figure 4.18: Illustration of the different steps for hPMs detachment from BNC substrate.
After ~15 days of culture, hPMs were detached by an enzymatic treatment for 45 min at 37°C and then gently scraped to be plated back on Standard after being evaluate for cell viability.

As first, I optimized a protocol to completely and gently detach the cells from the substrate (Figure 4.18 and Methods section 3.1.2.3.). After detachment (defined as post-BNC), BF pictures of “empty” cellulose substrate proved that the cells were completely removed from BNC using the new protocol (Figure 4.19A). Post-BNC cells were labeled with PI that is a fluorescent intercalating agent and indicator of cell death. The resulting range of dead cells is between 3% and 6% (Figure 4.19B) is similar to the one quantified in cells grown under standard condition (data not showed).

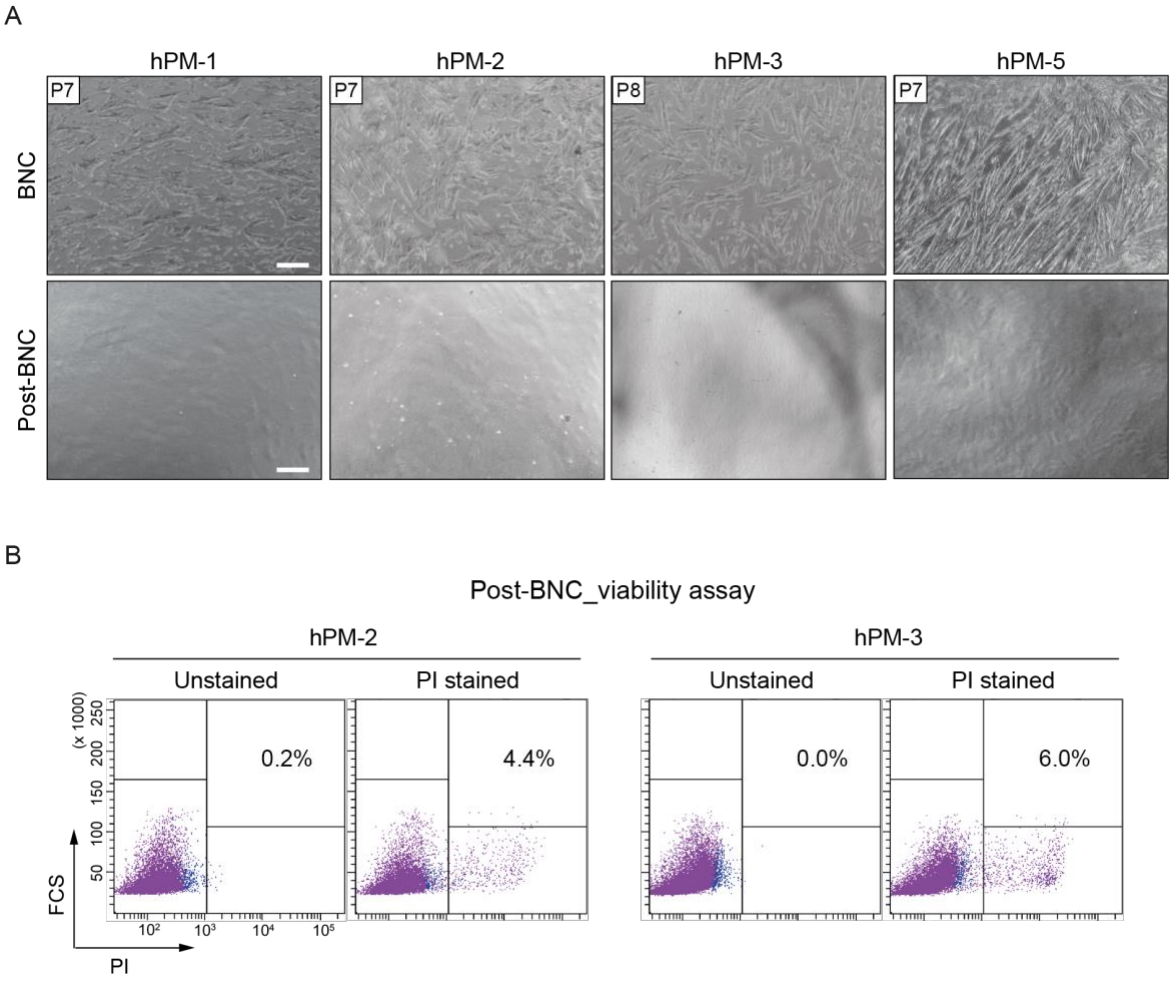

Figure 4.19: hPMs detachment from BNC and viability assay.
A) BF representative pictures of hPMs on BNC before detachment (upper row) and after detachment (lower row) (n=4 donors, hPM-1,2,3,5). Note the absence of cells on the BNC after detachment. **B)** Determination of cell viability using PI and flow cytometry analysis hPM-2 and hPM-3 after detachment from BNC.

Post-BNC, hPMs were plated on Standard and cultured for ~15 days (6 passages). During this period I assessed proliferation and differentiation ability (Figure 4.20).

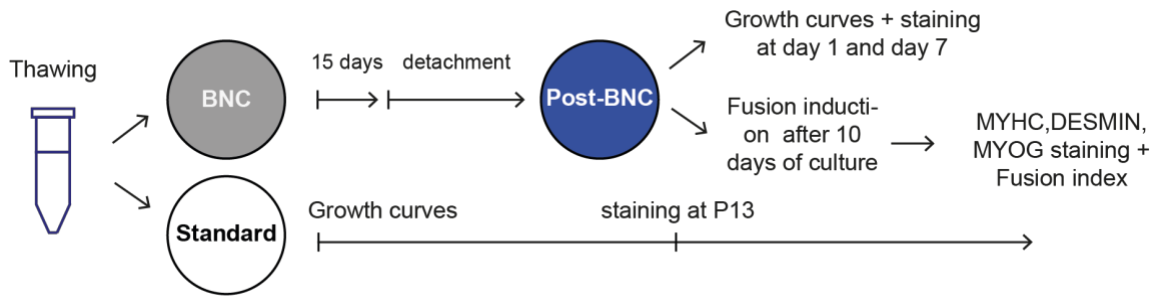

Figure 4.20: Experimental design to assess proliferation and differentiation potential of hPMs post-BNC.

After being kept on BNC for ~15 days, hPMs were detached and moved to Standard (post-BNC). Proliferation and differentiation were assessed 1 and 7 days after detachment in post-BNC and compared to Standard.

Proliferation in post-BNC hPMs started within 48 hours. I generated growth curves counting the cells every passage post-BNC in comparison with hPMs derived from Standard. Growth analysis showed that the cell number increased $1*10^4$ fold over ~15 days and 6 passages post-BNC. In addition, post-BNC hPMs (blue line) showed a faster proliferation velocity than hPMs that had been kept on Standard (black line) for the same period of time (Figure 4.21).

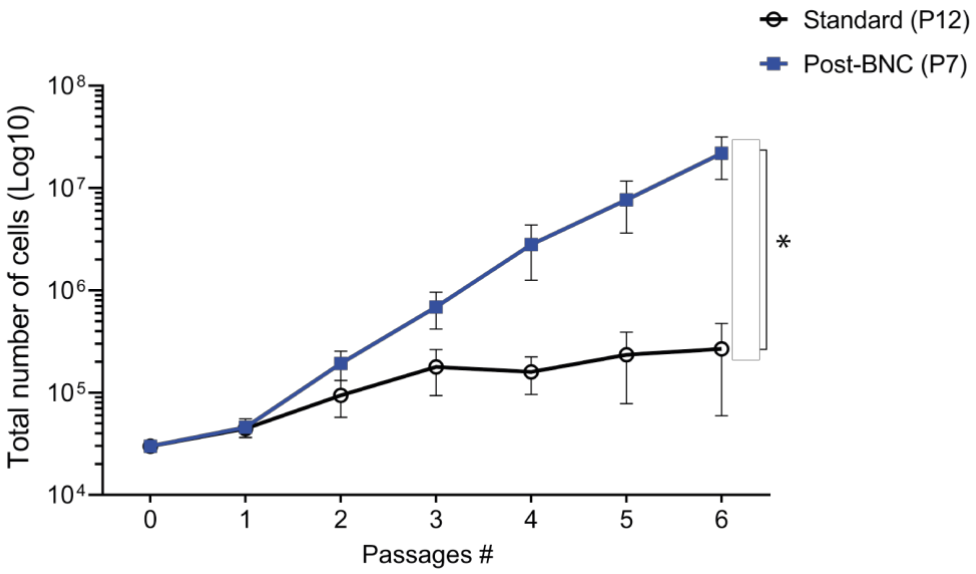

Figure 4.21: Recovery of proliferation potential of hPMs post-BNC.
Growth curves of Standard and post-BNC hPMs cultured up to 6 passages after ~15 days of culture; Standard hPMs in P12 and post-BNC in P7 (n=2 wells each donor; n=4 donors, hPM-1,2,3,5; mean±SEM). Two-way ANOVA. *=p<0.05

If post-BNC proliferation is regained, Ki-67 proliferation marker expression was also expected to vary. Staining for Ki-67 revealed a rapid increase of its expression between day 1 and day 7 in post-BNC hPMs, confirming the recovery of the proliferation capability (Figure 4.22A, B). At 7 days Ki-67 expression was significantly higher in post-BNC hPMs than in hPMs which had been kept on Standard, thus further confirming that hPMs, once retrieved from BMC, proliferate at a quicker rate. (Figure 4.22A). BF pictures at 7 days after detachment showed a similar hPMs morphology compared to the cells on Standard at early cell passage (P8) (Figure 4.22B).

No significant changes in protein expression of the myogenic markers desmin, Pax7 and MyoD1 were detected on hPMs 1 day and 7 days post-BNC compare to Standard (Figure 4.22A).

A

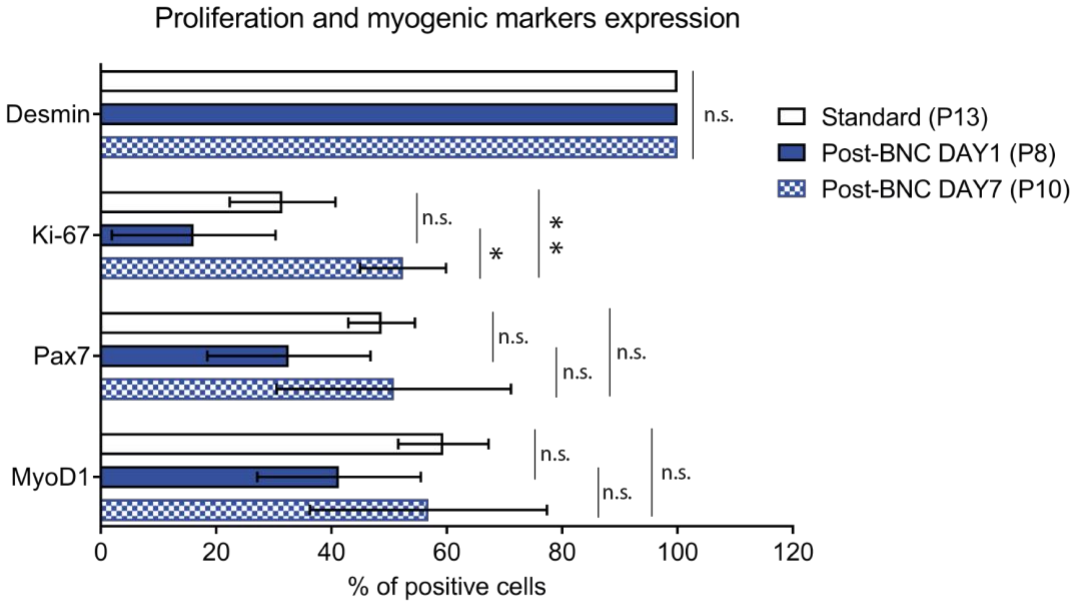

B

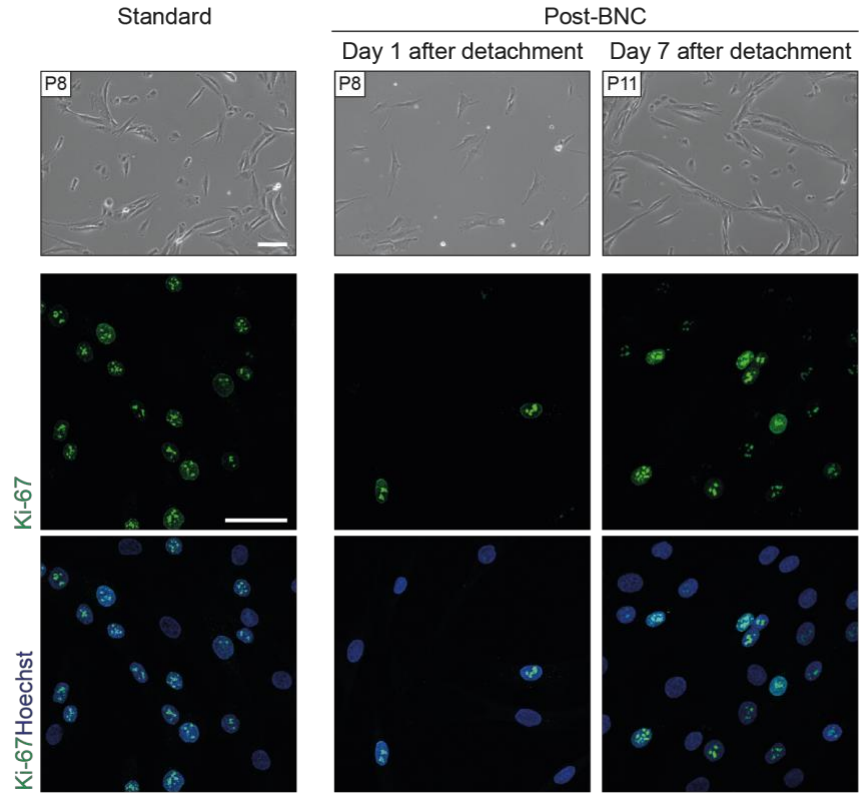

Figure 4.22: Recovery of morphology and Ki-67 expression of hPMs post-BNC.
A) Proliferation and myogenic markers protein expression in Standard hPMs and in post-BNC 1 day and 7 days after detachment. Standard hPMs: P13. Post-BNC hPMs: Day 1 at P8; Day 7 at P10 (n=2 wells each donors; n=4 donors, hPM-1,2,3,5; mean±SD). Two-sided unpaired t-test. *=p<0.05; **=p<0.01. **B)** Upper, representative BF pictures of P8 Standard hPM-1 compared to post-BNC hPM-1 at day 1 (P8) and day 7 (P10). Scale bar = 100 µm. Lower, IF staining for Ki-67 reveals a rapid increase of its expression between day 1 and day 7 in post-BNC hPMs to similar levels of Standard hPMs (n=4 donors, hPM-1,2,3,5). Scale bar = 25 µm.

To determine whether hPMs were still functional and able to terminally differentiate into multinucleated myotubes post-BNC, I induced post-BNC cells to fuse on Standard. The myotubes after fusion were multinucleated, expressed MYHC with clear sarcomeres' striation and showed MYOG (marker of differentiation) positive nuclei. The fusion index was shown to be comparable with hPMs that were kept on Standard only (57.1% (Figure 4.17) vs. 65% (Figure 4.23)).

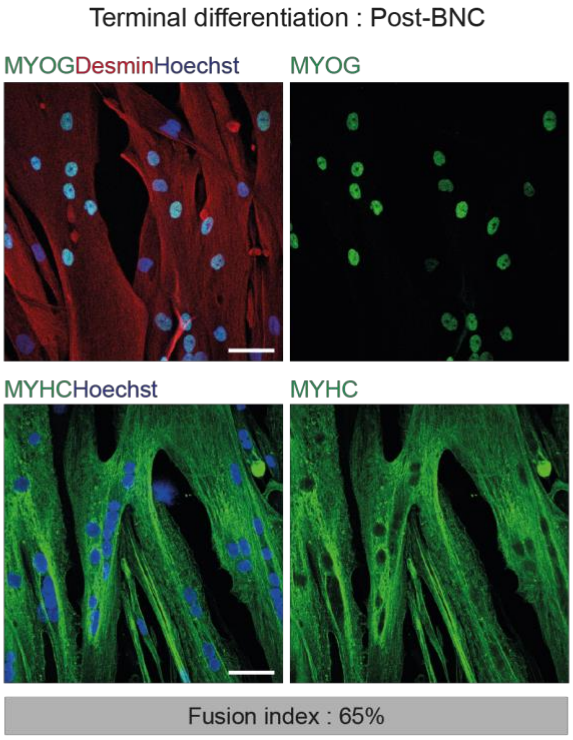

Figure 4.23: Recovery of differentiation potential of hPMs post-BNC.
IF staining for MYOG and MYHC demonstrates normal differentiation capacity of post-BNC hPMs with a fusion index of 65% (n=4 donors, hPM-1,2,3,5). Scale bar = 50 µm.

Here I showed that hPMs that were successfully and safely detached from BNC, display an enhanced proliferation potential, are still myogenic and are able to fuse into terminal differentiated myotubes.

4.3. Transcriptional profiling of hPMs on BNC vs. Standard.

To investigate the molecular mechanisms of the cellular phenotype displayed by hPMs cultured on BNC, we performed a total RNA sequencing experiment.

I thawed hPM-2 in P7 and seeded them on Standard. After 2 days of cell expansion I collected 1/3 of the hPMs for RNA isolation (Standard at DAY 0). The rest of the cells was seeded either on BNC or on Standard to be collected after 2 days (DAY 2) and 7 days (DAY 7) for RNA isolation (Figure 4.24). To obtain reliable results, two independent technical replicates per sample (a-b) were included in the analysis.

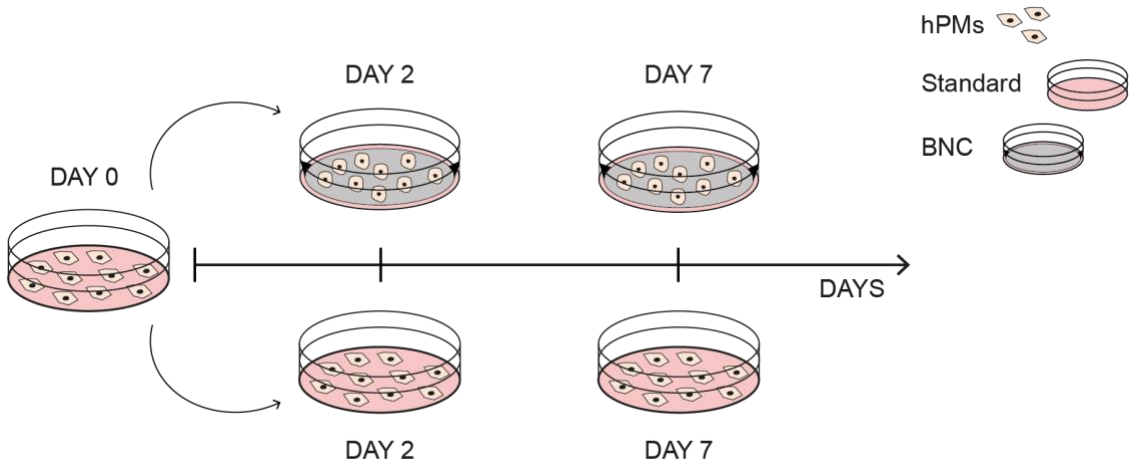

Figure 4.24: Illustration showing point of times and conditions of hPMs collection for RNA sequencing analysis.
hPMs at DAY 0 were in part collected for RNA isolation and the rest was seeded both on Standard and on BNC. Subsequently, cells collection was performed at DAY 2 and DAY 7 from both culture conditions.

RNA sequencing was completed in cooperation with the Genomics Platform (Dr. Sascha Sauer, Max Delbrück Center for Molecular Medicine, Berlin, Germany). For the differential transcript expression analysis, DEseq2 (Anders & Huber, 2010) with a padj<0.05, was run by Dr. Daniele Yumi Sunaga-Franze in the Genomics Platform. Differentially expressed transcripts (DETs) between BNC and Standard samples were identified using paired analysis and three different comparisons considered (Table 4.1).

4.3.1. RNA sequencing results indicate two different RNA signatures in hPMs on BNC vs. Standard

For RNA sequencing analysis, we performed the following comparisons (Table 4.1):

- Comparison #1: hPM-2 on Standard at DAY 0 vs. BNC at DAY 2.

Aim: to detect gene expression changes induced in hPMs throughout the first 2 days since the passage from Standard to BNC condition.

The DETs obtained from this comparison were normalized to the 43 DETs derived from the analysis of hPM-2 on plastic between DAY 0 and DAY 2 (hPM-2 on Standard at DAY 0 vs. DAY 2) and 3293 DETs were found.

- Comparison #2: hPM-2 on Standard at DAY 2 vs. BNC DAY 2;

Aim: to detect gene expression changes between hPMs on BNC or Standard at the same point of time: DAY 2. → 9127 DETs were identified

- Comparison #3: hPM-2 on Standard at DAY 7 vs. BNC at DAY 7

Aim: to detect gene expression changes between hPMs on BNC or Standard at the same point of time: DAY 7. → 1723 DETs were identified.

Comparison		DETs p<0.05	% of downregulated DETS
#1	hPM-2 on Standard at DAY 0 vs. BNC at DAY2 normalized to hPM-2 on Standard at DAY 0 vs. DAY2	3293	75.3
#2	hPM-2 on Standard at DAY 2 vs. BNC at DAY2	9127	75.1
#3	hPM-2 on Standard at DAY 7 vs. BNC at DAY7	1723	62.9

Table 4.1: DETs found via total RNA sequencing between BNC and Standard samples for each comparison.
Table showing the three different comparisons considered for the RNA sequencing analysis. The total number of found DETs and the percentage of downregulated DETs is reported in the table for each comparison.

The Heat-maps display an extract of the most significant DETs derived from RNA sequencing analysis for each comparison, filtered by Log2FC. A clear separation between (Figure 4.25A) from hPMs on BNC and Standard was already clear in Comparison #1 and was confirmed in #2 (Comparison #2) and #3 (Comparison #3) (Figure 4.25B,C). Moreover, most of the DETs that were detected, were downregulated on BNC, showing a low overall RNA expression level of cells cultured on BNC compared to Standard.

A

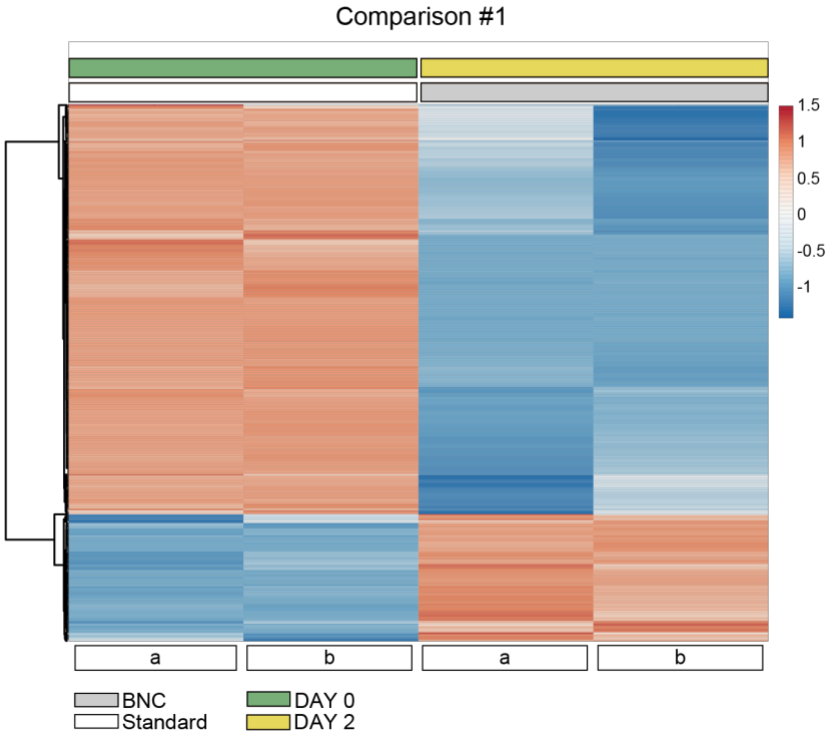

B

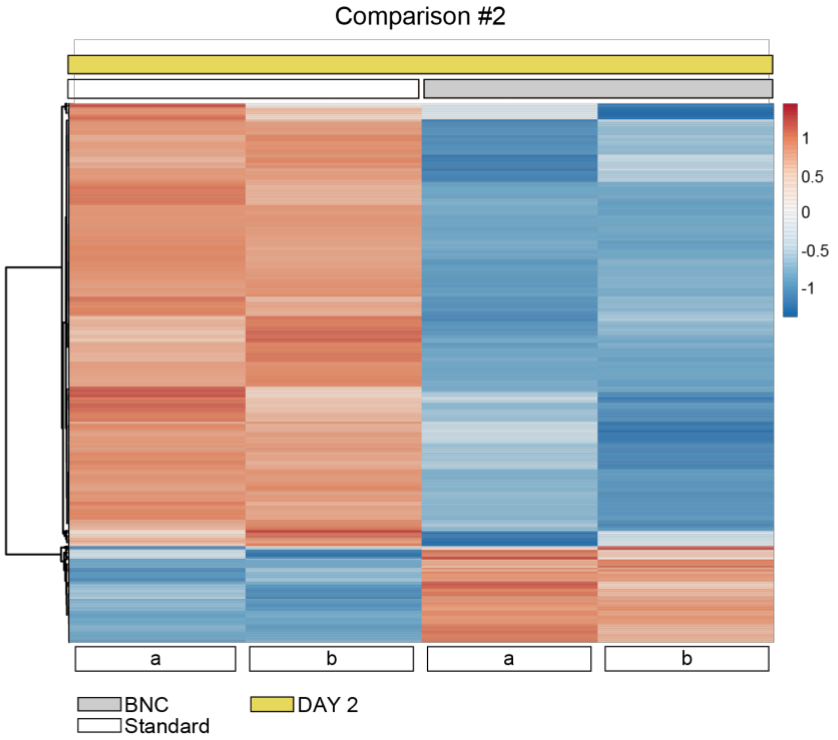

C

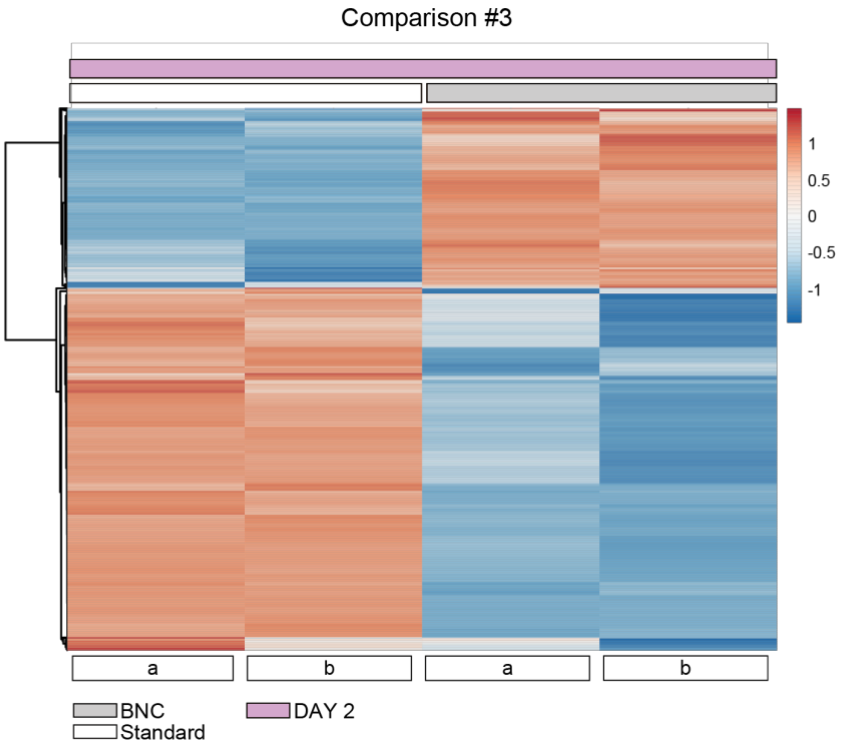

Figure 4.25: Heat-maps representation of total RNA sequencing of hPM-2 on BNC compared to Standard at different points of time.

Heat-maps showing the most significantly DETs (selected for protein-coding only) according to the padj value (padj<0.05) and filtered by Log2FC (all values >2 and <-2) for comparison #1 **(A)**, comparison #2 **(B)** and comparison #3 **(C)**. Orange represents the upregulated DETs and blue the downregulated DETs. DETs are shown according to their expression counts values (reads) ln(x + 1)-transformed. Rows and columns are

clustered using correlation distance and complete linkage. The two independent RNA sequencing replicates per sample (a – b) clearly clustered together in all comparisons.

4.3.2. RNA sequencing results confirm the cell cycle arrest in hPMs on BNC

We proceeded with an enrichment pathway analysis using a ConsensusPathDB database and applied it to all the comparisons. Some of the significantly enriched pathways or terms that we considered related to the cells phenotype described in the results part above are listed in Table 4.2.

PATHWAYS - COMPARISON #1	SOURCE	EXTERNAL ID	SIZE	P-VALUE
CELL CYCLE	Reactome	R-HSA-1640170	551	4.01E-92
CELL CYCLE, MITOTIC	Reactome	R-HSA-69278	468	2.51E-85
M PHASE	Reactome	R-HSA-68886	267	2.04E-51
RHO GTPASE EFFECTORS	Reactome	R-HSA-195258	299	6.97E-48
SIGNALING BY RHO GTPASES	Reactome	R-HSA-194315	434	3.07E-38
CELL CYCLE CHECKPOINTS	Reactome	R-HSA-69620	158	2.4788E-28
S PHASE	Reactome	R-HSA-69242	82	5.90424E-13
ECM-RECEPTOR INTERACTION	KEGG	path:hsa04512	82	0.000258373
INTEGRIN SIGNALING PATHWAY	BioCarta	integrinpathway	34	0.000538417
CELL-EXTRACELLULAR MATRIX INTERACTIONS	Reactome	R-HSA-446353	16	0.001020805

PATHWAYS - COMPARISON #2	SOURCE	EXTERNAL ID	SIZE	P-VALUE
CELL CYCLE	Reactome	R-HSA-1640170	551	3.12E-77
CELL CYCLE, MITOTIC	Reactome	R-HSA-69278	468	7.88E-75
M PHASE	Reactome	R-HSA-68886	267	5.79E-41
RHO GTPASE EFFECTORS	Reactome	R-HSA-195258	299	7.57E-27
SIGNALING BY RHO GTPASES	Reactome	R-HSA-194315	434	5.67E-23
CELL CYCLE CHECKPOINTS	Reactome	R-HSA-69620	158	7.53E-18
S PHASE	Reactome	R-HSA-69242	82	4.27E-11
INTEGRIN-MEDIATED CELL ADHESION	Wikipathways	WP185	101	0.000151
INTEGRIN SIGNALING PATHWAY	BioCarta	integrinpathway	34	0.000597

EXTRACELLULAR MATRIX ORGANIZATION	Reactome	R-HSA-1474244	295	0.001694
ECM-RECEPTOR INTERACTION	KEGG	path:hsa04512	82	0.009816

PATHWAYS - COMPARISON #3	**SOURCE**	**EXTERNAL ID**	**SIZE**	**P-VALUE**
CELL CYCLE, MITOTIC	Reactome	R-HSA-69278	468	6.77E-34
CELL CYCLE	Reactome	R-HSA-1640170	551	4.64E-32
RHO GTPASE EFFECTORS	Reactome	R-HSA-195258	299	1.35E-30
SIGNALING BY RHO GTPASES	Reactome	R-HSA-194315	434	4.24E-26
M PHASE	Reactome	R-HSA-68886	267	4.58E-25
CELL CYCLE CHECKPOINTS	Reactome	R-HSA-69620	158	1.4726E-10
INTEGRIN	INOH	None	124	7.24415E-06
EXTRACELLULAR MATRIX ORGANIZATION	Reactome	R-HSA-1474244	295	2.50959E-05
INTEGRIN-MEDIATED CELL ADHESION	Wikipathways	WP185	101	0.000362539

Table 4.2: ConsensusPathDB enrichment signaling pathways analysis obtained from total RNA sequencing.
The table show pathways of interest found to be among the most differentially regulated (according to the p-value score > 0.05) between hPM-2 on Standard at DAY 0 and BNC at DAY 2 (Comparison #1), hPM-2 on Standard and BNC at DAY 2 (Comparison #2) and hPM-2 on Standard and BNC at DAY 7 (Comparison #3).

Terms related to cell cycle regulation and progression (e.g. “Cell cycle”; “M phase”; “Cell cycle, mitotic”) were found to be among the most significant (lower p-value score) differentially regulated pathways between DAY 0 and DAY 2 on BNC compared to Standard (comparison #1; Table 4.2). Those pathways were still enriched for the duration of the 7 days of culture (comparison #2, #3; Table 4.2).

As previously shown, BNC induces the reduction of hPMs proliferation rate (Figure 4.13 and Figure 4.16) with a majority of the cells retained in G1/G0 cell cycle phases (Figure 4.15). As a consequence, I expected a downregulation of genes related to cell cycle in the RNA sequencing results. To confirm that, I selected the DETs related to “Cell cycle” of all three comparisons and plotted them into a volcano plot (source Reactome; external ID: R-HSA-1640170). As it is shown in Figure 4.26, almost all the DETs were significantly downregulated in hPM-2 on BNC compared to Standard (Figure 4.26A,B,C). This data corroborates our previous observations on a cell cycle “arrest” induced by BNC in hPMs. Moreover, cyclins (CCNs) (e.g. CCND2, CCNA2, CCNB1) have been found among the downregulated transcripts (Figure 4.26A,B,C). They are known to control both the G1/S and the G2/M transition phases of the cell cycle via complex formation with the cyclin-dependent protein kinases (CDKs), which were also found to be downregulated (Figure 4.26A,B,C) (Yang, Hitomi, and Stacey 2006; Pagano et al. 1992; Brown et al. 2007). Lastly, E2F1 (E2 promoter binding factor 1) expression was significantly decreased within the “Cell cycle” pathway (Figure 4.26A,B,C). E2F1 is a transcription factor responsible for the progression through

the G1-phase via transcriptional activation of genes involved in cell cycle regulation or in DNA replication (Paik et al. 2010).

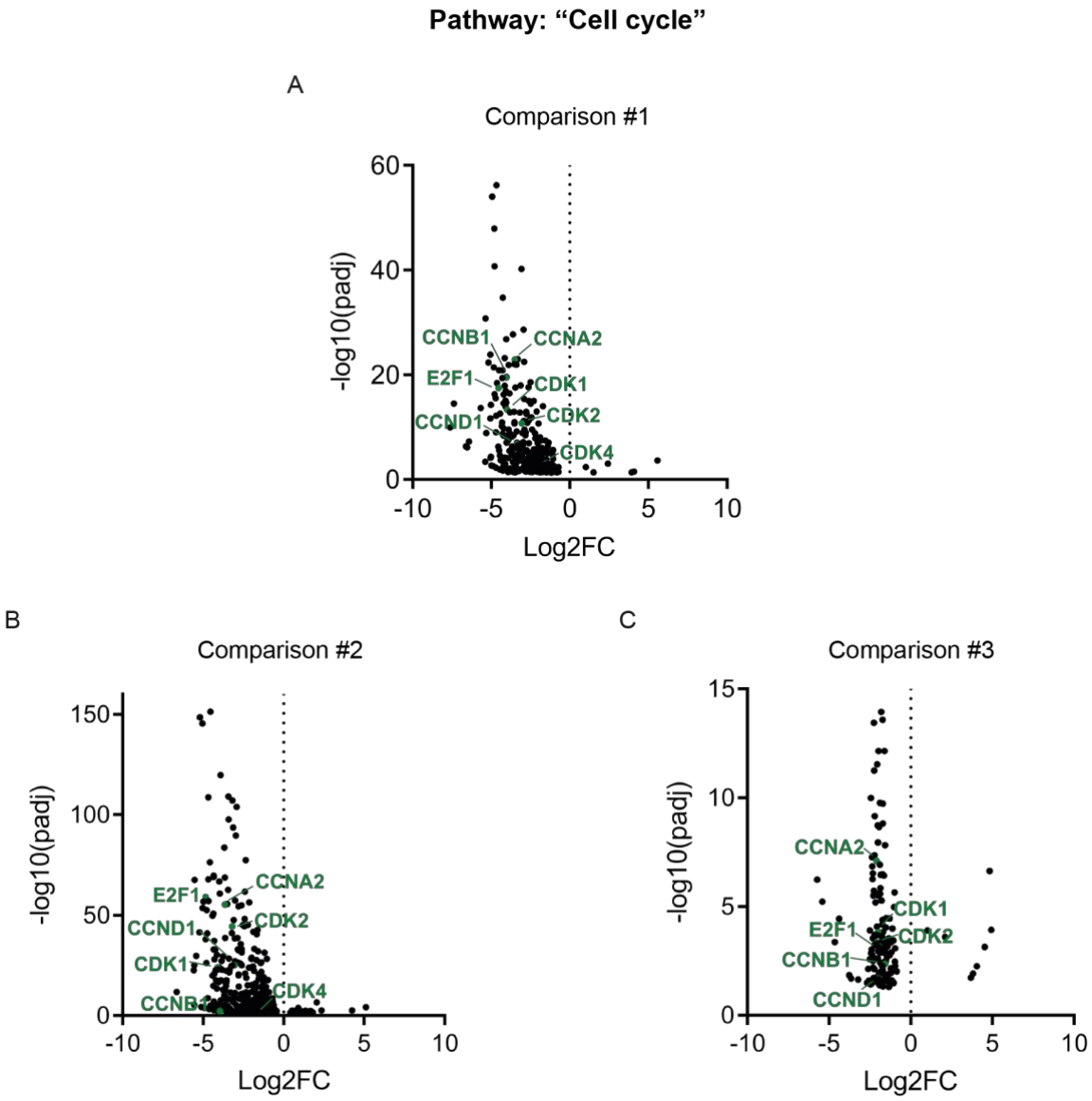

Figure 4.26: DETs trend of expression within a differentially regulated pathway of interest between BNC and Standard samples.
Volcano plots of statistical significance (-log10(padj)) against Log2FC, representing DETs (black dots) found within the term "Cell cycle" from the enrichment pathway analysis in comparison #1 (A), #2 (B) and #3 (C). Some of DETs of interest (CCNs, CDKs and E2F1) are marked (green dots).

The enrichment signaling analysis unveiled other pathways known to be involved in a wide range of cellular biological mechanisms, which could play a significant role in driving our cellular phenotype on BNC. Remarkably, pathways involving Rho GTPases activity and integrins belonged to the differentially regulated terms in all three comparisons (Figure 4.27A,B,C). Some genes of the GTPases Rho subfamily like Ras homolog family member (RHO) A, B, C, the Rac family small GTPase 1 (RAC1) and the cell division cycle 42 (CDC42) were found significantly differentially expressed (Figure 4.27A,B,C). These molecules are involved in many cellular processes such as

cytoskeleton remodeling, membrane trafficking (Olayioye, Noll, and Hausser 2019), cell transcription and cell cycle progression (Olson, Ashworth, and Hall 1995; Glassford et al. 2001). They are also known to act as molecular switches that convert extracellular signals into multiple cellular effects in cooperation with integrins (Etienne-Manneville and Hall 2002). For this reason, they may play an important role in regulating hPMs morphology and proliferation as response to different ECM stimuli when in contact with the BNC matrix.

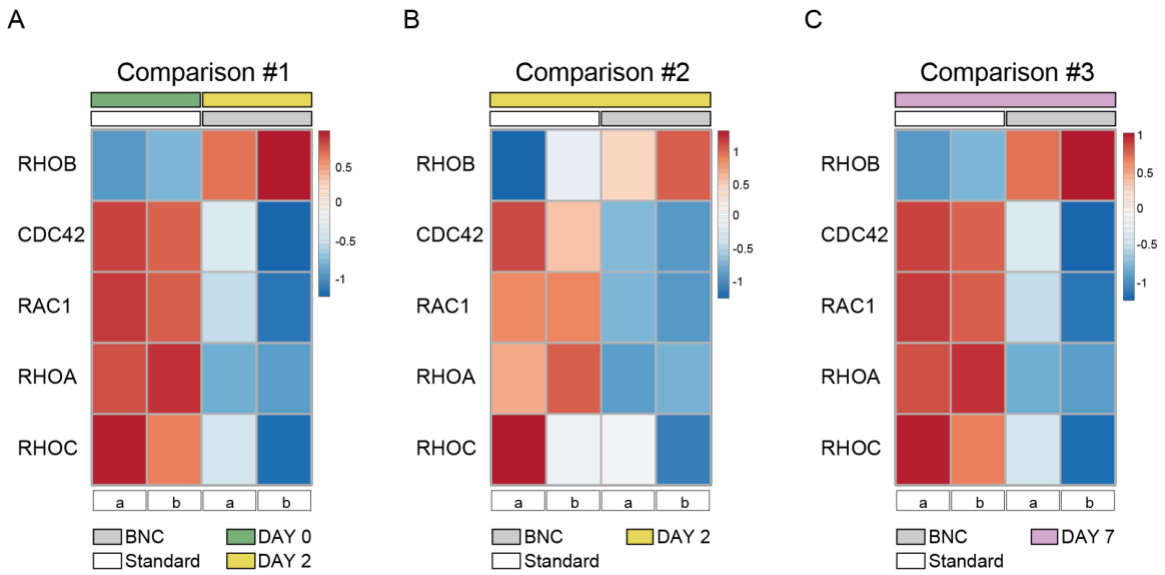

Figure 4.27: Heat-maps representation of GTPases Rho subfamily DETs.
Heat-maps showing DETs of the GTPases Rho subfamily as determined by RNA sequencing of hPM-2 on BNC compared to Standard. DETs (padj<0.05) are shown according to their expression counts values (reads), ln(x + 1)-transformed. Orange represents the upregulated DETs and blue the downregulated DETs. Two independent RNA sequencing replicates per sample (a – b).

Lastly, I found significant differences concerning extracellular re-organization and ECM-cell communication processes (e.g. “Extracellular matrix organization” or “Cell-extracellular matrix interactions”) (Table 4.2). Several DETs related to these pathways are shown to be upregulated in all three comparisons (Figure 4.28A,B,C). Among them we found ECM components like collagen V α-1/α-2/α-3 chain (COL5A1/3), collagen VI α-1/α-2/α-3 chain (COL6A1/2/3), collagen XXVIII α-1 chain (COL28A1) and fibronectin 1 (FN1) as well as matrix metalloproteinase-2 (MMP2), a protein responsible of ECM remodeling (Figure 4.28A,B,C).

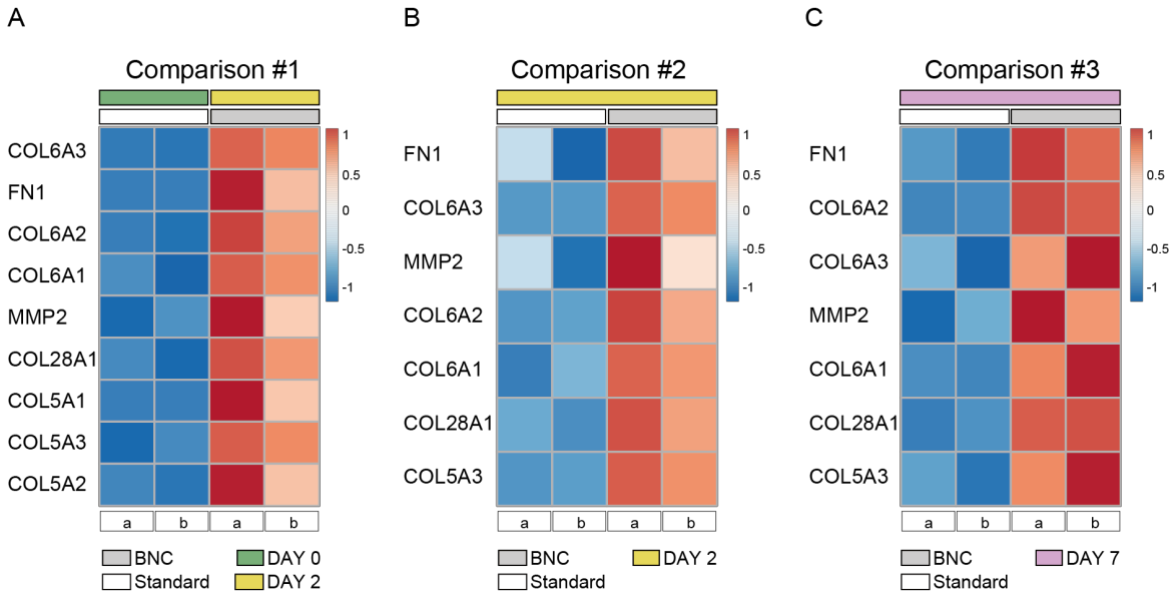

Figure 4.28: Heat-maps representation of ECM related DETs determined by RNA sequencing.
Heat-maps showing DETs related to cell-ECM communication and ECM re-organization as determined by RNA sequencing of hPM-2 on BNC compared to Standard. DETs (padj<0.05) are shown according to their expression counts values (reads), ln(x + 1)-transformed. Orange represents the upregulated DETs and blue the downregulated DETs. Two independent RNA sequencing replicates per sample (a – b).

To conclude, we provided an overview about the main molecular differences in hPMs between BNC and Standard via transcriptome analysis. We confirmed previous observations about the hPMs proliferation rate looking at the cell cycle-related pathways. Moreover, we suggested the involvement of Rho GTPases and ECM-associated genes in inducing hPMs changes on BNC, thus providing new insights for further investigations.

4.3.3. RNA sequencing results validated via RTq-PCR

I confirmed and validated a selection of DETs found in RNA sequencing via RTq-PCR. The experiments were performed in hPMs derived from three different donors hPM-1, hPM-3, hPM-5 and from donor hPM-2 (sample used for the total RNA sequencing experiment). The cells were analyzed on BNC or on Standard at the same points of time (DAY 0, DAY 2 and DAY 7) as in the RNA sequencing experiment (Table 4.1) and the same comparisons (#1, #2, #3) were investigated.

For the validation, I selected cell cycle-related genes among the downregulated (CCND1, CCNA2, CCNB1, and E2F1) (Figure 4.29) and ECM related genes among the upregulated (COL5A1, COL6A3, COL28A1, FN1, and MMP2) (Figure 4.30) DETs.

All cell cycle-related candidate-genes were confirmed via RTq-PCR to be significantly downregulated as found in the RNA sequence, in all three comparisons investigated (Figure 4.29).

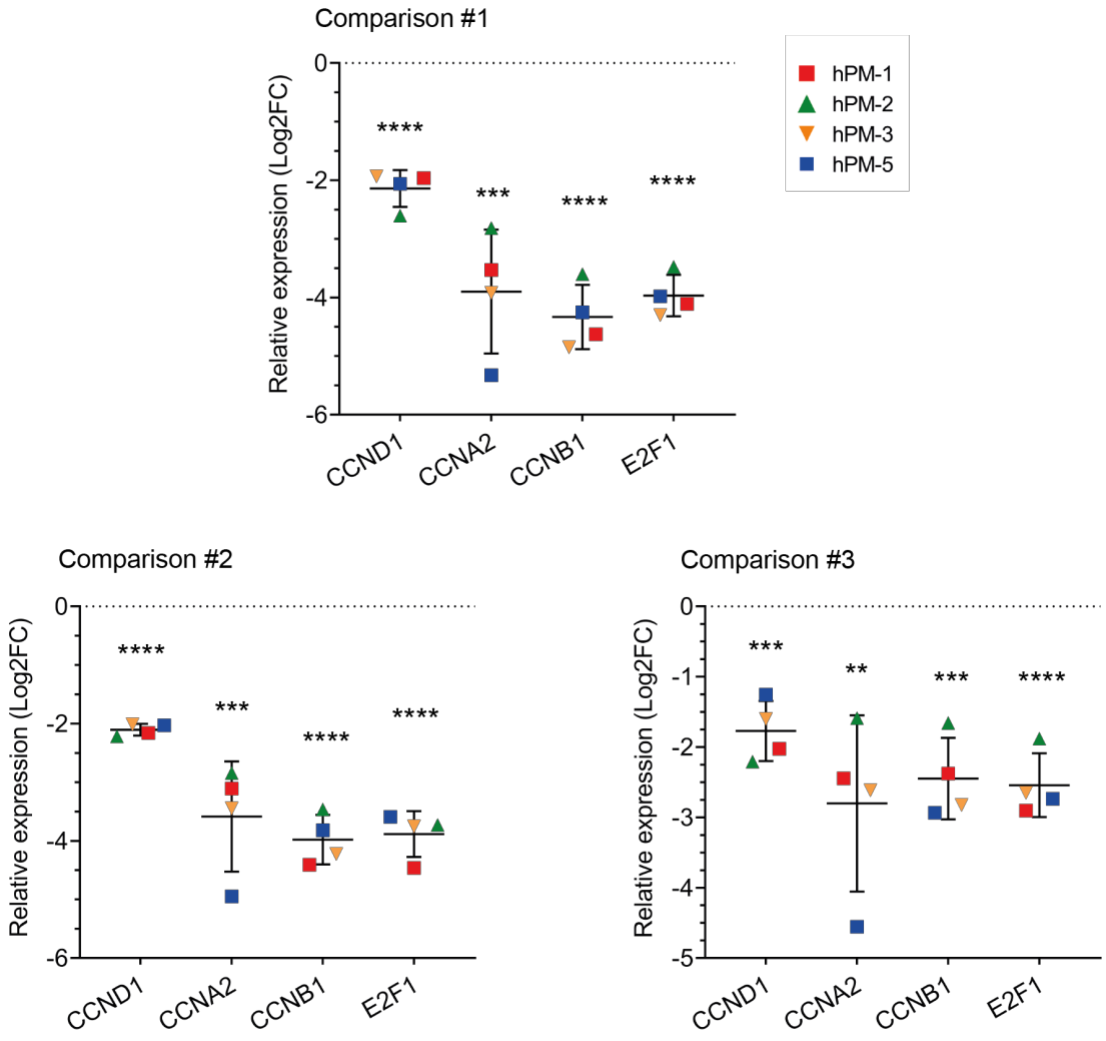

Figure 4.29: RTq-PCR validation of downregulated genes derived from total RNA sequencing results at different points of time.
RTq-PCR validation experiments for selected genes found downregulated in RNA sequencing results. DDCt values are shown as Log2FC relative to Standard for each point of time. n=4 donors; hPM-1,2,3,5; vertical black lines represent SD between different donors; horizontal black lines the mean. Two-sided unpaired t-test calculation on Log2FC values. *=p<0.05; **=p<0.01; ***=p<0.001 ****=p<0.0001

The ECM-related candidate-genes were as well confirmed to be significantly upregulated as found in the RNA sequence between in comparison #1, #2 and #3 (Figure 4.30).

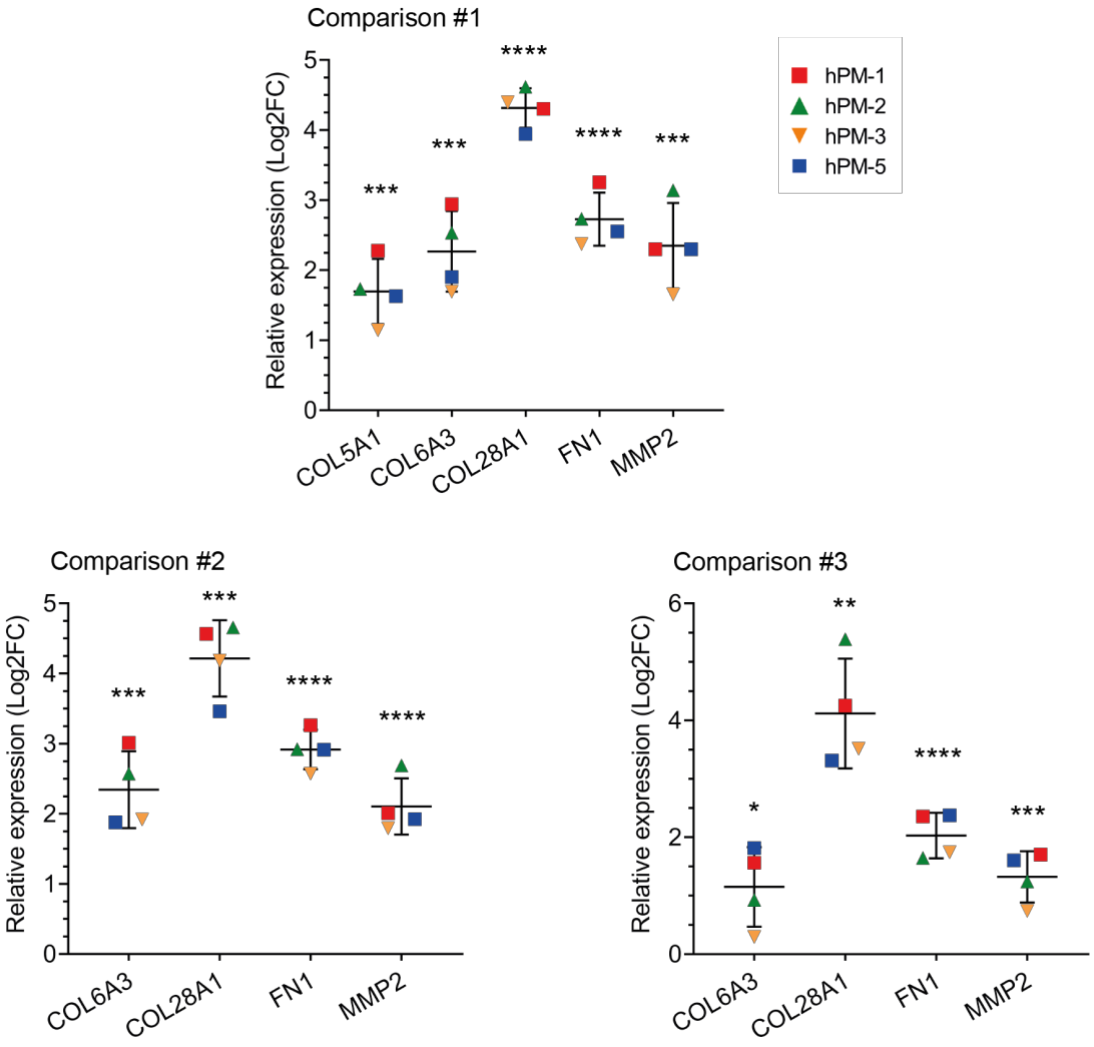

Figure 4.30: RTq-PCR validation of upregulated genes derived from total RNA sequencing results at different points of time.
RTq-PCR validation experiments for selected genes found upregulated in RNA sequencing results. DDCt values are shown as Log2FC relative to Standard for each point of time. n=4 donors; hPM-1,2,3,5; vertical black lines represent SD between different donors; horizontal black lines the mean. Two-sided paired t-test calculation on Log2FC values. *=p<0.05; **=p<0.01; ***=p<0.001; ****p=<0.0001.

4.4. *Ex vivo* CRISPR/Cas9-based gene editing in hPMs on BNC

In the first part of my results, I reported that CRISPR/Cas9-induced NHEJ DSBs repair can be applied either to achieve a specific knockout of *NCAM1* or to reframe mutant *DYSF* in hPMs on Standard. In the second part of this study, I introduced a novel culture method based on a cellulose substrate that allows to culture hPMs in a “slow-dividing” state for weeks. When placed back to Standard they regained a high proliferation ability and showed to be functional since they differentiated into myotubes.

As the next step I analyzed whether the CRISPR/Cas9-based strategies is as well applicable to the new BNC culture model.

4.4.1. Evaluation of transduction and transfection efficacy in hPMs on BNC

For genomic manipulation and gene editing (e.g. CRISPR/Cas9-based technique) on BNC I first wanted to test two different nucleic acid delivery methods.

Lentiviral vectors are widely used for delivery and expression of nucleic acids into cells. They are characterized by their ability to retro-transcribe their RNA genome into cDNA, which can be then stably integrated into the host cell genome (Warnock, Daigre, and Al-Rubeai 2011; Kimura et al. 2010). Lentiviral vectors can be potentially used to express the Cas9/sgRNA complex for efficient gene editing in hPMs (Xu et al. 2019; Bellec et al. 2015; Lyu et al. 2019).

I first tested the efficacy of a lentiviral vector to transduce hPMs and induce the expression of a GFP cassette. Cells that have been successfully infected, express a GFP (green) fluorescence signal. 48h after transduction, GFP positive (GFP+) hPMs were observed by BF microscopy and quantified via flow cytometry (Figure 4.31A). In both, Standard and BNC, hPMs were successfully infected and the number of GFP+ cells was comparable in either conditions (Figure 4.31B).

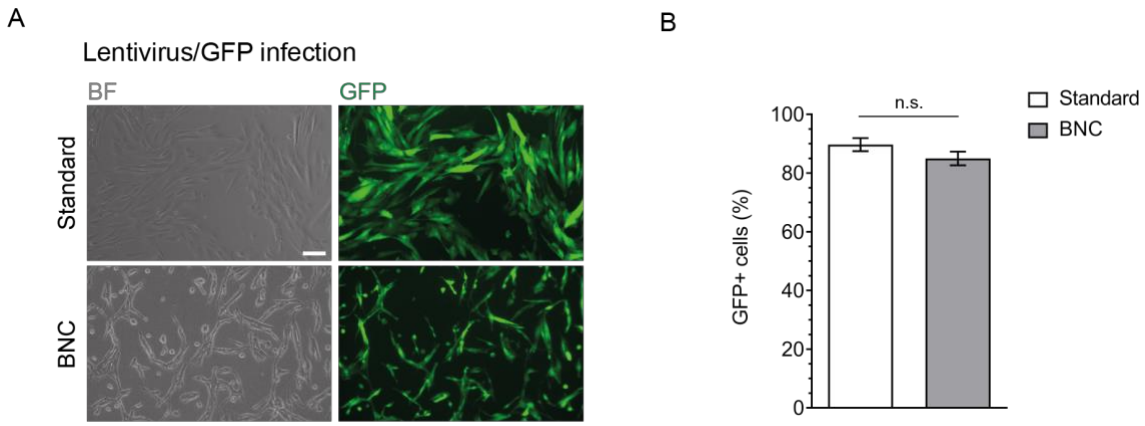

Figure 4.31: Lentiviral nucleic acids delivery on BNC.
Left, representative BF and fluorescence pictures of hPMs after lentivirus/GFP infection in Standard and on BNC. Scale bar = 100 µm. Right, quantification FACS analysis of GFP+ cells after infection in Standard and on BNC (n=3 donors, hPM-3,4,6; mean±SD). P value calculated by two-sided unpaired t-test.

I then verified the efficiency of lipo-transfection to deliver a Cas9/sgRNA-expressing plasmid in hPMs cultured on BNC. This method was also used to perform gene editing in hPMs on Standard (see Results section 4.1.). I transfected hPMs on Standard or BNC using Lipofectamine and the eSpCas9(1.1)::Venus plasmid. Venus signal was observed by BF microscopy and quantified via flow cytometry after 48h (Figure 4.32A). Cells were successfully transfected in either condition. However, the transfection on Standard resulted to be more efficient compared to BNC (Figure 4.32B).

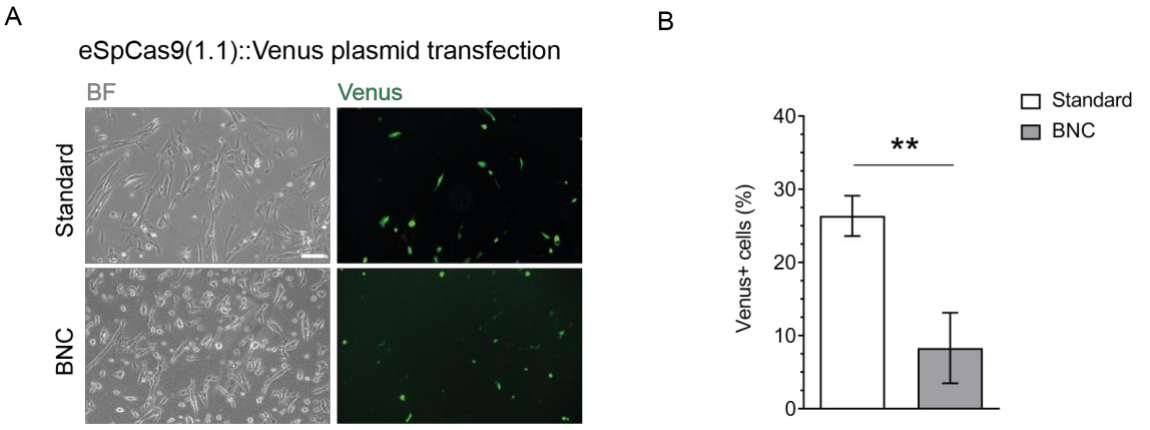

Figure 4.32: Nucleic acids delivery on BNC via lipo-transfection.
Left, representative BF and fluorescence pictures of hPMs after eSpCas9::Venus plasmid transfection in Standard and on BNC. Scale bar = 100 µm. Right, quantification FACS analysis of Venus+ cells after infection in Standard and on BNC (n=3 donors, hPM-1,2,5; mean±SD).

Here I concluded that Lentiviral transduction and lipo-transfection are both successful for DNA delivery in hPMs on BNC, although the lentivirus vector appeared to be more efficient.

4.4.2. CRISPR/Cas9-based gene editing in donor-derived PMs cultured on BNC induces *NCAM1* knockout

Since many safety and ethical issues raised from the use of lentiviral-based vectors in the clinic (Connolly 2002; Anson 2004), I decided to use lipo-transfection as a delivery method to perform a CRISPR/Cas9 gene editing experiment in hPMs on BNC. I used *NCAM1* knockout as a read-out of gene editing efficiency, as was already performed in Standard (see Results section 4.1.1., Figure 4.1 and Figure 4.2). I transfected donor-derived PMs cultured on BNC for 24h with an eSpCas9(1.1)::Venus plasmid containing the sgRNA targeting *NCAM1* exon 3 (*NCAM1*ex3wt#1) (Figure 4.33A and see Methods section 3.9.1., Table 3.3). The eSpCas9(1.1)::Venus vector w/o sgRNA was used as a control. After enrichment of eSpCas9(1.1)::Venus+ cells, I extracted gDNA from each condition and I PCR amplified the region around *NCAM1* exon 3 for Sanger sequencing. Sanger sequencing of the *NCAM1 exon 3* locus revealed chromatogram disturbance after the cleavage site of sgRNA due to formation via NHEJ, suggesting successful gene editing (Figure 4.33B), as similarly observed on Standard (Figure 4.2A).

Quantification of the editing efficiency is displayed in indel plots that revealed a predicted editing efficiency of 43.3% hPMs sgRNA samples, average of three independent experiments (Figure 4.33C, right). A single N deletion at the expected site, is the predicted preferred indel formation (Figure 4.33C, left).

Lastly, I confirmed the knockout of the gene by FACS-staining for NCAM1 protein expression. FACS dot plot analysis showed a mean of ~24% loss of NCAM1 protein expression in the edited hPMs after ~10 days expansion in Standard (Figure 4.33D).

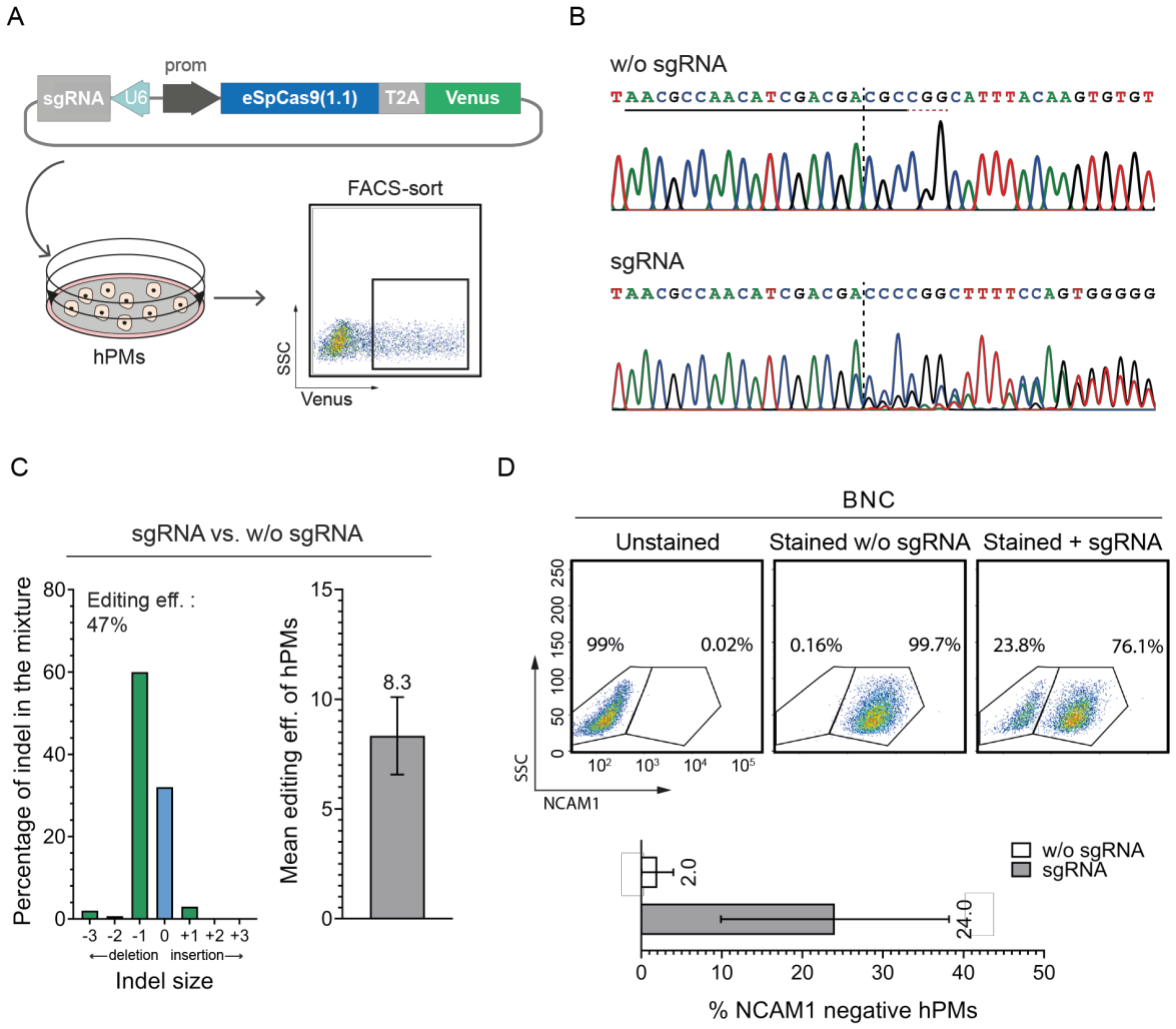

Figure 4.33: Depletion of NCAM1 protein in hPMs using CRISPR/Cas9-mediated genome editing approach.
A) Illustration of the plasmid encoding enhanced specificity eSpCas9(1.1)::Venus used for transfection of hPMs. Transfected cells express Venus fluorescence (green), allowing for selection of eSpCas9(1.1)::Venus+ cells by FACS. **B)** Sanger sequences in the region surrounding the sgRNA sequence from hPM-2 transfected with sgRNA (sgRNA) compared to a control unedited sequence (w/o sgRNA). Chromatogram variability is observed after the cleavage site (black dotted line). Horizontal black underline: sgRNA. Red dotted line: PAM site. **C)** Left, representative example of indel plot from ICE analysis showing the predicted editing efficiency relative to hPM-2. Right, average of editing efficiency (ICE) of three hPMs donors (n=3 donors; mean±SD). **D)** Upper, example of FACS dot plots from NCAM1 staining of w/o sgRNA and sgRNA relative to hPM-2. Lower, percentage mean value of NCAM1 negative cells of different hPMs donors after editing (n=3 donors; mean±SD).

In the second part of the work, I demonstrated that hPMs can be kept longer in culture then on Standard without losing their viability, proliferation and myogenic capabilities. With the last experiments, I also showed that BNC can be used as an alternative culture method to genetic manipulate hPMs via CRISPR/Cas9-based methods. These results are the first step towards the development of a method able to correct dystrophy-causing mutation in hPMs while preserving their proliferative and myogenic potential.

5. DISCUSSION

5.1. *Ex vivo* hPMs correction of a mutation in the *DYSF* gene using the CRISPR/Cas9 system

MDs are a group of heterogeneous genetic myogenic disorders associated with progressive loss of muscle mass and function (Emery 2002). Despite the effort in investigating different therapeutic options, a definitive treatment for these diseases has not been developed yet (Mercuri and Muntoni 2013; Nigro and Piluso 2015). Since many MDs are caused by single gene mutations, its replacement or correction by gene therapy is considered as a promising clinical application.

I.m. or vascular injection of AAVs expressing the missing gene has been shown to rescue protein expression and muscle function in a variety of dystrophic animal models (Grose et al. 2012; Sondergaard et al. 2015; Le Guiner et al. 2017; Duan 2018; Yue et al. 2015). In agreement with this therapeutic approach, several clinical trials have been approved for DMD (ClinicalTrials.gov: Pfizer, NCT03362502; Sarepta Therapeutics, NCT03375164; Solid Biosciences, NCT03368742) and LGMDs (ClinicalTrials.gov: NCT03652259; NCT01976091; NCT02710500). However, the dosage-dependent immune response to both AAV capsid (Martino et al. 2011; Mingozzi and High 2013; Shayakhmetov, Di Paolo, and Mossman 2010) and the transgenes delivered (Mendell et al. 2010) is still a major safety concern for the clinical procedure. AAVs have been also applied for *in vivo* CRISPR/Cas9-based gene editing of causing mutations in several myogenic disorders (Crudele and Chamberlain 2019). Systemic distribution via muscle-specific AVVs is ideal for the treatment of diseases affecting one of the largest tissues in the body. However, the constitutive expression of Cas9 nuclease by AAVs may lead to accumulation of “off-target” DNA mutations (Cho et al. 2014). Moreover, exogenous AAVs and Cas9 protein expression may trigger undesired immune system responses (Mingozzi and High 2013; Crudele and Chamberlain 2018). Altogether, these challenges limit the possibility of clinical application..

As an alternative, cell-based treatments can be applied for allogeneic transplantation of healthy or corrected myogenic cells that are able to sustain and enhance long-term muscle regeneration of dystrophic muscle. Several types of progenitor cells derived from skeletal muscle or from non-muscle tissues have been tested as sources for cell transplantation in MDs (Biressi, Filareto, and Rando 2020). iPSCs propagate indefinitely and can be used for autologous transplantation upon differentiation into myogenic cells. Different gene editing approaches (e.g. CRISPR/Cas9) have been used to correct mutations in iPSCs derived from MDs patients (Turan et al. 2016; Young et al. 2016; Min et al. 2019; Selvaraj et al. 2019). Corrected iPSCs-derived myogenic cells showed engraftment potential in dystrophic mouse models, rescuing the genetic defect without leading to the formation of tumors (Tedesco et al. 2012; Young et al. 2016). Despite these promising results, optimization of differentiation protocols for transplantation in humans are required and genomic instability, as well as their teratogenicity are still safety concerns.

CD133+ cells or MABs, myogenic cells with an endothelial origin, have also been proved to own good engraftment capability in skeletal muscle when systemically or locally delivered (Dellavalle et al. 2011; Torrente et al. 2007). Indeed, many studies showed the rescue of the dystrophic phenotype after transplantation of healthy or corrected MABs in different animal models (Sampaolesi et al. 2003; Sampaolesi, Blot, and D'Antona 2006; Díaz-Manera et al. 2010). However, a phase I/IIA clinical trial performed in 2011 (Eudract 2011-000176-33) did not show any beneficial effect in DMD patients and implementation of the transplantation protocol is needed (Cossu et al. 2015).

Myoblasts are myogenic progenitor cells deriving from adult SCs that can be isolated from human muscle biopsies, expanded *in vitro* and ideally transplanted after gene correction. Even if these cells are available in a lower number compared to iPSCs (Briggs and Morgan 2013), myoblasts are very well characterized (Tedesco et al. 2010; Yin, Price, and Rudnicki 2013) and they contribute to muscle regeneration once engrafted (Marg et al. 2014; Marg et al. 2019). The use of myoblasts in cell-therapy has indeed been supported by initial studies showing that healthy cells, derived from *in vitro* expansion of mouse stem cells, are able to rescue the genetic defect when injected in the muscle of DMD models (Partridge et al. 1989; Vilquin et al. 1996; Partridge 1991). Importantly, some of the transplanted myoblasts survived as precursor cells and repopulated the SCs niche suggesting a long-term therapeutic effect. In the last decades, several clinical trials demonstrated that healthy donor-derived myoblasts can be safely transplanted in muscles from DMD patients and restore dystrophin expression in the muscle tissue (Partridge 2002; Mendell, Sahenk, and Prior 1995; Briggs and Morgan 2013; Karpati et al. 1993; Skuk, Goulet, Roy, Piette, Côté, et al. 2007) but clinical benefits for the patients have not been proven yet. Nevertheless, this strategy appeared to be successful in small and more accessible muscles, as proved in less extended diseases such as OPMD (Périé et al. 2014).

Allogeneic transplantations harbor the risk for immunogenicity of the donor myoblasts once injected in the host muscle (Guérette et al. 1994). To avoid this issue, the use of *ex vivo* corrected patient-derived cells is considered as a therapeutic advantage. Recently, the CRISPR/Cas9 system has been explored as method for editing MDs-causing mutations and could be applied in patient-derived myogenic cells prior autologous transplantation. However, no data have been published yet about CRISPR/Cas9-based gene correction in myoblasts.

In this study, we reported an *ex vivo* CRISPR/Cas9-based strategy to restore the open reading frame of mutated *DYSF* in PMs derived from a patient affected by LGMD2B. LGMD2B is an autosomal recessive disorder belonging to the heterogeneous family of LGMDs (Wicklund and Hilton-Jones 2003; Domingos et al. 2017; Nigro and Savarese 2014). LGMD2B is prevalent in southern Europe with a frequency of 15–25% in the group of the LGMDs and, as for the rest of the MDs, no cure is available yet (Argov et al. 2000; Cagliani et al. 2003; Vilchez et al. 2005). A homozygous missense mutation (c.4872_4876delinsCCCC) in *DYSF* exon 44 was discovered to be a founder genetic defect with a 10% carrier frequency in the Libyan Jew population. A deletion of a G (4872delG) causes a frameshift of the *DYSF* open reading frame, a premature stop codon in exon 45 and a complete absence of dysferlin protein (Argov et al. 2000).

As shown in Figure 4.5, ~50% of mutated cells were efficiently edited by the delivery of SpCas9 nuclease and a mutation-specific sgRNA. Of note, the eSpCas9 and SpCas9 variants were compared and SpCas9 was proved to be the most efficient one (Figure 4.5). eSpCas9 has been engineered to have increased specificity and reduced "off-target" nuclease effects compared to SpCas9 (Slaymaker et al. 2016). However, further studies showed that the general activity of this variant is reduced and some target sites are poorly cleaved (Kim et al. 2017; Kulcsár et al. 2017; Anderson et al. 2018), explaining the fact that SpCas9 was more efficient in this study.

sgRNA guided SpCas9 induced DSBs at the cleavage site followed by NHEJ repair and led to a preferred indel formation of +1A (Figure 4.5B and Figure 4.6). As result of this insertion, *DYSF* open reading frame could be restored (Figure 4.7). We speculated that a single nucleotide insertion is a consequence of a so-called staggered DNA cleavage-repair model (Gisler et al. 2019). According to this model, Cas9 induction of staggered DSBs (Zuo and Liu 2016) leads to template-dependent insertions following a 1-nucleotide 5′ overhang on the opposite strand (Figure 5.1). Therefore, a duplication of a DNA base immediately downstream of the break site is occurring with high probability. This editing strategy minimizes undesirable variability of NHEJ repair outcomes, therefore achieving a more efficient and precise genome editing in mutated cells.

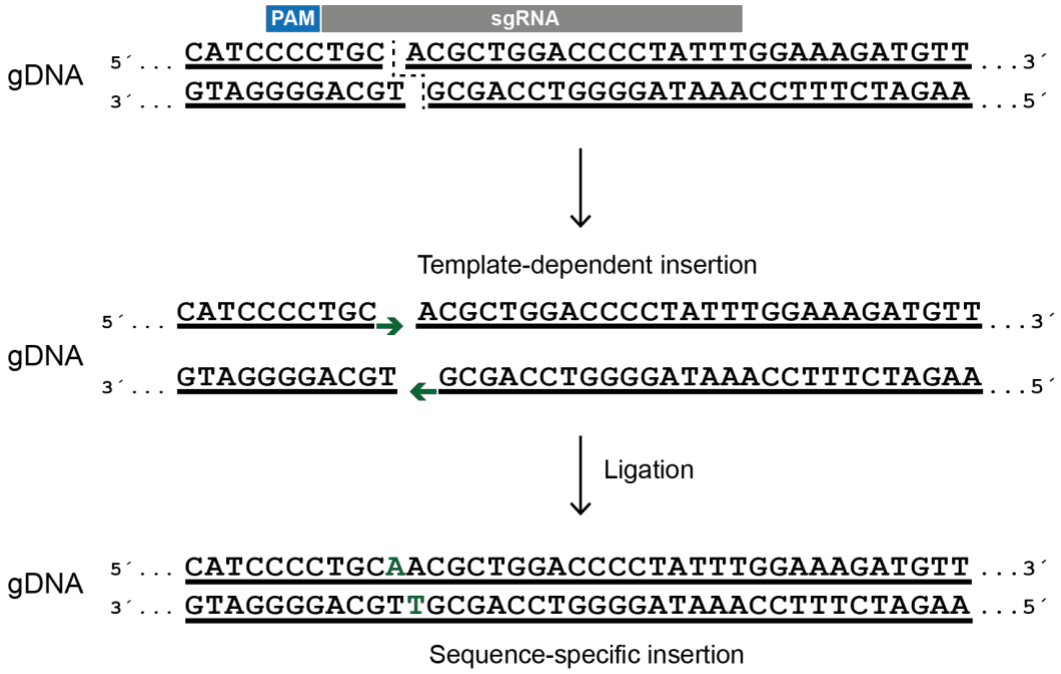

Figure 5.1: DNA repair outcome after Cas9-induced DSB following the staggered DNA cleavage-repair model.
After Cas9-mediated staggered DSBs between nucleotides 3/4 on the target DNA site and 4/5 on the non-target one, the resulting 5´ overhangs trigger polymerase-based fill-in at position 4 producing sgRNA specific insertion. The inserted nucleotide will be identical to the DNA base immediately downstream of the break site (A).

Because of the *DYSF* re-framing, *DYSF* mRNA is translated correctly (Figure 4.7). Indeed, I observed a significant rescue of the mRNA expression by RT q-PCR in the population of edited

cells (Figure 4.8A). Moreover, DYSF protein could be detected by WB (Figure 4.9A) and immunofluorescence (Figure 4.9B) in edited myoblasts and differentiated myotubes. Clearly, dysferlin localized at the membrane and at the myotubes/myoblasts fusion junction, showing a similar expression pattern to control healthy cells (Figure 4.9B). It is important to mention that the "re-framing" strategy, described in this study, generated 4 aa substitution (Thr>Asn, Leu>Ala, Glu>Gly, Val>Leu) in the edited dysferlin coding sequence (Figure 4.7). However, these changes appeared not to interfere with protein translation and localization at the membrane through its C terminal domain. As further confirmation, preliminary results obtained from laser wounding experiments demonstrated that dysferlin, together with annexin A1, was expressed at the "repair dome" 20 min after the membrane injury (Figure 4.10) as also shown in healthy control cells and previous studies (Marg et al. 2012). Here, laser wounding results suggested that the corrected dysferlin takes part in the sarcolemma Ca^{2+}-depended repair process. Nevertheless, conclusions about functional recovery in muscle fiber plasma membrane resealing have to be confirmed by increasing the number of observations.

The open reading frame resolution via NHEJ-mediated DNA repair and subsequent prevention of premature stop codons is known as "gene reframing therapy", which has been effective also for correction of DMD (Iyombe-Engembe et al. 2016; Min et al. 2019) and other non-muscular monogenic disease-causing mutations (e.g. recessive dystrophic epidermolysis bullosa) (Takashima et al. 2019). Gene reframing therapy can be potentially applied to any missense/frameshift mutations and in this study it was successful in LGMD2B. However, a number of technical limitations need to be discussed.

After lipo-transfection of the SpCas9::Venus vector, Venus+ cells were enriched by FACS. Transfection efficiency is critical since it influences the final number of sorted cells that can be expanded for further analysis and, potentially, transplanted. In the performed experiments a maximum of 18% (data not shown) of the total transfected cells have been sorted as Venus+ and, of those, half were edited (Figure 4.5B). After ~10 days of cell expansion, necessary for further analysis, the percentage of corrected cells dropped (Figure 4.8B). This would explain the partial rescue of *DYSF* mRNA, as well as the low protein abundance observed by immunoblot in the analysis of the bulk population of edited cells. Lower intensity of dysferlin protein was also observed in stained myotubes since they likely derived from the fusion of both edited and not edited nuclei with a consequent attenuation of the protein signal.

Several factors are known to be responsible for the poor transfection efficiency and can be improved. We observed that delivery of the editing machinery as nucleic acid via plasmid lipofection has a low efficiency and quite high cytotoxicity in hPMs. Recently, in our laboratory successful "proof of concept" experiments have been performed in the delivery of the Cas9 nuclease as mRNA or recombinant protein (RMP) into hPMs via nucleofection. We observed a considerable higher number of Cas9-expressing cell, as well as increased editing "rate" compared to lipofection using *NCAM1* as model gene. The presence of a higher percentage of edited myoblasts would reduce the expansion time and, accordingly, the "dilution" of the edited population of cells.

As previously mentioned, a general issue of *ex vivo* cell-based therapies is the loss of regenerative capability and limited proliferation of hPMs once isolated (Montarras et al. 2005). This is even more challenging when myoblasts are isolated from patients´ biopsies, which are characterized by an advanced dystrophic phenotype. As experienced in our laboratory, they result to be aged, less proliferative and going earlier towards senescence compared to healthy donor myoblasts. This might be related to extrinsic (e.g. dystrophic tissue microenvironment with continuous cycles of muscle degeneration/regeneration and induction of SCs exhaustion) (Goldstein and McNally 2010; Negroni et al. 2015; Wallace and McNally 2009; Mouly et al. 2005; Blau, Webster, and Pavlath 1983) or intrinsic (e.g. membrane instability, defective RNA processing, impaired SCs polarity, proteasome activation) (Dumont and Rudnicki 2016; Furling et al. 2001; Gastaldello et al. 2008) factors. If their replicative life span is reduced, the cells undergo senescence faster than the healthy counterpart and, even if successfully edited, they cannot proliferate nor efficiently regenerate muscle after transplantation (Blau, Webster, and Pavlath 1983; Webster and Blau 1990; Wright 1985). Anticipating the muscle biopsy in earlier stage of the disease progression might be a solution to address this problem. Additionally, different methods to overcome SCs-derived myoblasts loss of stemness and aging have been investigated and they will be discussed in the next paragraph.

5.2. BNC substrate as culture method for hPMs: advantages and caveats

For the improvement of muscle stem cells or myoblasts *ex vivo* culture conditions, several attempts have been made to directly modulate signaling pathways (Parker et al. 2012; Price et al. 2014; Zismanov et al. 2016; Sampath et al. 2018; Tierney et al. 2014) and epigenetic clues (Judson et al. 2018) that are known to preserve stemness and avoid terminal myogenic differentiation. Those approaches are based on the knowledge about quiescence retention of stem cells in the muscle niche (Evano and Tajbakhsh 2018; Yin, Price, and Rudnicki 2013; So and Cheung 2018; Conboy and Rando 2002). Charville et al. demonstrated that the inhibition of p38 MAP kinase enhances *ex vivo* human SCs expansion and engraftment efficiency upon xenotransplantation into immunodeficient mice (Charville et al. 2015; Jones et al. 2005). In addition, transplantation efficiency of mammalian progenitor muscle cells has been improved by manipulation of Notch signaling (Parker et al., 2012). In another study, a cocktail of four cytokines (IL-1α, IL-13, TNF-α, and IFN-γ) have been reported to promote mouse muscle stem cell proliferation and maintain them undifferentiated *in vitro* even after several passages (Fu et al. 2015). Oxygen levels have been also considered as an important factor influencing muscle stem cell behavior in culture. Indeed, maintaining the cells in hypoxic conditions as in muscle tissue, was proven to have a positive influence on myoblast self-renewal and transplantation efficiency in dystrophic mice (Liu et al. 2012).

Other approaches aimed to mimic the mechanical properties of the *in vivo* niche using moldable matrixes or substrates to sustain myogenic cell potency (Dellatore, Garcia, and Miller 2008; Gilbert et al. 2010; Quarta et al. 2016; Monge et al. 2017). This concept is based on reported evidence about how substrate properties (e.g. elasticity and/or rigidity) significantly influence mammalian muscle stem cells behavior in culture (Dellatore, Garcia, and Miller 2008; Engler et al. 2006; Gilbert et al. 2010; Monge et al. 2017). More in detail, materials that are characterized by an elastic module comparable to skeletal muscle (12kPa) have also proved to sustain the quiescence state of human muscle stem cells, reducing cell division and increasing engraftment efficiency (Gilbert et al. 2010; Quarta et al. 2016; Monge et al. 2017).

Here, I introduced for the first time a BNC material as a method for a long-term *in vitro* culture of hPMs. We showed that BNC allows the preservation of hPMs for several weeks at a very low proliferation rate without the need for cell passaging (Figure 4.13) and evidence of terminal differentiation (Figure 4.12C and Figure 4.17). BNC is a soft and flexible material (~15kPa) made of cellulose nano-fibers produced by *Gluconacetobacter Xylinus* (Hofinger, Bertholdt, and Weuster-Botz 2011; Feil et al. 2017; Wang, Tavakoli, and Tang 2019), (Figure 4.12A). Because of high purity, high biocompatibility and mechanical strength, BNC has been widely applied in tissue engineering (e.g. wound dressing) (Picheth et al. 2017) and regenerative medicine (e.g. BNC scaffolds for cell transfer) (Svensson et al. 2005; Dutta, Patel, and Lim 2019). Moreover, BNC structural properties and morphological similarities between nano-cellulose fibers and ECM proteins like collagen (Petersen and Gatenholm 2011; Geisel et al. 2016), suggested possible applications as alternative stem cells culture substrate for controlling differentiation and maintenance of stemness (Geisel et al. 2016; Tronser et al. 2018).

5.2.1. hPMs proliferation rate on BNC

When hPMs were cultured on the BNC substrate, a significant reduction of Ki-67 protein (Figure 4.15A) and mRNA levels (Figure 4.16) was consistent over 14 days of culture, proving that the cellulose properties significantly influence hPMs proliferation. These data are in line with the observation that hPMs never reached confluence when plated at low density on BNC over 21 days (Figure 4.14). Ki-67 is exclusively expressed in S-M-G2 phases of cell cycle (Sun and Kaufman 2018) suggesting that the majority of hPMs were in G0/G1 phases on the BNC substrate. Indeed, a cell cycle analysis via FACS confirmed that after 2 days of culture on BNC more than 90% of hPMs were “arrested” in G0/G1 phase (Figure 4.15B). Only a small percentage of cells was doubling (S/G2 phase: ~2%) (Figure 4.15B) and was still expressing Ki-67 (Figure 4.12A) over time, a phenomenon likely related to the functional heterogeneity within the population of activated SCs (Kuang et al. 2007; Kuang and Rudnicki 2008; Marg et al. 2019). Several studies proved the presence of transcriptional distinct SCs populations, which show dissimilar behavior in vitro assays and in vivo transplantation experiments (Kuang et al. 2007; Charville et al. 2015; Cho and Doles 2017; Barruet et al. 2020). As hPMs used in this study are a mixed population of myogenic cells derived from activated SCs, differences in cell cycle progression might correlate to their functional

heterogeneity. Further analysis (e.g. single cell sequencing) may give more insights about hPMs diversity on BNC.

In line with my first observations on Ki-67 expression and the cell cycle status, bulk RNA sequencing analysis confirmed a significant downregulation of the majority of transcripts related to proliferation and cell cycle in hPMs on BNC compared to Standard (Table 4.2). More importantly, 2 days of BNC culture were enough to induce a substantial downregulation of CCND1/A2/B1, CDKs and E2F1 transcripts that was maintained until the seventh day (Figure 4.26; validated via RTq-PCR in Figure 4.29). Proteins encoded by those genes are the main regulator of cell cycle progression (Sherr and Roberts 1999). CCND1 binds CDK4 and induces the dissociation of E2F1 from the Retinoblastoma protein (Rb) (Yang, Hitomi, and Stacey 2006; Baldin et al. 1993). E2F1 permits CCNE transcription and the transition from G0/G1 to S-phase (Moreno-Layseca and Streuli 2014). Cell adhesion via integrins is critical for cell cycle progression towards the S-phase (Moreno-Layseca and Streuli 2014). Integrins are transmembrane receptors known to mediate cell-sensing of biophysical signals such as substrate stiffness and mechanical force (Schiller and Fässler 2013; Ireland and Simmons 2015). They are responsible for cytoskeleton organization and influence signal transduction pathways in response to ECM-attachment. For proliferative responses, the major pathways regulated by integrins in cooperation with growth factors are the small GTPase (Rho and Rac) pathways known to be associated with adhesion-dependent cell cycle regulation (Welsh 2004; Mack et al. 2011). Interestingly, ConsensusPathDB signaling analysis in this study showed that integrins and Rho GTPase associated pathways were differentially regulated (Table 4.2). In detail, three principal members of the GTPase family (Rac1, RhoA and Cdc42) were downregulated during the first 2 days of BNC culture (Figure 4.27A). Modulations of integrins pathways due to cell-BNC fibers interaction might therefore inhibit the expression of the members of GTPases family ultimately leading to cell cycle arrest in hPMs on BNC.

5.2.2. hPMs morphologic changes on BNC

During the first days of culture on BNC, hPMs appeared morphologically roundish (Figure 4.12B,D,E) and F-actin displayed an altered organization re-localizing at the sub-sarcolemma space (Figure 4.12E). It was already reported that myoblast morphology is influenced by substrate biomechanical clues or elasticity (Engler et al. 2006) and a comparable roundish phenotype has been associated to a biopolymeric film or hydrogels with lower stiffness compared to plastic (~3 GPa) (Engler et al. 2006; Gilbert et al. 2010; Monge et al. 2017). Prolonged culture of hPMs on BNC resulted in increased spreading area, in new cell-substrate contacts and an more elongated morphology (see BF pictures in Figure 4.13 A,C). Since matrix stiffness is largely dependent on the composition of the ECM, changes in hPMs morphology along the culture period might be correlated with ECM proteins secretion. Indeed, transcripts encoding for collagens, FN1 and an ECM remodeling protein such as MMD2 were upregulated after 2 days on BNC according to RNA sequencing analysis (Figure 4.28). hPMs have been derived from SCs that are known to remodel

their own ECM *in vivo* (Tierney et al. 2016; Rayagiri et al. 2018). In detail, FN1 and COL6A1 which were upregulated in hPMs on BNC along 7 days of culture, (Figure 4.28) are both expressed by SCs *in vivo* and are important for SCs niche remodeling during regeneration (Bentzinger, Wang, von Maltzahn, Soleimani, et al. 2013; Urciuolo et al. 2013). Self-induced chances in ECM composition might allow cell spreading modulating signaling pathways such as integrins and Rho GTPase related pathways which were still differentially regulated after 7 days of culture on BNC (Table 4.2).

5.2.3. hPMs cell cycle status on BNC

Non-cycling cells in irreversible G1-phases are associated to a terminal differentiation or senescence. When in reversible G0-phase they are in a quiescent state (Kuang and Rudnicki 2008).

BNC did not induce terminal differentiation of hPMs (Figure 4.12B). Even when hPMs on BNC reached confluence (e.g. after ~30 days of culture) and were induced to fuse, they did not form multinucleated myotubes and did not express MYHC as on Standard (Figure 4.17). In the dynamic process of myoblasts fusion, actin fiber re-organization and “focus” formation are essential (Kesper et al. 2007; Richardson et al. 2007; Massarwa et al. 2007; Kim et al. 2007). The actin “focus” provides the traction force to induce membrane juxtaposition and fusion between 2 myoblasts. Rho1 and Rac proteins from the Rho GTPases family play an important role in the activation of genes required for the formation of the actin “focus” (e.g. SCAR/WAVE and WASP) (Berger et al. 2008; Richardson et al. 2007; Massarwa et al. 2007; Kim et al. 2007; Sens et al. 2010; Jin et al. 2011). It is therefore possible to hypothesize that the downregulation of Rho GTPases related genes affecting F-actin organization influences the fusion process while hPMs are on BNC.

However, BNC did not induce senescence either as the cells were able to re-enter the cell cycle and then differentiate. When I detached hPMs after ~15 days of culture on BNC and re-plated them in Standard (post-BNC) they rescued proliferation capability (Figure 4.21 and Figure 4.22). As observed in Figure 4.21, cell doubling was comparable to the controls (Standard) the first three days (between P0 and P1). However, after P1 the post-BNC hPMs were dividing even faster. In fact, Ki-67 protein expression significantly increased after 7 days of post-BNC compared to the control (Figure 4.22A). This data suggests that “arrested” hPMs could re-enter cell cycle “younger” (i.e. with a minor number of cell division) and, accordingly, with a higher proliferation capacity compared to the Standard. Indeed, a very low division rate might avoid telomeres shortening, which occurs at each round of cell division (Decary et al. 1997) and which is one of the main mechanisms associated to senescence (Meyne, Ratliff, and Moyzis 1989; de Lange et al. 1990; Bernadotte, Mikhelson, and Spivak 2016). Changes in telomerase length during long-term culture on BNC has to be evaluated to validate this hypothesis.

Moreover, post-BNC hPMs successfully fused in multinucleated myotubes when induced to terminal differentiation. They expressed differentiation makers (MYHC and MYOG) (Figure 4.23)

and showed a fusion index comparable with the one displayed by early-passage control myoblasts (Figure 4.17). This confirmed that the cells completely recovered their myogenic functional properties as well as proliferation and were able to terminally differentiate in vitro. Whether the regenerative capacity (i.e. new mature tissue formation and self-renewal in vivo) of the post-BNC hPMs has been maintained or enhanced is not known yet. The analysis of their engraftment potential compared to Standard after in vivo transplantation will address this question.

In contrast to senescent or terminally differentiated cells, quiescent cells are able to re-enter cell cycle from a reversible G0 state (Coller, Sang, and Roberts 2006). Muscle stem cells are quiescent when localized in the in vivo niche and usually defined by Pax7 expression (Kuang and Rudnicki 2008; Cheung and Rando 2013). A high number of genes are upregulated in quiescent SCs compared with activated cells (e.g. Cdkn1B and 1C, Rb1, Calcr, Notch1, Lama3, Pax7 etc.) (Fukada et al. 2007; Liu et al. 2013; Pietrosemoli et al. 2017) and several factors and signaling pathways are required for maintaining their state (e.g. Notch, p38 MAPK, mTOR signaling pathways, microRNAs, etc.) (Dumont, Wang, and Rudnicki 2015). Previous studies reported that the use of special matrix compositions maintain muscle stem cells in their quiescent state, thus enhancing engraftment efficiency in several animal models (Gilbert et al. 2010; Quarta et al. 2016; Monge et al. 2017). Pax7 expression at the expense of MyoD1 was used as marker to claim that cells are kept with a higher regenerative potential than on standard culture (Gilbert et al. 2010; Quarta et al. 2016; Monge et al. 2017). In our analysis, the myogenic markers Pax7 and MyoD1 were not found to be significantly altered on BNC (Figure 4.16), a result probably related to the type of cells used in our analysis compared to the other studies. In our experiments, hPMs underwent a freezing/thawing process and many cell divisions before use (e.g. donor-derived cells were used between P6 to P8) while in the other studies cells were analyzed closely after isolation. Additionally, the hPMs that I used in this work showed variable donor-dependent levels of Pax7 protein expression after isolation (see Methods section 3.1.1., Table 3.1.), which makes a proper evaluation challenging. Nevertheless, it has also been shown that Pax7 expression level in human biopsy specimen-derived myoblasts does not influence the potential of hPMs for muscle fibre formation after transplantation in an immunodeficient mouse model (Marg et al. 2019). Thus, the expression of the transcription marker Pax7 remains questionable as a proper marker for the regenerative potential of hPMs in our experimental condition.

COL5A1 or COLV was found up-regulated in hPMs (validated via RTq-PCR in Figure 4.30) on BNC between Day 0 and Day 2. It was recently reported that COLV participates in self-maintenance of the SC quiescent state in the SC niche (Baghdadi et al. 2018). COLV is deposited by SCs under the basal membrane acting as a surrogate ligand for the calcitonin receptor to inhibit SCs from escaping the quiescent state (Yamaguchi et al. 2015). Transcriptional induction of COLV is regulated by Notch signaling that is known to be the main regulator of quiescent muscle cells (Bjornson et al. 2012). However, Notch pathway has not been found enriched in the ConsensusPathDB signaling analysis in this study. On the other hand, other factors (e.g. Angiopoietin 1 [ANG1] and the family of FOXO genes), associated to quiescence and in vitro self-

renewal (Abou-Khalil et al. 2009; Yeo et al. 2013; García-Prat et al. 2020), were upregulated at 7 days of BNC culture (data not shown).

To summarize, we observed that a high percentage of hPMs on BNC were retained in a reversible G0 state of cell cycle and that some genes related to quiescence maintenance were upregulated (e.g. COLV) compared to Standard. However, we did not see changes in the Pax7/MyoD1 expression ratio or Notch signaling activation. Considering these controversial results, it is challenging to infer the induction of a "quiescence-like" state of hPMs when cultured on BNC. To answer this specific question, further investigations are necessary. For example, it is reported that lower metabolic activity characterizes the quiescent state (Takubo et al. 2013; Ryall et al. 2015; Pala et al. 2018) and metabolomics studies may be considered.

5.2.4. Possible limitations in using BNC for cell culture

Some limitations of BNC as a substrate are related to the experimental procedure and the manufacturing process. To perform each experiment on BNC, I had to modify several established standard cell culture protocols. For example, I used additional enzymes (e.g. collagenases and dispase) and longer time of incubation for cell detachment (Figure 4.18 and Methods section 3.1.2.4.). It is generally known that proteases disassemble peptide bonds in proteins and induce cell surface damage when used for cell detachment (Hayman et al. 2006; Danoviz and Yablonka-Reuveni 2012). Moreover, prolonged trypsin treatment delays the time to next cell division and by this can influence the proliferation of adherent cells (Hirai et al. 2002). Therefore, a development of a detachment protocols that involve other proteases and/or shorter incubation time would be beneficial for enhancing cell survival and accelerate proliferation recovery after detachment from BNC.

Conflicting results have been published concerning the general effect of BNC substrates on different cell types (see Introduction section 1.5.2.). Such variability can be explained by inconsistent bio-mechanical features from batch to batch if bacteria strains and manufacturing experimental technique are dissimilar (Gorgieva and Trček 2019). Moreover, we occasionally experience intrinsic differences within the single cellulose discs due to the irregularity in cellulose nanofibers organization and density. This is a limitation since changes in BNC stiffness, thickness and fiber organization and shape have been reported and experienced to strongly influence cell behavior. Therefore, a more standardized manufacturing procedure is necessary for constancy in cell culture applications.

To summarize, we showed for the first time that a cellulose-based substrate allows the culture of hPMs in a "rested", slow-dividing state for a prolonged time period without the need of cell passaging. This would avoid extensive cell propagation allowing preservation in culture for many days without undergoing differentiation or senescence. Moreover, hPMs were able to regain proliferation and myogenic potential (e.g. differentiation in multinucleated myotubes) after placed back in Standard.

5.3. BNC substrate: platform to test *ex vivo* gene editing in "resting" hPMs and other primary cells

BNC preserves hPMs in culture for several weeks temporally "arrested" in a slow-dividing state without losing their ability to re-enter cell cycle. Keeping the cells in a slow-proliferative state can be advantageous in experimental settings aimed to test genetic and pharmacological therapeutic approaches.

Here I demonstrated for the first time that hPMs can be edited when cultured on BNC. I used a CRISPR/Cas9-based strategy to successfully induce *NCAM1* gene knockout and protein depletion in donor-derived PMs (Figure 4.33). The percentage of *NCAM1* edited cells (Figure 4.33D) was lower than in Standard cell culture conditions (Figure 4.2D). The low number of edited cells on BNC was related to the lower transfection efficiency on the BNC using Lipofectamine compared to Standard (Figure 4.32). Differences in cytoskeletal organization, ECM environment and cell division between Standard and BNC culture may altogether influence the process of cellular uptake, intracellular trafficking and nuclear entry of Lipofectamine/DNA complexes (Cardarelli et al. 2016). For this reason, I additionally tested the transduction efficiency of a lentiviral-based method to deliver a GFP plasmid. This experiment showed a very high transduction efficiency of hPMs in both culture conditions (Figure 4.31). Lentiviruses have been already used for CRISPR/Cas9-based genome engineering in mammalian cells (Kabadi et al. 2014). However, since they are integrating in the genome of infected cells, the possibility of mutagenesis is a safety concern (Wilson and Cichutek 2009). For this reason, it not ideal in the contest of *in vivo* and *ex vivo* gene therapy. In addition, as discussed above (see section 5.1.) we are currently exploring more efficient methods to express the Cas9/sgRNAs complex into hPMs that are not based on DNA delivery (e.g. mRNA or RMP) via nucleofection.

Monogenic disorders like MDs affect mainly post-mitotic cells and stem cells that are not dividing (Rodwell and Aymé 2014). The treatment for these diseases is still limited in controlling the symptoms without addressing the genetic defect behind. Gene editing tools such as CRISPR/Cas9-mediated methods hold the promise of providing therapeutic cure for monogenic disorders (Porteus 2015) as shown in several preclinical studies (Kotagama, Jayasinghe, and Abeysinghe 2019). Cas9-induced HDR repair is exploited as process for higher precision editing. It requires a homologue donor DNA template and leads to sequence substitutions or insertion of the desired nucleotide sequence into the genomic target site (Paquet et al. 2016). However, since HDR is restricted to the S and G2-phases of the cell cycle (Rudin, Sugarman, and Haber 1989; Zhao et al. 2017), this approach is challenging in non-dividing cells (Nami et al. 2018). For this reason, intense research is being performed on developing repair strategies that can induce precise editing during the G0/G1-phase (Nami et al. 2018). Gene editing of stem cells like SCs which are non-dividing only when into the niche (Bischoff 1975; Konigsberg, Lipton, and Konigsberg 1975; Cheung and Rando 2013), can be tested only *in vivo*. Animal experiments are complex to set up, expensive, time consuming and hardly discussed because of ethical issues (Lewis 2019). The use of an *in vitro* system like BNC allows the testing of gene correction strategies in cells maintained in

a non-proliferative status, thus avoiding animal experiments. Moreover, a BNC-based culture system could save work-time, plastic use and medium because cells do not need passaging for many weeks.

Such application could be extended to other monogenic diseases and we are currently in the process of BNC manufactory standardization for the characterization of other primary cell types. For instance, hepatocytes, the major parenchymal liver cells, perform essential metabolic, endocrine and secretory functions (Ishibashi et al. 2009) and can be affected in hepatic inherited diseases (Clayton 2002). Hepatocytes are considered the gold standard for drug screening (Vilas-Boas et al. 2019) and disease modeling studies (Baruteau et al. 2017) when cultured *in vitro*. However, upon isolation, they can be maintained in monolayer only for a short period of time as they re-enter cell cycle and progressively de-differentiate (Zeilinger et al. 2016). Over the last years, many efforts have been made to develop new culture conditions (e.g. 3D cultivation methods) in order to preserve the liver-specific feature (Kim et al. 2010; Schyschka et al. 2013; Deegan et al. 2016; Ruoß et al. 2020). Allowing long-term culture of this type of cells while maintaining their viability and identity would be advantageous for the investigation of drug effects and gene editing approaches. The substrate we introduced in this study fit those requirements. Furthermore, BNC-based culture would permit large-scale screening of small-molecules or therapeutic compounds, otherwise challenging in the standard experimental settings.

5.4. Conclusion and future prospects

In this study, I first introduced an *ex vivo* CRISPR/Cas9-based method to correct *DYSF* c.4872_4876delinsCCCC founder mutation in LGMD2B patient-derived PMs. Dysferlin protein expression and membrane localization in corrected hPMs-derived myotubes suggested a rescue of the protein functionality. Edited dysferlin appeared also to participate to the Ca^{2+}-depended sarcolemma repair process in which the protein plays a crucial role.

Dr. Helena E. Fernandez from our laboratory (in collaboration with Dr. Ralf Kühn), developed a mouse model carrying a humanized *DYSF* exon 44 with and without the c.4872_4876delinsCCCC mutation and called HUMex44_MUT and HUMex44_WT respectively. A preliminary characterization proved that HUMex44_MUT muscles show similar histopathological symptoms to LGMD2B muscles. Since the limited availability of patient-derived PMs, this is a suitable model to ultimately confirm the efficiency of the re-framing approach through *ex vivo* and *in vivo* experiments. We are first planning to test the editing efficiency of *DYSF* in isolated mouse myoblasts. Corrected myoblasts will be analyzed for protein expression and differentiated into myotubes to investigate dysferlin functionality via laser wounding assay. By performing *in vivo* transplantation experiments, we will evaluate the engraftment efficiency of edited myoblasts and whether the protein is correctly localized at the membrane of newly generated fibers. Lastly, the re-framing efficiency can be tested directly *in vivo.* Viral or non-viral strategies can be used to systematically deliver muscle-specific Cas9 nucleases and sgRNAs in HUMex44_MUT mice. The

rescue of the dystrophic phenotype will eventually reveal the clinical relevance of the established method.

In the second part of my study, I introduced a novel BNC-based cell culture technique to maintain hPMs in slow-proliferative condition for weeks. The majority of the cells are preserved in the G0-phase of the cell cycle since they can re-enter the cell cycle when removed from BNC. Extensive proliferation of hPMs *in vitro* is known to reduce stemness (Montarras et al. 2005; Gilbert et al. 2010). Therefore, we can suppose that hPMs possess increased regenerative capabilities when detached from the substrate compared to the cells passaged simultaneously on standard conditions. To experimentally prove this, a transplantation assay could be performed. We already know that hPMs can regenerate muscle and self-renew when injected into irradiated muscle of immunocompromised mice (Marg et al. 2019). The same procedure could be applied using hPMs after long-term culture on BNC and Standard. This experiment would allow the comparison of their engraftment potential *in vivo.*

Finally, I showed that slow-dividing hPMs on BNC could also be edited via CRISPR/Cas9-based methods. This “proof of concept” experiment paved the way for its use as an *in vitro* model to study gene editing approaches in “resting” primary cells. This would permit the investigation of new treatments for monogenic diseases in which the affected cells are mainly in G0/G1-phase of the cell cycle. We aim to propose BNC as an *in vitro* tool applicable to a wide range of monogenic diseases. For this reason, our laboratory is working to standardize a large-scale BNC manufacturing procedure for the characterization of different primary cell types.

To conclude, the work of my thesis represents a step forward towards the application of *ex vivo* cell-based gene editing in the context of MDs. I provided a strategy to correct a specific dystrophy-causing mutation in patient primary myoblasts. Moreover, I presented a new culture method that helps to overcome one of the main limitations of Standard: extensive hPMs propagation leading to the loss of regenerative capabilities. This method can also be applied to perform gene editing, thus providing an *in vitro* platform to test new therapeutic approaches in “rested” and slow-dividing primary human cells.

6. CONTRIBUTIONS

hPMs characterization on BNC was based on preliminary experiments that have been performed in our laboratory by Dr. Eric Metzler.

Total RNA sequencing and preliminary data analysis was performed by Dr. Daniele Yumi Sunaga-Franze from the Genomics Platform (Dr. Sascha Sauer, Max Delbrück Center for Molecular Medicine, Berlin, Germany). Following analysis and data visualization was performed by me in close cooperation.

7. APPENDIX

7.1. Maps of plasmids encoding for SpCas9 nucleases

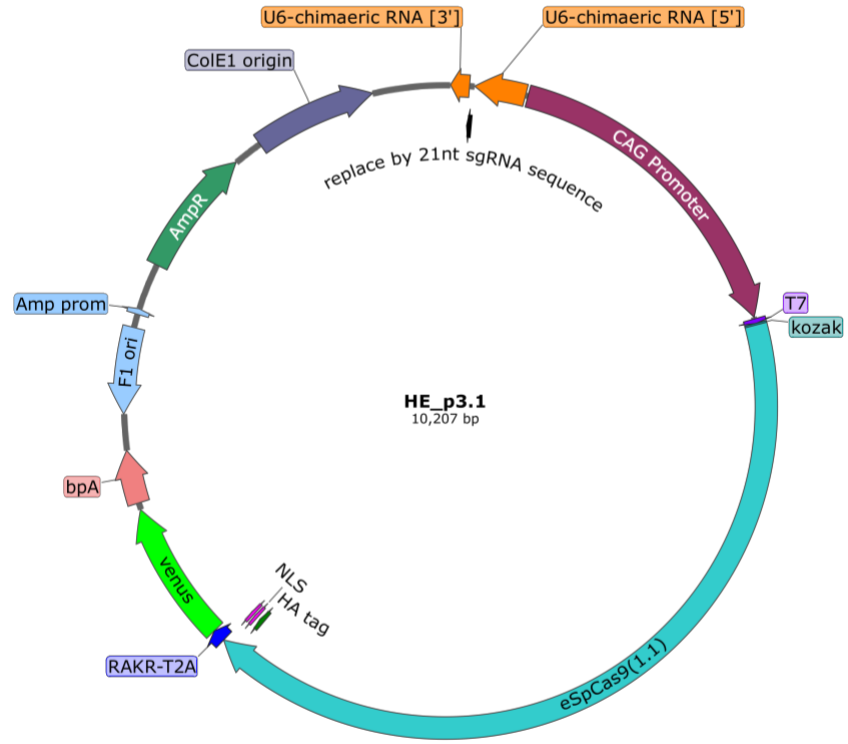

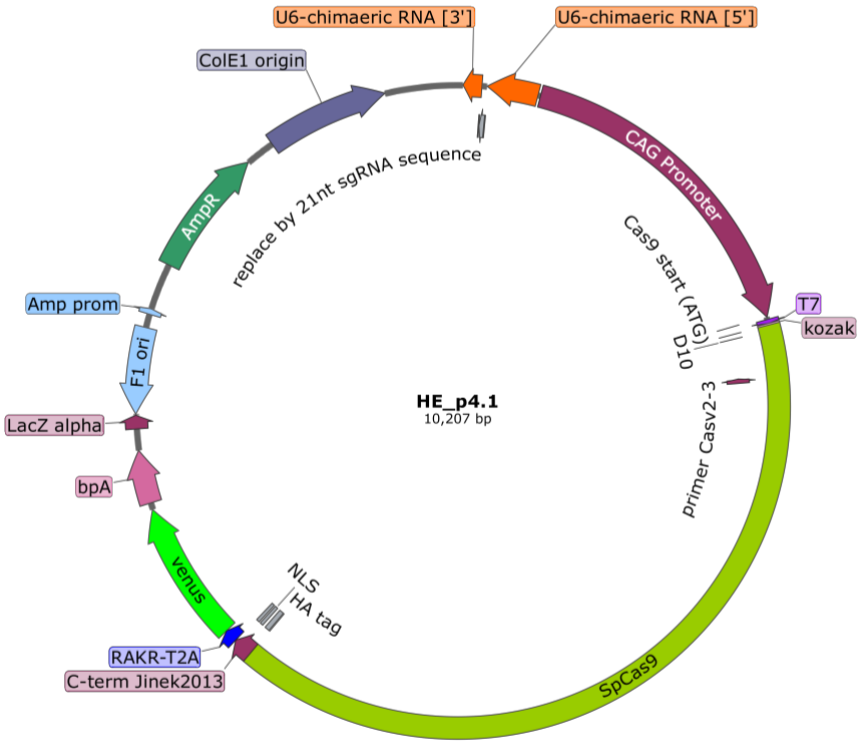

8. BIBLIOGRAPHY

Aartsma-Rus, A., M. Bremmer-Bout, A. A. Janson, J. T. den Dunnen, G. J. van Ommen, and J. C. van Deutekom. 2002. 'Targeted exon skipping as a potential gene correction therapy for Duchenne muscular dystrophy', *Neuromuscul Disord*, 12 Suppl 1: S71-7.

Aartsma-Rus, A., A. A. Janson, W. E. Kaman, M. Bremmer-Bout, J. T. den Dunnen, F. Baas, G. J. van Ommen, and J. C. van Deutekom. 2003. 'Therapeutic antisense-induced exon skipping in cultured muscle cells from six different DMD patients', *Hum Mol Genet*, 12: 907-14.

Aartsma-Rus, A., K. H. Singh, I. F. Fokkema, I. B. Ginjaar, G. J. van Ommen, J. T. den Dunnen, and S. M. van der Maarel. 2010. 'Therapeutic exon skipping for dysferlinopathies?', *Eur J Hum Genet*, 18: 889-94.

Abdullah, N., M. Padmanarayana, N. J. Marty, and C. P. Johnson. 2014. 'Quantitation of the calcium and membrane binding properties of the C2 domains of dysferlin', *Biophys J*, 106: 382-9.

Abou-Khalil, R., F. Le Grand, G. Pallafacchina, S. Valable, F. J. Authier, M. A. Rudnicki, R. K. Gherardi, S. Germain, F. Chretien, A. Sotiropoulos, P. Lafuste, D. Montarras, and B. Chazaud. 2009. 'Autocrine and paracrine angiopoietin 1/Tie-2 signaling promotes muscle satellite cell self-renewal', *Cell Stem Cell*, 5: 298-309.

Agarwal, A. K., K. Tunison, M. A. Mitsche, J. G. McDonald, and A. Garg. 2019. 'Insights into lipid accumulation in skeletal muscle in dysferlin-deficient mice', *J Lipid Res*, 60: 2057-73.

Akcakaya, P., M. L. Bobbin, J. A. Guo, J. Malagon-Lopez, K. Clement, S. P. Garcia, M. D. Fellows, M. J. Porritt, M. A. Firth, A. Carreras, T. Baccega, F. Seeliger, M. Bjursell, S. Q. Tsai, N. T. Nguyen, R. Nitsch, L. M. Mayr, L. Pinello, Y. M. Bohlooly, M. J. Aryee, M. Maresca, and J. K. Joung. 2018. 'In vivo CRISPR editing with no detectable genome-wide off-target mutations', *Nature*, 561: 416-19.

Allbrook, D. B., M. F. Han, and A. E. Hellmuth. 1971. 'Population of muscle satellite cells in relation to age and mitotic activity', *Pathology*, 3: 223-43.

Almada, A. E., and A. J. Wagers. 2016. 'Molecular circuitry of stem cell fate in skeletal muscle regeneration, ageing and disease', *Nat Rev Mol Cell Biol*, 17: 267-79.

Almeida, C. F., S. A. Fernandes, A. F. Ribeiro Junior, O. Keith Okamoto, and M. Vainzof. 2016. 'Muscle Satellite Cells: Exploring the Basic Biology to Rule Them', *Stem Cells Int*, 2016: 1078686.

Amoasii, L., J. C. W. Hildyard, H. Li, E. Sanchez-Ortiz, A. Mireault, D. Caballero, R. Harron, T. R. Stathopoulou, C. Massey, J. M. Shelton, R. Bassel-Duby, R. J. Piercy, and E. N. Olson. 2018. 'Gene editing restores dystrophin expression in a canine model of Duchenne muscular dystrophy', *Science*, 362: 86-91.

Amoasii, L., C. Long, H. Li, A. A. Mireault, J. M. Shelton, E. Sanchez-Ortiz, J. R. McAnally, S. Bhattacharyya, F. Schmidt, D. Grimm, S. D. Hauschka, R. Bassel-Duby, and E. N. Olson. 2017. 'Single-cut genome editing restores dystrophin expression in a new mouse model of muscular dystrophy', *Sci Transl Med*, 9.

Ampong, B. N., M. Imamura, T. Matsumiya, M. Yoshida, and S. Takeda. 2005. 'Intracellular localization of dysferlin and its association with the dihydropyridine receptor', *Acta Myol*, 24: 134-44.

Anders, C., O. Niewoehner, A. Duerst, and M. Jinek. 2014. 'Structural basis of PAM-dependent target DNA recognition by the Cas9 endonuclease', *Nature*, 513: 569-73.

Anderson, K.R., M. Haeussler, C. Watanabe, V. Janakiraman, J. Lund, Z. Modrusan, J. Stinson, Q. Bei, A. Buechler, C.Yu, S. R. Thamminana, L. Tam, M.-A. Sowick, T. Alcantar, N. O'Neil, J. Li, L. Ta, L. Lima, M. Roose-Girma, X. Rairdan, S. Durinck, and S. Warming. 2018. 'CRISPR off-target analysis in genetically engineered rats and mice', *Nature Methods*, 15: 512-14.

Anderson, L. V., K. Davison, J. A. Moss, C. Young, M. J. Cullen, J. Walsh, M. A. Johnson, R. Bashir, S. Britton, S. Keers, Z. Argov, I. Mahjneh, F. Fougerousse, J. S. Beckmann, and K. M. Bushby. 1999. 'Dysferlin is a plasma membrane protein and is expressed early in human development', *Hum Mol Genet*, 8: 855-61.

Andersson, J., H. Stenhamre, H. Bäckdahl, and P. Gatenholm. 2010. 'Behavior of human chondrocytes in engineered porous bacterial cellulose scaffolds', *J Biomed Mater Res A*, 94: 1124-32.

Andrade, F. K., Renata Pértile, Fernando Dourado, and Francisco Gama. 2010. *Bacterial cellulose: Properties, production and applications*.

Angelini, C., L. Giaretta, and R. Marozzo. 2018. 'An update on diagnostic options and considerations in limb-girdle dystrophies', *Expert Rev Neurother*, 18: 693-703.
Anson, D. S. 2004. 'The use of retroviral vectors for gene therapy-what are the risks? A review of retroviral pathogenesis and its relevance to retroviral vector-mediated gene delivery', *Genet Vaccines Ther*, 2: 9.
Aoki, M., J. Liu, I. Richard, R. Bashir, S. Britton, S. M. Keers, J. Oeltjen, H. E. Brown, S. Marchand, N. Bourg, C. Beley, D. McKenna-Yasek, K. Arahata, S. Bohlega, E. Cupler, I. Illa, I. Majneh, R. J. Barohn, J. A. Urtizberea, M. Fardeau, A. Amato, C. Angelini, K. Bushby, J. S. Beckmann, and R. H. Brown, Jr. 2001. 'Genomic organization of the dysferlin gene and novel mutations in Miyoshi myopathy', *Neurology*, 57: 271-8.
Aoki, Y., T. Nagata, T. Yokota, A. Nakamura, M. J. Wood, T. Partridge, and S. Takeda. 2013. 'Highly efficient in vivo delivery of PMO into regenerating myotubes and rescue in laminin-α2 chain-null congenital muscular dystrophy mice', *Hum Mol Genet*, 22: 4914-28.
Arai, F., and T. Suda. 2008. 'Quiescent stem cells in the niche.' in, *StemBook* (Cambridge (MA)).
Argov, Z., M. Sadeh, K. Mazor, D. Soffer, E. Kahana, I. Eisenberg, S. Mitrani-Rosenbaum, I. Richard, J. Beckmann, S. Keers, R. Bashir, K. Bushby, and H. Rosenmann. 2000. 'Muscular dystrophy due to dysferlin deficiency in Libyan Jews. Clinical and genetic features', *Brain*, 123 (Pt 6): 1229-37.
Azakir, B. A., S. Di Fulvio, C. Therrien, and M. Sinnreich. 2010. 'Dysferlin interacts with tubulin and microtubules in mouse skeletal muscle', *PLoS One*, 5: e10122.
Bäckdahl, H., M. Esguerra, D. Delbro, B. Risberg, and P. Gatenholm. 2008. 'Engineering microporosity in bacterial cellulose scaffolds', *J Tissue Eng Regen Med*, 2: 320-30.
Bäckdahl, H., G. Helenius, A. Bodin, U. Nannmark, B. R. Johansson, B. Risberg, and P. Gatenholm. 2006. 'Mechanical properties of bacterial cellulose and interactions with smooth muscle cells', *Biomaterials*, 27: 2141-9.
Baghdadi, M. B., D. Castel, L. Machado, S. I. Fukada, D. E. Birk, F. Relaix, S. Tajbakhsh, and P. Mourikis. 2018. 'Reciprocal signalling by Notch-Collagen V-CALCR retains muscle stem cells in their niche', *Nature*, 557: 714-18.
Baldin, V., J. Lukas, M. J. Marcote, M. Pagano, and G. Draetta. 1993. 'Cyclin D1 is a nuclear protein required for cell cycle progression in G1', *Genes Dev*, 7: 812-21.
Bansal, D., and K. P. Campbell. 2004. 'Dysferlin and the plasma membrane repair in muscular dystrophy', *Trends Cell Biol*, 14: 206-13.
Bansal, D., K. Miyake, S. S. Vogel, S. Groh, C. C. Chen, R. Williamson, P. L. McNeil, and K. P. Campbell. 2003. 'Defective membrane repair in dysferlin-deficient muscular dystrophy', *Nature*, 423: 168-72.
Barruet, E., S. M. Garcia, K. Striedinger, J. Wu, S. Lee, L. Byrnes, A. Wong, S. Xuefeng, S. Tamaki, A. S. Brack, and J. H. Pomerantz. 2020. 'Functionally heterogeneous human satellite cells identified by single cell RNA sequencing', *Elife*, 9.
Barthelemy, F., C. Blouin, N. Wein, V. Mouly, S. Courrier, E. Dionnet, V. Kergourlay, Y. Mathieu, L. Garcia, G. Butler-Browne, C. Lamaze, N. Levy, M. Krahn, and M. Bartoli. 2015. 'Exon 32 Skipping of Dysferlin Rescues Membrane Repair in Patients' Cells', *J Neuromuscul Dis*, 2: 281-90.
Barthelemy, F., N. Wein, M. Krahn, N. Levy, and M. Bartoli. 2011. 'Translational research and therapeutic perspectives in dysferlinopathies', *Mol Med*, 17: 875-82.
Baruteau, J., S. N. Waddington, I. E. Alexander, and P. Gissen. 2017. 'Gene therapy for monogenic liver diseases: clinical successes, current challenges and future prospects', *J Inherit Metab Dis*, 40: 497-517.
Bashir, R., S. Britton, T. Strachan, S. Keers, E. Vafiadaki, M. Lako, I. Richard, S. Marchand, N. Bourg, Z. Argov, M. Sadeh, I. Mahjneh, G. Marconi, M. R. Passos-Bueno, S. Moreira Ede, M. Zatz, J. S. Beckmann, and K. Bushby. 1998. 'A gene related to Caenorhabditis elegans spermatogenesis factor fer-1 is mutated in limb-girdle muscular dystrophy type 2B', *Nat Genet*, 20: 37-42.
Bellec, J., M. Bacchetta, D. Losa, I. Anegon, M. Chanson, and T. H. Nguyen. 2015. 'CFTR inactivation by lentiviral vector-mediated RNA interference and CRISPR-Cas9 genome editing in human airway epithelial cells', *Curr Gene Ther*, 15: 447-59.
Belles-Isles, M., R. Roy, G. Dansereau, M. Goulet, B. Roy, J. P. Bouchard, and J. P. Tremblay. 1993. 'Rapid selection of donor myoblast clones for muscular dystrophy therapy using cell surface expression of NCAM', *Eur J Histochem*, 37: 375-80.
Bengtsson, N. E., J. K. Hall, G. L. Odom, M. P. Phelps, C. R. Andrus, R. D. Hawkins, S. D. Hauschka, J. R. Chamberlain, and J. S. Chamberlain. 2017. 'Muscle-specific CRISPR/Cas9

dystrophin gene editing ameliorates pathophysiology in a mouse model for Duchenne muscular dystrophy', *Nat Commun*, 8: 14454.
Bentzinger, C. F., Y. X. Wang, J. von Maltzahn, and M. A. Rudnicki. 2013. 'The emerging biology of muscle stem cells: implications for cell-based therapies', *Bioessays*, 35: 231-41.
Bentzinger, C. F., Y. X. Wang, J. von Maltzahn, V. D. Soleimani, H. Yin, and M. A. Rudnicki. 2013. 'Fibronectin regulates Wnt7a signaling and satellite cell expansion', *Cell Stem Cell*, 12: 75-87.
Berger, S., G. Schäfer, D. A. Kesper, A. Holz, T. Eriksson, R. H. Palmer, L. Beck, C. Klämbt, R. Renkawitz-Pohl, and S.-F. Önel. 2008. 'WASP and SCAR have distinct roles in activating the Arp2/3 complex during myoblast fusion', *Journal of Cell Science*, 121: 1303.
Bernadotte, A., V. M. Mikhelson, and I. M. Spivak. 2016. 'Markers of cellular senescence. Telomere shortening as a marker of cellular senescence', *Aging (Albany NY)*, 8: 3-11.
Biressi, S., A. Filareto, and T. A. Rando. 2020. 'Stem cell therapy for muscular dystrophies', *J Clin Invest*.
Bischoff, R. 1975. 'Regeneration of single skeletal muscle fibers in vitro', *Anat Rec*, 182: 215-35.
Bjornson, C. R., T. H. Cheung, L. Liu, P. V. Tripathi, K. M. Steeper, and T. A. Rando. 2012. 'Notch signaling is necessary to maintain quiescence in adult muscle stem cells', *Stem Cells*, 30: 232-42.
Blau, H. M., C. Webster, and G. K. Pavlath. 1983. 'Defective myoblasts identified in Duchenne muscular dystrophy', *Proc Natl Acad Sci U S A*, 80: 4856-60.
Bodin, A., H. Bäckdahl, H. Fink, L. Gustafsson, B. Risberg, and P. Gatenholm. 2007. 'Influence of cultivation conditions on mechanical and morphological properties of bacterial cellulose tubes', *Biotechnol Bioeng*, 97: 425-34.
Booth, D. G., and W. C. Earnshaw. 2017. 'Ki-67 and the Chromosome Periphery Compartment in Mitosis', *Trends Cell Biol*, 27: 906-16.
Briggs, D., and J. E. Morgan. 2013. 'Recent progress in satellite cell/myoblast engraftment -- relevance for therapy', *Febs j*, 280: 4281-93.
Brimah, K., J. Ehrhardt, V. Mouly, G. S. Butler-Browne, T. A. Partridge, and J. E. Morgan. 2004. 'Human muscle precursor cell regeneration in the mouse host is enhanced by growth factors', *Hum Gene Ther*, 15: 1109-24.
Brown, N. R., E. D. Lowe, E. Petri, V. Skamnaki, R. Antrobus, and L. N. Johnson. 2007. 'Cyclin B and cyclin A confer different substrate recognition properties on CDK2', *Cell Cycle*, 6: 1350-9.
Bustin, S. A., V. Benes, J. A. Garson, J. Hellemans, J. Huggett, M. Kubista, R. Mueller, T. Nolan, M. W. Pfaffl, G. L. Shipley, J. Vandesompele, and C. T. Wittwer. 2009. 'The MIQE guidelines: minimum information for publication of quantitative real-time PCR experiments', *Clin Chem*, 55: 611-22.
Cagliani, R., F. Fortunato, R. Giorda, C. Rodolico, M. C. Bonaglia, M. Sironi, M. G. D'Angelo, A. Prelle, F. Locatelli, A. Toscano, N. Bresolin, and G. P. Comi. 2003. 'Molecular analysis of LGMD-2B and MM patients: identification of novel DYSF mutations and possible founder effect in the Italian population', *Neuromuscul Disord*, 13: 788-95.
Cai, C., H. Masumiya, N. Weisleder, N. Matsuda, M. Nishi, M. Hwang, J. K. Ko, P. Lin, A. Thornton, X. Zhao, Z. Pan, S. Komazaki, M. Brotto, H. Takeshima, and J. Ma. 2009. 'MG53 nucleates assembly of cell membrane repair machinery', *Nat Cell Biol*, 11: 56-64.
Cai, C., N. Weisleder, J. K. Ko, S. Komazaki, Y. Sunada, M. Nishi, H. Takeshima, and J. Ma. 2009. 'Membrane repair defects in muscular dystrophy are linked to altered interaction between MG53, caveolin-3, and dysferlin', *J Biol Chem*, 284: 15894-902.
Capkovic, Katie L., Severin Stevenson, Marc C. Johnson, Jay J. Thelen, and D. D. W. Cornelison. 2008. 'Neural cell adhesion molecule (NCAM) marks adult myogenic cells committed to differentiation', *Experimental cell research*, 314: 1553-65.
Cardarelli, F., L. Digiacomo, C. Marchini, A. Amici, F. Salomone, G. Fiume, A. Rossetta, E. Gratton, D. Pozzi, and G. Caracciolo. 2016. 'The intracellular trafficking mechanism of Lipofectamine-based transfection reagents and its implication for gene delivery', *Scientific Reports*, 6: 25879.
Cárdenas, A. M., A. M. González-Jamett, L. A. Cea, J. A. Bevilacqua, and P. Caviedes. 2016. 'Dysferlin function in skeletal muscle: Possible pathological mechanisms and therapeutical targets in dysferlinopathies', *Exp Neurol*, 283: 246-54.
Chakkalakal, J. V., J. Christensen, W. Xiang, M. T. Tierney, F. S. Boscolo, A. Sacco, and A. S. Brack. 2014. 'Early forming label-retaining muscle stem cells require p27kip1 for maintenance of the primitive state', *Development*, 141: 1649-59.

Chakkalakal, J. V., K. M. Jones, M. A. Basson, and A. S. Brack. 2012. 'The aged niche disrupts muscle stem cell quiescence', *Nature*, 490: 355-60.
Chakrabarti, A. M., T. Henser-Brownhill, J. Monserrat, A. R. Poetsch, N. M. Luscombe, and P. Scaffidi. 2019. 'Target-Specific Precision of CRISPR-Mediated Genome Editing', *Molecular Cell*, 73: 699-713.e6.
Chal J, Oginuma M, Al Tanoury Z, Gobert B, Sumara O, Hick A, Bousson F, Zidouni Y, Mursch C, Moncuquet P, Tassy O, Vincent S, Miyanari A, Bera A, Garnier JM, Guevara G, Hestin M, Kennedy L, Hayashi S, Drayton B, Cherrier T, Gayraud-Morel B, Gussoni E, Relaix F, Tajbakhsh S, Pourquié O. Differentiation of pluripotent stem cells to muscle fiber to model Duchenne muscular dystrophy. Nat Biotechnol. 2015 Sep;33(9):962-9.
Charville, G. W., T. H. Cheung, B. Yoo, P. J. Santos, G. K. Lee, J. B. Shrager, and T. A. Rando. 2015. 'Ex Vivo Expansion and In Vivo Self-Renewal of Human Muscle Stem Cells', *Stem Cell Reports*, 5: 621-32.
Cheung, T. H., and T. A. Rando. 2013. 'Molecular regulation of stem cell quiescence', *Nat Rev Mol Cell Biol*, 14: 329-40.
Cho, D. S., and J. D. Doles. 2017. 'Single cell transcriptome analysis of muscle satellite cells reveals widespread transcriptional heterogeneity', *Gene*, 636: 54-63.
Cho, S. W., S. Kim, J. M. Kim, and J. S. Kim. 2013. 'Targeted genome engineering in human cells with the Cas9 RNA-guided endonuclease', *Nat Biotechnol*, 31: 230-2.
Cho, S. W., S. Kim, Y. Kim, J. Kweon, H. S. Kim, S. Bae, and J. S. Kim. 2014. 'Analysis of off-target effects of CRISPR/Cas-derived RNA-guided endonucleases and nickases', *Genome Res*, 24: 132-41.
Chu, V. T., T. Weber, B. Wefers, W. Wurst, S. Sander, K. Rajewsky, and R. Kühn. 2015. 'Increasing the efficiency of homology-directed repair for CRISPR-Cas9-induced precise gene editing in mammalian cells', *Nature Biotechnology*, 33: 543-48.
Clayton, P. T. 2002. 'Inborn errors presenting with liver dysfunction', *Semin Neonatol*, 7: 49-63.
Coller, H. A., L. Sang, and J. M. Roberts. 2006. 'A new description of cellular quiescence', *PLoS Biol*, 4: e83.
Collins, C. A., I. Olsen, P. S. Zammit, L. Heslop, A. Petrie, T. A. Partridge, and J. E. Morgan. 2005. 'Stem cell function, self-renewal, and behavioral heterogeneity of cells from the adult muscle satellite cell niche', *Cell*, 122: 289-301.
Conboy, I. M., and T. A. Rando. 2002. 'The regulation of Notch signaling controls satellite cell activation and cell fate determination in postnatal myogenesis', *Dev Cell*, 3: 397-409.
Concordet, J.-P., and M. Haeussler. 2018. 'CRISPOR: intuitive guide selection for CRISPR/Cas9 genome editing experiments and screens', *Nucleic Acids Research*, 46: W242-W45.
Cong, L., F. A. Ran, D. Cox, S. Lin, R. Barretto, N. Habib, P. D. Hsu, X. Wu, W. Jiang, L. A. Marraffini, and F. Zhang. 2013. 'Multiplex genome engineering using CRISPR/Cas systems', *Science*, 339: 819-23.
Connolly, J. B. 2002. 'Lentiviruses in gene therapy clinical research', *Gene Ther*, 9: 1730-4.
Cooper, R. N., D. Thiesson, D. Furling, J. P. Di Santo, G. S. Butler-Browne, and V. Mouly. 2003. 'Extended amplification in vitro and replicative senescence: key factors implicated in the success of human myoblast transplantation', *Hum Gene Ther*, 14: 1169-79.
Cooper, S. T., and P. L. McNeil. 2015. 'Membrane Repair: Mechanisms and Pathophysiology', *Physiol Rev*, 95: 1205-40.
Cossu, G., Previtali, S. C., Napolitano, S., Cicalese, M. P., Tedesco, F. S., Nicastro, F., Noviello, M., Roostalu, U., Natali Sora, M. G., Scarlato, M., De Pellegrin, M., Godi, C., Giuliani, S., Ciotti, F., Tonlorenzi, R., Lorenzetti, I., Rivellini, C., Benedetti, S., Gatti, R., Marktel, S., … Ciceri, F. 2015. 'Intra-arterial transplantation of HLA-matched donor mesoangioblasts in Duchenne muscular dystrophy' EMBO molecular medicine, 7(12), 1513–1528.
Crudele, J. M., and J. S. Chamberlain. 2019. 'AAV-based gene therapies for the muscular dystrophies', *Hum Mol Genet*, 28: R102-R07.
Crudele, Julie M., and Jeffrey S. Chamberlain. 2018. 'Cas9 immunity creates challenges for CRISPR gene editing therapies', *Nature Communications*, 9: 3497.
Cuylen, Sara, Claudia Blaukopf, Antonio Z. Politi, Thomas Müller-Reichert, Beate Neumann, Ina Poser, Jan Ellenberg, Anthony A. Hyman, and Daniel W. Gerlich. 2016. 'Ki-67 acts as a biological surfactant to disperse mitotic chromosomes', *Nature*, 535: 308-12.
Czaja, W., A. Krystynowicz, S. Bielecki, and R. M. Brown, Jr. 2006. 'Microbial cellulose--the natural power to heal wounds', *Biomaterials*, 27: 145-51.

Danoviz, M. E., and Z. Yablonka-Reuveni. 2012. 'Skeletal muscle satellite cells: background and methods for isolation and analysis in a primary culture system', *Methods Mol Biol*, 798: 21-52.
Darabi, R., R. W. Arpke, S. Irion, J. T. Dimos, M. Grskovic, M. Kyba, and R. C. Perlingeiro. 2012. 'Human ES- and iPS-derived myogenic progenitors restore DYSTROPHIN and improve contractility upon transplantation in dystrophic mice', *Cell Stem Cell*, 10: 610-9.
De Angelis, L., L. Berghella, M. Coletta, L. Lattanzi, M. Zanchi, M. G. Cusella-De Angelis, C. Ponzetto, and G. Cossu. 1999. 'Skeletal myogenic progenitors originating from embryonic dorsal aorta coexpress endothelial and myogenic markers and contribute to postnatal muscle growth and regeneration', *J Cell Biol*, 147: 869-78.
de Lange, T., L. Shiue, R. M. Myers, D. R. Cox, S. L. Naylor, A. M. Killery, and H. E. Varmus. 1990. 'Structure and variability of human chromosome ends', *Molecular and cellular biology*, 10: 518-27.
De Luna, N., E. Gallardo, and I. Illa. 2004. 'In vivo and in vitro dysferlin expression in human muscle satellite cells', *J Neuropathol Exp Neurol*, 63: 1104-13.
Decary, S., V. Mouly, and G. S. Butler-Browne. 1996. 'Telomere length as a tool to monitor satellite cell amplification for cell-mediated gene therapy', *Hum Gene Ther*, 7: 1347-50.
Decary, S., V. Mouly, C. B. Hamida, A. Sautet, J. P. Barbet, and G. S. Butler-Browne. 1997. 'Replicative potential and telomere length in human skeletal muscle: implications for satellite cell-mediated gene therapy', *Hum Gene Ther*, 8: 1429-38.
Deegan, D. B., C.Zimmerman, A. Skardal, A. Atala, and T. D. Shupe. 2016. 'Stiffness of hyaluronic acid gels containing liver extracellular matrix supports human hepatocyte function and alters cell morphology', *Journal of the Mechanical Behavior of Biomedical Materials*, 55: 87-103.
Dellatore, S. M., A. S. Garcia, and W. M. Miller. 2008. 'Mimicking stem cell niches to increase stem cell expansion', *Curr Opin Biotechnol*, 19: 534-40.
Dellavalle, A., G. Maroli, D. Covarello, E. Azzoni, A. Innocenzi, L. Perani, S. Antonini, R. Sambasivan, S. Brunelli, S. Tajbakhsh, and G. Cossu. 2011. 'Pericytes resident in postnatal skeletal muscle differentiate into muscle fibres and generate satellite cells', *Nature Communications*, 2: 499.
Dellavalle, A., M. Sampaolesi, R. Tonlorenzi, E. Tagliafico, B. Sacchetti, L. Perani, A. Innocenzi, B. G. Galvez, G. Messina, R. Morosetti, S. Li, M. Belicchi, G. Peretti, J. S. Chamberlain, W. E. Wright, Y. Torrente, S. Ferrari, P. Bianco, and G. Cossu. 2007. 'Pericytes of human skeletal muscle are myogenic precursors distinct from satellite cells', *Nat Cell Biol*, 9: 255-67.
Deltcheva, E., K. Chylinski, C. M. Sharma, K. Gonzales, Y. Chao, Z. A. Pirzada, M. R. Eckert, J. Vogel, and E. Charpentier. 2011. 'CRISPR RNA maturation by trans-encoded small RNA and host factor RNase III', *Nature*, 471: 602-7.
Demonbreun, A. R., J. P. Fahrenbach, K. Deveaux, J. U. Earley, P. Pytel, and E. M. McNally. 2011. 'Impaired muscle growth and response to insulin-like growth factor 1 in dysferlin-mediated muscular dystrophy', *Human Molecular Genetics*, 20: 779-89.
Diaz-Manera, J., R. Fernandez-Torron, L. Lauger J, M. K. James, A. Mayhew, F. E. Smith, U. R. Moore, A. M. Blamire, P. G. Carlier, L. Rufibach, P. Mittal, M. Eagle, M. Jacobs, T. Hodgson, D. Wallace, L. Ward, M. Smith, R. Stramare, A. Rampado, N. Sato, T. Tamaru, B. Harwick, S. Rico Gala, … K. Bushby, and V. Straub. 2018. 'Muscle MRI in patients with dysferlinopathy: pattern recognition and implications for clinical trials', *J Neurol Neurosurg Psychiatry*, 89: 1071-81.
Díaz-Manera, J., T. Touvier, A. Dellavalle, R. Tonlorenzi, F. S. Tedesco, G. Messina, M. Meregalli, C. Navarro, L. Perani, C. Bonfanti, I. Illa, Y. Torrente, and G. Cossu. 2010. 'Partial dysferlin reconstitution by adult murine mesoangioblasts is sufficient for full functional recovery in a murine model of dysferlinopathy', *Cell Death Dis*, 1: e61.
Diecke, S., L. Ye, S. Zhang, and J. Zhang. 2013. 'Generation and Differentiation of Human iPS Cells.' in H. Ardehali, R. Bolli and D.W. Losordo (eds.), *Manual of Research Techniques in Cardiovascular Medicine* (John Wiley & Sons, Ltd.).
Doherty, Katherine R., Andrew Cave, Dawn Belt Davis, Anthony J. Delmonte, Avery Posey, Judy U. Earley, Michele Hadhazy, and Elizabeth M. McNally. 2005. 'Normal myoblast fusion requires myoferlin', *Development (Cambridge, England)*, 132: 5565-75.
Domingos, J., A. Sarkozy, M. Scoto, and F. Muntoni. 2017. 'Dystrophinopathies and limb-girdle muscular dystrophies', *Neuropediatrics*, 48: 262-72.
Dominov, Janice A., Ozgün Uyan, Peter C. Sapp, Diane McKenna-Yasek, Babi R. R. Nallamilli, Madhuri Hegde, and Robert H. Brown, Jr. 2014. 'A novel dysferlin mutant pseudoexon

bypassed with antisense oligonucleotides', *Annals of clinical and translational neurology*, 1: 703-20.
Dong, J. Y., P. D. Fan, and R. A. Frizzell. 1996. 'Quantitative analysis of the packaging capacity of recombinant adeno-associated virus', *Hum Gene Ther*, 7: 2101-12.
Doudna, J. A., and E. Charpentier. 2014. 'Genome editing. The new frontier of genome engineering with CRISPR-Cas9', *Science*, 346: 1258096.
Duan, Dongsheng. 2018. 'Systemic AAV Micro-dystrophin Gene Therapy for Duchenne Muscular Dystrophy', *Molecular therapy : the journal of the American Society of Gene Therapy*, 26: 2337-56.
Dull, T., R. Zufferey, M. Kelly, R. J. Mandel, M. Nguyen, D. Trono, and L. Naldini. 1998. 'A third-generation lentivirus vector with a conditional packaging system', *J Virol*, 72: 8463-71.
Dumont, N. A., and M. A. Rudnicki. 2016. 'Targeting muscle stem cell intrinsic defects to treat Duchenne muscular dystrophy', *NPJ Regen Med*, 1: 16006-.
Dumont, N. A., Y. X. Wang, and M. A. Rudnicki. 2015. 'Intrinsic and extrinsic mechanisms regulating satellite cell function', *Development*, 142: 1572-81.
Dunckley, M. G., M. Manoharan, P. Villiet, I. C. Eperon, and G. Dickson. 1998. 'Modification of splicing in the dystrophin gene in cultured Mdx muscle cells by antisense oligoribonucleotides', *Hum Mol Genet*, 7: 1083-90.
Dutta, S. D., D. K. Patel, and K. T. Lim. 2019. 'Functional cellulose-based hydrogels as extracellular matrices for tissue engineering', *J Biol Eng*, 13: 55.
Emery, A. E. 2002. 'The muscular dystrophies', *Lancet*, 359: 687-95.
Engler, A. J., S. Sen, H. L. Sweeney, and D. E. Discher. 2006. 'Matrix elasticity directs stem cell lineage specification', *Cell*, 126: 677-89.
Escobar, H., V. Schowel, S. Spuler, A. Marg, and Z. Izsvak. 2016. 'Full-length Dysferlin Transfer by the Hyperactive Sleeping Beauty Transposase Restores Dysferlin-deficient Muscle', *Mol Ther Nucleic Acids*, 5: e277.
Etienne-Manneville, S., and A. Hall. 2002. 'Rho GTPases in cell biology', *Nature*, 420: 629-35.
Evano, B., and S. Tajbakhsh. 2018. 'Skeletal muscle stem cells in comfort and stress', *NPJ Regen Med*, 3: 24.
Fan, Y., M. Maley, M. Beilharz, and M. Grounds. 1996. 'Rapid death of injected myoblasts in myoblast transfer therapy', *Muscle Nerve*, 19: 853-60.
Feil, G., R. Horres, J. Schulte, A. F. Mack, S. Petzoldt, C. Arnold, C. Meng, L. Jost, J. Boxleitner, N. Kiessling-Wolf, E. Serbest, D. Helm, B. Kuster, I. Hartmann, T. Korff, and H. Hahne. 2017. 'Bacterial Cellulose Shifts Transcriptome and Proteome of Cultured Endothelial Cells Towards Native Differentiation', *Mol Cell Proteomics*, 16: 1563-77.
Feldmann, E. M., J. F. Sundberg, B. Bobbili, S. Schwarz, P. Gatenholm, and N. Rotter. 2013. 'Description of a novel approach to engineer cartilage with porous bacterial nanocellulose for reconstruction of a human auricle', *J Biomater Appl*, 28: 626-40.
Figueiredo, Andrea G. P. R., Ana R. P. Figueiredo, Ana Alonso-Varona, Susana C. M. Fernandes, Teodoro Palomares, Eva Rubio-Azpeitia, Ana Barros-Timmons, Armando J. D. Silvestre, Carlos Pascoal Neto, and Carmen S. R. Freire. 2013. 'Biocompatible bacterial cellulose-poly(2-hydroxyethyl methacrylate) nanocomposite films', *BioMed research international*, 2013: 698141-41.
Flamini, V., R. S. Ghadiali, P. Antczak, A. Rothwell, J. E. Turnbull, and A. Pisconti. 2018. 'The Satellite Cell Niche Regulates the Balance between Myoblast Differentiation and Self-Renewal via p53', *Stem Cell Reports*, 10: 970-83.
Floyd, S. S., Jr., P. R. Clemens, M. R. Ontell, S. Kochanek, C. S. Day, J. Yang, S. D. Hauschka, L. Balkir, J. Morgan, M. S. Moreland, G. W. Feero, M. Epperly, and J. Huard. 1998. 'Ex vivo gene transfer using adenovirus-mediated full-length dystrophin delivery to dystrophic muscles', *Gene Ther*, 5: 19-30.
Fontana, J. D., A. M. de Souza, C. K. Fontana, I. L. Torriani, J. C. Moreschi, B. J. Gallotti, S. J. de Souza, G. P. Narcisco, J. A. Bichara, and L. F. Farah. 1990. 'Acetobacter cellulose pellicle as a temporary skin substitute', *Appl Biochem Biotechnol*, 24-25: 253-64.
Frangoul, H., D. Altshuler, M. D. Cappellini, Y. S. Chen, J. Domm, B. K. Eustace, J. Foell, J. de la Fuente, S. Grupp, R. Handgretinger, T. W. Ho, A. Kattamis, A. Kernytsky, J. Lekstrom-Himes, A. M. Li, F. Locatelli, M. Y. Mapara, M. de Montalembert, D. Rondelli, A. Sharma, S. Sheth, S. Soni, M. H. Steinberg, D. Wall, A. Yen, and S. Corbacioglu. 2020. 'CRISPR-Cas9 Gene Editing for Sickle Cell Disease and β-Thalassemia', *N Engl J Med*.
Frontera, W. R., and J. Ochala. 2015. 'Skeletal muscle: a brief review of structure and function', *Calcif Tissue Int*, 96: 183-95.

Fu, X., J. Xiao, Y. Wei, S. Li, Y. Liu, J. Yin, K. Sun, H. Sun, H. Wang, Z. Zhang, B. T. Zhang, C. Sheng, H. Wang, and P. Hu. 2015. 'Combination of inflammation-related cytokines promotes long-term muscle stem cell expansion', *Cell Res*, 25: 655-73.

Fu, Y., J. A. Foden, C. Khayter, M. L. Maeder, D. Reyon, J. K. Joung, and J. D. Sander. 2013. 'High-frequency off-target mutagenesis induced by CRISPR-Cas nucleases in human cells', *Nat Biotechnol*, 31: 822-6.

Fukada, S., A. Uezumi, M. Ikemoto, S. Masuda, M. Segawa, N. Tanimura, H. Yamamoto, Y. Miyagoe-Suzuki, and S. Takeda. 2007. 'Molecular signature of quiescent satellite cells in adult skeletal muscle', *Stem Cells*, 25: 2448-59.

Furling, D., L. Coiffier, V. Mouly, J. P. Barbet, J. L. St Guily, K. Taneja, G. Gourdon, C. Junien, and G. S. Butler-Browne. 2001. 'Defective satellite cells in congenital myotonic dystrophy', *Hum Mol Genet*, 10: 2079-87.

Gabr, H., M. K. El Ghamrawy, A. H. Almaeen, A. S. Abdelhafiz, A. O. S. Hassan, and M. H. El Sissy. 2020. 'CRISPR-mediated gene modification of hematopoietic stem cells with beta-thalassemia IVS-1-110 mutation', *Stem Cell Res Ther*, 11: 390.

Gao, Zongliang, Alex Harwig, Ben Berkhout, and Elena Herrera-Carrillo. 2017. 'Mutation of nucleotides around the +1 position of type 3 polymerase III promoters: The effect on transcriptional activity and start site usage', *Transcription*, 8: 275-87.

García-Prat, L., E. Perdiguero, S. Alonso-Martín, S. Dell'Orso, S. Ravichandran, S. R. Brooks, A. H. Juan, S. Campanario, K. Jiang, X. Hong, L. Ortet, V. Ruiz-Bonilla, M. Flández, V. Moiseeva, E. Rebollo, M. Jardí, H. W. Sun, A. Musarò, M. Sandri, A. Del Sol, V. Sartorelli, and P. Muñoz-Cánoves. 2020. 'FoxO maintains a genuine muscle stem-cell quiescent state until geriatric age', *Nat Cell Biol*, 22: 1307-18.

Garcia, S. M., S. Tamaki, S. Lee, A. Wong, A. Jose, J. Dreux, G. Kouklis, H. Sbitany, R. Seth, P. D. Knott, C. Heaton, W. R. Ryan, E. A. Kim, S. L. Hansen, W. Y. Hoffman, and J. H. Pomerantz. 2018. 'High-Yield Purification, Preservation, and Serial Transplantation of Human Satellite Cells', *Stem Cell Reports*, 10: 1160-74.

Gasiunas, G., R. Barrangou, P. Horvath, and V. Siksnys. 2012. 'Cas9-crRNA ribonucleoprotein complex mediates specific DNA cleavage for adaptive immunity in bacteria', *Proc Natl Acad Sci U S A*, 109: E2579-86.

Gastaldello S, D'Angelo S, Franzoso S, Fanin M, Angelini C, Betto R, Sandonà D. 2008. 'Inhibition of proteasome activity promotes the correct localization of disease-causing alpha-sarcoglycan mutants in HEK-293 cells constitutively expressing beta-, gamma-, and delta-sarcoglycan' Am J Pathol., 173(1):170-81.

Gayathri, N., R. Alefia, A. Nalini, T. C. Yasha, M. Anita, V. Santosh, and S. K. Shankar. 2011. 'Dysferlinopathy: spectrum of pathological changes in skeletal muscle tissue', *Indian J Pathol Microbiol*, 54: 350-4.

Geisel, N., J. Clasohm, X. Shi, L. Lamboni, J. Yang, K. Mattern, G. Yang, K. H. Schäfer, and M. Saumer. 2016. 'Microstructured Multilevel Bacterial Cellulose Allows the Guided Growth of Neural Stem Cells', *Small*, 12: 5407-13.

Gelin, Kristina, Aase Bodin, Paul Gatenholm, Albert Mihranyan, Katarina Edwards, and Maria Strømme. 2007. 'Characterization of water in bacterial cellulose using dielectric spectroscopy and electron microscopy', *Polymer*, 48: 7623-31.

Gerdes, J., U. Schwab, H. Lemke, and H. Stein. 1983. 'Production of a mouse monoclonal antibody reactive with a human nuclear antigen associated with cell proliferation', *Int J Cancer*, 31: 13-20.

Gilbert, P. M., K. L. Havenstrite, K. E. G. Magnusson, A. Sacco, N. A. Leonardi, P. Kraft, N. K. Nguyen, S. Thrun, M. P. Lutolf, and H. M. Blau. 2010. 'Substrate elasticity regulates skeletal muscle stem cell self-renewal in culture', *Science (New York, N.Y.)*, 329: 1078-81.

Gillies, A. R., and R. L. Lieber. 2011. 'Structure and function of the skeletal muscle extracellular matrix', *Muscle Nerve*, 44: 318-31.

Gisler, Santiago, Joana P. Gonçalves, Waseem Akhtar, Johann de Jong, Alexey V. Pindyurin, Lodewyk F. A. Wessels, and Maarten van Lohuizen. 2019. 'Multiplexed Cas9 targeting reveals genomic location effects and gRNA-based staggered breaks influencing mutation efficiency', *Nature Communications*, 10: 1598.

Glassford, J., M. Holman, L. Banerji, E. Clayton, G. G. Klaus, M. Turner, and E. W. Lam. 2001. 'Vav is required for cyclin D2 induction and proliferation of mouse B lymphocytes activated via the antigen Receptor', *J Biol Chem*, 276: 41040-8.

Goldstein, J. A., and E. M. McNally. 2010. 'Mechanisms of muscle weakness in muscular dystrophy', *J Gen Physiol*, 136: 29-34.

Gonçalves, M. A. F. V., M. Holkers, C. Cudré-Mauroux, G. P. van Nierop, S. Knaän-Shanzer, L. van der Velde, D. Valerio, and A. A. F. de Vries. 2006. 'Transduction of myogenic cells by retargeted dual high-capacity hybrid viral vectors: robust dystrophin synthesis in duchenne muscular dystrophy muscle cells', *Molecular Therapy*, 13: 976-86.

Gonzalez, M. L., N. I. Busse, C. M. Waits, and S. E. Johnson. 2020. 'Satellite cells and their regulation in livestock', *J Anim Sci*.

Gorgieva, S., and J. Trček. 2019. 'Bacterial Cellulose: Production, Modification and Perspectives in Biomedical Applications', *Nanomaterials (Basel)*, 9.

Goudenege, S., C. Lebel, N. B. Huot, C. Dufour, I. Fujii, J. Gekas, J. Rousseau, and J. P. Tremblay. 2012. 'Myoblasts derived from normal hESCs and dystrophic hiPSCs efficiently fuse with existing muscle fibers following transplantation', *Mol Ther*, 20: 2153-67.

Gregorevic, P., M. J. Blankinship, J. M. Allen, and J. S. Chamberlain. 2008. 'Systemic microdystrophin gene delivery improves skeletal muscle structure and function in old dystrophic mdx mice', *Mol Ther*, 16: 657-64.

Griggs, R. C., B. E. Herr, A. Reha, G. Elfring, L. Atkinson, V. Cwik, E. McColl, R. Tawil, S. Pandya, M. P. McDermott, and K. Bushby. 2013. 'Corticosteroids in Duchenne muscular dystrophy: major variations in practice', *Muscle Nerve*, 48: 27-31.

Grose, William E., K. Reed Clark, Danielle Griffin, Vinod Malik, Kimberly M. Shontz, Chrystal L. Montgomery, Sarah Lewis, Robert H. Brown, Jr., Paul M. L. Janssen, Jerry R. Mendell, and Louise R. Rodino-Klapac. 2012. 'Homologous Recombination Mediates Functional Recovery of Dysferlin Deficiency following AAV5 Gene Transfer', *PLoS One*, 7: e39233.

Grounds, M. D., J. R. Terrill, H. G. Radley-Crabb, T. Robertson, J. Papadimitriou, S. Spuler, and T. Shavlakadze. 2014. 'Lipid accumulation in dysferlin-deficient muscles', *Am J Pathol*, 184: 1668-76.

Guérette, B., I. Asselin, D. Skuk, M. Entman, and J. P. Tremblay. 1997. 'Control of inflammatory damage by anti-LFA-1: increase success of myoblast transplantation', *Cell Transplant*, 6: 101-7.

Guérette, B., I. Asselin, J. T. Vilquin, R. Roy, and J. P. Tremblay. 1994. 'Lymphocyte infiltration following allo- and xenomyoblast transplantation in mice', *Transplant Proc*, 26: 3461-2.

Gullo, M., S. La China, P. M. Falcone, and P. Giudici. 2018. 'Biotechnological production of cellulose by acetic acid bacteria: current state and perspectives', *Appl Microbiol Biotechnol*.

Han, R. 2011. 'Muscle membrane repair and inflammatory attack in dysferlinopathy', *Skelet Muscle*, 1: 10.

Han, R., and K. P. Campbell. 2007. 'Dysferlin and muscle membrane repair', *Curr Opin Cell Biol*, 19: 409-16.

Harper, S. Q., R. W. Crawford, C. DelloRusso, and J. S. Chamberlain. 2002. 'Spectrin-like repeats from dystrophin and alpha-actinin-2 are not functionally interchangeable', *Hum Mol Genet*, 11: 1807-15.

Hart, T., M. Chandrashekhar, M. Aregger, Z. Steinhart, K. R. Brown, G. MacLeod, M. Mis, M. Zimmermann, A. Fradet-Turcotte, S. Sun, P. Mero, P. Dirks, S. Sidhu, F. P. Roth, O. S. Rissland, D. Durocher, S. Angers, and J. Moffat. 2015. 'High-Resolution CRISPR Screens Reveal Fitness Genes and Genotype-Specific Cancer Liabilities', *Cell*, 163: 1515-26.

Hayman, Danika M., Todd J. Blumberg, C. Corey Scott, and Kyriacos A. Athanasiou. 2006. 'The Effects of Isolation on Chondrocyte Gene Expression', *Tissue Engineering*, 12: 2573-81.

Haynes, V. R., S. N. Keenan, J. Bayliss, E. M. Lloyd, P. J. Meikle, M. D. Grounds, and M. J. Watt. 2019. 'Dysferlin deficiency alters lipid metabolism and remodels the skeletal muscle lipidome in mice', *J Lipid Res*, 60: 1350-64.

Helenius, G., H. Bäckdahl, A. Bodin, U. Nannmark, P. Gatenholm, and B. Risberg. 2006. 'In vivo biocompatibility of bacterial cellulose', *J Biomed Mater Res A*, 76: 431-8.

Hernandez-Hernandez, J. M., E. G. Garcia-Gonzalez, C. E. Brun, and M. A. Rudnicki. 2017. 'The myogenic regulatory factors, determinants of muscle development, cell identity and regeneration', *Semin Cell Dev Biol*, 72: 10-18.

Hestrin, S., and M. Schramm. 1954. 'Synthesis of cellulose by Acetobacter xylinum. II. Preparation of freeze-dried cells capable of polymerizing glucose to cellulose', *The Biochemical journal*, 58: 345-52.

Hicks, M. R., J. Hiserodt, K. Paras, W. Fujiwara, A. Eskin, M. Jan, H. Xi, C. S. Young, D. Evseenko, S. F. Nelson, M. J. Spencer, B. V. Handel, and A. D. Pyle. 2018. 'ERBB3 and NGFR mark a distinct skeletal muscle progenitor cell in human development and hPSCs', *Nat Cell Biol*, 20: 46-57.

Hilton, Isaac B., and Charles A. Gersbach. 2015. 'Enabling functional genomics with genome engineering', *Genome research*, 25: 1442-55.
Hirai H, Umegaki R, Kino-Oka M, Taya M. 2002. ´Characterization of cellular motions through direct observation of individual cells at early stage in anchorage-dependent culture´ J Biosci Bioeng, 94(4):351-6.
Hirakawa, Matthew P., Raga Krishnakumar, Jerilyn A. Timlin, James P. Carney, and Kimberly S. Butler. 2020. 'Gene editing and CRISPR in the clinic: current and future perspectives', *Bioscience reports*, 40: BSR20200127.
Hoffman, E. P., A. P. Monaco, C. C. Feener, and L. M. Kunkel. 1987. 'Conservation of the Duchenne muscular dystrophy gene in mice and humans', *Science*, 238: 347-50.
Hoffman, E. P., D. Rao, and L. M. Pachman. 2002. 'Clarifying the boundaries between the inflammatory and dystrophic myopathies: insights from molecular diagnostics and microarrays', *Rheum Dis Clin North Am*, 28: 743-57.
Hofinger, M., G. Bertholdt, and D. Weuster-Botz. 2011. 'Microbial production of homogeneously layered cellulose pellicles in a membrane bioreactor', *Biotechnol Bioeng*, 108: 2237-40.
Hoppeler, H., and M. Fluck. 2002. 'Normal mammalian skeletal muscle and its phenotypic plasticity', *J Exp Biol*, 205: 2143-52.
Hornsey, M. A., S. H. Laval, R. Barresi, H. Lochmuller, and K. Bushby. 2013. 'Muscular dystrophy in dysferlin-deficient mouse models', *Neuromuscul Disord*, 23: 377-87.
Hsu, P. D., E. S. Lander, and F. Zhang. 2014. 'Development and applications of CRISPR-Cas9 for genome engineering', *Cell*, 157: 1262-78.
Huang, Yang, Chunlin Zhu, Jiazhi Yang, Ying Nie, Chuntao Chen, and Dongping Sun. 2014. 'Recent advances in bacterial cellulose', *Cellulose*, 21: 1-30.
Iguchi, M., S. Yamanaka, and A. Budhiono. 2000. 'Bacterial cellulose—a masterpiece of nature's arts', *Journal of Materials Science*, 35: 261-70.
Illa, I., M. Leon-Monzon, and M. C. Dalakas. 1992. 'Regenerating and denervated human muscle fibers and satellite cells express neural cell adhesion molecule recognized by monoclonal antibodies to natural killer cells', *Ann Neurol*, 31: 46-52.
Illa, I., C. Serrano-Munuera, E. Gallardo, A. Lasa, R. Rojas-García, J. Palmer, P. Gallano, M. Baiget, C. Matsuda, and R. H. Brown. 2001. 'Distal anterior compartment myopathy: a dysferlin mutation causing a new muscular dystrophy phenotype', *Ann Neurol*, 49: 130-4.
Im, W. B., S. F. Phelps, E. H. Copen, E. G. Adams, J. L. Slightom, and J. S. Chamberlain. 1996. 'Differential expression of dystrophin isoforms in strains of mdx mice with different mutations', *Hum Mol Genet*, 5: 1149-53.
Ireland, R. G., and C. A. Simmons. 2015. 'Human Pluripotent Stem Cell Mechanobiology: Manipulating the Biophysical Microenvironment for Regenerative Medicine and Tissue Engineering Applications', *Stem Cells*, 33: 3187-96.
Ishibashi, Hiromi, Minoru Nakamura, Atsumasa Komori, Kiyoshi Migita, and Shinji Shimoda. 2009. 'Liver architecture, cell function, and disease', *Seminars in Immunopathology*, 31: 399.
Ishida, K., P. Gee, and A. Hotta. 2015. 'Minimizing off-Target Mutagenesis Risks Caused by Programmable Nucleases', *Int J Mol Sci*, 16: 24751-71.
Ishino, Y., H. Shinagawa, K. Makino, M. Amemura, and A. Nakata. 1987. 'Nucleotide sequence of the iap gene, responsible for alkaline phosphatase isozyme conversion in Escherichia coli, and identification of the gene product', *J Bacteriol*, 169: 5429-33.
Iyombe-Engembe, Jean-Paul, Dominique L. Ouellet, Xavier Barbeau, Joël Rousseau, Pierre Chapdelaine, Patrick Lagüe, and Jacques P. Tremblay. 2016. 'Efficient Restoration of the Dystrophin Gene Reading Frame and Protein Structure in DMD Myoblasts Using the CinDel Method', *Molecular Therapy - Nucleic Acids*, 5: e283.
Jacinto, F. V., W. Link, and B. I. Ferreira. 2020. 'CRISPR/Cas9-mediated genome editing: From basic research to translational medicine', *J Cell Mol Med*, 24: 3766-78.
Jahn, C. E., D. A. Selimi, J. D. Barak, and A. O. Charkowski. 2011. 'The Dickeya dadantii biofilm matrix consists of cellulose nanofibres, and is an emergent property dependent upon the type III secretion system and the cellulose synthesis operon', *Microbiology (Reading)*, 157: 2733-44.
Jansen, R., J. D. Embden, W. Gaastra, and L. M. Schouls. 2002. 'Identification of genes that are associated with DNA repeats in prokaryotes', *Mol Microbiol*, 43: 1565-75.
Jeong, Seong Il, Seung Eun Lee, Hana Yang, Young-Ho Jin, Cheung-Seog Park, and Yong Seek Park. 2010. 'Toxicologic evaluation of bacterial synthesized cellulose in endothelial cells and animals', *Molecular & Cellular Toxicology*, 6: 370-77.

Jin, P., R. Duan, F. Luo, G. Zhang, S. N. Hong, and E. H. Chen. 2011. 'Competition between Blown fuse and WASP for WIP binding regulates the dynamics of WASP-dependent actin polymerization in vivo', *Dev Cell*, 20: 623-38.
Jinek, M., K. Chylinski, I. Fonfara, M. Hauer, J. A. Doudna, and E. Charpentier. 2012. 'A programmable dual-RNA-guided DNA endonuclease in adaptive bacterial immunity', *Science*, 337: 816-21.
Jinek, M., A. East, A. Cheng, S. Lin, E. Ma, and J. Doudna. 2013. 'RNA-programmed genome editing in human cells', *Elife*, 2: e00471.
Jinek, M., F. Jiang, D. W. Taylor, S. H. Sternberg, E. Kaya, E. Ma, C. Anders, M. Hauer, K. Zhou, S. Lin, M. Kaplan, A. T. Iavarone, E. Charpentier, E. Nogales, and J. A. Doudna. 2014. 'Structures of Cas9 endonucleases reveal RNA-mediated conformational activation', *Science*, 343: 1247997.
Jones, N. C., K. J. Tyner, L. Nibarger, H. M. Stanley, D. D. Cornelison, Y. V. Fedorov, and B. B. Olwin. 2005. 'The p38alpha/beta MAPK functions as a molecular switch to activate the quiescent satellite cell', *J Cell Biol*, 169: 105-16.
Judson, R. N., M. Quarta, M. J. Oudhoff, H. Soliman, L. Yi, C. K. Chang, G. Loi, R. Vander Werff, A. Cait, M. Hamer, J. Blonigan, P. Paine, L. T. N. Doan, E. Groppa, W. He, L. Su, R. H. Zhang, P. Xu, C. Eisner, M. Low, I. Barta, C. B. Lewis, C. Zaph, M. M. Karimi, T. A. Rando, and F. M. Rossi. 2018. 'Inhibition of Methyltransferase Setd7 Allows the In Vitro Expansion of Myogenic Stem Cells with Improved Therapeutic Potential', *Cell Stem Cell*, 22: 177-90.e7.
Kabadi, A. M., D. G. Ousterout, I. B. Hilton, and C. A. Gersbach. 2014. 'Multiplex CRISPR/Cas9-based genome engineering from a single lentiviral vector', *Nucleic Acids Res*, 42: e147.
Kang, P. B., and R. C. Griggs. 2015. 'Advances in Muscular Dystrophies', *JAMA Neurol*, 72: 741-2.
Karpati, G., D. Ajdukovic, D. Arnold, R. B. Gledhill, R. Guttmann, P. Holland, P. A. Koch, E. Shoubridge, D. Spence, M. Vanasse, and et al. 1993. 'Myoblast transfer in Duchenne muscular dystrophy', *Ann Neurol*, 34: 8-17.
Kazuki, Yasuhiro, Masaharu Hiratsuka, Masato Takiguchi, Mitsuhiko Osaki, Naoyo Kajitani, Hidetoshi Hoshiya, Kei Hiramatsu, Toko Yoshino, Kanako Kazuki, Chie Ishihara, Shoko Takehara, Katsumi Higaki, Masato Nakagawa, Kazutoshi Takahashi, Shinya Yamanaka, and Mitsuo Oshimura. 2010. 'Complete genetic correction of ips cells from Duchenne muscular dystrophy', *Molecular therapy : the journal of the American Society of Gene Therapy*, 18: 386-93.
Kerr, J. P., A. P. Ziman, A. L. Mueller, J. M. Muriel, E. Kleinhans-Welte, J. D. Gumerson, S. S. Vogel, C. W. Ward, J. A. Roche, and R. J. Bloch. 2013. 'Dysferlin stabilizes stress-induced Ca2+ signaling in the transverse tubule membrane', *Proc Natl Acad Sci U S A*, 110: 20831-6.
Kesper, Dörthe Andrea, Christiana Stute, Detlev Buttgereit, Nina Kreisköther, Smitha Vishnu, Karl-Friedrich Fischbach, and Renate Renkawitz-Pohl. 2007. 'Myoblast fusion in Drosophila melanogaster is mediated through a fusion-restricted myogenic-adhesive structure (FuRMAS)', *Developmental Dynamics*, 236: 404-15.
Khalid, A., R. Khan, M. Ul-Islam, T. Khan, and F. Wahid. 2017. 'Bacterial cellulose-zinc oxide nanocomposites as a novel dressing system for burn wounds', *Carbohydr Polym*, 164: 214-21.
Kim, D., S. Bae, J. Park, E. Kim, S. Kim, H. R. Yu, J. Hwang, J. I. Kim, and J. S. Kim. 2015. 'Digenome-seq: genome-wide profiling of CRISPR-Cas9 off-target effects in human cells', *Nat Methods*, 12: 237-43, 1 p following 43.
Kim, S., K. Shilagardi, S. Zhang, S. N. Hong, K. L. Sens, J. Bo, G. A. Gonzalez, and E. H. Chen. 2007. 'A critical function for the actin cytoskeleton in targeted exocytosis of prefusion vesicles during myoblast fusion', *Dev Cell*, 12: 571-86.
Kim, Sojung, Taegeun Bae, Jaewoong Hwang, and Jin-Soo Kim. 2017. 'Rescue of high-specificity Cas9 variants using sgRNAs with matched 5' nucleotides', *Genome Biology*, 18: 218.
Kim, Y., C. D. Lasher, L. M. Milford, T. M. Murali, and P. Rajagopalan. 2010. 'A comparative study of genome-wide transcriptional profiles of primary hepatocytes in collagen sandwich and monolayer cultures', *Tissue Eng Part C Methods*, 16: 1449-60.
Kimura, E., S. Li, P. Gregorevic, B. M. Fall, and J. S. Chamberlain. 2010. 'Dystrophin delivery to muscles of mdx mice using lentiviral vectors leads to myogenic progenitor targeting and stable gene expression', *Mol Ther*, 18: 206-13.
Kinoshita, I., J. T. Vilquin, B. Guerette, I. Asselin, R. Roy, and J. P. Tremblay. 1994. 'Very efficient myoblast allotransplantation in mice under FK506 immunosuppression', *Muscle Nerve*, 17: 1407-15.

Kleinstiver, B. P., V. Pattanayak, M. S. Prew, S. Q. Tsai, N. T. Nguyen, Z. Zheng, and J. K. Joung. 2016. 'High-fidelity CRISPR-Cas9 nucleases with no detectable genome-wide off-target effects', *Nature*, 529: 490-5.

Klemm, D., B. Heublein, H. P. Fink, and A. Bohn. 2005. 'Cellulose: fascinating biopolymer and sustainable raw material', *Angew Chem Int Ed Engl*, 44: 3358-93.

Klinge, L., J. Harris, C. Sewry, R. Charlton, L. Anderson, S. Laval, Y. H. Chiu, M. Hornsey, V. Straub, R. Barresi, H. Lochmüller, and K. Bushby. 2010. 'Dysferlin associates with the developing T-tubule system in rodent and human skeletal muscle', *Muscle Nerve*, 41: 166-73.

Klinge, L., S. Laval, S. Keers, F. Haldane, V. Straub, R. Barresi, and K. Bushby. 2007. 'From T-tubule to sarcolemma: damage-induced dysferlin translocation in early myogenesis', *FASEB J*, 21: 1768-76.

Kocher, Thomas, Oliver March, Johannes Bischof, Bernadette Liemberger, Stefan Hainzl, Alfred Klausegger, Anna Hoog, Dirk Strunk, Johann Bauer, and Ulrich Koller. 2020. 'Predictable CRISPR/Cas9-Mediated COL7A1 Reframing for Dystrophic Epidermolysis Bullosa', *Journal of Investigative Dermatology*, 140.

Koike-Yusa, H., Y. Li, E. P. Tan, C. Velasco-Herrera Mdel, and K. Yusa. 2014. 'Genome-wide recessive genetic screening in mammalian cells with a lentiviral CRISPR-guide RNA library', *Nat Biotechnol*, 32: 267-73.

Konigsberg, U. R., B. H. Lipton, and I. R. Konigsberg. 1975. 'The regenerative response of single mature muscle fibers isolated in vitro'.

Kotagama, O. W., C. D. Jayasinghe, and T. Abeysinghe. 2019. 'Era of Genomic Medicine: A Narrative Review on CRISPR Technology as a Potential Therapeutic Tool for Human Diseases', *Biomed Res Int*, 2019: 1369682.

Kowalska-Ludwicka, Karolina, Jaroslaw Cala, Bartlomiej Grobelski, Dominik Sygut, Dorota Jesionek-Kupnicka, Marek Kolodziejczyk, Stanislaw Bielecki, and Zbigniew Pasieka. 2013. 'Modified bacterial cellulose tubes for regeneration of damaged peripheral nerves', *Archives of medical science : AMS*, 9: 527-34.

Krahn, M., C. Béroud, V. Labelle, K. Nguyen, R. Bernard, G. Bassez, D. Figarella-Branger, C. Fernandez, J. Bouvenot, I. Richard, E. Ollagnon-Roman, J. A. Bevilacqua, E. Salvo, S. Attarian, F. Chapon, J. F. Pellissier, J. Pouget, H. Hammouda el, P. Laforêt, J. A. Urtizberea, B. Eymard, F. Leturcq, and N. Lévy. 2009. 'Analysis of the DYSF mutational spectrum in a large cohort of patients', *Hum Mutat*, 30: E345-75.

Krahn, M., N. Wein, M. Bartoli, W. Lostal, S. Courrier, N. Bourg-Alibert, K. Nguyen, C. Vial, N. Streichenberger, V. Labelle, D. DePetris, C. Pécheux, F. Leturcq, P. Cau, I. Richard, and N. Lévy. 2010. 'A naturally occurring human minidysferlin protein repairs sarcolemmal lesions in a mouse model of dysferlinopathy', *Sci Transl Med*, 2: 50ra69.

Kuang, S., S. B. Charge, P. Seale, M. Huh, and M. A. Rudnicki. 2006. 'Distinct roles for Pax7 and Pax3 in adult regenerative myogenesis', *J Cell Biol*, 172: 103-13.

Kuang, S., K. Kuroda, F. Le Grand, and M. A. Rudnicki. 2007. 'Asymmetric self-renewal and commitment of satellite stem cells in muscle', *Cell*, 129: 999-1010.

Kuang, S., and M. A. Rudnicki. 2008. 'The emerging biology of satellite cells and their therapeutic potential', *Trends Mol Med*, 14: 82-91.

Kulcsár, Péter István, András Tálas, Krisztina Huszár, Zoltán Ligeti, Eszter Tóth, Nóra Weinhardt, Elfrieda Fodor, and Ervin Welker. 2017. 'Crossing enhanced and high fidelity SpCas9 nucleases to optimize specificity and cleavage', *Genome Biology*, 18: 190.

Kunin, Victor, Rotem Sorek, and Philip Hugenholtz. 2007. 'Evolutionary conservation of sequence and secondary structures in CRISPR repeats', *Genome Biology*, 8: R61.

Kuscu, C., S. Arslan, R. Singh, J. Thorpe, and M. Adli. 2014. 'Genome-wide analysis reveals characteristics of off-target sites bound by the Cas9 endonuclease', *Nat Biotechnol*, 32: 677-83.

Labrie, Simon J., Julie E. Samson, and Sylvain Moineau. 2010. 'Bacteriophage resistance mechanisms', *Nature Reviews Microbiology*, 8: 317-27.

Le Guiner, C., L. Servais, M. Montus, T. Larcher, B. Fraysse, S. Moullec, M. Allais, V. Francois, M. Dutilleul, A. Malerba, T. Koo, J. L. Thibaut, B. Matot, M. Devaux, J. Le Duff, J. Y. Deschamps, I. Barthelemy, S. Blot, I. Testault, K. Wahbi, S. Ederhy, S. Martin, P. Veron, C. Georger, T. Athanasopoulos, C. Masurier, F. Mingozzi, P. Carlier, B. Gjata, J. Y. Hogrel, O. Adjali, F. Mavilio, T. Voit, P. Moullier, and G. Dickson. 2017. 'Long-term microdystrophin gene therapy is effective in a canine model of Duchenne muscular dystrophy', *Nat Commun*, 8: 16105.

Lee, Joshua J. A., Rika Maruyama, William Duddy, Hidetoshi Sakurai, and Toshifumi Yokota. 2018. 'Identification of Novel Antisense-Mediated Exon Skipping Targets in DYSF for Therapeutic Treatment of Dysferlinopathy', *Molecular therapy. Nucleic acids*, 13: 596-604.
Lepper, C., S. J. Conway, and C. M. Fan. 2009. 'Adult satellite cells and embryonic muscle progenitors have distinct genetic requirements', *Nature*, 460: 627-31.
Lerario, A., F. Cogiamanian, C. Marchesi, M. Belicchi, Ne. Bresolin, L. Porretti, and Y. Torrente. 2010. 'Effects of rituximab in two patients with dysferlin-deficient muscular dystrophy', *BMC musculoskeletal disorders*, 11: 157-57.
Leriche-Guérin, K., L. V. Anderson, K. Wrogemann, B. Roy, M. Goulet, and J. P. Tremblay. 2002. 'Dysferlin expression after normal myoblast transplantation in SCID and in SJL mice', *Neuromuscul Disord*, 12: 167-73.
Leshinsky-Silver, E., Z. Argov, L. Rozenboim, S. Cohen, Z. Tzofi, Y. Cohen, Y. Wirguin, R. Dabby, D. Lev, and M. Sadeh. 2007. 'Dysferlinopathy in the Jews of the Caucasus: a frequent mutation in the dysferlin gene', *Neuromuscul Disord*, 17: 950-4.
Lewis, D. I. 2019. 'Animal experimentation: implementation and application of the 3Rs', *Emerg Top Life Sci*, 3: 675-79.
Li, H. L., Fujimoto, N., Sasakawa, N., Shirai, S., Ohkame, T., Sakuma, T., Tanaka, M., Amano, N., Watanabe, A., Sakurai, H., Yamamoto, T., Yamanaka, S., & Hotta, A. 2015. 'Precise correction of the dystrophin gene in duchenne muscular dystrophy patient induced pluripotent stem cells by TALEN and CRISPR-Cas9', *Stem Cell Reports*, 4: 143-54.
Lieber, Michael R. 2010. 'The mechanism of double-strand DNA break repair by the nonhomologous DNA end-joining pathway', *Annual review of biochemistry*, 79: 181-211.
Lilja, K. C., N. Zhang, A. Magli, V. Gunduz, C. J. Bowman, R. W. Arpke, R. Darabi, M. Kyba, R. Perlingeiro, and B. D. Dynlacht. 2017. 'Pax7 remodels the chromatin landscape in skeletal muscle stem cells', *PLoS One*, 12: e0176190.
Lim, K. R., R. Maruyama, and T. Yokota. 2017. 'Eteplirsen in the treatment of Duchenne muscular dystrophy', *Drug Des Devel Ther*, 11: 533-45.
Lindstrom, M., F. Pedrosa-Domellof, and L. E. Thornell. 2010. 'Satellite cell heterogeneity with respect to expression of MyoD, myogenin, Dlk1 and c-Met in human skeletal muscle: application to a cohort of power lifters and sedentary men', *Histochem Cell Biol*, 134: 371-85.
Lindstrom, M., and L. E. Thornell. 2009. 'New multiple labelling method for improved satellite cell identification in human muscle: application to a cohort of power-lifters and sedentary men', *Histochem Cell Biol*, 132: 141-57.
Liu, J., M. Aoki, I. Illa, C. Wu, M. Fardeau, C. Angelini, C. Serrano, J. A. Urtizberea, F. Hentati, M. B. Hamida, S. Bohlega, E. J. Culper, A. A. Amato, K. Bossie, J. Oeltjen, K. Bejaoui, D. McKenna-Yasek, B. A. Hosler, E. Schurr, K. Arahata, P. J. de Jong, and R. H. Brown, Jr. 1998. 'Dysferlin, a novel skeletal muscle gene, is mutated in Miyoshi myopathy and limb girdle muscular dystrophy', *Nat Genet*, 20: 31-6.
Liu, L., T. H. Cheung, G. W. Charville, B. M. Hurgo, T. Leavitt, J. Shih, A. Brunet, and T. A. Rando. 2013. 'Chromatin modifications as determinants of muscle stem cell quiescence and chronological aging', *Cell Rep*, 4: 189-204.
Liu, W., Y. Wen, P. Bi, X. Lai, X. S. Liu, X. Liu, and S. Kuang. 2012. 'Hypoxia promotes satellite cell self-renewal and enhances the efficiency of myoblast transplantation', *Development*, 139: 2857-65.
Lo, W. S., E. Gardiner, Z. Xu, C. F. Lau, F. Wang, J. J. Zhou, J. D. Mendlein, L. A. Nangle, K. P. Chiang, X. L. Yang, K. F. Au, W. H. Wong, M. Guo, M. Zhang, and P. Schimmel. 2014. 'Human tRNA synthetase catalytic nulls with diverse functions', *Science*, 345: 328-32.
Loh, E. Y. X., N. Mohamad, M. B. Fauzi, M. H. Ng, S. F. Ng, and M. C. I. Mohd Amin. 2018. 'Development of a bacterial cellulose-based hydrogel cell carrier containing keratinocytes and fibroblasts for full-thickness wound healing', *Sci Rep*, 8: 2875.
Long, C., J. R. McAnally, J. M. Shelton, A. A. Mireault, R. Bassel-Duby, and E. N. Olson. 2014. 'Prevention of muscular dystrophy in mice by CRISPR/Cas9-mediated editing of germline DNA', *Science*, 345: 1184-88.
Lostal, W., M. Bartoli, C. Roudaut, N. Bourg, M. Krahn, M. Pryadkina, P. Borel, L. Suel, J. A. Roche, D. Stockholm, R. J. Bloch, N. Levy, R. Bashir, and I. Richard. 2012. 'Lack of correlation between outcomes of membrane repair assay and correction of dystrophic changes in experimental therapeutic strategy in dysferlinopathy', *PLoS One*, 7: e38036.
Lyu, P., P. Javidi-Parsijani, A. Atala, and B. Lu. 2019. 'Delivering Cas9/sgRNA ribonucleoprotein (RNP) by lentiviral capsid-based bionanoparticles for efficient 'hit-and-run' genome editing', *Nucleic Acids Res*, 47: e99.

Machado, L., J. Esteves de Lima, O. Fabre, C. Proux, R. Legendre, A. Szegedi, H. Varet, L. R. Ingerslev, R. Barrès, F. Relaix, and P. Mourikis. 2017. 'In Situ Fixation Redefines Quiescence and Early Activation of Skeletal Muscle Stem Cells', *Cell Rep*, 21: 1982-93.

Mack, Natalie A., Helen J. Whalley, Sonia Castillo-Lluva, and Angeliki Malliri. 2011. 'The diverse roles of Rac signaling in tumorigenesis', *Cell Cycle*, 10: 1571-81.

Makarova, K. S., N. V. Grishin, S. A. Shabalina, Y. I. Wolf, and E. V. Koonin. 2006. 'A putative RNA-interference-based immune system in prokaryotes: computational analysis of the predicted enzymatic machinery, functional analogies with eukaryotic RNAi, and hypothetical mechanisms of action', *Biol Direct*, 1: 7.

Makarova, K. S., Y. I. Wolf, O. S. Alkhnbashi, F. Costa, S. A. Shah, S. J. Saunders, R. Barrangou, S. J. Brouns, E. Charpentier, D. H. Haft, P. Horvath, S. Moineau, F. J. Mojica, R. M. Terns, M. P. Terns, M. F. White, A. F. Yakunin, R. A. Garrett, J. van der Oost, R. Backofen, and E. V. Koonin. 2015. 'An updated evolutionary classification of CRISPR-Cas systems', *Nat Rev Microbiol*, 13: 722-36.

Makarova, K. S., D. H Haft, R. Barrangou, S. J. Brouns, E. Charpentier, P. Horvath, S. Moineau, F. J. Mojica, Y. I. Wolf, A. F. Yakunin,J. van der Oost, E. V. Koonin. 2011. 'Evolution and classification of the CRISPR–Cas systems', *Nature Reviews Microbiology*, 9: 467-77.

Malcher, J., L. Heidt, A. Goyenvalle, H. Escobar, A. Marg, C. Beley, R. Benchaouir, M. Bader, S. Spuler, L. Garcia, and V. Schowel. 2018. 'Exon Skipping in a Dysf-Missense Mutant Mouse Model', *Mol Ther Nucleic Acids*, 13: 198-207.

Mali, P., L. Yang, K. M. Esvelt, J. Aach, M. Guell, J. E. DiCarlo, J. E. Norville, and G. M. Church. 2013. 'RNA-guided human genome engineering via Cas9', *Science*, 339: 823-6.

Mao, Z., M. Bozzella, A. Seluanov, and V. Gorbunova. 2008. 'Comparison of nonhomologous end joining and homologous recombination in human cells', *DNA repair*, 7: 1765-71.

Marg, A., H. Escobar, S. Gloy, M. Kufeld, J. Zacher, A. Spuler, C. Birchmeier, Z. Izsvak, and S. Spuler. 2014. 'Human satellite cells have regenerative capacity and are genetically manipulable', *J Clin Invest*, 124: 4257-65.

Marg, A., H. Escobar, N. Karaiskos, S. A. Grunwald, E. Metzler, J. Kieshauer, S. Sauer, D. Pasemann, E. Malfatti, D. Mompoint, S. Quijano-Roy, A. Boltengagen, J. Schneider, M. Schulke, S. Kunz, R. Carlier, C. Birchmeier, H. Amthor, A. Spuler, C. Kocks, N. Rajewsky, and S. Spuler. 2019. 'Human muscle-derived CLEC14A-positive cells regenerate muscle independent of PAX7', *Nat Commun*, 10: 5776.

Marg, A., V. Schoewel, T. Timmel, A. Schulze, C. Shah, O. Daumke, and S. Spuler. 2012. 'Sarcolemmal repair is a slow process and includes EHD2', *Traffic*, 13: 1286-94.

Martino, A. T., M. Suzuki, D. M. Markusic, I. Zolotukhin, R. C. Ryals, B. Moghimi, H. C. Ertl, D. A. Muruve, B. Lee, and R. W. Herzog. 2011. 'The genome of self-complementary adeno-associated viral vectors increases Toll-like receptor 9-dependent innate immune responses in the liver', *Blood*, 117: 6459-68.

Maruyama, Takeshi, Stephanie K. Dougan, Matthias C. Truttmann, Angelina M. Bilate, Jessica R. Ingram, and Hidde L. Ploegh. 2015. 'Increasing the efficiency of precise genome editing with CRISPR-Cas9 by inhibition of nonhomologous end joining', *Nature Biotechnology*, 33: 538-42.

Mashal, R. D., J. Koontz, and J. Sklar. 1995. 'Detection of mutations by cleavage of DNA heteroduplexes with bacteriophage resolvases', *Nat Genet*, 9: 177-83.

Mashinchian, O., A. Pisconti, E. Le Moal, and C. F. Bentzinger. 2018. 'The Muscle Stem Cell Niche in Health and Disease', *Curr Top Dev Biol*, 126: 23-65.

Massarwa, R., S. Carmon, B. Z. Shilo, and E. D. Schejter. 2007. 'WIP/WASp-based actin-polymerization machinery is essential for myoblast fusion in Drosophila', *Dev Cell*, 12: 557-69.

Matsuda, C., Y. K. Hayashi, M. Ogawa, M. Aoki, K. Murayama, I. Nishino, I. Nonaka, K. Arahata, and R. H. Brown, Jr. 2001. 'The sarcolemmal proteins dysferlin and caveolin-3 interact in skeletal muscle', *Hum Mol Genet*, 10: 1761-6.

Matsuo, M., T. Masumura, H. Nishio, T. Nakajima, Y. Kitoh, T. Takumi, J. Koga, and H. Nakamura. 1991. 'Exon skipping during splicing of dystrophin mRNA precursor due to an intraexon deletion in the dystrophin gene of Duchenne muscular dystrophy kobe', *J Clin Invest*, 87: 2127-31.

Maule, Giulia, Antonio Casini, Claudia Montagna, Anabela S. Ramalho, Kris De Boeck, Zeger Debyser, Marianne S. Carlon, Gianluca Petris, and Anna Cereseto. 2019. 'Allele specific repair of splicing mutations in cystic fibrosis through AsCas12a genome editing', *Nature Communications*, 10: 3556.

Mauro, A. 1961. 'Satellite cell of skeletal muscle fibers', *J Biophys Biochem Cytol*, 9: 493-5.
McCarthy, J. J., J. Mula, M. Miyazaki, R. Erfani, K. Garrison, A. B. Farooqui, R. Srikuea, B. A. Lawson, B. Grimes, C. Keller, G. Van Zant, K. S. Campbell, K. A. Esser, E. E. Dupont-Versteegden, and C. A. Peterson. 2011. 'Effective fiber hypertrophy in satellite cell-depleted skeletal muscle', *Development*, 138: 3657-66.
McNeil, P. L. 2002. 'Repairing a torn cell surface: make way, lysosomes to the rescue', *J Cell Sci*, 115: 873-9.
Mello, Luis Renato, Leonir T. Feltrin, Paulo T. Fontes Neto, and Fernando A. P. Ferraz. 1997. 'Duraplasty with biosynthetic cellulose: an experimental study', *Journal of Neurosurgery*, 86: 143.
Mendell, J. R., K. Campbell, L. Rodino-Klapac, Z. Sahenk, C. Shilling, S. Lewis, D. Bowles, S. Gray, C. Li, G. Galloway, V. Malik, B. Coley, K. R. Clark, J. Li, X. Xiao, J. Samulski, S. W. McPhee, R. J. Samulski, and C. M. Walker. 2010. 'Dystrophin immunity in Duchenne's muscular dystrophy', *N Engl J Med*, 363: 1429-37.
Mendell, J. R., L. G. Chicoine, S. A. Al-Zaidy, Z. Sahenk, K. Lehman, L. Lowes, N. Miller, L. Alfano, B. Galliers, S. Lewis, D. Murrey, E. Peterson, D. A. Griffin, K. Church, S. Cheatham, J. Cheatham, M. J. Hogan, and L. R. Rodino-Klapac. 2019. 'Gene Delivery for Limb-Girdle Muscular Dystrophy Type 2D by Isolated Limb Infusion', *Hum Gene Ther*, 30: 794-801.
Mendell, J. R., J. T. Kissel, A. A. Amato, W. King, L. Signore, T. W. Prior, Z. Sahenk, S. Benson, P. E. McAndrew, R. Rice, and et al. 1995. 'Myoblast transfer in the treatment of Duchenne's muscular dystrophy', *N Engl J Med*, 333: 832-8.
Mendell, J. R., Z. Sahenk, and T. W. Prior. 1995. 'The childhood muscular dystrophies: diseases sharing a common pathogenesis of membrane instability', *J Child Neurol*, 10: 150-9.
Meng, Jinhong, Soyon Chun, Rowan Asfahani, Hanns Lochmüller, Francesco Muntoni, and Jennifer Morgan. 2014. 'Human Skeletal Muscle–derived CD133+ Cells Form Functional Satellite Cells After Intramuscular Transplantation in Immunodeficient Host Mice', *Molecular Therapy*, 22: 1008-17.
Meng, Jinhong, Francesco Muntoni, and Jennifer Morgan. 2018. 'CD133+ cells derived from skeletal muscles of Duchenne muscular dystrophy patients have a compromised myogenic and muscle regenerative capability', *Stem Cell Research*, 30: 43-52.
Mercuri, E., and F. Muntoni. 2013. 'Muscular dystrophies', *Lancet*, 381: 845-60.
Meyne, J., R. L. Ratliff, and R. K. Moyzis. 1989. 'Conservation of the human telomere sequence (TTAGGG)n among vertebrates', *Proceedings of the National Academy of Sciences of the United States of America*, 86: 7049-53.
Min, Y. L., H. Li, C. Rodriguez-Caycedo, A. A. Mireault, J. Huang, J. M. Shelton, J. R. McAnally, L. Amoasii, P. P. A. Mammen, R. Bassel-Duby, and E. N. Olson. 2019. 'CRISPR-Cas9 corrects Duchenne muscular dystrophy exon 44 deletion mutations in mice and human cells', *Sci Adv*, 5: eaav4324.
Minasi, M. G., M. Riminucci, L. De Angelis, U. Borello, B. Berarducci, A. Innocenzi, A. Caprioli, D. Sirabella, M. Baiocchi, R. De Maria, R. Boratto, T. Jaffredo, V. Broccoli, P. Bianco, and G. Cossu. 2002. 'The meso-angioblast: a multipotent, self-renewing cell that originates from the dorsal aorta and differentiates into most mesodermal tissues', *Development*, 129: 2773.
Mingozzi, F., and K. A. High. 2013. 'Immune responses to AAV vectors: overcoming barriers to successful gene therapy', *Blood*, 122: 23-36.
Mintz, B., and W. W. Baker. 1967. 'Normal mammalian muscle differentiation and gene control of isocitrate dehydrogenase synthesis', *Proc Natl Acad Sci U S A*, 58: 592-8.
Miyoshi, K., H. Kawai, M. Iwasa, K. Kusaka, and H. Nishino. 1986. 'Autosomal recessive distal muscular dystrophy as a new type of progressive muscular dystrophy. Seventeen cases in eight families including an autopsied case', *Brain*, 109 (Pt 1): 31-54.
Moisset, P. A., Y. Gagnon, G. Karpati, and J. P. Tremblay. 1998. 'Expression of human dystrophin following the transplantation of genetically modified mdx myoblasts', *Gene Therapy*, 5: 1340-46.
Mojica, Francisco J. M., Chc sar Díez-Villaseñor, Jesús García-Martínez, and Elena Soria. 2005. 'Intervening Sequences of Regularly Spaced Prokaryotic Repeats Derive from Foreign Genetic Elements', *Journal of Molecular Evolution*, 60: 174-82.
Monaco, A. P., C. J. Bertelson, S. Liechti-Gallati, H. Moser, and L. M. Kunkel. 1988. 'An explanation for the phenotypic differences between patients bearing partial deletions of the DMD locus', *Genomics*, 2: 90-5.

Monge, C., N. DiStasio, T. Rossi, M. Sébastien, H. Sakai, B. Kalman, T. Boudou, S. Tajbakhsh, I. Marty, A. Bigot, V. Mouly, and C. Picart. 2017. 'Quiescence of human muscle stem cells is favored by culture on natural biopolymeric films', *Stem Cell Research & Therapy*, 8: 104.
Montarras, D., J. Morgan, C. Collins, F. Relaix, S. Zaffran, A. Cumano, T. Partridge, and M. Buckingham. 2005. 'Direct isolation of satellite cells for skeletal muscle regeneration', *Science*, 309: 2064-7.
Moore, U., M. Jacobs, M. K. James, A. G. Mayhew, R. Fernandez-Torron, J. Feng, A. Cnaan, M. Eagle, K. Bettinson, L. E. Rufibach, R. M. Lofra, A. M. Blamire, P. G. Carlier, P. Mittal, L. P. Lowes, L. Alfano, K. Rose, T. Duong, K. M. Berry, E. Montiel-Morillo, … K. Bushby, and V. Straub. 2019. 'Assessment of disease progression in dysferlinopathy: A 1-year cohort study', *Neurology*, 92: e461-74.
Moore, Ursula R., Marni Jacobs, Roberto Fernandez-Torron, Jiji Jang, Meredith K. James, Anna Mayhew, Laura Rufibach, Plavi Mittal, Michelle Eagle, Avital Cnaan, Pierre G. Carlier, Andrew Blamire, Heather Hilsden, Hanns Lochmüller, Ulrike Grieben, Simone Spuler, Carolina Tesi Rocha, … Kate Bushby, and Volker Straub. 2018. 'Teenage exercise is associated with earlier symptom onset in dysferlinopathy: a retrospective cohort study', *Journal of Neurology, Neurosurgery & Psychiatry*: jnnp-2017-317329.
Moreno-Layseca, P., and C. H. Streuli. 2014. 'Signalling pathways linking integrins with cell cycle progression', *Matrix Biol*, 34: 144-53.
Moretti, A., L. Fonteyne, F. Giesert, P. Hoppmann, A. B. Meier, T. Bozoglu, A. Baehr, C. M. Schneider, D. Sinnecker, K. Klett, T. Frohlich, F. A. Rahman, T. Haufe, S. Sun, V. Jurisch, B. Kessler, R. Hinkel, … W. Wurst, and C. Kupatt. 2020. 'Somatic gene editing ameliorates skeletal and cardiac muscle failure in pig and human models of Duchenne muscular dystrophy', *Nat Med*, 26: 207-14.
Morrison, J. I., S. Loof, P. He, and A. Simon. 2006. 'Salamander limb regeneration involves the activation of a multipotent skeletal muscle satellite cell population', *J Cell Biol*, 172: 433-40.
Morse, D. E., and C. Yanofsky. 1969. 'Polarity and the degradation of mRNA', *Nature*, 224: 329-31.
Moss, F. P., and C. P. Leblond. 1970. 'Nature of dividing nuclei in skeletal muscle of growing rats', *J Cell Biol*, 44: 459-62.
Mouly, V., A. Aamiri, A. Bigot, R. N. Cooper, S. Di Donna, D. Furling, T. Gidaro, V. Jacquemin, K. Mamchaoui, E. Negroni, S. Périé, V. Renault, S. D. Silva-Barbosa, and G. S. Butler-Browne. 2005. 'The mitotic clock in skeletal muscle regeneration, disease and cell mediated gene therapy', *Acta Physiol Scand*, 184: 3-15.
Nami, F., M. Basiri, L. Satarian, C. Curtiss, H. Baharvand, and C. Verfaillie. 2018. 'Strategies for In Vivo Genome Editing in Nondividing Cells', *Trends Biotechnol*, 36: 770-86.
Negroni, E., T. Gidaro, A. Bigot, G. S. Butler-Browne, V. Mouly, and C. Trollet. 2015. 'Invited review: Stem cells and muscle diseases: advances in cell therapy strategies', *Neuropathol Appl Neurobiol*, 41: 270-87.
Nelson, C. E., C. H. Hakim, D. G. Ousterout, P. I. Thakore, E. A. Moreb, R. M. Castellanos Rivera, S. Madhavan, X. Pan, F. A. Ran, W. X. Yan, A. Asokan, F. Zhang, D. Duan, and C. A. Gersbach. 2016. 'In vivo genome editing improves muscle function in a mouse model of Duchenne muscular dystrophy', *Science*, 351: 403-7.
Nigro, V., and G. Piluso. 2015. 'Spectrum of muscular dystrophies associated with sarcolemmal-protein genetic defects', *Biochim Biophys Acta*, 1852: 585-93.
Nigro, V., and M. Savarese. 2014. 'Genetic basis of limb-girdle muscular dystrophies: the 2014 update', *Acta Myol*, 33: 1-12.
Nishi, Y., M. Uryu, S. Yamanaka, K. Watanabe, N. Kitamura, M. Iguchi, and S. Mitsuhashi. 1990. 'The structure and mechanical properties of sheets prepared from bacterial cellulose', *Journal of Materials Science*, 25: 2997-3001.
Nishimasu, H., F. A. Ran, P. D. Hsu, S. Konermann, S. I. Shehata, N. Dohmae, R. Ishitani, F. Zhang, and O. Nureki. 2014. 'Crystal structure of Cas9 in complex with guide RNA and target DNA', *Cell*, 156: 935-49.
Nunes, A. M., R. D. Wuebbles, A. Sarathy, T. M. Fontelonga, M. Deries, D. J. Burkin, and S. Thorsteinsdottir. 2017. 'Impaired fetal muscle development and JAK-STAT activation mark disease onset and progression in a mouse model for merosin-deficient congenital muscular dystrophy', *Hum Mol Genet*, 26: 2018-33.
Olayioye, M. A., B. Noll, and A. Hausser. 2019. 'Spatiotemporal Control of Intracellular Membrane Trafficking by Rho GTPases', *Cells*, 8.
Olguin, H. C., and B. B. Olwin. 2004. 'Pax-7 up-regulation inhibits myogenesis and cell cycle progression in satellite cells: a potential mechanism for self-renewal', *Dev Biol*, 275: 375-88.

Olguin, H. C., and A. Pisconti. 2012. 'Marking the tempo for myogenesis: Pax7 and the regulation of muscle stem cell fate decisions', *J Cell Mol Med*, 16: 1013-25.
Olson, M. F., A. Ashworth, and A. Hall. 1995. 'An essential role for Rho, Rac, and Cdc42 GTPases in cell cycle progression through G1', *Science*, 269: 1270.
Ono, Y., S. Masuda, H. S. Nam, R. Benezra, Y. Miyagoe-Suzuki, and S. Takeda. 2012. 'Slow-dividing satellite cells retain long-term self-renewal ability in adult muscle', *J Cell Sci*, 125: 1309-17.
Ortiz-Vitali, Jose L., and Radbod Darabi. 2019. 'iPSCs as a Platform for Disease Modeling, Drug Screening, and Personalized Therapy in Muscular Dystrophies', *Cells*, 8: 20.
Pagano, M., R. Pepperkok, F. Verde, W. Ansorge, and G. Draetta. 1992. 'Cyclin A is required at two points in the human cell cycle', *EMBO J*, 11: 961-71.
Paik, J. C., B. Wang, K. Liu, J. K. Lue, and W. C. Lin. 2010. 'Regulation of E2F1-induced apoptosis by the nucleolar protein RRP1B', *J Biol Chem*, 285: 6348-63.
Pala, F., D. Di Girolamo, S. Mella, S. Yennek, L. Chatre, M. Ricchetti, and S. Tajbakhsh. 2018. 'Distinct metabolic states govern skeletal muscle stem cell fates during prenatal and postnatal myogenesis', *Journal of Cell Science*, 131: jcs212977.
Paquet, D., D. Kwart, A. Chen, A. Sproul, S. Jacob, S. Teo, K. M. Olsen, A. Gregg, S. Noggle, and M. Tessier-Lavigne. 2016. 'Efficient introduction of specific homozygous and heterozygous mutations using CRISPR/Cas9', *Nature*, 533: 125-9.
Parker, M. H., C. Loretz, A. E. Tyler, W. J. Duddy, J. K. Hall, B. B. Olwin, I. D. Bernstein, R. Storb, and S. J. Tapscott. 2012. 'Activation of Notch signaling during ex vivo expansion maintains donor muscle cell engraftment', *Stem Cells*, 30: 2212-20.
Partridge, T. 2002. 'Myoblast transplantation', *Neuromuscul Disord*, 12 Suppl 1: S3-6.
Partridge, T. A. 1991. 'Invited review: myoblast transfer: a possible therapy for inherited myopathies?', *Muscle Nerve*, 14: 197-212.
Partridge, T. A., J. E. Morgan, G. R. Coulton, E. P. Hoffman, and L. M. Kunkel. 1989. 'Conversion of mdx myofibres from dystrophin-negative to -positive by injection of normal myoblasts', *Nature*, 337: 176-9.
Patel, N. J., K. W. Van Dyke, and L. R. Espinoza. 2017. 'Limb-Girdle Muscular Dystrophy 2B and Miyoshi Presentations of Dysferlinopathy', *Am J Med Sci*, 353: 484-91.
Peltz, S. W., A. H. Brown, and A. Jacobson. 1993. 'mRNA destabilization triggered by premature translational termination depends on at least three cis-acting sequence elements and one trans-acting factor', *Genes Dev*, 7: 1737-54.
Périé, S., C. Trollet, V. Mouly, V. Vanneaux, K. Mamchaoui, B. Bouazza, J. P. Marolleau, P. Laforêt, F. Chapon, B. Eymard, G. Butler-Browne, J. Larghero, and J. L. St Guily. 2014. 'Autologous myoblast transplantation for oculopharyngeal muscular dystrophy: a phase I/IIa clinical study', *Mol Ther*, 22: 219-25.
Petersen, N., and P. Gatenholm. 2011. 'Bacterial cellulose-based materials and medical devices: current state and perspectives', *Appl Microbiol Biotechnol*, 91: 1277-86.
Philippi, S., S. Lorain, C. Beley, C. Peccate, G. Precigout, S. Spuler, and L. Garcia. 2015. 'Dysferlin rescue by spliceosome-mediated pre-mRNA trans-splicing targeting introns harbouring weakly defined 3' splice sites', *Hum Mol Genet*, 24: 4049-60.
Picheth, G. F., C. L. Pirich, M. R. Sierakowski, M. A. Woehl, C. N. Sakakibara, C. F. de Souza, A. A. Martin, R. da Silva, and R. A. de Freitas. 2017. 'Bacterial cellulose in biomedical applications: A review', *Int J Biol Macromol*, 104: 97-106.
Pickar-Oliver, Adrian, and Charles A. Gersbach. 2019. 'The next generation of CRISPR–Cas technologies and applications', *Nature Reviews Molecular Cell Biology*, 20: 490-507.
Pietrosemoli, N., S. Mella, S. Yennek, M. B. Baghdadi, H. Sakai, R. Sambasivan, F.Pala, D. Di Girolamo, and S. Tajbakhsh. 2017. 'Comparison of multiple transcriptomes exposes unified and divergent features of quiescent and activated skeletal muscle stem cells', *Skeletal muscle*, 7: 28-28.
Platt, R. J., S. Chen, Y. Zhou, M. J. Yim, L. Swiech, H. R. Kempton, J. E. Dahlman, O. Parnas, T. M. Eisenhaure, M. Jovanovic, D. B. Graham, S. Jhunjhunwala, M. Heidenreich, R. J. Xavier, R. Langer, D. G. Anderson, N. Hacohen, A. Regev, G. Feng, P. A. Sharp, and F. Zhang. 2014. 'CRISPR-Cas9 knockin mice for genome editing and cancer modeling', *Cell*, 159: 440-55.
Portela, R., C. R. Leal, P. L. Almeida, and R. G. Sobral. 2019. 'Bacterial cellulose: a versatile biopolymer for wound dressing applications', *Microb Biotechnol*, 12: 586-610.
Porteus, Matthew H. 2015. 'Towards a new era in medicine: therapeutic genome editing', *Genome Biology*, 16: 286.

Pramono, Z. A., C. L. Tan, I. A. Seah, J. S. See, S. Y. Kam, P. S. Lai, and W. C. Yee. 2009. 'Identification and characterisation of human dysferlin transcript variants: implications for dysferlin mutational screening and isoforms', *Hum Genet*, 125: 413-20.
Price, F. D., J. von Maltzahn, C. F. Bentzinger, N. A. Dumont, H. Yin, N. C. Chang, D. H. Wilson, J. Frenette, and M. A. Rudnicki. 2014. 'Inhibition of JAK-STAT signaling stimulates adult satellite cell function', *Nat Med*, 20: 1174-81.
Quarta, M., J. O. Brett, R. DiMarco, A. De Morree, S. C. Boutet, R. Chacon, M. C. Gibbons, V. A. Garcia, J. Su, J. B. Shrager, S. Heilshorn, and T. A. Rando. 2016. 'An artificial niche preserves the quiescence of muscle stem cells and enhances their therapeutic efficacy', *Nat Biotechnol*, 34: 752-9.
Quenneville, S. P., P. Chapdelaine, D. Skuk, M. Paradis, M. Goulet, J. Rousseau, X. Xiao, L. Garcia, and J. P. Tremblay. 2007. 'Autologous transplantation of muscle precursor cells modified with a lentivirus for muscular dystrophy: human cells and primate models', *Mol Ther*, 15: 431-8.
Rajwade, J. M., K. M. Paknikar, and J. V. Kumbhar. 2015. 'Applications of bacterial cellulose and its composites in biomedicine', *Appl Microbiol Biotechnol*, 99: 2491-511.
Ramos, J. N., K. Hollinger, N. E. Bengtsson, J. M. Allen, S. D. Hauschka, and J. S. Chamberlain. 2019. 'Development of Novel Micro-dystrophins with Enhanced Functionality', *Mol Ther*, 27: 623-35.
Rayagiri, S. S., D. Ranaldi, A. Raven, N. I. F. Mohamad Azhar, O. Lefebvre, P. S. Zammit, and A. G. Borycki. 2018. 'Basal lamina remodeling at the skeletal muscle stem cell niche mediates stem cell self-renewal', *Nat Commun*, 9: 1075.
Recouvreux, Derce O. S., Carlos R. Rambo, Fernanda V. Berti, Claudimir A. Carminatti, Regina V. Antônio, and Luismar M. Porto. 2011. 'Novel three-dimensional cocoon-like hydrogels for soft tissue regeneration', *Materials Science and Engineering: C*, 31: 151-57.
Relaix, F., D. Montarras, S. Zaffran, B. Gayraud-Morel, D. Rocancourt, S. Tajbakhsh, A. Mansouri, A. Cumano, and M. Buckingham. 2006. 'Pax3 and Pax7 have distinct and overlapping functions in adult muscle progenitor cells', *J Cell Biol*, 172: 91-102.
Relaix, F., D. Rocancourt, A. Mansouri, and M. Buckingham. 2005. 'A Pax3/Pax7-dependent population of skeletal muscle progenitor cells', *Nature*, 435: 948-53.
Relaix, F., and P. S. Zammit. 2012. 'Satellite cells are essential for skeletal muscle regeneration: the cell on the edge returns centre stage', *Development*, 139: 2845-56.
Retegi, A., Nagore Gabilondo, Cristina Peña, Robin Zuluaga, Cristina Castro, Piedad Gañán, Koro De la Caba, and I. Mondragon. 2010. 'Bacterial cellulose films with controlled microstructure-mechanical property relationships', *Cellulose*, 17: 661-69.
Reznik, M. 1969. 'Thymidine-3H uptake by satellite cells of regenerating skeletal muscle', *J Cell Biol*, 40: 568-71.
Richardson, Brian E., Karen Beckett, Scott J. Nowak, and Mary K. Baylies. 2007. 'SCAR/WAVE and Arp2/3 are crucial for cytoskeletal remodeling at the site of myoblast fusion', *Development*, 134: 4357.
Rocheteau, P., B. Gayraud-Morel, I. Siegl-Cachedenier, M. A. Blasco, and S. Tajbakhsh. 2012. 'A subpopulation of adult skeletal muscle stem cells retains all template DNA strands after cell division', *Cell*, 148: 112-25.
Römling, U. 2002. 'Molecular biology of cellulose production in bacteria', *Res Microbiol*, 153: 205-12.
Rong, Y. S., and K. G. Golic. 2000. 'Gene targeting by homologous recombination in Drosophila', *Science*, 288: 2013-8.
Rosales, X. Q., J. M. Gastier-Foster, S. Lewis, M. Vinod, D. L. Thrush, C. Astbury, R. Pyatt, S. Reshmi, Z. Sahenk, and J. R. Mendell. 2010. 'Novel diagnostic features of dysferlinopathies', *Muscle Nerve*, 42: 14-21.
Rozo, M., L. Li, and C. M. Fan. 2016. 'Targeting beta1-integrin signaling enhances regeneration in aged and dystrophic muscle in mice', *Nat Med*, 22: 889-96.
Rudin, N., E. Sugarman, and J. E. Haber. 1989. 'Genetic and physical analysis of double-strand break repair and recombination in Saccharomyces cerevisiae', *Genetics*, 122: 519-34.
Ruoß, M., M. Vosough, A. Königsrainer, S. Nadalin, S. Wagner, S. Sajadian, D. Huber, Z. Heydari, S. Ehnert, J. G. Hengstler, and A. K. Nussler. 2020. 'Towards improved hepatocyte cultures: Progress and limitations', *Food Chem Toxicol*, 138: 111188.
Ryall, J. G., S. Dell'Orso, A. Derfoul, A. Juan, H. Zare, X. Feng, D. Clermont, M. Koulnis, G. Gutierrez-Cruz, M. Fulco, and V. Sartorelli. 2015. 'The NAD(+)-dependent SIRT1

deacetylase translates a metabolic switch into regulatory epigenetics in skeletal muscle stem cells', *Cell Stem Cell*, 16: 171-83.
Sacco, A., R. Doyonnas, P. Kraft, S. Vitorovic, and H. M. Blau. 2008. 'Self-renewal and expansion of single transplanted muscle stem cells', *Nature*, 456: 502-6.
Salani, S., S. Lucchiari, F. Fortunato, M. Crimi, S. Corti, F. Locatelli, P. Bossolasco, N. Bresolin, and G. P. Comi. 2004. 'Developmental and tissue-specific regulation of a novel dysferlin isoform', *Muscle Nerve*, 30: 366-74.
Sampaolesi, M., Y. Torrente, A. Innocenzi, R. Tonlorenzi, G. D'Antona, M. A. Pellegrino, R. Barresi, N. Bresolin, M. G. De Angelis, K. P. Campbell, R. Bottinelli, and G. Cossu. 2003. 'Cell therapy of alpha-sarcoglycan null dystrophic mice through intra-arterial delivery of mesoangioblasts', *Science*, 301: 487-92.
Sampaolesi, M., S. Blot, and Giuseppe D'Antona. 2006. 'Mesoangioblast stem cells ameliorate muscle function in dystrophic dogs', *Nature*, 127: 1304-06.
Sampath, S. C., S. C. Sampath, A. T. V. Ho, S. Y. Corbel, J. D. Millstone, J. Lamb, J. Walker, B. Kinzel, C. Schmedt, and H. M. Blau. 2018. 'Induction of muscle stem cell quiescence by the secreted niche factor Oncostatin M', *Nat Commun*, 9: 1531.
Scadden, D. T. 2006. 'The stem-cell niche as an entity of action', *Nature*, 441: 1075-9.
Scharner, J., and P. S. Zammit. 2011. 'The muscle satellite cell at 50: the formative years', *Skelet Muscle*, 1: 28.
Schiller, Herbert B., and Reinhard Fässler. 2013. 'Mechanosensitivity and compositional dynamics of cell-matrix adhesions', *EMBO reports*, 14: 509-19.
Schmidt, Manuel, Svenja C. Schüler, Sören S. Hüttner, Björn von Eyss, and Julia von Maltzahn. 2019. 'Adult stem cells at work: regenerating skeletal muscle', *Cellular and Molecular Life Sciences*, 76: 2559-70.
Schnyder, S., and C. Handschin. 2015. 'Skeletal muscle as an endocrine organ: PGC-1alpha, myokines and exercise', *Bone*, 80: 115-25.
Schoewel, V., A. Marg, S. Kunz, T. Overkamp, R. S. Carrazedo, U. Zacharias, P. T. Daniel, and S. Spuler. 2012. 'Dysferlin-peptides reallocate mutated dysferlin thereby restoring function', *PLoS One*, 7: e49603.
Schofield, R. 1978. 'The relationship between the spleen colony-forming cell and the haemopoietic stem cell', *Blood Cells*, 4: 7-25.
Schumann, Dieter A., J. Wippermann, D. O. Klemm, F. Kramer, D. Koth, H. Kosmehl, T. Wahlers, and S. Salehi-Gelani. 2009. 'Artificial vascular implants from bacterial cellulose: preliminary results of small arterial substitutes', *Cellulose*, 16: 877-85.
Schwank, G., B. K. Koo, V. Sasselli, J. F. Dekkers, I. Heo, T. Demircan, N. Sasaki, S. Boymans, E. Cuppen, C. K. van der Ent, E. E. Nieuwenhuis, J. M. Beekman, and H. Clevers. 2013. 'Functional repair of CFTR by CRISPR/Cas9 in intestinal stem cell organoids of cystic fibrosis patients', *Cell Stem Cell*, 13: 653-8.
Schyschka, L., J. J. Sánchez, Z. Wang, B. Burkhardt, U. Müller-Vieira, K. Zeilinger, A. Bachmann, S. Nadalin, G. Damm, and A. K. Nussler. 2013. 'Hepatic 3D cultures but not 2D cultures preserve specific transporter activity for acetaminophen-induced hepatotoxicity', *Arch Toxicol*, 87: 1581-93.
Seale, P., L. A. Sabourin, A. Girgis-Gabardo, A. Mansouri, P. Gruss, and M. A. Rudnicki. 2000. 'Pax7 is required for the specification of myogenic satellite cells', *Cell*, 102: 777-86.
Selvaraj, S., N. R. Dhoke, J. Kiley, A. J. Mateos-Aierdi, S. Tungtur, R. Mondragon-Gonzalez, G. Killeen, V. K. P. Oliveira, A. López de Munain, and R. C. R. Perlingeiro. 2019. 'Gene Correction of LGMD2A Patient-Specific iPSCs for the Development of Targeted Autologous Cell Therapy', *Mol Ther*, 27: 2147-57.
Sens, K. L., S. Zhang, P. Jin, R. Duan, G. Zhang, F. Luo, L. Parachini, and E. H. Chen. 2010. 'An invasive podosome-like structure promotes fusion pore formation during myoblast fusion', *Journal of Cell Biology*, 191: 1013-27.
Shah, N., M. Ul-Islam, W. A. Khattak, and J. K. Park. 2013. 'Overview of bacterial cellulose composites: a multipurpose advanced material', *Carbohydr Polym*, 98: 1585-98.
Shalem, O., N. E. Sanjana, E. Hartenian, X. Shi, D. A. Scott, T. Mikkelson, D. Heckl, B. L. Ebert, D. E. Root, J. G. Doench, and F. Zhang. 2014. 'Genome-scale CRISPR-Cas9 knockout screening in human cells', *Science*, 343: 84-87.
Shayakhmetov, D. M., N. C. Di Paolo, and K. L. Mossman. 2010. 'Recognition of virus infection and innate host responses to viral gene therapy vectors', *Molecular therapy : the journal of the American Society of Gene Therapy*, 18: 1422-29.

Shelton, M., J. Metz, J. Liu, R. L. Carpenedo, S.-P. Demers, W. L. Stanford, and I. S. Skerjanc. 2014. 'Derivation and expansion of PAX7-positive muscle progenitors from human and mouse embryonic stem cells', *Stem Cell Reports*, 3: 516-29.
Sherr, C. J., and J. M. Roberts. 1999. 'CDK inhibitors: positive and negative regulators of G1-phase progression', *Genes Dev*, 13: 1501-12.
Shieh, P. B. 2015. 'Duchenne muscular dystrophy: clinical trials and emerging tribulations', *Curr Opin Neurol*, 28: 542-6.
Shin, J. H., X. Pan, C. H. Hakim, H. T. Yang, Y. Yue, K. Zhang, R. L. Terjung, and D. Duan. 2013. 'Microdystrophin ameliorates muscular dystrophy in the canine model of duchenne muscular dystrophy', *Mol Ther*, 21: 750-7.
Shmakov, Sergey, Omar O. Abudayyeh, Kira S. Makarova, Yuri I. Wolf, Jonathan S. Gootenberg, Ekaterina Semenova, Leonid Minakhin, Julia Joung, Silvana Konermann, Konstantin Severinov, Feng Zhang, and Eugene V. Koonin. 2015. 'Discovery and Functional Characterization of Diverse Class 2 CRISPR-Cas Systems', *Molecular Cell*, 60: 385-97.
Shoda, M., and Y. Sugano. 2005. 'Recent advances in bacterial cellulose production', *Biotechnology and Bioprocess Engineering*, 10: 1.
Skuk, D., M. Goulet, B. Roy, P. Chapdelaine, J. P. Bouchard, R. Roy, F. J. Dugre, M. Sylvain, J. G. Lachance, L. Deschenes, H. Senay, and J. P. Tremblay. 2006. 'Dystrophin expression in muscles of duchenne muscular dystrophy patients after high-density injections of normal myogenic cells', *J Neuropathol Exp Neurol*, 65: 371-86.
Skuk, D., M. Goulet, B. Roy, V. Piette, C. H. Cote, P. Chapdelaine, J. Y. Hogrel, M. Paradis, J. P. Bouchard, M. Sylvain, J. G. Lachance, and J. P. Tremblay. 2007. 'First test of a "high-density injection" protocol for myogenic cell transplantation throughout large volumes of muscles in a Duchenne muscular dystrophy patient: eighteen months follow-up', *Neuromuscul Disord*, 17: 38-46.
Skuk, D., M. Goulet, B. Roy, V. Piette, C. H. Côté, P. Chapdelaine, J. Y. Hogrel, M. Paradis, J. P. Bouchard, M. Sylvain, J. G. Lachance, and J. P. Tremblay. 2007. 'First test of a "high-density injection" protocol for myogenic cell transplantation throughout large volumes of muscles in a Duchenne muscular dystrophy patient: eighteen months follow-up', *Neuromuscul Disord*, 17: 38-46.
Skuk, D., M. Goulet, B. Roy, and J. P. Tremblay. 2002. 'Efficacy of myoblast transplantation in nonhuman primates following simple intramuscular cell injections: toward defining strategies applicable to humans', *Exp Neurol*, 175: 112-26.
Skuk, D., M. Goulet, and J. P. Tremblay. 2014. 'Intramuscular transplantation of myogenic cells in primates: importance of needle size, cell number, and injection volume', *Cell Transplant*, 23: 13-25.
Slaymaker, I. M., L. Gao, B. Zetsche, D. A. Scott, W. X. Yan, and F. Zhang. 2016. 'Rationally engineered Cas9 nucleases with improved specificity', *Science*, 351: 84-8.
So, W. K., and T. H. Cheung. 2018. 'Molecular Regulation of Cellular Quiescence: A Perspective from Adult Stem Cells and Its Niches', *Methods Mol Biol*, 1686: 1-25.
Sondergaard, P. C., D. A. Griffin, E. R. Pozsgai, R. W. Johnson, W. E. Grose, K. N. Heller, K. M. Shontz, C. L. Montgomery, J. Liu, K. R. Clark, Z. Sahenk, J. R. Mendell, and L. R. Rodino-Klapac. 2015. 'AAV.Dysferlin Overlap Vectors Restore Function in Dysferlinopathy Animal Models', *Ann Clin Transl Neurol*, 2: 256-70.
Song, B., Y. Fan, W. He, D. Zhu, X. Niu, D. Wang, Z. Ou, M. Luo, and X. Sun. 2015. 'Improved hematopoietic differentiation efficiency of gene-corrected beta-thalassemia induced pluripotent stem cells by CRISPR/Cas9 system', *Stem Cells Dev*, 24: 1053-65.
Soriano-Arroquia, A., P. D. Clegg, A. P. Molloy, and K. Goljanek-Whysall. 2017. 'Preparation and Culture of Myogenic Precursor Cells/Primary Myoblasts from Skeletal Muscle of Adult and Aged Humans', *J Vis Exp*.
Souza, C. M., L. A. Mesquita, D. Souza, A. C. Irioda, J. C. Francisco, C. F. Souza, L. C. Guarita-Souza, M. R. Sierakowski, and K. A. Carvalho. 2014. 'Regeneration of skin tissue promoted by mesenchymal stem cells seeded in nanostructured membrane', *Transplant Proc*, 46: 1882-6.
Spuler, S., M. Carl, J. Zabojszcza, V. Straub, K. Bushby, S. A. Moore, S. Bahring, K. Wenzel, U. Vinkemeier, and C. Rocken. 2008. 'Dysferlin-deficient muscular dystrophy features amyloidosis', *Ann Neurol*, 63: 323-8.
Stein, C. A. 2016. 'Eteplirsen Approved for Duchenne Muscular Dystrophy: The FDA Faces a Difficult Choice', *Mol Ther*, 24: 1884-85.

Sternberg, S. H., S. Redding, M. Jinek, E. C. Greene, and J. A. Doudna. 2014. 'DNA interrogation by the CRISPR RNA-guided endonuclease Cas9', *Nature*, 507: 62-7.
Sun, C., L. Shen, Z. Zhang, and X. Xie. 2020. 'Therapeutic Strategies for Duchenne Muscular Dystrophy: An Update', *Genes (Basel)*, 11.
Sun, X., and P. D. Kaufman. 2018. 'Ki-67: more than a proliferation marker', *Chromosoma*, 127: 175-86.
Svensson, A., E. Nicklasson, T. Harrah, B. Panilaitis, D. L. Kaplan, M. Brittberg, and P. Gatenholm. 2005. 'Bacterial cellulose as a potential scaffold for tissue engineering of cartilage', *Biomaterials*, 26: 419-31.
Tabebordbar, M., K. Zhu, J. K. W. Cheng, W. L. Chew, J. J. Widrick, W. X. Yan, C. Maesner, E. Y. Wu, R. Xiao, F. A. Ran, L. Cong, F. Zhang, L. H. Vandenberghe, G. M. Church, and A. J. Wagers. 2016. 'In vivo gene editing in dystrophic mouse muscle and muscle stem cells', *Science*, 351: 407-11.
Tajbakhsh, S., E. Bober, C. Babinet, S. Pournin, H. Arnold, and M. Buckingham. 1996. 'Gene targeting the myf-5 locus with nlacZ reveals expression of this myogenic factor in mature skeletal muscle fibres as well as early embryonic muscle', *Dev Dyn*, 206: 291-300.
Takashima, S., S. Shinkuma, Y. Fujita, T. Nomura, H. Ujiie, K. Natsuga, H. Iwata, H. Nakamura, A. Vorobyev, R. Abe, and H. Shimizu. 2019. 'Efficient Gene Reframing Therapy for Recessive Dystrophic Epidermolysis Bullosa with CRISPR/Cas9', *J Invest Dermatol*, 139: 1711-21.e4.
Takubo, K., G. Nagamatsu, C. I. Kobayashi, A. Nakamura-Ishizu, H. Kobayashi, E. Ikeda, N. Goda, Y. Rahimi, R. S. Johnson, T. Soga, A. Hirao, M. Suematsu, and T. Suda. 2013. 'Regulation of glycolysis by Pdk functions as a metabolic checkpoint for cell cycle quiescence in hematopoietic stem cells', *Cell Stem Cell*, 12: 49-61.
Tedesco, F. S., A. Dellavalle, J. Diaz-Manera, G. Messina, and G. Cossu. 2010. 'Repairing skeletal muscle: regenerative potential of skeletal muscle stem cells', *J Clin Invest*, 120: 11-9.
Tedesco, F. S., M. F. Gerli, L. Perani, S. Benedetti, F. Ungaro, M. Cassano, S. Antonini, E. Tagliafico, V. Artusi, E. Longa, R. Tonlorenzi, M. Ragazzi, G. Calderazzi, H. Hoshiya, O. Cappellari, M. Mora, B. Schoser, P. Schneiderat, M. Oshimura, R. Bottinelli, M. Sampaolesi, Y. Torrente, V. Broccoli, and G. Cossu. 2012. 'Transplantation of genetically corrected human iPSC-derived progenitors in mice with limb-girdle muscular dystrophy', *Sci Transl Med*, 4: 140ra89.
Tedesco, F. S., H. Hoshiya, G. D'Antona, M. F. Gerli, G. Messina, S. Antonini, R. Tonlorenzi, S. Benedetti, L. Berghella, Y. Torrente, Y. Kazuki, R. Bottinelli, M. Oshimura, and G. Cossu. 2011. 'Stem cell-mediated transfer of a human artificial chromosome ameliorates muscular dystrophy', *Sci Transl Med*, 3: 96ra78.
Therrien, C., S. Di Fulvio, S. Pickles, and M. Sinnreich. 2009. 'Characterization of lipid binding specificities of dysferlin C2 domains reveals novel interactions with phosphoinositides', *Biochemistry*, 48: 2377-84.
Therrien, C., D. Dodig, G. Karpati, and M. Sinnreich. 2006. 'Mutation impact on dysferlin inferred from database analysis and computer-based structural predictions', *J Neurol Sci*, 250: 71-8.
Thomson, J. A., J. Itskovitz-Eldor, S. S. Shapiro, M. A. Waknitz, J. J. Swiergiel, V. S. Marshall, and J. M. Jones. 1998. 'Embryonic stem cell lines derived from human blastocysts', *Science*, 282: 1145-7.
Tierney, M. T., T. Aydogdu, D. Sala, B. Malecova, S. Gatto, P. L. Puri, L. Latella, and A. Sacco. 2014. 'STAT3 signaling controls satellite cell expansion and skeletal muscle repair', *Nat Med*, 20: 1182-6.
Tierney, M.T., A. Gromova, F. B. Sesillo, D. Sala, C. Spenlé, G. Orend, and A. Sacco. 2016. 'Autonomous Extracellular Matrix Remodeling Controls a Progressive Adaptation in Muscle Stem Cell Regenerative Capacity during Development', *Cell Reports*, 14: 1940-52.
Torrente, Y., M. Belicchi, C. Marchesi, G. D'Antona, F. Cogiamanian, F. Pisati, M. Gavina, R. Giordano, R. Tonlorenzi, G. Fagiolari, C. Lamperti, L. Porretti, R. Lopa, M. Sampaolesi, L. Vicentini, N. Grimoldi, F. Tiberio, V. Songa, P. Baratta, A. Prelle, L. Forzenigo, M. Guglieri, O. Pansarasa, C. Rinaldi, V. Mouly, G. S. Butler-Browne, G. P. Comi, P. Biondetti, M. Moggio, S. M. Gaini, N. Stocchetti, A. Priori, M. G. D'Angelo, A. Turconi, R. Bottinelli, G. Cossu, P. Rebulla, and N. Bresolin. 2007. 'Autologous transplantation of muscle-derived CD133+ stem cells in Duchenne muscle patients', *Cell Transplant*, 16: 563-77.
Torrente, Y., M. Belicchi, M. Sampaolesi, F. Pisati, M. Meregalli, G. D'Antona, R. Tonlorenzi, L. Porretti, M. Gavina, K. Mamchaoui, M. A. Pellegrino, D. Furling, V. Mouly, G. S. Butler-Browne, R. Bottinelli, G. Cossu, and N. Bresolin. 2004. 'Human circulating AC133(+) stem

cells restore dystrophin expression and ameliorate function in dystrophic skeletal muscle', *J Clin Invest*, 114: 182-95.
Tremblay, J. P., F. Malouin, R. Roy, J. Huard, J. P. Bouchard, A. Satoh, and C. L. Richards. 1993. 'Results of a triple blind clinical study of myoblast transplantations without immunosuppressive treatment in young boys with Duchenne muscular dystrophy', *Cell Transplant*, 2: 99-112.
Tronser, T., A. Laromaine, A. Roig, and P. A. Levkin. 2018. 'Bacterial Cellulose Promotes Long-Term Stemness of mESC', *ACS Appl Mater Interfaces*, 10: 16260-69.
Tsai, S. Q., Z. Zheng, N. T. Nguyen, M. Liebers, V. V. Topkar, V. Thapar, N. Wyvekens, C. Khayter, A. J. Iafrate, L. P. Le, M. J. Aryee, and J. K. Joung. 2015. 'GUIDE-seq enables genome-wide profiling of off-target cleavage by CRISPR-Cas nucleases', *Nat Biotechnol*, 33: 187-97.
Turan, S., A. P. Farruggio, W. Srifa, J. W. Day, and M. P. Calos. 2016. 'Precise Correction of Disease Mutations in Induced Pluripotent Stem Cells Derived From Patients With Limb Girdle Muscular Dystrophy', *Mol Ther*, 24: 685-96.
Tyler, F. H., and F. E. Stephens. 1951. 'Studies in disorders of muscle. IV. The clinical manifestations and inheritance of childhood progressive muscular dystrophy', *Ann Intern Med*, 35: 169-85.
Ullah, M. W., M. Ul-Islam, S. Khan, Y. Kim, and J. K. Park. 2016. 'Structural and physico-mechanical characterization of bio-cellulose produced by a cell-free system', *Carbohydrate polymers*, 136: 908-16.
Urciuolo, A., M. Quarta, V. Morbidoni, F. Gattazzo, S. Molon, P. Grumati, F. Montemurro, F. S. Tedesco, B. Blaauw, G. Cossu, G. Vozzi, T. A. Rando, and P. Bonaldo. 2013. 'Collagen VI regulates satellite cell self-renewal and muscle regeneration', *Nat Commun*, 4: 1964.
Valera, M. J., M. J. Torija, A. Mas, and E. Mateo. 2015. 'Cellulose production and cellulose synthase gene detection in acetic acid bacteria', *Appl Microbiol Biotechnol*, 99: 1349-61.
van der Oost, J., M. M. Jore, E. R. Westra, M. Lundgren, and S. J. Brouns. 2009. 'CRISPR-based adaptive and heritable immunity in prokaryotes', *Trends Biochem Sci*, 34: 401-7.
van Overbeek, M., D. Capurso, M. M. Carter, M. S. Thompson, E. Frias, C. Russ, J. S. Reece-Hoyes, C. Nye, S. Gradia, B. Vidal, J. Zheng, G. R. Hoffman, C. K. Fuller, and A. P. May. 2016. 'DNA Repair Profiling Reveals Nonrandom Outcomes at Cas9-Mediated Breaks', *Mol Cell*, 63: 633-46.
Vilas-Boas, V., A. Cooreman, E. Gijbels, R. Van Campenhout, E. Gustafson, S. Ballet, P. Annaert, B. Cogliati, and M. Vinken. 2019. 'Primary hepatocytes and their cultures for the testing of drug-induced liver injury', *Adv Pharmacol*, 85: 1-30.
Vilchez, J. J., P. Gallano, E. Gallardo, A. Lasa, R. Rojas-Garcia, A. Freixas, N. De Luna, F. Calafell, T. Sevilla, F. Mayordomo, M. Baiget, and I. Illa. 2005. 'Identification of a novel founder mutation in the DYSF gene causing clinical variability in the Spanish population', *Arch Neurol*, 62: 1256-9.
Vilquin, J. T., I. Kinoshita, B. Roy, M. Goulet, E. Engvall, F. Tomé, M. Fardeau, and J. P. Tremblay. 1996. 'Partial laminin alpha2 chain restoration in alpha2 chain-deficient dy/dy mouse by primary muscle cell culture transplantation', *Journal of Cell Biology*, 133: 185-97.
von Maltzahn, J., A. E. Jones, R. J. Parks, and M. A. Rudnicki. 2013. 'Pax7 is critical for the normal function of satellite cells in adult skeletal muscle', *Proc Natl Acad Sci U S A*, 110: 16474-9.
von Maltzahn, Julia, C Florian Bentzinger, and Michael A Rudnicki. 2014. 'Characteristics of satellite cells and multipotent adult stem cells in the skeletal muscle.' in, *Stem Cells and Cancer Stem Cells, Volume 12* (Springer).
Wallace, G. Q., and E. M. McNally. 2009. 'Mechanisms of muscle degeneration, regeneration, and repair in the muscular dystrophies', *Annu Rev Physiol*, 71: 37-57.
Walter, M. C., P. Reilich, S. Thiele, J. Schessl, H. Schreiber, K. Reiners, W. Kress, C. Muller-Reible, M. Vorgerd, P. Urban, B. Schrank, M. Deschauer, B. Schlotter-Weigel, R. Kohnen, and H. Lochmuller. 2013. 'Treatment of dysferlinopathy with deflazacort: a double-blind, placebo-controlled clinical trial', *Orphanet J Rare Dis*, 8: 26.
Wang, B., J. Li, and X. Xiao. 2000. 'Adeno-associated virus vector carrying human minidystrophin genes effectively ameliorates muscular dystrophy in mdx mouse model', *Proc Natl Acad Sci U S A*, 97: 13714-9.
Wang, H., H. Yang, C. S. Shivalila, M. M. Dawlaty, A. W. Cheng, F. Zhang, and R. Jaenisch. 2013. 'One-step generation of mice carrying mutations in multiple genes by CRISPR/Cas-mediated genome engineering', *Cell*, 153: 910-8.

Wang, J., J. Tavakoli, and Y. Tang. 2019. 'Bacterial cellulose production, properties and applications with different culture methods - A review', *Carbohydr Polym*, 219: 63-76.
Wang, Y. X., and M. A. Rudnicki. 2011. 'Satellite cells, the engines of muscle repair', *Nat Rev Mol Cell Biol*, 13: 127-33.
Warnock, J. N., C. Daigre, and M. Al-Rubeai. 2011. 'Introduction to viral vectors', *Methods Mol Biol*, 737: 1-25.
Watanabe, K., Y. Eto, S. Takano, S. Nakamori, H. Shibai, and S. Yamanaka. 1993. 'A new bacterial cellulose substrate for mammalian cell culture', *Cytotechnology*, 13: 107-14.
Watchko, J., T. O'Day, B. Wang, L. Zhou, Y. Tang, J. Li, and X. Xiao. 2002. 'Adeno-associated virus vector-mediated minidystrophin gene therapy improves dystrophic muscle contractile function in mdx mice', *Hum Gene Ther*, 13: 1451-60.
Webster, C., and H. M. Blau. 1990. 'Accelerated age-related decline in replicative life-span of Duchenne muscular dystrophy myoblasts: implications for cell and gene therapy', *Somat Cell Mol Genet*, 16: 557-65.
Weiler, T., R. Bashir, L. V. Anderson, K. Davison, J. A. Moss, S. Britton, E. Nylen, S. Keers, E. Vafiadaki, C. R. Greenberg, C. R. Bushby, and K. Wrogemann. 1999. 'Identical mutation in patients with limb girdle muscular dystrophy type 2B or Miyoshi myopathy suggests a role for modifier gene(s)', *Hum Mol Genet*, 8: 871-7.
Welsh, C. F. 2004. 'Rho GTPases as key transducers of proliferative signals in g1 cell cycle regulation', *Breast Cancer Res Treat*, 84: 33-42.
Wenzel, K., M. Carl, A. Perrot, J. Zabojszcza, M. Assadi, M. Ebeling, C. Geier, P. N. Robinson, W. Kress, K. J. Osterziel, and S. Spuler. 2006. 'Novel sequence variants in dysferlin-deficient muscular dystrophy leading to mRNA decay and possible C2-domain misfolding', *Hum Mutat*, 27: 599-600.
Wenzel, K., J. Zabojszcza, M. Carl, S. Taubert, A. Lass, C. L. Harris, M. Ho, H. Schulz, O. Hummel, N. Hubner, K. J. Osterziel, and S. Spuler. 2005. 'Increased susceptibility to complement attack due to down-regulation of decay-accelerating factor/CD55 in dysferlin-deficient muscular dystrophy', *J Immunol*, 175: 6219-25.
Wicklund, M. P., and D. Hilton-Jones. 2003. 'The limb-girdle muscular dystrophies: genetic and phenotypic definition of a disputed entity', *Neurology*, 60: 1230-1.
Wilson, C. A., and K. Cichutek. 2009. 'The US and EU regulatory perspectives on the clinical use of hematopoietic stem/progenitor cells genetically modified ex vivo by retroviral vectors', *Methods Mol Biol*, 506: 477-88.
Wright, W. E. 1985. 'Myoblast senescence in muscular dystrophy', *Exp Cell Res*, 157: 343-54.
Wyatt, E. J., A. R. Demonbreun, E. Y. Kim, M. J. Puckelwartz, A. H. Vo, L. M. Dellefave-Castillo, Q. Q. Gao, M. Vainzof, R. C. M. Pavanello, M. Zatz, and E. M. McNally. 2018. 'Efficient exon skipping of SGCG mutations mediated by phosphorodiamidate morpholino oligomers', *JCI Insight*, 3.
Xie, Fei, Lin Ye, Judy C. Chang, Ashley I. Beyer, Jiaming Wang, Marcus O. Muench, and Yuet Wai Kan. 2014. 'Seamless gene correction of β-thalassemia mutations in patient-specific iPSCs using CRISPR/Cas9 and piggyBac', *Genome research*, 24: 1526-33.
Xu, C. L., M. Z. C. Ruan, V. B. Mahajan, and S. H. Tsang. 2019. 'Viral Delivery Systems for CRISPR', *Viruses*, 11: 28.
Xu, X., K. J. Wilschut, G. Kouklis, H. Tian, R. Hesse, C. Garland, H. Sbitany, S. Hansen, R. Seth, P. D. Knott, W. Y. Hoffman, and J. H. Pomerantz. 2015. 'Human Satellite Cell Transplantation and Regeneration from Diverse Skeletal Muscles', *Stem Cell Reports*, 5: 419-34.
Yablonka-Reuveni, Z. 2011. 'The skeletal muscle satellite cell: still young and fascinating at 50', *J Histochem Cytochem*, 59: 1041-59.
Yamaguchi, M., Y. Watanabe, T. Ohtani, A. Uezumi, N. Mikami, M. Nakamura, T. Sato, M. Ikawa, M. Hoshino, K. Tsuchida, Y. Miyagoe-Suzuki, K. Tsujikawa, S. Takeda, H. Yamamoto, and S. Fukada. 2015. 'Calcitonin Receptor Signaling Inhibits Muscle Stem Cells from Escaping the Quiescent State and the Niche', *Cell Reports*, 13: 302-14.
Yamanaka, S, K Watanabe, N Kitamura, M Iguchi, S Mitsuhashi, Y Nishi, and M Uryu. 1989. 'The structure and mechanical properties of sheets prepared from bacterial cellulose', *Journal of Materials Science*, 24: 3141-45.
Yang, G., and X. Huang. 2019. 'Methods and applications of CRISPR/Cas system for genome editing in stem cells', *Cell Regen (Lond)*, 8: 33-41.
Yang, K., M. Hitomi, and D. W. Stacey. 2006. 'Variations in cyclin D1 levels through the cell cycle determine the proliferative fate of a cell', *Cell division*, 1: 32.

Yeo, H., C. A. Lyssiotis, Y. Zhang, H. Ying, J. M. Asara, L. C. Cantley, and J. H. Paik. 2013. 'FoxO3 coordinates metabolic pathways to maintain redox balance in neural stem cells', *EMBO J*, 32: 2589-602.
Yin, H., F. Price, and M. A. Rudnicki. 2013. 'Satellite cells and the muscle stem cell niche', *Physiol Rev*, 93: 23-67.
Young, C. S., M. R. Hicks, N. V. Ermolova, H. Nakano, M. Jan, S. Younesi, S. Karumbayaram, C. Kumagai-Cresse, D. Wang, J. A. Zack, D. B. Kohn, A. Nakano, S. F. Nelson, M. C. Miceli, M. J. Spencer, and A. D. Pyle. 2016. 'A Single CRISPR-Cas9 Deletion Strategy that Targets the Majority of DMD Patients Restores Dystrophin Function in hiPSC-Derived Muscle Cells', *Cell Stem Cell*, 18: 533-40.
Young, C. S., E. Mokhonova, M. Quinonez, A. D. Pyle, and M. J. Spencer. 2017. 'Creation of a Novel Humanized Dystrophic Mouse Model of Duchenne Muscular Dystrophy and Application of a CRISPR/Cas9 Gene Editing Therapy', *J Neuromuscul Dis*, 4: 139-45.
Yue, Yongping, Xiufang Pan, Chady H. Hakim, Kasun Kodippili, Keqing Zhang, Jin-Hong Shin, Hsiao T. Yang, Thomas McDonald, and Dongsheng Duan. 2015. 'Safe and bodywide muscle transduction in young adult Duchenne muscular dystrophy dogs with adeno-associated virus', *Human Molecular Genetics*, 24: 5880-90.
Zammit, P. S., J. J. Carvajal, J. P. Golding, J. E. Morgan, D. Summerbell, J. Zolnerciks, T. A. Partridge, P. W. Rigby, and J. R. Beauchamp. 2004. 'Myf5 expression in satellite cells and spindles in adult muscle is controlled by separate genetic elements', *Dev Biol*, 273: 454-65.
Zanou, N., and P. Gailly. 2013. 'Skeletal muscle hypertrophy and regeneration: interplay between the myogenic regulatory factors (MRFs) and insulin-like growth factors (IGFs) pathways', *Cell Mol Life Sci*, 70: 4117-30.
Zeilinger, K., N. Freyer, G. Damm, D. Seehofer, and F. Knöspel. 2016. 'Cell sources for in vitro human liver cell culture models', *Exp Biol Med (Maywood)*, 241: 1684-98.
Zhang, W., X. C. Wang, X. Y. Li, L. L. Zhang, and F. Jiang. 2020. 'A 3D porous microsphere with multistage structure and component based on bacterial cellulose and collagen for bone tissue engineering', *Carbohydr Polym*, 236: 116043.
Zhang, Y., H. Li, Y. L. Min, E. Sanchez-Ortiz, J. Huang, A. A. Mireault, J. M. Shelton, J. Kim, P. P. A. Mammen, R. Bassel-Duby, and E. N. Olson. 2020. 'Enhanced CRISPR-Cas9 correction of Duchenne muscular dystrophy in mice by a self-complementary AAV delivery system', *Sci Adv*, 6: eaay6812.
Zhang, Y., C. Long, H. Li, J. R. McAnally, K. K. Baskin, J. M. Shelton, R. Bassel-Duby, and E. N. Olson. 2017. 'CRISPR-Cpf1 correction of muscular dystrophy mutations in human cardiomyocytes and mice', *Sci Adv*, 3: e1602814.
Zhao, X., C. Wei, J. Li, P. Xing, J. Li, S. Zheng, and X. Chen. 2017. 'Cell cycle-dependent control of homologous recombination', *Acta Biochim Biophys Sin (Shanghai)*, 49: 655-68.
Zhou, J. J., F. Wang, Z. Xu, W. S. Lo, C. F. Lau, K. P. Chiang, L. A. Nangle, M. A. Ashlock, J. D. Mendlein, X. L. Yang, M. Zhang, and P. Schimmel. 2014. 'Secreted histidyl-tRNA synthetase splice variants elaborate major epitopes for autoantibodies in inflammatory myositis', *J Biol Chem*, 289: 19269-75.
Zhu, P., F. Wu, J. Mosenson, H. Zhang, T. C. He, and W. S. Wu. 2017. 'CRISPR/Cas9-Mediated Genome Editing Corrects Dystrophin Mutation in Skeletal Muscle Stem Cells in a Mouse Model of Muscle Dystrophy', *Mol Ther Nucleic Acids*, 7: 31-41.
Zincarelli, C., S. Soltys, G. Rengo, and J. E. Rabinowitz. 2008. 'Analysis of AAV serotypes 1-9 mediated gene expression and tropism in mice after systemic injection', *Mol Ther*, 16: 1073-80.
Zismanov, V., V. Chichkov, V. Colangelo, S. Jamet, S. Wang, A. Syme, A. E. Koromilas, and C. Crist. 2016. 'Phosphorylation of eIF2α Is a Translational Control Mechanism Regulating Muscle Stem Cell Quiescence and Self-Renewal', *Cell Stem Cell*, 18: 79-90.
Zufferey, R., T. Dull, R. J. Mandel, A. Bukovsky, D. Quiroz, L. Naldini, and D. Trono. 1998. 'Self-inactivating lentivirus vector for safe and efficient in vivo gene delivery', *J Virol*, 72: 9873-80.
Zuo, Z., and J. Liu. 2016. 'Cas9-catalyzed DNA Cleavage Generates Staggered Ends: Evidence from Molecular Dynamics Simulations', *Scientific Reports*, 6: 37584.